

Biomass Burning Emissions - Composition, Uptake, and Evolution

by

Max Loebel Roson

A thesis submitted in partial fulfillment of the requirements for the degree of

Doctor of Philosophy

Department of Chemistry
University of Alberta

© Max Loebel Roson, 2023

Abstract

Biomass burning, from wildfires to cooking stoves, is a major contributor to atmospheric pollution on a global scale, affecting the quality of the air we breathe. Emissions from biomass burning are both health and climate affecting, and vary considerably in composition depending on how the fuel is burned. Currently, millions depend on biomass fuels for energy production, cooking, and heating purposes. And yet, we still do not fully understand the composition of biomass burning emissions, their evolution once travelling through the atmosphere, or their impacts. The effects of biomass combustion are compounded for people living in developing regions such as Sub-Saharan Africa, where reliance on unrefined biomass like wood or cow dung is widespread. Usage of unrefined fuels and inefficient stoves aggravates the impacts of biomass burning; impacts which can only be accurately predicted with a comprehensive understanding of emission composition. The matter is also urgent, considering that wildfire incidence and severity is expected to rise in the coming years.

The goal of this thesis is to forward our understanding of biomass burning emissions from understudied fuels, from composition to evolution in the atmosphere. In Chapter 2, I discuss the composition of biomass burning emissions through the study of wood and cow dung fuels combusted in a tube furnace capable of highly reproducible burns. I report that the composition of the base fuel directly impacts that of the emissions, which for dung comprise a complex matrix of light-absorbing and nitrogen-containing compounds. Additionally, I detail that levoglucosan and its isomers galactosan and mannosan - tracers generally used to source-apportion wood burns - are also emitted from burning cow dung, and report their emission factors.

I conclude that the effects of biomass burning in regions which rely on dung fuels could be underestimated. And, that on a per-mass basis, the climate impacts of dung burning are likely greater than wood.

In Chapter 3, I apply novel analytical and statistical techniques to the study of biomass burning emissions. Here, I describe which burn parameters, such as heating temperature, air flow rate, or fuel type, contribute to altering the composition of the emissions. This was achieved through the coupling of two-dimensional gas chromatography mass spectrometry (GC×GC-MS) and principal component analysis (PCA). While GC×GC-MS separates the emissions, PCA identifies which components are characteristic to each burn parameter. I report that the major driver for differentiation between emissions are flow rate and temperature. As well, I show that low flow rate combustion of cow dung is associated with more diverse emissions, including health-affecting furans and thiazoles. This chapter demonstrates that coupling GC×GC-MS and PCA can effectively deconvolute biomass emissions too convoluted to otherwise characterize; a combination of techniques which has not been applied to the study of biomass burning emissions in a laboratory setting previously.

In Chapter 4, I focus on the evolution of anhydrides in the atmosphere. Specifically, I discuss how anhydrides can reactively uptake to the surface of biomass burning emissions, and report the uptake coefficients of phthalic anhydride under increasing loading masses. I detail how electrophilic anhydrides can react with a variety of nucleophiles present in biomass burning emissions to form larger water-stable products, including with the tracer levoglucosan. This mechanism might explain how volatile compounds like anhydrides end up irreversibly partitioned to the particle-phase in the atmosphere, improving our understanding of the evolution of burn plumes.

Overall, this thesis provides novel data and methods for the study of biomass burning and its emissions. The information provided within will help differentiate emissions from previously understudied biomass fuels, and ultimately, aid in the creation of atmospheric models to predict the impacts of biomass burning.

Preface

My contributions to each chapter of this thesis are listed below. Chapters 1, 3, and 5 include unpublished material. Chapters 2 and 4 consist of published work.

Chapter 1

Introduction

Contributions: The introduction was written by Max Loebel Roson with review and feedback by Dr. Ran Zhao.

Chapter 2

Chemical Characterization of Emissions Arising from Solid Fuel Combustion - Contrasting Wood and Cow Dung Burning

M. Loebel Roson, R. Duruisseau-Kuntz, M. Wang, K. Klimchuk, R. J. Abel, J. J. Harynuk, and R. Zhao, “Chemical characterization of emissions arising from solid fuel combustion—contrasting wood and cow dung burning,” *ACS Earth and Space Chemistry*, vol. 5, no. 10, pp. 2925–2937, 2021. DOI: 10.1021/acsearthspacechem.1c00268 [1]

Contributions: The combustion experiments were designed by Max Loebel Roson with critical input by Dr. Robin J. Abel and Dr. Ran Zhao. Combustion samples were gathered and analyzed by Max Loebel Roson and Meng Wang. Levoglucosan experiments were carried out by Ryan Duruisseau Kuntz and Keifer Klimchuk. Mass absorption coefficient, mass spectrometry, and scanning mobility particle sizer

experiments, as well as data analysis for these experiments was performed by Max Loebel Roson. Total organic carbon and total nitrogen experiments were carried out by the University of Alberta Natural Resources Analytical Laboratory. The manuscript was written by Max Loebel Roson, with in-depth review by Dr. Ran Zhao and feedback by Dr. Robin J. Abel and Dr. James J. Harynuk.

Chapter 3

Comprehensive Two-Dimensional Gas Chromatographic Analysis of Biomass Burning Emissions

M. Loebel Roson, S. A. Schmidt, V. Choudhary, T. A. Johnson, A. P. de la Mata, J. J. Harynuk, and R. Zhao

Contributions: The combustion experiments were designed by Max Loebel Roson. Samples were gathered by Max Loebel Roson and Vikram Choudhary. Two-dimensional gas chromatography analyses were carried out by Max Loebel Roson, with feedback by Sheri A. Schmidt, Dr. Trevor A. Johnson, and Dr. A. Paulina de la Mata. Data was analyzed by Max Loebel Roson with feedback by Sheri A. Schmidt. The chapter was written by Max Loebel Roson, with in-depth review by Dr. Ran Zhao.

Chapter 4

Unexpected Electrophiles in the Atmosphere - Anhydride Nucleophile Reactions and Uptake to Biomass Burning Emissions

M. Loebel Roson, M. Abou-Ghanem, E. Kim, S. Wu, D. Long, S. A. Styler, and R. Zhao, "Unexpected electrophiles in the atmosphere – anhydride nucleophile reactions and uptake to biomass burning emissions," *Phys. Chem. Chem. Phys.*, 2023. DOI: 10.1039/D3CP01751F [2]

Contributions: The uptake, stability, and separation experiments were designed and carried by Max Loebel Roson with feedback by Dr. Ran Zhao. Uptake calculations were performed by Max Loebel Roson with feedback and validation by Dr. Maya Abou-Ghanem based on previous supervision by Dr. Sarah A. Styler. Gas and liquid chromatography mass spectrometry data were analyzed by Max Loebel Roson. Nuclear magnetic resonance determination was performed by the University of Alberta nuclear magnetic resonance facility, with data analysis by Erica Kim. Shuang Wu and Dylan Long provided resources for the uptake and liquid chromatographic analysis respectively. The manuscript was written by Max Loebel Roson, with in-depth review by Dr. Ran Zhao and feedback by Dr. Maya Abou-Ghanem.

Chapter 5

Conclusions, Recommendations, and Future Work

Contributions: The conclusion was written by Max Loebel Roson with review and feedback by Dr. Ran Zhao.

Acknowledgements

First and foremost, I would like to thank my supervisor Dr. Ran Zhao, for being an unending well of knowledge, support, and positivity. His guidance and ingenuity were invaluable over the past five years, and I aspire to display a fraction of his qualities. I also credit Ran for fostering an environment of collaboration and inclusivity, I could not have been luckier to be a part of the Zhao group. Building the foundations of the laboratory has been a formative experience in problem-solving and independence, and I am grateful for how it has shaped my approach to research today. I have no doubts that the group will keep being successful under Ran's continued leadership.

I would also like to express my gratitude to each member of my supervisory committee, Dr. Wolfgang Jäger and Dr. Jason Olfert, as well as Dr. Sarah Styler, for their continued advice and support. I also thank Daniel R. Aldrich for his continuing contributions to the University of Alberta. More specifically, I would like to acknowledge the work that he put into creating the L^AT_EX template for this thesis, without which the formatting process have been even more arduous.

I also thank all my past and present collaborators, mentees, and Zhao group members, including but not limited to: Amanda Hanashiro Moraes, Chester Lau, Christian Fotang, Dylan Long, Keifer Klimchuk, Dr. Maya Abou-Ghanem, Meng Wang, Dr. Ming Lyu, Mst Rowshon Afroz, Ryan Duruisseau-Kuntz, Shakiba Talebian, Toluwatise Ehindero, and Wayne Cheng. You are the bedrock of this thesis. I would also like to thank those who undertook this journey with me, Tania Gautam, Shuang Wu, Vikram Choudhary and Xinyang Guo. Every one of you inspired me in distinct ways and I could not have asked for kinder friends and colleagues. I am indebted to each

of you, and will greatly miss our discussions over coffee.

Outside of the laboratory, I thank my Edmontonian friends, who made the Canadian winters more bearable with their warmth, Ally, Fiorella, and Wayne. In particular, I would like to thank Jéssica and Morgan Vejdani Amorim. You have become a second family throughout my stay, and I cherish you both immensely. I also thank my intercontinental friends, who often sacrificed their sleep schedules for online hangouts, Carlos, Dionysos, Ivo, Jason, Marc, Marie, Maxine, and Tristan-Pablo. You have always been there for me and I hold you all dearly. By extension, I would also like to thank the “Metal Leaping Glass” server and all of its other members, for their companionship and peculiar brand of life-affirming sardonic humor.

Finally, I would also like to thank my partner Caroline, who painstakingly supported me throughout my thesis-writing seclusion. I am eternally grateful. I also thank all members of the Roson family for their unconditional love, with special mention to my sister Lola, for her support and commiserations throughout her own studies, as well as my mother Susana, for being the driving force behind my decision to pursue a PhD; I dedicate this thesis to them.

Table of Contents

1	Introduction	1
1.1	What is biomass burning	2
1.1.1	On particulate matter	3
1.1.1.1	Black carbon	5
1.1.1.2	Brown carbon	5
1.1.2	On volatile organic compounds	7
1.2	Evolution of biomass burning emissions	9
1.2.1	Physical changes	10
1.2.1.1	Transport	10
1.2.1.2	Dry Deposition	10
1.2.1.3	Wet Deposition	11
1.2.1.4	Partitioning - evaporation and condensation	13
1.2.1.5	Phase changes	14
1.2.2	Chemical changes	15
1.2.2.1	Photochemistry - direct photolysis and photooxidation	15
1.2.2.2	Nucleophilic addition	19
1.2.2.3	Heterogeneous reactions and uptake	20
1.3	Combustion	21
1.3.1	Combustion efficiency	23
1.3.1.1	On emission composition and its variability	24
1.3.2	Approaches to study fire	25
1.3.2.1	Sampling in the field versus a fire lab, and other sim- plified methods	25
1.3.2.2	Reproducible versus representative combustion strate- gies	26
1.3.2.3	On the tube furnace	28
1.4	Analysis of physical properties	28
1.4.1	Size and optical properties	28

1.4.1.1	Aerodynamic particle sizer	29
1.4.1.2	Scanning mobility particle sizer	29
1.4.2	Phase state	30
1.5	Analysis of chemical properties	31
1.5.1	Online Techniques	31
1.5.1.1	Aerosol mass spectrometry	31
1.5.1.2	Proton transfer reaction mass spectrometry	33
1.5.2	Offline Techniques	33
1.5.2.1	Benefits and difficulties	33
1.5.3	Targeted versus non-targeted	35
1.5.3.1	An aside on tracers	37
1.5.4	Separation-based techniques	38
1.5.4.1	Gas Chromatography	38
1.5.4.2	Liquid chromatography mass spectrometry	39
1.5.4.3	Two-dimensional gas chromatography mass spectrometry	40
1.5.5	Uptake measurement techniques	41
1.5.5.1	Coated wall flow tubes and Knudsen cells	41
1.6	Motivation	42
1.7	Thesis Objectives	43
1.8	Thesis Outline	44
	References	45

2 Chemical Characterization of Emissions Arising from Solid Fuel Combustion - Contrasting Wood and Cow Dung Burning **74**

2.1	Introduction	75
2.2	Materials and Methods	77
2.2.1	Solid Fuels	77
2.2.2	Elemental Analysis of Solid Fuels	77
2.2.3	Solid Fuel Burning and Sample Collection	78
2.2.4	Quantification of Levoglucosan using GC-MS	80
2.2.5	Total Organic Carbon (TOC) and Total Nitrogen (TN) Measurements	81
2.2.6	Characterization of Light Absorption	81
2.2.7	Non-Targeted Organic Analysis with LC-MS	82
2.3	Results and discussion	83
2.3.1	Elemental Composition of Solid Fuels	83

2.3.2	Combustion Process	84
2.3.3	Total Organic Carbon and Total Nitrogen	86
2.3.4	UV-Vis Absorption of Filter Extracts and Mass Absorption Coefficients	87
2.3.5	Emission Factors of Levoglucosan and its Structural Isomers	89
2.3.6	Non-Targeted Organic Analysis with LC-MS	92
2.3.7	Major Peaks Detected	93
2.3.8	Detailed MS Assignments	95
2.3.9	Targeted Analysis of Representative Biomass Burning Compounds	96
2.3.10	Implication and Conclusion	97
2.4	Acknowledgements	99
2.5	Supporting Information	100
	References	101
3	Comprehensive Two-Dimensional Gas Chromatographic Analysis of Biomass Burning Emissions	112
3.1	Introduction	113
3.2	Materials and methods	115
3.2.1	Sample combustion and collection	115
3.2.2	Thermal desorption and GC×GC-MS analysis	115
3.2.3	Peak detection	116
3.2.4	Feature selection	116
3.2.5	Principal component analysis	117
3.2.5.1	Concepts and definitions	117
3.3	Results and discussion	119
3.3.1	GC×GC-ToF-MS Results	119
3.3.2	Principal component analysis	125
3.4	Conclusion and future work	129
	References	130
4	Unexpected Electrophiles in the Atmosphere - Anhydride Nucleophile Reactions and Uptake to Biomass Burning Emissions	139
4.1	Introduction	140
4.2	Materials and Methods	143
4.2.1	Choice of Anhydrides and Nucleophiles	143
4.2.2	Nucleophilic Addition in the Condensed-Phase	144

4.2.3	Uptake Experiments	145
4.2.4	Coating Material Collection and Solid Fuel Burning	147
4.2.5	Tube Coating	148
4.2.6	LC-MS Analysis of the Coating Material	148
4.2.7	Uptake Calculations	149
4.3	Results and discussion	151
4.3.1	Fundamental Investigation of Nucleophilic Addition	151
4.3.1.1	Anhydrides in Protic and Aprotic Solvents - NMR Characterization	151
4.3.1.2	Reaction Confirmation using LC-MS	151
4.3.1.3	Reaction Competition and Product Stability in Water	152
4.3.2	Uptake of Anhydrides to Biomass Burning Material	155
4.3.2.1	Uptake of Phthalic Anhydride	155
4.3.3	Evidence of Reactive Uptake	158
4.3.3.1	Mass Dependence	159
4.3.3.2	Linoleic Acid	160
4.3.3.3	Removal of Semivolatile Species	161
4.3.3.4	Presence of Uptake Products - Tube Doping Experi- ments	163
4.3.4	Additional Factors Affecting the Uptake - Relative Humidity	165
4.4	Conclusions	166
4.5	Author Contributions	168
4.6	Conflicts of interest	168
4.7	Acknowledgements	168
4.8	Supporting Information	168
	References	169
5	Conclusions, Recommendations, and Future Work	180
5.1	Thesis Summary	181
5.2	Future Work and recommendations	182
5.2.1	On fire research	182
5.2.2	On the application of GC×GC-MS to biomass burning emission analysis	182
5.2.3	Proposed research directions	183
5.2.3.1	Improving bulk identification - inspiration from metabolomic databases	183
5.2.3.2	Re-emission of VOCs from biomass burning films	184

5.2.3.3	Towards low-cost accessible detection of levoglucosan	185
References		186
Bibliography		188
Appendix A: Chapter 2		234
A.1	Supplementary information for Chapter 2	234
A.1.1	Levoglucosan Derivatization	234
A.1.2	Particle Emission from Biomass Burning	235
A.1.3	Mass Absorption Coefficients	236
A.1.4	Individual GC-MS Chromatograms	237
A.1.5	Levoglucosan Fragmentation Pattern	239
A.1.6	Individual ESI- MS Chromatograms	240
A.1.7	Individual ESI+ MS Chromatograms	242
A.1.8	MS Assignments	244
A.1.9	Standard Compounds	246
Appendix B: Chapter 3		247
B.1	Supplementary information for Chapter 3	247
B.1.1	GC×GC-ToF-MS Results	247
Appendix C: Chapter 4		249
C.1	Supplementary information for Chapter 4	249
C.1.1	NMR Analysis	249
C.1.2	Anhydride Gas-Phase Concentration Determination	251
C.1.3	Typical LC-MS Chromatograms	252
C.1.4	Burn Parameters	254
C.1.5	Coated Tube Uptake Parameters	255
C.1.6	Anhydride Nucleophilic Addition	255
C.1.7	Reaction Competition and Product Stability in Water	256

List of Tables

1.1	Combustion parameters and their influence on combustion efficiency .	25
2.1	Mean Elemental Composition of Ground Biomass \pm Standard Deviation.	84
2.2	Total Organic Carbon and Total Nitrogen Content of each Biomass. Mean \pm Standard Deviation.	87
2.3	Mean Levoglucosan and Isomer Emission Factors \pm Standard Deviation.	90
4.1	Maleic (M) or phthalic (P) anhydride nucleophile reaction products detected using LC-MS. In each instance, the listed product peak mass to charges (m/z) were those that yielded the highest intensity LC-MS signals.	152
4.2	Range of γ values obtained for phthalic anhydride during uptake as loading mass is decreased under variable relative humidity (RH). . . .	158
A.1	Top 100 Molecular Assignments Unique to Indian and Canadian Dung using the ESI+ mode. High (left column) to low (right column) in descending order of intensity. Columns 3. and 6. ‘Prev. Rep.’ list whether a compound has been identified in a study by Fleming <i>et</i> <i>al.</i> [249] as unique to dung samples (1), common to wood and dung samples (2), or not detected (0).	244
A.2	Standard Analysis: ESI- Compound Detection Intensity	246
A.3	Standard Analysis: ESI+ Compound Detection Intensity	246
C.1	^1H NMR anhydride and acid analysis in protic (D_2O) and aprotic (CDCl_3) solvents. The calculated concentration range represents du- plicate analyses.	249
C.2	Individual filter burn parameters.	254
C.3	Parameters used to calculate the uptake coefficient (γ) in Chapter 4 PA = Phthalic Anhydride, RM = Molecular Reduced Mass	255

List of Figures

1.1	Proportion of the population with primary reliance on clean fuels and technology for cooking in 2016 (%). Figure obtained (with adapted caption) from: (WHO)“Global Household Energy Database,” <i>World Health Organization</i> , 2023 [6]	2
1.2	Emissions during the May 15th 2023 Alberta wildfires, captured by a National Aeronautics Space Administration (NASA) satellite. The red dots represent temperature anomalies, i.e. the origin of the emissions as a result of the fires. Image (with adapted caption) obtained from NASA Worldview. 2023 [33].	4

1.3 RF bar chart for the period 1750–2011 based on emitted compounds (gases, aerosols or aerosol precursors) or other changes. Numerical values and their uncertainties are shown in the Supplementary Material Tables 8.SM.6 and 8.SM.7. Note that a certain part of CH₄ attribution is not straightforward and discussed further in Section 8.3.3. Red (positive RF) and blue (negative forcing) are used for emitted components which affect few forcing agents, whereas for emitted components affecting many compounds several colours are used as indicated in the inset at the upper part the figure. The vertical bars indicate the relative uncertainty of the RF induced by each component. Their length is proportional to the thickness of the bar, that is, the full length is equal to the bar thickness for a ±50% uncertainty. The net impact of the individual contributions is shown by a diamond symbol and its uncertainty (5 to 95% confidence range) is given by the horizontal error bar. ERF_{aci} is ERF due to aerosol–cloud interaction. BC and OC are co-emitted, especially for biomass burning emissions (given as Biomass Burning in the figure) and to a large extent also for fossil and biofuel emissions (given as Fossil and Biofuel in the figure where biofuel refers to solid biomass fuels). SOA have not been included because the formation depends on a variety of factors not currently sufficiently quantified. Figure and caption reprinted with permission from: IPCC. “Climate Change 2013 – The Physical Science Basis: Working Group I Contribution to the Fifth Assessment Report of the Intergovernmental Panel on Climate Change”, ch. 8, pp. 698, 2014, Figure 8.17 [34]. Copyright Cambridge University Press 7

1.4 Volatility, oxidation state, and approximate oxygen to carbon ratio for important organic aerosol (OA) and vapours. The shaded areas represent the classification of each OA. Oxidized organic aerosol (OOA) are split into low volatility (LV) and semi-volatile (SV) fractions. The HOA fraction represents hydrocarbon-like organic aerosol. Figure reprinted under Creative Commons Attribution (CC BY 3.0) from: Donahue *et al.* “A two-dimensional volatility basis set – part 2: Diagnostics of organic-aerosol evolution,” *Atmospheric Chemistry and Physics*, vol. 12, no. 2, pp. 615–634, 2012 [58] 8

1.5	Major sources and processes affecting the amount and quality of organic carbon found in wet deposition. SOA refers to secondary organic aerosol, CCN are cloud condensation nuclei, VOCs are volatile organic compounds, CO is carbon monoxide gas, and CO ₂ is carbon dioxide gas. Figure reprinted under Creative Commons Attribution (CC BY-NC-ND 4.0) from: Iavorivska <i>et al.</i> “Atmospheric deposition of organic carbon via precipitation,” <i>Atmospheric Environment</i> , vol. 146, pp. 153–163, 2016 [91]	12
1.6	Schematics of the kinetic multilayer model of gas-particle interactions in aerosols and clouds (KM-GAP). Concentrations of species Z _i and Z _j in the gas (g) and near-surface gas-phase, at the sorption layer (s) and in the surface (ssb) and in the bulk (b) layers. J are the transport fluxes between each layer, including the gas-phase diffusion flux (J _g), the adsorption (J _{ads}) and desorption (J _{des}) fluxes, surface-bulk exchange fluxes (J _{s,ssb} , J _{ssb,s}), and bulk diffusion fluxes (J _b). Figure reprinted with permission from: Arangio <i>et al.</i> “Multiphase Chemical Kinetics of OH Radical Uptake by Molecular Organic Markers of Biomass Burning Aerosols: Humidity and Temperature Dependence, Surface Reaction, and Bulk Diffusion,” <i>J. Phys. Chem. A</i> , vol. 119, pp. 4533-4544, 2015 [118]. Copyright 2023 American Chemical Society	16
1.7	BrC chromophores present in the BBOA sample before (a) and after (b) 300 nm irradiation for a conifer fuel: lodgepole pine. Figure reprinted under Creative Commons Attribution (CC BY 4.0) from: Fleming <i>et al.</i> “Molecular composition and photochemical lifetimes of brown carbon chromophores in biomass burning organic aerosol,” <i>Atmos. Chem. and Phys.</i> , vol. 20, pp. 1105-1129, 2020 [124]	18

1.8	A more advanced conceptual model that captures the effects of the competitive thermokinetics inherent in the combustion of cellulosic fuels. Arrows indicate direction of flows. The low activation energy, exothermic pathway of char formation occurs in competition with the higher activation, endothermic pathway of volatile formation. Oxidation of volatiles and char provide the bulk of the heat released during combustion and create three different feedback paths that lead to sustained combustion. The heat generated by the formation of char is retained in the fuel substrate (yellow pathway) and in conjunction with the oxidation of char (red pathway) provides the mechanism by which a fuel can transition to flaming combustion. In most instances, it is the oxidation of volatiles (blue pathway) that drives the spread of a wildland fire. However, it is the char pathways that enable a biomass fire to sustain combustion under marginal conditions. Reproduced with permission from Springer Nature: Sullivan <i>et al.</i> “Inside the Inferno: Fundamental Processes of Wildland Fire Behaviour,” <i>Curr. Forestry Rep.</i> , vol. 3, pp. 132-149, 2017 [153]	23
1.9	Simplified and reproducible tube furnace burn (A) versus a prescribed representative burn in a fire lab (B). Picture (B) reprinted (with adapted caption) from: “Experimental fire studied in the Missoula Fire Lab combustion chamber,” <i>Missoula Fire Sciences Laboratory</i> , U.S Department of Agriculture, 2023 [172]	27
1.10	Estimation of the phase state of the film substrate as shown for a glucose/1,2,6-hexanetriol (GLU/HEX) mixture (mass ratio of 4 : 1). Deformation and recovery were monitored for different time periods due to the poking of the substrate at different temperatures. The microscope images are 200 μm wide. Figure reprinted under Creative Commons Attribution (CC BY 4.0) from: Li <i>et al.</i> “Heterogeneous oxidation of amorphous organic aerosol surrogates by O_3 , NO_3 , and OH at typical tropospheric temperatures,” <i>Atmos. Chem. and Phys.</i> , vol. 20, pp. 6055-6080, 2020 [117]	32

1.11	Number percentages of elemental formulas identified from biomass burning solvent-extractable organic compounds measured with high resolution mass spectrometry (HRMS) depending on whether direct infusion electrospray ionization (ESI) or atmospheric pressure photo ionization (APPI) is used. The charge used for ionization is represented by + or -. Figure reprinted with permission from: Lin <i>et al.</i> “Comprehensive Molecular Characterization of Atmospheric Brown Carbon by High Resolution Mass Spectrometry with Electrospray and Atmospheric Pressure Photoionization,” <i>Analytical Chemistry</i> , vol. 90, no. 21, pp. 12493–12502, 2018 [109]. Copyright 2023 American Chemical Society	36
1.12	Schematic diagram of a coated wall flow tube coupled to a mass spectrometer applied to the uptake of SO ₂ on Saharan dust. Figure reprinted with adapted caption under Creative Commons Attribution (CC BY-NC-SA 2.5 CA) from: Adams <i>et al.</i> “The uptake of SO ₂ on Saharan dust: a flow tube study,” <i>Atmos. Chem. and Phys.</i> , vol. 5, pp. 2679-2689, 2005 [245]	42
2.1	Schematic Diagram of Tube Furnace Setup (a) and Pictures of Wood (b), CAD (c), and IND (d) Biomass Fuels.	79
2.2	Normalized mass concentration (dM/dlogD _p) and particle diameter (nm) of biomass burning emissions throughout the IND heating process. The heatmap represents the particle mass concentration (dM) in μg/m ³ normalized by the number of channels per decade of particle resolution (dlogD _p) of the instrument. The black line represents the median particle diameter. The red line represents the temperature measured throughout the heating process using a thermocouple inside the quartz tube.	85
2.3	Mass Absorption Coefficient (MAC) of water soluble fraction of emissions from the three types of biomass fuels. The sub window contains biomass MACs obtained in the current study as well as values reported by Pandey <i>et al.</i> [267] and Fleming <i>et al.</i> [249] at 350 nm.	88
2.4	GC-MS chromatogram of biomass burning filter extracts.	89
2.5	Species detected in emissions from each fuel by LC-MS in ESI- and ESI+, by number (a). The intensity-weighted breakdown of CHN, CHON, and CHO compounds detected by the ESI+ mode are presented in (b).	92

2.6	ESI- LC-MS Base Peak Chromatogram (BPC) of biomass burning emissions. IND and Wood spectra offset by 30 and 60 counts respectively.	94
2.7	Total Ion Chromatogram (TIC)(a) and Base Peak Chromatogram (BPC)(b) ESI+ LC-MS chromatograms of biomass burning emissions. CAD and IND spectra in base peak chromatogram are offset by 30 and 60 counts respectively.	95
3.1	Two-dimensional gas chromatography time of flight mass spectrometry (GC×GC-ToF-MS) chromatogram of wood biomass burning particulate matter gathered at 500 °C and 0.2 slpm of airflow. The yellow square represents levoglucosan. The red square displays a series of syringaldehyde-like compounds of increasing molecular mass. The blue and green squares represent interferences from the glass wool and column bleed respectively. An enlarged version of this figure is available in the Supporting Information (B.1.1)	120
3.2	Double bond equivalent (DBE) and carbon number obtained from the combustion of Indian cow dung (IND) (green triangles, offset by -0.25 counts on the x- and y-axis), wood (red squares), and Canadian cow dung (CAD) (blue circles, offset by 0.25 counts on the x- and y-axis) biomass. The marker shading represents the number of nitrogen atoms detected in each compound.	122
3.3	Double bond equivalence (DBE) and carbon number obtained from the combustion of Indian cow dung (IND) samples at 500 °C using 0.2 (green triangles) and 10 (blue triangles, offset on the x- and y-axis by 0.25 counts) slpm of air, unique detections only. The marker shading represents the number of nitrogen atoms detected in each compound. The size of the markers indicates the logarithmic peak volume of each compound, normalized by the average loading mass of each filter punch class. The peak volumes of a compound that appears multiple times at a given flow rate are summed. n = 3 for each flow rate.	123

3.4	Hydrogen to carbon (H/C) and oxygen to carbon (O/C) ratio obtained from: A), species unique to the combustion of Indian cow dung (green triangles), wood (red squares), and Canadian cow dung (blue circles) biomass, and B), the combustion of Indian cow dung (IND) at 500 °C using 0.2 (downwards green triangles) and 10 (upwards blue triangles) slpm of air. The interior marker shading represents the number of nitrogen atoms identified in each detection. The size of the markers indicates the logarithmic peak volume of each compound.	124
3.5	Principal component analysis (PCA) of biomass burning emissions after feature selection and classification by biomass fuel type.	126
3.6	Principal component analysis (PCA) of biomass burning emissions after feature selection and classification by heating temperature at 10 slpm.	127
3.7	Principal component analysis (PCA) of biomass burning emissions after feature selection and classification by flow rate and heating temperature. The point at which the lines from each marker meet indicates the average score for all samples of that classification.	128
4.1	Acid catalyzed acid anhydride nucleophilic addition reaction, alcohol and amine driven additions are simplified.	143
4.2	Anhydride uptake experimental setup.	147
4.3	LC-MS peak area signals obtained from increasing fractions of water in acetonitrile (ACN) after the 24 hour and 1 week-long analysis period for A) Maleic anhydride vanillin product (MVP), B) Maleic acid, C) Phthalic anhydride levoglucosan product (PLP), D) Phthalic acid. Error bars represent the range between duplicate experiments. . . .	153
4.4	Phthalic anhydride (PA) uptake experiment. The top blue curve represents a typical GC-FID PA peak vertically offset by 1 count, taken at 2.7 min intervals throughout the experiment and from which the bottom uptake graph is constructed. The bottom gray and red shaded areas represent the anhydride flowing through the uncoated and coated tubes respectively, γ is calculated over the length of the red area. The green marker on the bottom graph indicates the time at which the top peak is taken.	156

4.5	Range of γ values obtained for phthalic anhydride on tubes coated with biomass burning material as a function of loading mass of the coating. Each data point represents the averaged γ values obtained over 2 hours of uptake at a relative humidity of 0. The shaded blue area depicts the range of γ values observed from tubes which underwent 24 hours of semivolatile removal. The green dot portrays the γ obtained from a tube which did not go through the semivolatile removal procedure. The red triangle represents the γ from a tube in which 0.0167 g of vanillin were dissolved during the coating process, in addition to the biomass burning material. The brown squares illustrate the γ obtained from tubes coated with linoleic acid, an unreactive material. The dashed line indicates the average γ obtained for uncoated (blank) tubes. . . .	160
4.6	GC-FID phthalic anhydride chromatogram of a tube rested under continued airflow for 24 hours versus a tube from which semivolatile species were not removed. The top peak signal is offset by 0.8 counts. . . .	162
4.7	Maleic anhydride levoglucosan product negative electrospray ionization (ESI-) total ion chromatogram (TIC) mass spectra. The top spectrum is gathered from a levoglucosan doped tube through which gas-phase anhydride was flown. The mirrored blue bottom spectrum tube was prepared under the same conditions, without the anhydride uptake step.	164
A.1	Levoglucosan Derivatization Mechanism	234
A.2	Normalized mass concentration ($dM/d\log D_p$) and particle diameter (nm) of biomass burning emissions throughout the wood heating process. The heatmap represents the particle mass concentration (dM) in $\mu g/m^3$ normalized by the number of channels per decade of particle resolution ($d\log D_p$) of the instrument. The black line represents the median particle diameter.	235
A.3	Normalized mass concentration ($dM/d\log D_p$) and particle diameter (nm) of biomass burning emissions throughout the CAD heating process. The heatmap represents the particle mass concentration (dM) in $\mu g/m^3$ normalized by the number of channels per decade of particle resolution ($d\log D_p$) of the instrument. The black line represents the median particle diameter.	235
A.4	Mass Absorption Coefficient of water soluble fraction of emissions from the three types of biomass fuels. The shaded area represents the difference between two burns.	236

A.5	GC-MS chromatogram of IND biomass burning filter extracts.	237
A.6	GC-MS chromatogram of CAD biomass burning filter extracts.	237
A.7	GC-MS chromatogram of Wood biomass burning filter extracts.	238
A.8	Fragmentation pattern observed for silylated levoglucosan (top) vs NISTMS library pattern (bottom)	239
A.9	ESI- LC-MS Base Peak Chromatogram (BPC) of IND biomass burning emissions.	240
A.10	ESI- LC-MS Base Peak Chromatogram (BPC) of CAD biomass burn- ing emissions.	240
A.11	ESI- LC-MS Base Peak Chromatogram (BPC) of Wood biomass burn- ing emissions.	241
A.12	Total Ion Chromatogram (TIC)(a) and Base Peak Chromatogram (BPC)(b) ESI+ LC-MS chromatograms of IND biomass burning emissions.	242
A.13	Total Ion Chromatogram (TIC)(a) and Base Peak Chromatogram (BPC)(b) ESI+ LC-MS chromatograms of CAD biomass burning emissions.	242
A.14	Total Ion Chromatogram (TIC)(a) and Base Peak Chromatogram (BPC)(b) ESI+ LC-MS chromatograms of Wood biomass burning emissions.	243
B.1	Two-dimensional gas chromatography time of flight mass spectrometry (GC×GC-ToF-MS) chromatogram of wood biomass burning particu- late matter gathered at 500 °C and 0.2 slpm of airflow. Each cir- cle represents a separate detection. The yellow square represents the biomass burning tracer levoglucosan. The red square displays a series of syringaldehyde compounds of increasing carbon chain length. The blue and green squares represent interferences from the glass wool and column bleed respectively.	248
C.1	¹ H NMR plot of Maleic Anhydride dissolved in CDCl ₃	250
C.2	¹ H NMR plot of Maleic Anhydride dissolved in D ₂ O	250
C.3	¹ H NMR plot of Maleic Acid dissolved in CDCl ₃	250
C.4	¹ H NMR plot of Maleic Acid dissolved in D ₂ O	250

C.5	Liquid Chromatography Negative Electrospray Ionization Mass Spectrometry (LC-MS) Plots of Coated Tube Extract After Maleic Anhydride Uptake in: (A) Total Ion Chromatogram (TIC), (B) Maleic Acid Extracted Ion Chromatogram (EIC) at a mass to charge (m/z) of 115, (C) Levoglucosan EIC at m/z 207, (D) Maleic Anhydride Levoglucosan Product EIC at m/z 259. NL represents the intensity of the largest peak in each chromatogram.	252
C.6	LC-MS chromatogram of 0.01mM maleic acid dissolved in acetonitrile, TIC (top) and EIC at 115 m/z (bottom).	253
C.7	LC-MS chromatogram of 0.1mM maleic anhydride dissolved in acetonitrile, TIC (top) and EIC at 115 m/z (bottom).	253
C.8	LC-MS chromatogram of 1mM phthalic acid dissolved in acetonitrile, TIC (top) and EIC at 165 m/z (bottom).	253
C.9	Predicted product structures of the nucleophilic addition of anhydrides where: A) Anisyl Alcohol + Phthalic Anhydride, B) Coniferyl Aldehyde + Maleic Anhydride, C) Histidine + Maleic Anhydride, D) Levoglucosan + Phthalic Anhydride, E) Vanillin + Maleic Anhydride, F) Aniline + Phthalic Anhydride, and G) Triethylene Glycol + Maleic Anhydride.	256
C.10	LC-MS peak area signals obtained from increasing fractions of water in acetonitrile after the 24 hour and 1 week-long analysis period for A) Phthalic Anhydride Vanillin Product (PVP), B) Maleic Anhydride Levoglucosan Product (MLP), C) Phthalic Anhydride Anisyl Alcohol Product (PAP), D) Maleic Anhydride Anisyl Alcohol Product (MAP).	257

Abbreviations

ACN Acetonitrile.

AMS Aerosol mass spectrometer.

APS Aerodynamic particle sizer.

BBE Biomass burning emissions.

BBOA Biomass burning organic aerosol.

BC Black carbon.

BPC Base peak chromatogram.

BrC Brown carbon.

CAD Canadian cow dung.

CCN Cloud condensation nuclei.

CPC Condensation particle counter.

DBE Double bond equivalent.

DMA Differential mobility analyzer.

EC Elemental carbon.

EI Electron impact.

ELVOC Extreme low volatility organic compounds.

ESI- Negative electrospray ionization.

ESI+ Positive electrospray ionization.

FID Flame ionization detector.

GC Gas chromatography.

GCxGC Two-dimensional gas chromatography.

IND Indian cow dung.

LC Liquid chromatography.

LVOC Low-volatile organic compound.

m/z Mass to charge.

MAC Mass absorption coefficient.

MFC Mass flow controller.

MS Mass spectrometry.

NMR Nuclear magnetic resonance.

NPOC Non-purgeable organic carbon.

OA Organic aerosol.

OC Organic carbon.

OOA Oxidized organic aerosol.

PAH Polycyclic aromatic hydrocarbons.

PC Principal component.

PCA Principal component analysis.

PM₁ Particulate matter below 1 μm in diameter.

PM_{2.5} Particulate matter below 2.5 μm in diameter.

PTR Proton transfer reaction.

RH Relative humidity.

SMPS Scanning mobility particle sizer.

SOA Secondary organic aerosol.

SVOC Semi-volatile organic compound.

TD Thermal desorption.

TIC Total ion chromatogram.

TN Total nitrogen.

TOC Total organic carbon.

ToF Time of flight.

tR Retention time.

VOC Volatile organic compound.

Chapter 1

Introduction

Contributions: The introduction was written by Max Loebel Roson with review and feedback by Dr. Ran Zhao.

1.1 What is biomass burning

Arguably, control of fire represents one of the earliest inventions of the human race [3]. As a result, we have been exposed to its emissions for the better part of a million years [3, 4]. Considering the Stone Age was a very long time ago, it is surprising we still do not fully understand the emissions of certain fuels. In particular, biomass has been the predominant fire-making combustible since prehistory [3, 4], and still remains the main source of energy for cooking and heating in many developing countries [5, 6]. For example, in 2016, 50% of households in India relied on biomass for cooking and heating; in Sub-Saharan Africa, this number reached 86%, as can be seen in Figure 1.1 [6]. Globally, up to 3 billion people are estimated to still be dependent on biomass for cooking and heating [5]. As a source of energy, biomass supplies more than 10% of the global energy demand [7]. Within this context, biomass is an umbrella term for the diverse types of biological materials used to fuel a fire, such as wood, animal dung, grass, hay, and crop residue [8].

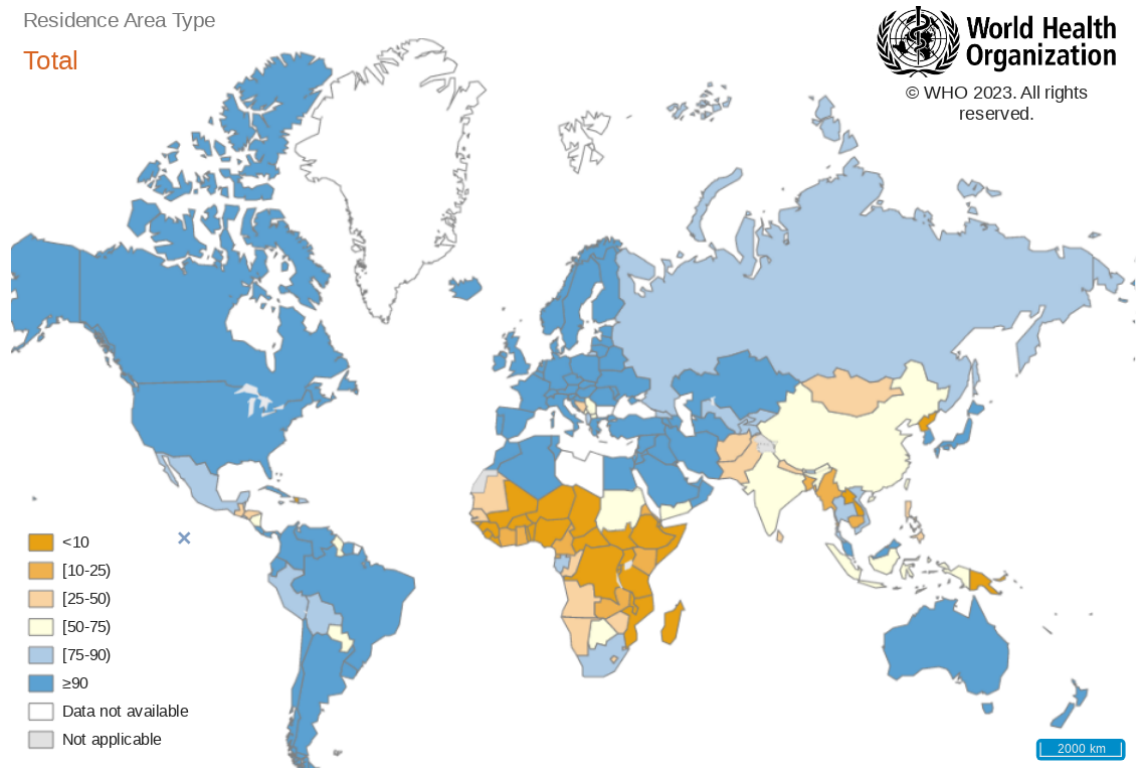


Figure 1.1: Proportion of the population with primary reliance on clean fuels and technology for cooking in 2016 (%). Figure obtained (with adapted caption) from: (WHO) “Global Household Energy Database,” *World Health Organization*, 2023 [6]

1.1.1 On particulate matter

When burned, biomass releases - in addition to many gas-phase molecules - harmful particulate matter into the surrounding air [9]. The term particulate matter describes both liquid droplets and solid particles, usually emitted into the atmosphere as suspended aerosol [10]. When breathed in, fine particulate matter can cause a variety of respiratory and cardiovascular disorders leading to premature mortality [11–13]. The size of the particle dictates where it is most likely to be deposited in the human body when breathed in, with particles above $6.7 \mu\text{m}$ not reaching the thorax (remaining trapped in the nose or throat), and particles below $0.8 \mu\text{m}$ passing all the way through to the alveoli [14]. Specifically, particulate matter with a diameter below the size of 1 or $2.5 \mu\text{m}$ (PM_1 and $\text{PM}_{2.5}$ respectively) is associated with adverse health outcomes [11, 15, 16]. Particles below these sizes can penetrate deep into the lungs, becoming trapped or transferred into the bloodstream from there [11]. Evidence of particulate matter exposure has even been found in Egyptian mummies, in the form of soot deposits in the lungs [17]. Despite its significant health impacts, increased mortality associated specifically with exposure to PM_1 and $\text{PM}_{2.5}$ has only been widely reported in the past 30 years [12, 15, 18].

Mostly emitted through anthropogenic air pollution, $\text{PM}_{2.5}$ is recognized by the World Health Organization (WHO), the European Environmental Agency (EEA), as well as the Environmental Protection Agency (EPA) as strongly air quality affecting [19–21]. By mass, it is believed that up to 90% of PM_1 may be comprised of organic aerosol (OA) particles, and up to 90% of global combustion OA may come from biomass burning [9, 22–24]. To make matters worse, carbonaceous particulate matter emitted from combustion has a significant surface area to size ratio [25], which promotes the adsorption of other chemical species [26–28]. Using particulate matter as a vector, adsorbed or absorbed compounds can be transferred into the human body, with unpredictable health effects [29]. A 2012 global health risk assessment by Lim *et al.* identified household air pollution from solid fuels as one of the three leading health risk factors worldwide (third for males and second for females) leading to premature death [11]. Thankfully, this risk has been mitigated over time, as the use of biomass has become less prevalent worldwide [16]. Still, with the rising incidence and sever-

ity of open biomass burning in recent years [30, 31](such as wildfires, as exemplified by Figure 1.2), the worldwide climate and health effects of biomass burning remain considerable [32].



Figure 1.2: Emissions during the May 15th 2023 Alberta wildfires, captured by a National Aeronautics Space Administration (NASA) satellite. The red dots represent temperature anomalies, i.e. the origin of the emissions as a result of the fires. Image (with adapted caption) obtained from NASA Worldview. 2023 [33].

From a climate perspective, biomass burning emissions (BBE) affect the balance of heating and cooling effects on the Earth (radiative budget) [9, 34–37]. The heating effect of greenhouse gases such as carbon dioxide (CO_2) and methane (CH_4) has been widely reported, and has been the zeitgeist of the conversation on climate change since the late 1980s [34, 38]. However, the effects of biomass burning aerosol in the atmosphere are more intricate. In addition to affecting local and regional visibility, biomass burning aerosol can have both heating (by trapping light or inhibiting the formation of light-scattering clouds) or cooling (by scattering light themselves or promoting cloud formation) effects depending on their physical and chemical properties [32, 39, 40]. To date, there is still considerable uncertainty in the effects of certain biomass burning aerosol, such as black and brown carbon (BC and BrC respectively). BC is categorized as elemental carbon (EC) (soot or graphite-like), while BrC is classified as organic carbon (OC) and is a major fraction of biomass burning organic aerosol (BBOA) [32, 41–44]. Aside from emitted greenhouse gases, BC and BrC are

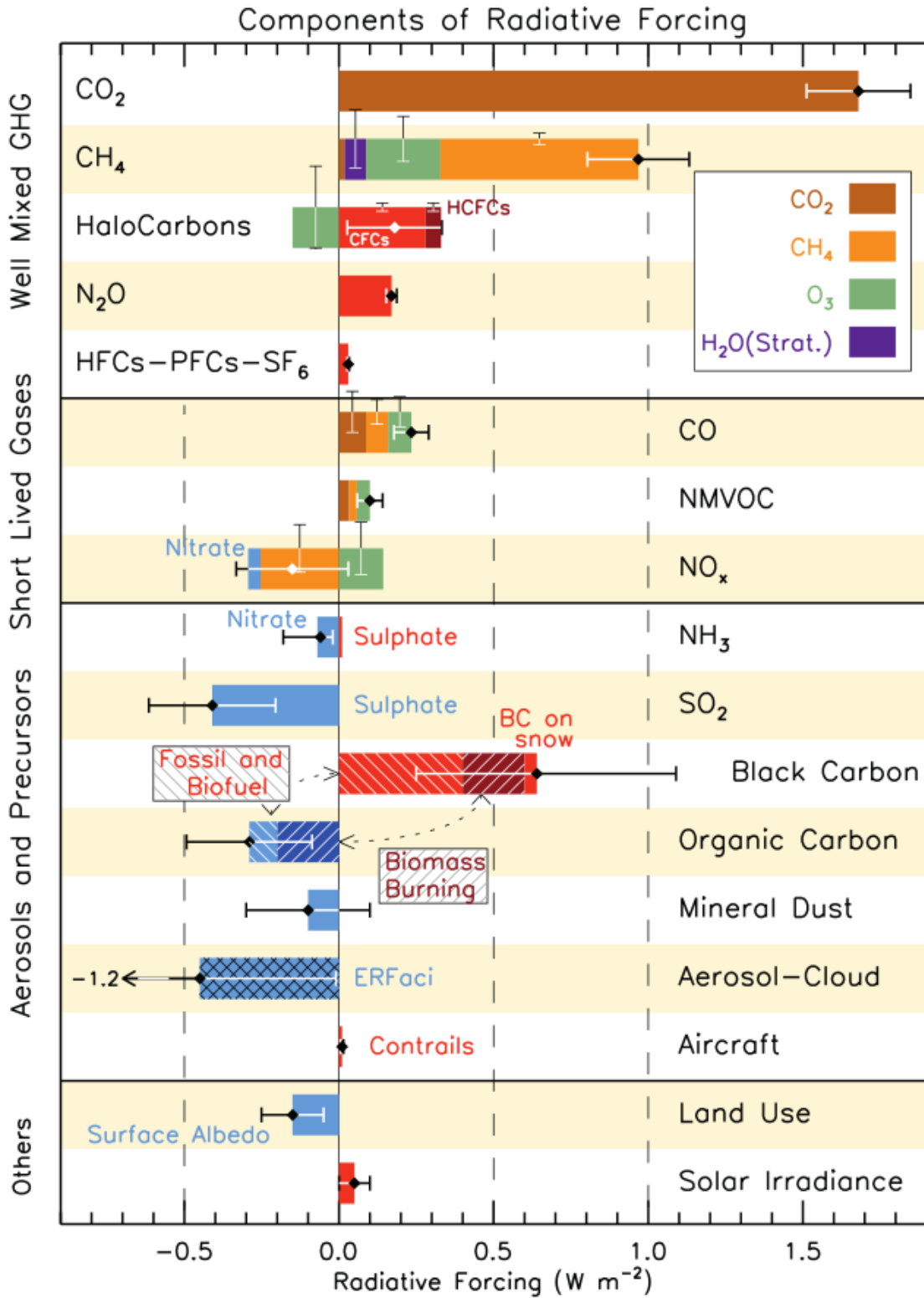
estimated to be the two strongest climate-affecting components of BBE [32, 34–37].

1.1.1.1 Black carbon

BC are carbonaceous fine particles emitted from the incomplete combustion of biomass and fossil fuels [44, 45]. BC is the most effective light-absorbing combustion aerosol in the atmosphere, leading directly to atmospheric warming [32, 36, 44]. By absorbing light, BC can enhance evaporation mechanisms in clouds and contribute to the melting of ice and snow [32, 46]. Additionally, as a fraction of $\text{PM}_{2.5}$, BC can also have significant health impacts after being breathed in [45]. For instance, the Great London Smog of 1952, which hospitalized over 150,000 people in less than a week, had a large BC component as part of soot emissions from coal burning [47]. This incident caused a surge in health and air-quality related science, which, as climate change became more apparent, transitioned into a meticulous investigation on the warming and cooling effects of BC. As a result, while the uncertainty associated with the climate-forcing effect of BC has shrunk considerably over the past 40 years, it still remains considerable, as shown in Figure 1.3 [32, 34, 35, 38, 43].

1.1.1.2 Brown carbon

BrC is a more recent discovery, it is a carbonaceous aerosol component of BBOA comprised of visible and ultraviolet light-absorbing organic particulates [32, 43, 44, 48]. BrC absorbs light in the ultraviolet and near-visible spectrum more strongly than BC, giving biomass burning smoke plumes their characteristic brown colour and BrC its moniker [43, 44, 48, 49]. While biomass burning is the largest source of BrC emitted into the atmosphere, BrC emission factors are highly uncertain as most studies report $\text{PM}_{2.5}$ [43]. Modelling studies have estimated that BrC may constitute 80% of all OC in areas which rely heavily on biomass burning (such as South Africa), this number is estimated to be much lower (between 20-40%) in North America and Western Europe [50]. Although a smaller source, secondary BrC may also form through photo-oxidation of both anthropogenic and biogenic VOC in the gas-phase [51, 52], photochemical processing in clouds [53], and heterogeneous night-time reactions with NO_3 and N_2O_5 [54].



Original caption available on the subsequent page.

Figure 1.3: RF bar chart for the period 1750–2011 based on emitted compounds (gases, aerosols or aerosol precursors) or other changes. Numerical values and their uncertainties are shown in the Supplementary Material Tables 8.SM.6 and 8.SM.7. Note that a certain part of CH_4 attribution is not straightforward and discussed further in Section 8.3.3. Red (positive RF) and blue (negative forcing) are used for emitted components which affect few forcing agents, whereas for emitted components affecting many compounds several colours are used as indicated in the inset at the upper part the figure. The vertical bars indicate the relative uncertainty of the RF induced by each component. Their length is proportional to the thickness of the bar, that is, the full length is equal to the bar thickness for a $\pm 50\%$ uncertainty. The net impact of the individual contributions is shown by a diamond symbol and its uncertainty (5 to 95% confidence range) is given by the horizontal error bar. ERFaci is ERF due to aerosol–cloud interaction. BC and OC are co-emitted, especially for biomass burning emissions (given as Biomass Burning in the figure) and to a large extent also for fossil and biofuel emissions (given as Fossil and Biofuel in the figure where biofuel refers to solid biomass fuels). SOA have not been included because the formation depends on a variety of factors not currently sufficiently quantified. Figure and caption reprinted with permission from: IPCC. “Climate Change 2013 – The Physical Science Basis: Working Group I Contribution to the Fifth Assessment Report of the Intergovernmental Panel on Climate Change”, ch. 8, pp. 698, 2014, Figure 8.17 [34]. Copyright Cambridge University Press

While BC is properly considered in most global climate forcing models and calculations [41, 42], BrC is still referred to as a purely scattering aerosol [36, 41, 55]. Currently, BrC is one of the main source of uncertainty in predicting the climate effects of biomass burning [48, 50]. Similarly to BC, emission of BrC is promoted by inefficient burning conditions, such as insufficient temperature or airflow, which are typical of household stoves [45, 56, 57]. In fact, the temperatures which promote the emission of BrC are even lower than BC [48]. Unsurprisingly, the impacts of BBE are felt more heavily in areas where biomass remains the main source of energy for heating and cooking [5, 56].

1.1.2 On volatile organic compounds

Aside from particulate matter, BC, and BrC, biomass burning also releases a variety of volatile organic compounds (VOC), intermediate-volatile organic compounds (IVOC), and some semi-volatile organic compounds (SVOC) as vapours [32, 43, 58]. VOC are a large group of carbon-containing species characterized by their high vapour

pressure, which causes them to readily evaporate [59, 60]. During biomass combustion, the cracking of larger molecules promotes the formation of VOC, IVOC, and SVOC, while the high temperatures enhance their evaporation and release [61]. The volatility of VOC, IVOC, and SVOC is experimentally distinguished by their saturation concentrations (usually measured using a thermodenuder), a broad classification is listed in Figure 1.4 [58].

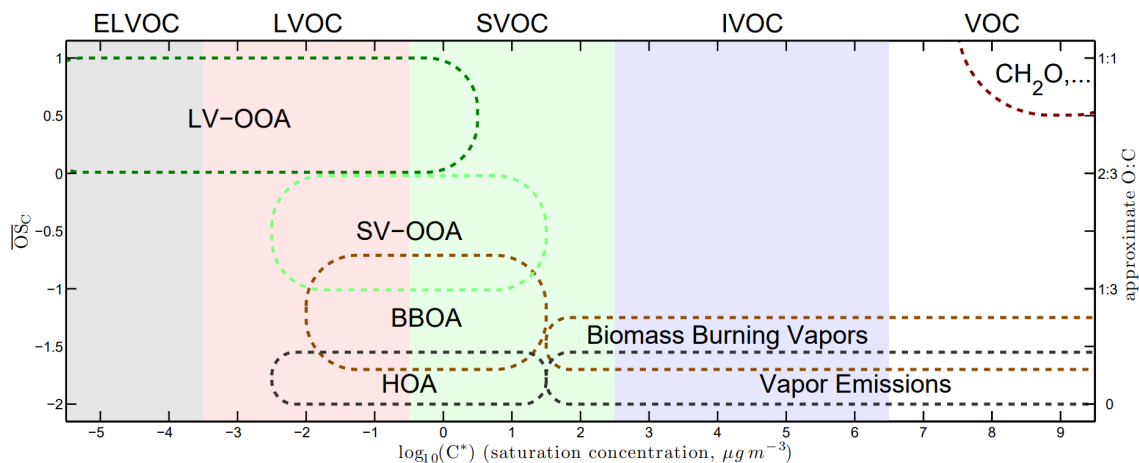


Figure 1.4: Volatility, oxidation state, and approximate oxygen to carbon ratio for important organic aerosol (OA) and vapours. The shaded areas represent the classification of each OA. Oxidized organic aerosol (OOA) are split into low volatility (LV) and semi-volatile (SV) fractions. The HOA fraction represents hydrocarbon-like organic aerosol. Figure reprinted under Creative Commons Attribution (CC BY 3.0) from: Donahue *et al.* “A two-dimensional volatility basis set – part 2: Diagnostics of organic-aerosol evolution,” *Atmospheric Chemistry and Physics*, vol. 12, no. 2, pp. 615–634, 2012 [58]

Compounds with an even lower volatility than SVOC can be classified as low volatility organic compounds (LVOC), and further as extremely low volatility organic compounds (ELVOC) [43, 58]. As can be seen in Figure 1.4 the majority of BBOA (including most BrC) have a volatility somewhere between SVOC and LVOC [58]. However, the burning of fuels such as Boreal peatlands - when smouldering, in particular - can release ELVOC in the form of highly absorptive BrC containing “tar balls” and humic like substances [43, 48, 62]. The evaporative tendencies of VOC cause them to readily move into the atmosphere, where they may impact climate and health [32]. These impacts are quite distinct from those of particulate matter. From a health perspective, both VOC and their oxidation products cause a variety of tox-

icological effect, including skin, eye and throat irritation, neuro- and hemo-toxicity, as well as carcinogenicity [63–65].

With regards to the climate, among the variety of reactions VOC can undergo once emitted [59, 66, 67], the formation of organic peroxy-radicals (RO_2) through hydroxyl radical (OH) oxidation is particularly significant [59]. Following its formation, RO_2 can react with nitric oxide (NO) to form nitrogen dioxide (NO_2), which when exposed to sunlight will in turn produce climate and health affecting ozone (O_3) [10, 59]. Unfortunately, since both VOC and NO_2 are common anthropogenic emissions from urban centers, O_3 generated following their interaction is - due to its position - pre-disposed to affect human health [59, 68]. This is one of the reasons why photochemical smog is largely bound to polluted cities [59], and why the skies above urban centers can adopt a brownish haze in the mornings when sunlight begins photolyzing the reservoir of NO_2 accumulated in the atmosphere during the previous night [68]. VOC are also generated biogenically from vegetation [23, 69]. Globally, the mass of emitted biogenic VOC is much larger than that of anthropogenic sources [23]. Similarly to anthropogenic VOC, biogenic VOC also contribute to cloud formation by acting as cloud condensation nuclei (CCN), with a net cooling effect on the atmosphere [69]. VOC are the largest precursors to secondary organic aerosol (SOA) formation in the atmosphere [23, 32]. As opposed to their VOC precursors, the impacts of SOA in the atmosphere are more similar to those of the aforementioned particulate matter (i.e. highly variable, with a net cooling or heating effect depending on their chemical makeup) [32]. Since the impacts of SOA are highly composition dependent, the processes that lead to their formation and transformation in the atmosphere are directly responsible for their climate burden [23]. Hence, tracking the evolution of VOC and SOA in the atmosphere is crucial towards predicting their effects.

1.2 Evolution of biomass burning emissions

Once in the atmosphere, BBE continuously undergo physical and chemical changes from light, temperature, and transport through the highly oxygenated environment [70, 71]. These changes can be broadly split into physical (where the emission state, phase, or position in the atmosphere changes without affecting its molecular compo-

sition), or chemical (where the emissions themselves or the species they interact with undergo chemical modification) [70, 71]. Fittingly, changes continue until emissions are either physically removed from the atmosphere (through wet or dry deposition, for example), or are sufficiently transformed (aged) into highly volatile oxidised products such as formaldehyde (HCHO), CO, or CO₂ through photochemical degradation [58, 72]. Ordinarily, atmospheric aging will migrate emissions to the top right corner of Figure 1.4 over time [58].

1.2.1 Physical changes

1.2.1.1 Transport

Like any other pollutant, BBE are transported by air currents - due to wind patterns or temperature gradients - through the atmosphere after emission [73, 74]. This transport can be horizontal through advection, vertical through convection, or both horizontal and vertical through turbulent dispersion [74–77]. As a consequence of atmospheric transport, emissions are diffused and exposed to a variety of atmospheric conditions, such as changes in temperature and humidity [75, 77]. In particular, vertical transport is associated with more drastic changes in temperature which may alter the phase of the emissions [75, 77, 78]. Transport can occur over long distances (even intercontinentally [13, 79]), depending on the atmospheric residence-time of the emission in question and air current velocity [75]. As a result, the lifetime of a compound in the atmosphere strongly hinges on its resistivity to various removal and aging processes, which are detailed in the following sections.

1.2.1.2 Dry Deposition

As particulate matter and gases move through the atmosphere, they may come into contact with and settle on physical barriers such as vegetation, soil, or man-made structures. When this process does not involve water, it is referred to as dry deposition [80]. Large and heavy particulate matter is especially prone to atmospheric removal through dry deposition [81, 82], particularly so in areas with heavy vegetation or man-made structures, where the surface area available for contact is greater [80]. Conversely, fine particulate matter (with more detrimental health effects [11]), remains in the atmosphere longer than the larger coarse fraction [81].

Dry deposition can cause the accumulation of pollutants on surfaces, with subsequent deleterious effects. For example, toxic heavy metals such as cadmium can accumulate in soil through deposition, be absorbed by crop, and eventually affect the health of those who consume them [83]. Particulate matter deposited on vegetation may affect photosynthesis efficiency [84]. If accumulated on buildings, particulate matter can be re-suspended with changes in wind speed or humidity, affecting air quality long after deposition [85].

1.2.1.3 Wet Deposition

Atmospheric pollutants can also be removed through wet deposition when they come into contact with water in the form of water vapour, precipitation, fog, or clouds [86, 87]. While dry deposition is mostly effective at removing particulate matter, wet deposition can efficiently eliminate both gases and particulate matter, and is therefore the main removal pathway for most aerosol species [82, 88]. The Earth’s atmosphere is comprised of almost 0 to 4% water by volume, depending on atmospheric conditions [89]. For this reason, the occurrence and effectiveness of wet deposition is highly location dependent [90].

Figure 1.5 depicts the major sources, processes, and sinks which can affect OC aerosol in the atmosphere [91]. Clouds are the largest reservoirs of water in the atmosphere, they capture emissions through nucleation or impaction scavenging [86–89]. Atmospheric water dissolves gases such as sulphur dioxide (SO_2) and nitrogen oxide species (NO_x) which after conversion to sulphuric and nitric acid (H_2SO_4 and HNO_3 respectively), can acidify soil or damage infrastructure through precipitation [86, 87]. Water vapour can also condense on particulate matter, promoting the formation of clouds which affect the Earth’s radiative budget [88]. Simultaneously, particles may become larger and less aerodynamic after water condenses on their surface, increasing the likelihood of them being removed through collision and deposition [81, 88]. Similarly, removal of particles through transfer to cloud droplets (rainout) affects mostly large particles [82, 88]. Most atmospheric OC is removed from the atmosphere through deposition. Of this removal, $\sim 60\%$ is expected to occur through wet versus 40% through dry deposition [72, 75]. In precipitation, the vast majority ($>75\%$) of carbon has been found to be organic [92].

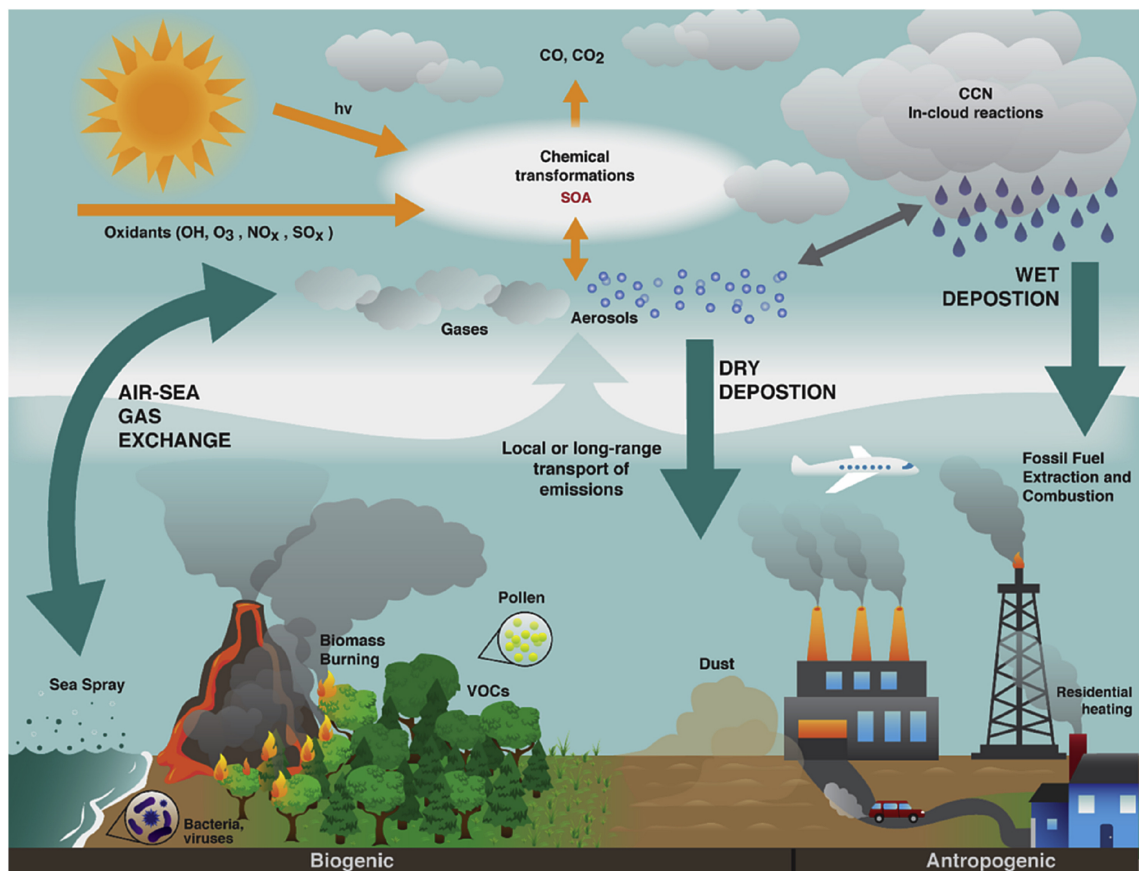


Figure 1.5: Major sources and processes affecting the amount and quality of organic carbon found in wet deposition. SOA refers to secondary organic aerosol, CCN are cloud condensation nuclei, VOCs are volatile organic compounds, CO is carbon monoxide gas, and CO₂ is carbon dioxide gas. Figure reprinted under Creative Commons Attribution (CC BY-NC-ND 4.0) from: Iavorivska *et al.* “Atmospheric deposition of organic carbon via precipitation,” *Atmospheric Environment*, vol. 146, pp. 153–163, 2016 [91]

Wet deposition efficiency is dependent on the chemical properties of the compound being removed [36, 91]. For instance, most BC (~80%) is emitted as hydrophobic BC and is only converted to hydrophilic BC once aged in the atmosphere [36, 93, 94]. While hydrophobic BC can be removed through wet deposition, the change in total aerosol mass is negligible compared to when hydrophilic BC experiences analogous collisions with atmospheric water [36, 88]. Similarly, VOC and other gas-phase molecules are more likely to be removed through wet deposition if they have a high Henry’s law coefficient (higher solubility in the water) [72, 82]. Therefore,

understanding the composition of pollutants is essential towards predicting by which mechanisms they are removed from the atmosphere.

1.2.1.4 Partitioning - evaporation and condensation

Partitioning typically refers to how pollutants are distributed between environmental compartments [95]. This includes both large-scale systems, such as how molecules are dispersed in air, water, and soil, as well as smaller ones, such as how gases are distributed between the surface or bulk of single particles [95, 96]. Water-soluble compounds will tend to partition into the aqueous-phase, while highly volatile species will usually partition to the gas-phase [58, 72, 82, 97, 98]. The two most significant mechanisms driving partitioning in the atmosphere are evaporation and condensation [89].

Evaporation involves the transfer from a solid or liquid surface to the gas-phase. The rate of this transfer is highly dependent on atmospheric conditions such as wind speed and temperature [89]. Additionally, different chemical species will also evaporate at distinct rates according to their vapour pressures, which are dependent on their physical and chemical properties [99]. This means that by monitoring key atmospheric conditions, the distribution of chemical species in the environment can be predicted [99]. For example, pollutants removed from the atmosphere through wet deposition may re-evaporate if local temperatures rise, and in turn impact air-quality anew [100]. From a climate perspective, evaporation inhibits the formation of clouds from CCN [101], indirectly heating the Earth's surface [32]. This is a pressing environmental concern, as our current understanding indicates that with rising temperatures cloud cover will continue thinning [32].

Condensation is the reverse process to evaporation, it refers to the formation of a liquid-phase from a gas-phase. It is the major pathway for the formation of clouds, fog, and precipitation, as water vapour condenses into the liquid-phase [89]. Unsurprisingly, condensation is similarly affected by temperature, wind speed, and other atmospheric conditions [89]. Condensation is enhanced in the presence of a surface or particle, and is why CCN are a prerequisite for the formation of clouds in most circumstances [102]. Aerosol can become activated as CCN at supersaturation relative humidity (RH), with the degree of hygroscopicity of the aerosol minimizing the

RH required for activation [103]. On the other hand, hydrophobic aerosol such as graphitized soot particles resist the addition of water, and may act as CCN only (if at all) at an even greater degree of supersaturation [104]. While condensation to form clouds has a net positive cooling effect considering the current climate crisis [32], it can also contribute to the formation of SOA [105]. For example, particulate matter emitted from biomass burning contains a wide variety of reactive organic species. When water, VOC, IVOC, or SVOC condense on the particle surface, they may alter the composition and partitioning of the emission matrix [97, 106]. These compositional changes often involve the formation and release of climate affecting SOA [106, 107].

Condensation is more common for VOCs with lower vapour pressures. For this reason, biomass burning emitted compounds such as light-absorbing polycyclic aromatic hydrocarbons (PAHs) are more likely to be found in the particle-phase following a temperature drop [108, 109]. Condensation of VOCs affects the composition of particulate matter, which may enhance their light-absorbing capabilities (in the case of PAHs for example) [110], or their capacity to act as CCN [111]. Additionally, condensation of compounds on the surface of particles can provide novel reaction partners to bulk-phase species, which may form SOA [106]. For instance, condensation of carboxylic acids can decrease the pH of the bulk particle-phase [112], which may catalyze the hydrolysis reaction of anhydrides emitted from biomass burning [2].

1.2.1.5 Phase changes

As emissions move through the atmosphere, variations in temperature and pressure may also cause phase changes without condensation and evaporation induced partitioning [113]. The phase of aerosol has significant effects on their reactivity in the atmosphere as well as their capacity to act as CCN, largely due to changes in viscosity [113–115]. Viscosity increases with descending temperature and humidity, hindering the diffusion of particles in the surrounding gas, heterogeneous reactions, as well as the uptake of gases to the particle [113, 116]. These changes are not linear however, as for example, phase-changes from liquid to solid (or more specifically, from a liquid to a glassy-solid) can drastically increase and plateau the viscosity of a particle [117]. This indicates that there might be low “breakthrough” temperatures intrinsic to each

compound which renders them less susceptible to degradation in the atmosphere. Since disparate species will solidify at different temperatures according to their physical and chemical properties, a given compound's breakthrough temperature might not be attainable in the environment. Considering the composition, temperature, humidity, and therefore the phase of a pollutant is essential to accurately track its fate in the atmosphere.

However, the composition of particulate matter emitted from biomass burning can not be simplified to a single type of compound. To complicate matters further, the various compounds which comprise a particle will partition themselves along concentration gradients on, in, and out of that particle over time [118]. Hence, if conditions vary enough for only some compounds in the bulk-phase to change into a solid state, formation of a solid coating may shield the remaining species closer to the core of the particle (irrespective of their phase) from degradation. Specifically, the formation of a protective glassy phase at low temperatures may be why pollutants are capable of reaching remote regions such as the Antarctic before being processed by atmospheric oxidants [77, 78]. Alternatively, changes in RH may also cause phase-separation in organic and mixed inorganic-organic aerosol [115, 116]. Phase-separation has unpredictable effects, it has been shown to form a protective coating which hinders uptake and the formation of SOA [116], and to drastically enhance hygroscopic growth and CCN properties for liquid-liquid phases [115].

Accordingly, particles may be thought of as containing various layers of fluid compositions and phases, sometimes around a solid core, which continuously partition and equilibrate between each other and the surrounding environment, as can be seen in Figure 1.6 [118]. And consequently, comprehensive investigations of particle composition become indispensable for atmospheric lifetime predictions.

1.2.2 Chemical changes

1.2.2.1 Photochemistry - direct photolysis and photooxidation

Photochemistry drives a wide variety of reactions in the atmosphere, it plays a crucial role in climate change, the lifetime of pollutants, and air quality [23, 106, 119]. Of the atmospheric photochemical processes, photolysis is responsible for the even-

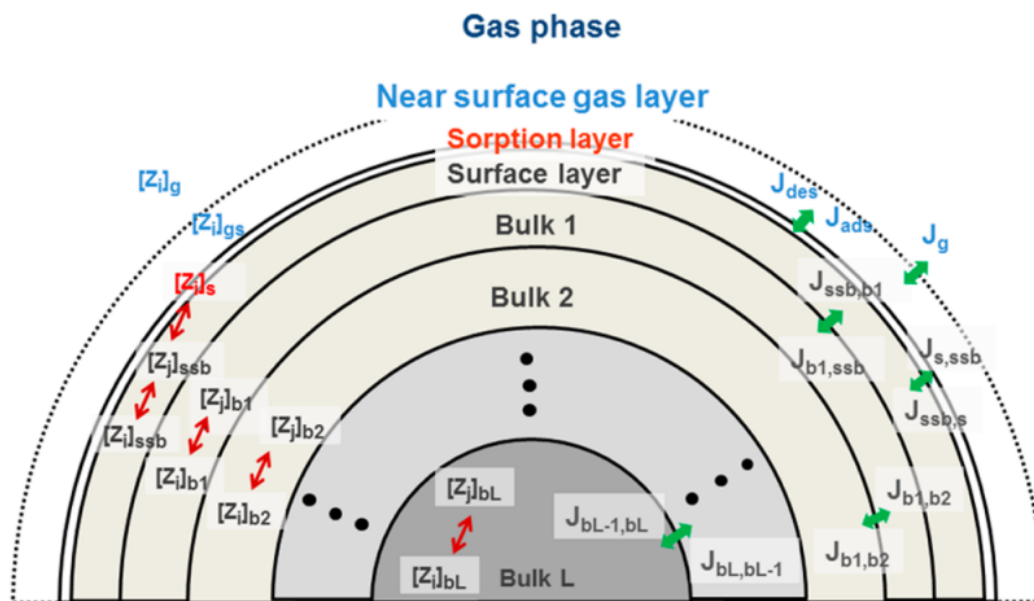


Figure 1.6: Schematics of the kinetic multilayer model of gas-particle interactions in aerosols and clouds (KM-GAP). Concentrations of species Z_i and Z_j in the gas (g) and near-surface gas-phase, at the sorption layer (s) and in the surface (ssb) and in the bulk (b) layers. J are the transport fluxes between each layer, including the gas-phase diffusion flux (J_g), the adsorption (J_{ads}) and desorption (J_{des}) fluxes, surface-bulk exchange fluxes ($J_{s,ssb}$, $J_{ssb,s}$), and bulk diffusion fluxes (J_b). Figure reprinted with permission from: Arangio *et al.* “Multiphase Chemical Kinetics of OH Radical Uptake by Molecular Organic Markers of Biomass Burning Aerosols: Humidity and Temperature Dependence, Surface Reaction, and Bulk Diffusion,” *J. Phys. Chem. A*, vol. 119, pp. 4533-4544, 2015 [118]. Copyright 2023 American Chemical Society

tual breakdown of pollutants into smaller fragments [23, 106]. Photolysis contributes directly to the removal of pollutants from the atmosphere, as well as the indirect formation of SOA by generating reactive precursors [23, 106]. For example, stratospheric photo-dissociation of diatomic oxygen is a fundamental step in the formation of O_3 [119]. On the other hand, tropospheric O_3 can be photolyzed to form highly reactive OH, which initiates the oxidation of a variety of VOC, this reaction is termed photooxidation [120].

Photooxidation involves the reaction of trace gases with reactive oxygen species (ROS) such as OH, O_3 , and NO_3 generated by the action of solar radiation, often forming SOA [23, 106, 120]. The reactions between trace gases and ROS may also generate reactive intermediate RO_2 species, which also react with atmospheric pollutants to form SOA [106]. For example, OH formed through photolysis can oxidize CH_4 into

methyl radicals. In turn, methyl radicals can react with O_2 to form the lachrymator formaldehyde (HCHO) [121]. This reaction is one of main mechanisms regulating the concentration of CH_4 in the atmosphere [32, 121], the greenhouse gas with the highest net positive impact on radiative forcing after CO_2 [32]. While it could be presumed that reducing the amount of CH_4 in the atmosphere would only have a cooling effect, the reality of the atmospheric environment is more complex. HCHO formed during the photooxidation of CH_4 is an intermediate product in the photochemical formation of a variety of SOA, with unpredictable climate and health effects. In fact, there is evidence that HCHO contributes to the formation of NO_x components [122] responsible for photochemical smog [32]. These reactions are only one example of the complex inter-connected processes which regulate the fate and impacts of pollutants in the atmospheric environment. They reinforce the need for comprehensive investigations on pollutant interactions both individually, and as a system. Even now, the mechanisms that lead to the formation of SOA are not fully understood [106].

BBE are also photochemically aged in the atmosphere, greatly increasing the chemical complexity of the emission matrix and forming climate and health affecting SOA [43, 48]. Particularly, the identification and quantification of compounds present on the surface of biomass burning aerosol is necessary to understand how it behaves in the atmosphere [43, 123]. For example, some of the species in biomass burning emissions, such as potassium, can form hygroscopic salts during atmospheric aging that may cause physical changes in individual biomass burning particles, altering their light scattering and cloud forming capabilities [55]. Alternatively, photobleaching driven by light-induced aging can irreversibly inhibit BBOA's capacity to absorb light [124]. For instance, as can be seen in Figure 1.7, Fleming *et al.* have reported that the light-absorptive species (chromophores) in a wood BBOA sample are universally photobleached under short wavelength UV light exposure for 6 hours [124].

Another example is sinapaldehyde, a breakdown product of the molecular tracer lignin (tracers are expanded on in Section 1.5.3.1) [124, 125]. Sinapaldehyde is one of the species with major abundance in fresh (un-aged) wood BBOA [125], and one of the most light absorptive components of BrC [124]. However, sinapaldehyde is also one of the biomass burning emitted compounds found to decay the most rapidly under photo-oxidative conditions [125]. This is just one example illustrating the

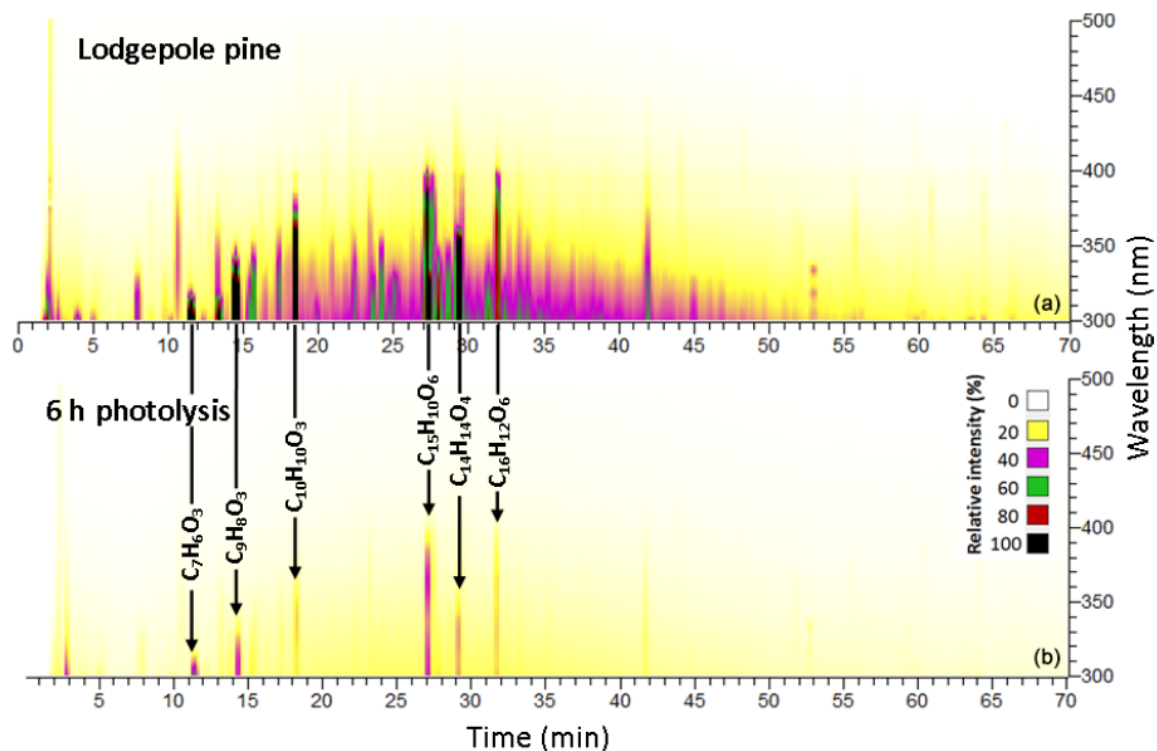


Figure 1.7: BrC chromophores present in the BBOA sample before (a) and after (b) 300 nm irradiation for a conifer fuel: lodgepole pine. Figure reprinted under Creative Commons Attribution (CC BY 4.0) from: Fleming *et al.* “Molecular composition and photochemical lifetimes of brown carbon chromophores in biomass burning organic aerosol,” *Atmos. Chem. and Phys.*, vol. 20, pp. 1105-1129, 2020 [124]

need for emission readings to be contextualized with where, how, and when they were studied. While sinapaldehyde may be a useful tool to associate plant matter derived OA to a particular burn incident, it is only effective if the characterization is performed before the emissions are aged. On the other hand, other biomass burning tracers such as syringaldehyde, guaiacol, or vanillin, exhibit an upwards trends in abundance 1-3 days after being emitted and photochemically aged. In fact, as found by Fortenberry *et al.*, their abundance only proceeds downwards after 6-10 days of aging, affording them a much longer atmospheric lifetime [125]. In any case, this further demonstrates the high amount of variation photochemical processes bestow on specific BBOA degradation products, and how vital knowing the degree of BBE aging is for characterization and impact prediction.

1.2.2.2 Nucleophilic addition

Nucleophilic additions are a broad class of non-photochemical reactions with atmospheric significance. Nucleophiles are molecules or atoms which react with positively charged nuclei (such as electrophiles), providing an electron pair during the reaction [126]. As the name implies, a nucleophilic addition reaction involves the addition of a nucleophile to an electrophilic center, forming a covalent bond between them and occasionally causing the loss of a leaving group [126]. Nucleophilic additions are commonly used in organic chemistry to synthesize carbon-carbon bonds, amines, and convert carbonyl groups into various other functional groups [126–128]. Perhaps the most famous nucleophilic addition is the Nobel prize winning Grignard reaction [129]. Carbonyls are common electrophiles in the atmosphere [130]. By reacting with nucleophiles, carbonyls will form higher molecular mass compounds such as geminal diols [131]. A similar reaction may also occur when nucleophiles react with electrophilic aldehydes to form diols [126, 131], or with organic nitrates to form carboxylic acids [132, 133]. These higher molecular mass compounds are more likely to partition into the condensed-phase, impacting SOA formation [43, 77]. In particular, formation of carboxylic acids is atmospherically significant as it contributes to the acidification of aerosol [134, 135], which in turn influences their cloud forming properties and their deposition rate [91, 104, 136]. Carboxylic acids are especially prone to acidifying aerosol as they tend to condense on the surface of particles more readily than their precursors [104, 106, 112, 136]. Nevertheless, there are other atmospheric electrophiles which have not been previously studied from this point of view. For instance, acid anhydrides have electrophilic properties and are evolved in large quantities as primary and secondary emissions from biomass burning [137, 138]. Through hydrolysis, acid anhydrides also form climate-affecting carboxylic acids [2, 139, 140]. Usually, water takes on the role of the nucleophile both here and in the examples given above. However, other compounds with lone-pair electrons can act as nucleophiles and may be significant in water-deficient environments [2, 130]. As a matter of fact, BBE contain numerous nucleophiles in the condensed-phase [1, 141], which are capable of reacting with acid anhydrides [2]. Still, the mechanism by which vapour-phase acid anhydrides would interact with the less volatile bulk-phase nucleophiles present in

BBE is unexplained.

1.2.2.3 Heterogeneous reactions and uptake

Heterogeneous reactions occur at the interface between two phases. In the context of BBE, this is typically between particulate matter - one of the only substrates available for reaction in the atmosphere - and the surrounding gas-phase [142]. As discussed previously, O_3 , OH, and NO_3 are significant reactive oxidants and one of the main sources of atmospheric degradation [106]. However, to react with particle-bound organic compounds, species like O_3 must either interact directly with the surface of particulate matter, or be heterogeneously uptaken on its surface or into its bulk-phase [26].

Uptake is the mechanism by which a molecule or particle becomes trapped on a substrate after colliding with it. The probability of capture occurring after a collision is described as the uptake coefficient (γ) [26]. γ can be experimentally derived by measuring relative concentration of a molecule before and after moving over an absorptive medium, typically a coated wall flow tube or Knudsen cell [26]. The uptake mechanism can be physical, driven by partitioning, or reactive, where the molecule being uptaken chemically reacts with the substrate [26, 28, 143]. As the name implies, reactive uptake is common for highly reactive gas-phase radicals such as OH [26]. On the other hand, carbonaceous particulate matter such as those emitted from biomass burning will promote physical uptake due to their large surface area [25]. In either case, a molecule or particle must come into direct contact with a surface for uptake into that surface to occur [26]. Therefore, differentiating between physical and reactive uptake is challenging, as experimentally both types of uptake lead to a reduction in signal.

The impacts and efficiency of uptake are highly dependent on the physical and chemical properties of both the molecule being uptaken and the adsorbing or absorbing substrate [26]. After uptake, reactive species such as O_3 or glyoxal can alter the composition of the surface directly [144, 145], or lead to the formation of secondary products in the bulk-phase [146]. Secondary compounds usually remain bound to the particle, further altering its physical or chemical properties [145, 146]. More concretely, acid anhydrides can for example be reactively uptaken to the surface of

BBE, and as described previously, react with particle-bound nucleophiles to form carboxylic acid containing compounds [2]. Alternatively, formation of an organic layer on the surface of particulate matter may shield their more reactive bulk-phase from OH uptake, increasing their lifetime in the atmosphere [145].

Despite this, heterogeneous reactions do not have to chemically involve particulate matter. For example, there is evidence that NO_2 will heterogeneously react on particles in the presence of water and light to form nitrous acid (HONO), a significant daytime pollutant and contributor to photochemical smog [147]. In this instance, the surface of particulate matter is expected to act only as a catalyst for the heterogeneous reaction.

Overall, Sections 1.1.1 through 1.2.2.3 reinforce how BBE not only interact with atmospheric sinks and oxidants, solar radiation, temperature, and each other, but also the particles they are bound to or collide with. Each of these factors as well as their interactions with one another influence the physical and chemical properties of BBE. In fact, even the position and diffusivity of a pollutant within a single particle may affect its atmospheric lifetime [118]. Therefore, BBE impact prediction is incumbent on a proper understanding of how each of these factors are interlaced with each other and the environment. This understanding can only be achieved through a combined effort of laboratory studies (which are uniquely capable of deconvoluting each compartment individually), as well as field and modelling based efforts (which focus on a more aggregate approach).

1.3 Combustion

To fully understand the mechanisms that gives rise to BBE, one must consider the process of combustion and flaming. Plant matter is mostly made up of water, which accounts for up to 60% of its undried weight, and may be the main factor accounting for fire propagation [148, 149]. Additionally, plant matter also contains cellulose and hemicellulose, which represents the majority of the dry weight of most plants [150, 151]. Most biomass fuels also contain lignin, proteins, amino acids, and other volatile materials, as well as a variety of different minerals [150, 151]. Each of these constituents can affect the burning process in different ways, enhancing or inhibiting

flame formation, for example. Other components, such as nitrogen, sulphur, phosphorous, and chlorine, have a bearing on the composition of the flaming emissions without directly contributing to the combustion step itself [148, 149]. These species can still be useful as a tool for tracking what type of fuel gave rise to a fire. For instance, a direct linear relationship has been shown between the nitrogen content of a fuel, and its emission of nitrogenous compounds during efficient combustion as far back as 1990 [152].

The first step in the combustion of plant material is drying, during which the water and volatile plant matter is given off or moves towards the inner layers of the material [148, 149]. Water content is important for the future flaming step, as high amounts of water or a heat source of insufficient intensity will not induce a flame [149]. The second step is pyrolysis, which begins at variable temperatures depending on the fuel type and does not involve oxygen. For wood, pyrolysis begins at around 400K and becomes self-sustaining above 450K [148]. During pyrolysis high-molecular weight compounds – such as dehydrocellulose – are cracked into intermediate-molecular weight products such as charcoal [149, 153]. Tar, a group of high molecular mass ELVOC, are also formed. These compounds are then further decomposed into VOC on the surface of the material, off of which a flame can be sparked [148, 149, 153]. If no volatile gases are formed, pyrolysis continues without reaching the flaming step, as the majority fuels must liberate fuel gases or vapours for a flame to be sparked [149]. Most cellulose-based materials must also be pyrolyzed to char before flaming, and if the ratio of char to tar is too high, combustion is prevented [148, 149, 153]. For wood fuel and only if oxygen is readily available, the process becomes glowing combustion at temperatures around 800K [148]. Here, char is directly oxidized to CO and then to CO₂. At this point, the volatile gases emitted by pyrolysis of the material and the emission of tar are diluted with ambient oxygen, forming an ignitable mixture and sparking a flame [149, 153]. The thermokinetic exchange processes of such a flame are depicted in Figure 1.8 [153]. After a flame is formed, a burn may fluidly shift between smouldering, pyrolysis, developing a flame multiple times throughout a single combustion [149]. Solid material can smoulder either after flaming or when flaming is not possible. A smouldering fire is an oxidative process characterized by its lack of flames and by its much lower oxygen requirements (5% vs 15% for a flame) [148]. Due to being a rel-

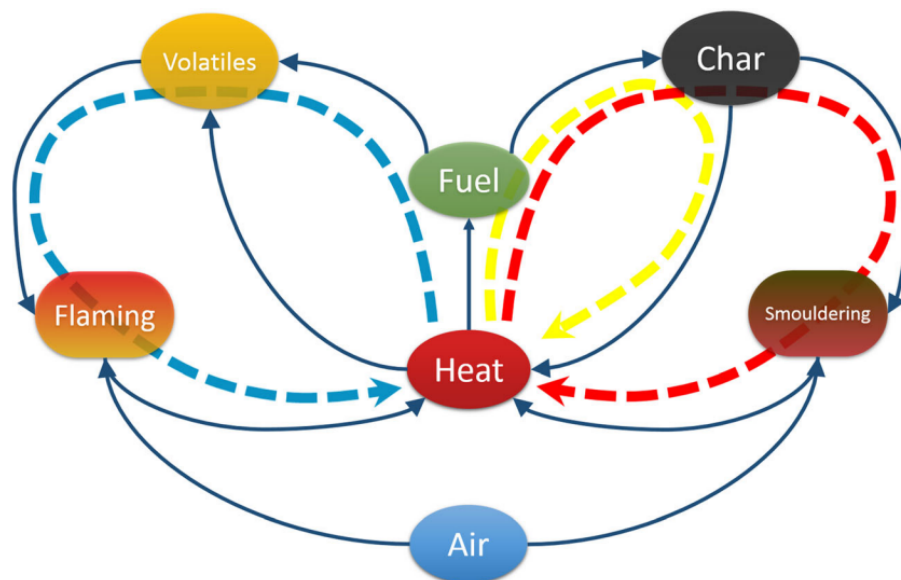


Figure 1.8: A more advanced conceptual model that captures the effects of the competitive thermokinetics inherent in the combustion of cellulosic fuels. Arrows indicate direction of flows. The low activation energy, exothermic pathway of char formation occurs in competition with the higher activation, endothermic pathway of volatile formation. Oxidation of volatiles and char provide the bulk of the heat released during combustion and create three different feedback paths that lead to sustained combustion. The heat generated by the formation of char is retained in the fuel substrate (yellow pathway) and in conjunction with the oxidation of char (red pathway) provides the mechanism by which a fuel can transition to flaming combustion. In most instances, it is the oxidation of volatiles (blue pathway) that drives the spread of a wildland fire. However, it is the char pathways that enable a biomass fire to sustain combustion under marginal conditions. Reproduced with permission from Springer Nature: Sullivan *et al.* “Inside the Inferno: Fundamental Processes of Wildland Fire Behaviour,” *Curr. Forestry Rep.*, vol. 3, pp. 132-149, 2017 [153]

atively lower temperature process, smouldering is long-lasting, and can continuously evolve emissions over week-long time periods in certain types of fuels [149, 153]. This increased duration coupled with the inefficiency of the process makes smouldering the main release step of $PM_{2.5}$ from biomass burning, and why it has attracted interest since the advent of fine particulate matter research [154].

1.3.1 Combustion efficiency

Combustion efficiency is an indication of the efficiency of energy transfer between a fuel and its surroundings when combusted, it is measured by the fraction of total carbon in the fuel versus the amount transformed into CO_2 during a burn [155]. The

more efficient a burn, the fewer secondary products are evolved and the more the reaction moves towards emitting only CO₂, water and heat, the main products of combustion [149, 155]. Typically, a lower combustion efficiency will yield lower temperatures, and produce a much larger number of byproducts per unit of fuel mass burned [149, 155]. Inefficient combustion promotes the formation of BrC over BC, as well as BBOA [43]. At low temperatures the combustion may become flameless, in which case the reaction subsists on oxygen reacting directly with the solid-phase fuel. This is the PM_{2.5} releasing smouldering process described previously, and why materials which become a liquid when heated are incapable of smouldering [149]. Similarly to inefficient flaming combustion, both smouldering and pyrolysis emit relatively larger particles and higher molecular mass compounds [43, 109]. Emissions are termed primary so long as they have not gone structural modification (hence the “secondary” nomenclature for aerosol formed after emission). Inefficient burning conditions also emit more primary organic aerosol, which are in turn more likely to form secondary aerosol through atmospheric processing [43, 109].

Highly efficient burn conditions are unusual in uncontrolled scenarios. For instance, farmers burning crop residue are rarely concerned about the efficiency of the combustion. Wildfire burn efficiency is also highly variable - although still less efficient than fuels prepared for combustion - as evidenced by the large amounts of evolved smoke [149, 156]. And unfortunately, the biomass stoves employed in developing countries are notorious for their inefficiency [45, 56, 57, 157]. This means that most biomass use-cases are bound to form large amounts of particulate matter, including health and climate affecting BC, BrC, and PM_{2.5} [43, 45, 56]. And by extension, that the users most affected by BBE are those which employ biomass through necessity rather than preference.

1.3.1.1 On emission composition and its variability

The major fraction of all BBE (CO₂, water, and heat) remains consistent between burns [156]. However, as mentioned previously, the composition of particulate matter is strongly impacted by changes in the burning conditions [9, 44, 48, 158]. A non-exhaustive list of important burning conditions is provided in Table 1.1 [149]. For simplicity, impacts are split depending on whether they typically enhance or hinder

the combustion efficiency.

Table 1.1: Combustion parameters and their influence on combustion efficiency

Combustion Parameter	Combustion Efficiency
Temperature	Enhanced
Humidity (Fuel)	Inhibited
Humidity (Environment)	Inhibited
Airflow	Enhanced*
Fuel Surface Area	Enhanced
Fuel Density	Enhanced
Fuel Purity	Enhanced

*When airflow becomes faster than the speed of the flame front, combustion efficiency is inhibited due to the snuffing out effect.

Environmental effects, such as cloud cover, have unpredictable effects on the burn efficiency that are difficult to reproduce in a laboratory setting [149]. Therefore, the benefit of methods which give up some representativity in favour of reproducibility, is that the parameters in Table 1.1 do not vary as significantly between experiments, yielding emissions which are more consistent in composition [158–160]. As such, throughout each chapter of the following thesis, great care has been placed on ensuring each combustion experiment is reproducible from its initial design, to its setup, and for the duration of the sampling process. To this end, a tube furnace capable of uniformly heating fuels was used as the sample combustion chamber.

1.3.2 Approaches to study fire

1.3.2.1 Sampling in the field versus a fire lab, and other simplified methods

There are three broad experimental approaches to collecting BBE samples:

1. The most representative samples are captured in the field, typically as aircraft measurements directly above a burn (for wildfires) or over an area of heavy

biomass use (for household combustion). While these are the most representative type of emission sample, reproducibility between combustion events is usually poor and inherently unpredictable [153, 158, 161–164].

2. An alternative to in-situ measurements are fire labs. Here, the outdoor burning environment is reproduced as faithfully as experimentally feasible in a closed environment. Fire labs strike a balance between sample representativity and reproducibility [107, 110, 158, 165–167].
3. Finally, simplified burns take a fundamental experimental approach to gathering samples. Here, the focus is typically on ensuring each burn is as reproducible is possible. To achieve this, known burn-affecting environmental variables are streamlined into more simplified controllable factors [1, 159, 160, 168–170].

1.3.2.2 Reproducible versus representative combustion strategies

When studying biomass burning in a laboratory setting, substantial effort is usually put towards ensuring the combustion process is as reproducible and representative as possible [158, 166]. Experimental studies replicating wildfire combustion are typically focused on establishing representative burns, since simulating the large outdoor environment is challenging and impractical in a laboratory setting [158, 166, 171]. During these studies, samples (usually large quantities of wood or other plant matter) are customarily combusted under a sampling flame stack, emissions are then routed through the flame stack and either gathered on tiered filters (if analyzing particulate matter) or sampled through various gas analyzers (See Figure 1.9 (B)) [107, 110, 165, 166, 172]. While this method does account (relatively) for the large amounts of vegetation burned during wildfires, it fails to replicate other environmental factors intrinsic to the outdoor environment which might affect the emission composition. For example, wind speed and direction will influence combustion, with higher wind speeds generally enhancing fire spread and temperature [149]. While a closed setup can control the airflow volume and speed, changes in airflow direction over the fuel or variations to the speed of that flow are not customarily accounted for [107, 110, 166]. Similarly, the shape, density, and moisture content of the fuel, or its positioning under the flame stack can also significantly alter the burn efficiency [149, 158, 173]. While the studies

listed here excel at being representative, their results are often difficult to replicate due to the large number of variable factors which affect the emission composition, even when imitating fuel characteristics such as species or mass [158].

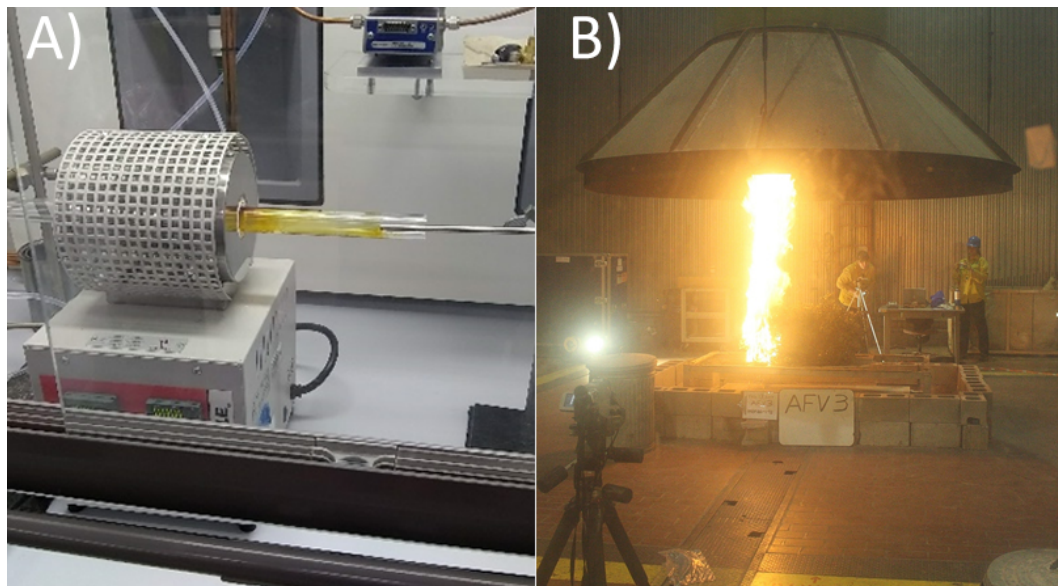


Figure 1.9: Simplified and reproducible tube furnace burn (A) versus a prescribed representative burn in a fire lab (B). Picture (B) reprinted (with adapted caption) from: “Experimental fire studied in the Missoula Fire Lab combustion chamber,” *Missoula Fire Sciences Laboratory*, U.S Department of Agriculture, 2023 [172]

Since achieving a fully representative burn is inherently challenging, some experimental studies have shifted their focus towards ensuring reproducibility (See Figure 1.9 (A)) [1, 159, 170]. That is to say, negating as many of the variable factors as possible in an attempt to ensure burns are the same between experiments, as opposed to attempting to fully replicate the “real” burning environment. For example, some studies [174, 175] will mechanically grind biomass before combustion, while this is rarely the way biomass is burned in the environment, it likely counteracts some of the shape-induced emission variability [149]. Likewise, fuels can be dried to ensure homogeneous humidity and burn efficiency, or burned in a chamber containing only a single inlet and outlet to establish a uniform (laminar) airflow [1, 158]. Reproducibility becomes essential when aiming for comprehensive characterization, as the exact molecular formulae of BBE can vary considerably with changes in the burning conditions [1, 44, 48, 158].

1.3.2.3 On the tube furnace

Throughout this thesis, reproducibility was improved by combusting samples inside a tube furnace [159]. The tube furnace is comprised of a cylindrical heating section through which a glass or quartz tube can be placed. The two ends of the tube can then sit outside the heating section on either side of the furnace. The benefit of this setup is that the tube is heated uniformly around its surface, and samples placed inside the tube are combusted with similar conditions during each burn [1, 159, 168]. Additionally, the speed and composition of the air flowing through the tube can be accurately controlled [1, 159, 168]. Depending on the flow velocity and the tube dimensions, the air flow can be made laminar, which further improves the reproducibility [176]. By applying a vacuum on the opposite end of the tube, emissions can be sampled directly on a filter, or routed to a secondary instrument for online analysis [1, 159, 170]. Although experimentally closed fuel burning (such as is conducted in fire labs) is still the more common combustion method, use of tube furnaces for the combustion of biomass has grown in recent years [1, 159, 160, 168–170]. A picture of the tube furnace is available in Figure 1.9 (A).

1.4 Analysis of physical properties

1.4.1 Size and optical properties

As mentioned regularly throughout this thesis, the size and composition of particulate matter is responsible for its light scattering and absorptive properties, its residence time in the atmosphere, and its health effects when breathed in. Specifically, particulate matter will reflect light in different directions according to Rayleigh, Mie, or geometric scattering. The wavelength of the incoming light and the size of the particle dictates which type of scattering occurs [89, 177–179]. For example, cloud droplets are large enough that their scattering is independent of wavelength in the visible light spectrum (larger than the wavelength of the incoming light), hence their white color [89]. On the other hand, the blue color of the sky is due to Rayleigh scattering of the much smaller air molecules at short wavelengths [89].

Interestingly, the major size distribution of biomass burning particulate matter is

somewhere in this range, between 0.02 to 2 μm [180–182]. This makes their scattering wavelength dependent (Mie), and why polluted atmospheres can appear grey in color [89]. Mie scattering reflects light more strongly in the vector of incidence, driving more solar radiation towards the surface of the Earth [89]. As a property common to all particulate matter, size measurements are usually the first step in predicting its health and climate impacts. In the following subsections, a few common techniques for particle size measurements are outlined.

1.4.1.1 Aerodynamic particle sizer

An aerodynamic particle sizer (APS) measures the size distribution of particulate matter; it was the first technique capable of fast, high-resolution particle size measurements [183]. The APS uses an accelerating flow field to sample aerosol and air. Particles will lag in the flow according to their size and shape. The time of flight (ToF) of the particles is measured by their travel time between two lasers. Finally, the aerodynamic diameter of the particle is obtained by comparing the measured ToF to known reference data [183–185]. Over the course of a set sampling period, the APS outputs the size distribution of the particles, typically as a number or volume concentration over a series of specific size bins [184]. However, the range of particle sizes APS instruments can measure is usually between 0.5–20 μm , which removes some of the fine, nucleation mode particles emitted from biomass burning [180–182, 184]. Additionally, accurate measurements are dependent on frequent instrument recalibration [184, 186]. Despite this, as a relatively low-complexity instrument, the APS is well-suited towards field deployment and continuous particle size monitoring [184, 187–189].

1.4.1.2 Scanning mobility particle sizer

A scanning mobility particle sizer (SMPS) is similarly used to measure the size distribution of particles. It consists of two sections, one capable of separating particles according to their size, and another which counts the particles [185, 190, 191].

The fundamental mechanism of operation of the SMPS is similar to the APS. After an initial pre-conditioning step, the particles are charged so they respond to an electric field, before passing into a differential mobility analyzer (DMA) [192, 193]. The DMA

consists of a cylindrical chamber containing an applied electric field through which the particles flow. The electric field causes particles to migrate towards the wall of the cylinder according to their electric mobility [192, 193]. Particles of different sizes can therefore be detected by varying the strength of the applied electric field. Additionally, the particles can be classified into size bins by scanning through electric field strengths over time [185, 194].

After size classification in the DMA, the particles are routed towards a particle detector for counting, such as a condensation particle counter (CPC) [194]. The particle detector counts particles by how they interact with a light source, typically a laser beam. Simply, particles scatter the beam of light as they pass through the particle detector, leading to them being counted individually [194]. To aid in detection, the particles may also undergo a condensation step in the CPC before counting [185, 190, 192]. The CPC chamber contains supersaturated liquid such as butanol which condenses on particles as they travel. The condensate increases both the size and light-scattering capacity of the particles. This is particularly useful for particles which might be too small to detect ordinarily [190, 192].

The signals from the DMA and the CPC are processed to obtain size distributions in number or volume concentrations, as well as particle surface areas or mass concentrations [189, 194, 195]. Akin to the APS, accurate detection is contingent on frequent calibration [186, 194]. However, the SMPS is better suited towards sizing and counting much smaller particles, anywhere between 0.001-1 μm [184, 191]. Therefore, which instrument is employed is dependent on the research or monitoring objectives, as well as the size range of interest. In fact, APS and SMPS are often applied in parallel to obtain a more comprehensive understanding of aerosol size distributions [185, 188, 189, 196].

1.4.2 Phase state

While the size and optical characteristics of BBE are more customarily analyzed for, the phase of the emissions can hint at their capacity for uptake, reactivity, and atmospheric lifetime [197–199]. Experimentally, the phase of a compound can be estimated by observing its viscosity. A convenient method to qualitatively measure the phase and viscosity of a liquid or solid is the “poke-flow” technique [117, 199–201].

This technique involves inserting a needle into a sample under a microscope. After poking, the sample experiences deformation characteristic of its phase, as displayed in Figure 1.10 [199]. For example, solid or glassy material will crack (Figure 1.10 (D)) while liquids will be pushed away from the needle (Figure 1.10 (A)) [117]. The viscosity can then be approximated by how long it takes for the sample to return to its original shape [117, 199]. Additionally, the analysis can be performed at variable RH, or in a heated or cooled environment to estimate when a phase-change occurs, and whether that phase-change leads to characteristic changes in viscosity [117, 200].

1.5 Analysis of chemical properties

The largest unknown - and experimental challenge - in the analysis of BBE is associated with the deconvolution of their chemical structures and properties [1, 43, 54, 55, 109, 158, 202–204]. Broadly, instrumentation capable of analyzing BBE can be split into online and offline techniques. Online techniques sample and analyze emissions directly from the source, while offline methods separate sampling and analysis, and sometimes include a pre-treatment between these steps.

1.5.1 Online Techniques

1.5.1.1 Aerosol mass spectrometry

Numerous studies utilize an aerosol mass spectrometer (AMS) for their particulate measurements [55, 205–207]. The AMS is capable of both sizing single aerosol particles and obtaining their molecular composition [207, 208]. First, the aerosol is sampled into the AMS vacuum using an aerodynamic lens. Similarly to the APS and SMPS, the aerodynamic size of the particle is usually determined through a ToF measurement. Once sized, the particles are ionized through electron impact (EI) and directed into a mass analyzer, typically a quadrupole or ToF, which separates the produced ions according to their mass to charge ratio (m/z) [207, 208]. The obtained m/z is characteristic of the molecular mass of the compound which produced it. However, using EI splinters each compound into multiple ion fragments (known as a hard ionization technique) [207, 208]. Therefore, the original molecular mass of the compound must usually be reconstructed by comparing the fragment spectra to a known

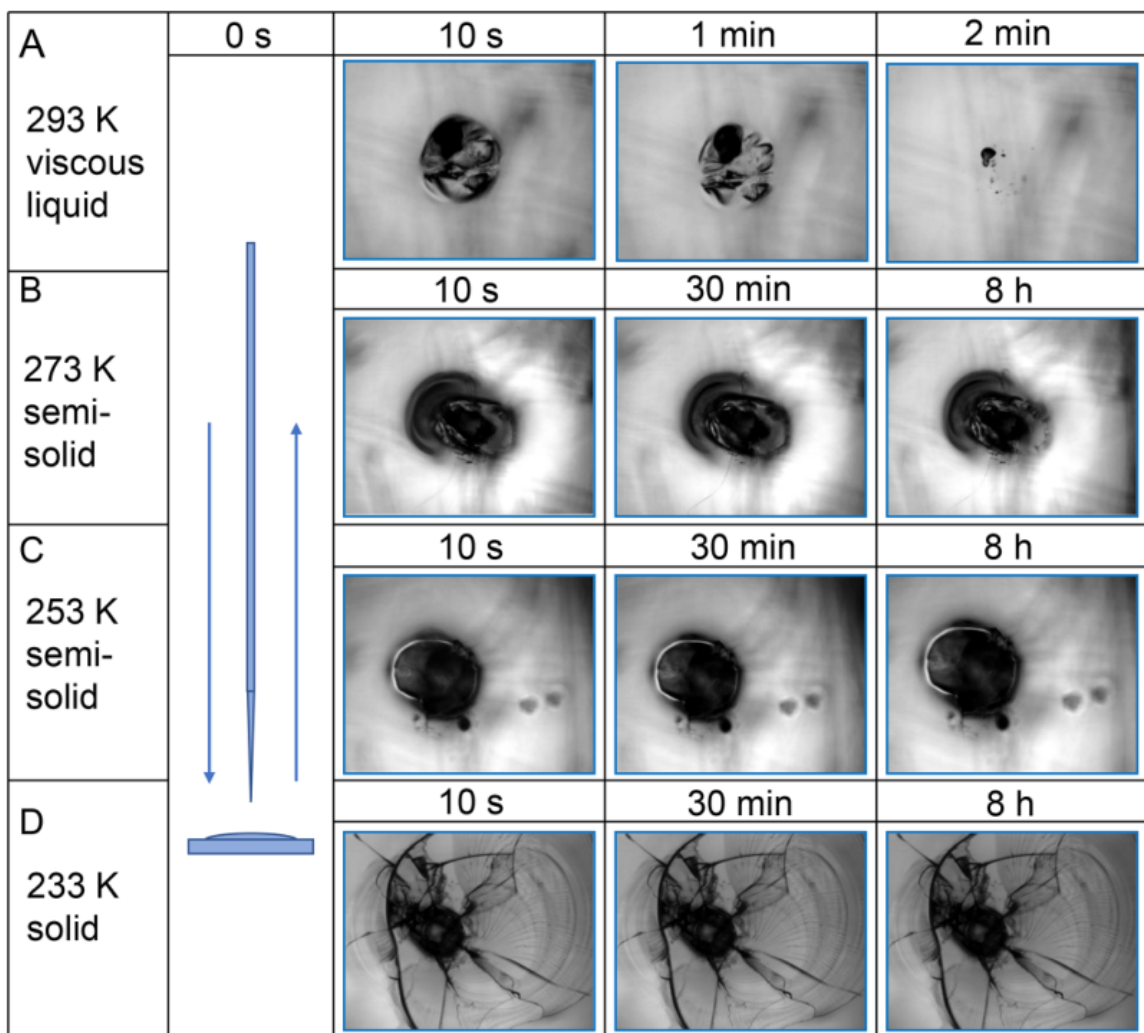


Figure 1.10: Estimation of the phase state of the film substrate as shown for a glucose/1,2,6-hexanetriol (GLU/HEX) mixture (mass ratio of 4 : 1). Deformation and recovery were monitored for different time periods due to the poking of the substrate at different temperatures. The microscope images are 200 μm wide. Figure reprinted under Creative Commons Attribution (CC BY 4.0) from: Li *et al.* “Heterogeneous oxidation of amorphous organic aerosol surrogates by O_3 , NO_3 , and OH at typical tropospheric temperatures,” *Atmos. Chem. and Phys.*, vol. 20, pp. 6055-6080, 2020 [117]

library, which is not always feasible for trace species [207]. Consequently, the AMS can struggle to differentiate complex sample mixtures with overlapping fragment m/z [207, 209]. The usefulness of the AMS comes from its “all in one” capabilities, including the ability to perform on-site field measurements. Accordingly, the technique is commonly applied to monitor and study the evolution of the bulk particle-phase or

its heterogeneous reactions with the surrounding gas-phase [205, 206]. For example, the origin and age of OA can be inferred by the composition of the particles detected at a given moment in time, which simplifies source apportionment and air quality impact prediction [55].

1.5.1.2 Proton transfer reaction mass spectrometry

A proton transfer reaction mass spectrometer (PTR-MS) is a technique used for the online monitoring of trace VOC gases [209–211]. Here, protonated water vapour H_3O^+ ionizes the sampled molecules by charged proton (H^+) transfer [209–211]. VOC can be continuously sampled and ionized without fragmentation (soft ionization technique) by addition of a H^+ . This means that the detected m/z is in most cases equal to the molecular mass of the VOC + 1 [209, 211]. Additionally, the range of VOC which can be effectively ionized and detected is very wide [211]. As opposed to hard ionization techniques, the identity of any ionized species can be inferred without having to compare detections to a known library of compounds [207]. This also avoids interference issues associated with analyzing complex sample mixtures - which are common for hard ionization techniques - as PTR-MS does not generate overlapping m/z unless the molecular formulae for two compounds are equal [209]. If m/z overlap does occur, ions can be separated using gas chromatography (GC), which is described in detail in Section 1.5.4.1 [211]. PTR-MS has also been applied to measure the chemical composition of aerosol. This can be achieved by volatilizing previously sampled aerosol, using thermal desorption for example [212]. Overall, PTR-MS is a convenient way to continuously monitor complex gas mixtures, both in the field and in a laboratory setting.

1.5.2 Offline Techniques

1.5.2.1 Benefits and difficulties

While online techniques have the benefit (and downsides) of sampling a more representative sample of the burn matrix, offline techniques have the advantage of selecting when and how the analysis is performed. Generally, more complex, bulkier, or time consuming analyses such as two-dimensional gas chromatography mass spectrometry (GC×GC-MS) can only be performed using samples gathered offline [213, 214]. Al-

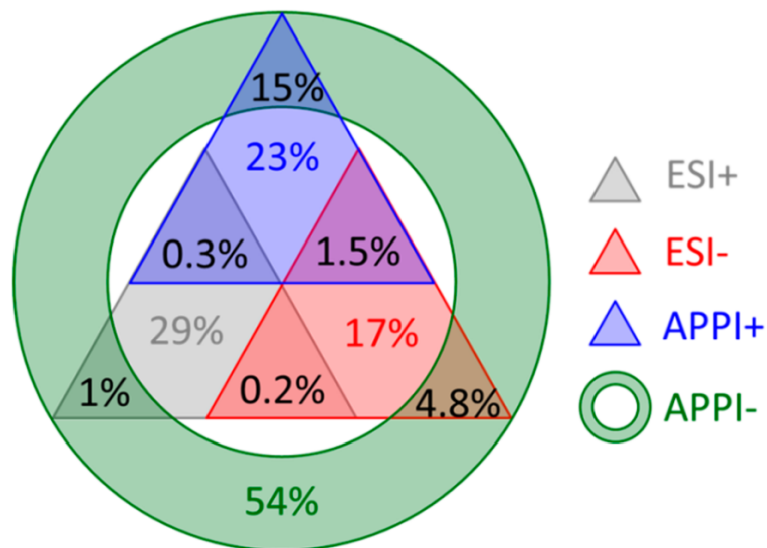
ternatively, some methods require a pre-treatment step which can only be performed offline after sampling [215], such as the derivatization of levoglucosan for gas chromatography mass spectrometry (GC-MS) analysis [1]. However, perhaps the biggest benefit of not being constrained by time is the capacity to pre-concentrate samples before offline analysis. This is particularly useful for environmental samples present in trace concentrations which would ordinarily be below the detection limit of the instrument [216].

One of the downsides of offline analyses is that they do not provide time-resolved information. As a result, samples gathered and analysed offline are composites of the entirety of the sampling period. Using biomass burning as an example, offline analysis can not distinguish whether the emission of a given product is only occurring during certain stages of combustion unless samples are taken at each stage. Therefore, the eventual detection of a compound can only be as accurate as the method used for its initial sampling. That is to say, there is an inherent bias introduced by the sampling method used, which makes gathering a fully representative sample burdensome. For instance, online measurements such as AMS have the benefit of sampling aerosol emissions directly, this means that the molecular compositions obtained are a direct representation of the emissions entering the AMS inlet at that point in time [208]. On the other hand, particle composition analyses using GC×GC are bound by how particles partition on a filter first, and further by how that filter is sampled into the instrument [167]. This bias is exacerbated in liquid chromatography mass spectrometry (LC-MS), where the filter must be extracted into a liquid before injection [1, 217]. When this happens, the extraction method selected directly influences which compounds are preferentially removed from the filter and injected into the LC-MS. Despite this downside, pre-treatment steps can be used to the advantage of the analyst. By selecting an extraction method specific to the organic component of emissions, information characteristic to that component can be derived. For example, since the light-absorbing properties of BrC are believed to be largely due to the organic component [43], preferentially extracting that component avoids interference from the remaining polar fraction, a significant concern for BBE [217, 218].

1.5.3 Targeted versus non-targeted

Just as there is a split in combustion science between reproducible and representative analyses, there is simultaneously a divide between targeted and non-targeted investigations of emission composition. This is due to the main emissions from biomass burning being consistent between burns [149, 156], while the remaining fraction has highly variable compositions [1, 9, 48]. Targeted here refers to experiments in which what is being studied is known, and where the means to measure the target are typically optimized for its detection. On the other hand, non-targeted analyses involve a more broad method. Here, the goal is often to detect as many different unknowns (physicochemical properties, specific compounds) as feasible from a sample, i.e. to cast as wide a net as possible, while maintaining enough resolution to separate each part from the whole. Non-targeted analyses of BBE are particularly challenging as no single analytical method is capable of efficiently separating and detecting the entirety of the burn matrix [43, 55, 109, 124, 125, 171, 218–220]. To illustrate this point, Figure 1.11 displays the percentage and overlap of elemental formulas detected in organic compounds extracted from BBE, obtained by merely changing the MS ionization method [109].

Outside of a laboratory, the vast majority of analyses are targeted. The tracking of BBE in the atmosphere is usually based on the major emissions, and therefore a targeted effort. Health and climate standards are also based on targeted analyses of known deleterious substances such as $\text{PM}_{2.5}$ [20, 21, 45]. Or alternatively, on compounds which while innocuous, indicate the presence or origin of other more harmful species (such as the molecular tracer levoglucosan indicating emissions originated from biomass burning, for example) [221–223]. However, there is evidence that the species responsible for a substantial fraction of the climate and health effects of biomass burning are part of the - relatively unknown - variable emission fraction [43, 109, 124]. Therefore, understanding the composition of the fluctuating fraction and how it is affected by fuel type, or burn and atmospheric conditions, is imperative towards predicting its effects. Historically, the type of widespread approach required to analyse the variable fraction has been non-targeted, due to a deficiency in analytical methods capable of separating the complex emission matrix while identifying



% of formulas in each ionization mode

Figure 1.11: Number percentages of elemental formulas identified from biomass burning solvent-extractable organic compounds measured with high resolution mass spectrometry (HRMS) depending on whether direct infusion electrospray ionization (ESI) or atmospheric pressure photo ionization (APPI) is used. The charge used for ionization is represented by + or -. Figure reprinted with permission from: Lin *et al.* “Comprehensive Molecular Characterization of Atmospheric Brown Carbon by High Resolution Mass Spectrometry with Electrospray and Atmospheric Pressure Photoionization,” *Analytical Chemistry*, vol. 90, no. 21, pp. 12493–12502, 2018 [109]. Copyright 2023 American Chemical Society

every individual compound [17, 220]. For this reason, there have been arguments made against the practicality of obtaining detailed molecular information on each BBE component. Generally, such claims suggest that extrapolating from compound properties, classes, or known tracers can be sufficient to predict the impact of biomass burning [73, 79, 202, 219, 224, 225].

A more recent approach, and perhaps considered the most useful (pragmatic) solution to this dichotomy, has been to classify emissions by a series of health or climate effect predictors, or compositional markers (this method is sometimes called fingerprinting) [153, 222, 224–227]. For example, rather than obtaining exact molecular compositions for each of the light-absorbing compounds in biomass burning emissions, emissions can instead be classified by their nitrogen content - an indicator for enhanced absorbance in BrC - relative to their carbon and hydrogen content [109, 217]. Grouping of compounds is especially useful for separation-based techniques such as LC-MS,

which can struggle to isolate BBE completely [1, 109, 217]. This “semi-targeted” classification approach is reflected in a large body of research focusing on identifying the underlying emission trends rather than specific compounds [109, 217, 224–227], going as far as to classify them by only two factors [228]. This is a logical path when confronted with the large amount of species that could be present on the surface of a single biomass burning particle, let alone how they age as part of the entirety of a burn plume [229]. Classification is particularly useful for representative studies which struggle with reproducibility, considering that while the exact molecular composition is variable between burns, compound classes tend to remain consistent [1, 9, 228].

However, as this thesis will come to argue, classification-based approaches sometimes insufficiently inform the wider trends observed in the overall emissions. In this case, a detailed, analytical, and reproducible characterization is necessary to truly understand emissions from biomass burning. The following sections outline a few common targeted and non-targeted instrumental techniques for the analysis of biomass burning emissions, as well as some of the challenges associated with them.

1.5.3.1 An aside on tracers

In the context of biomass burning, tracers are compounds or emissions with properties characteristic of the fuel being studied. Tracers aid in source apportionment and emission trajectory prediction [61, 79, 221, 223]. The most commonly used biomass burning molecular tracer is levoglucosan - a byproduct of cellulose pyrolysis - due to its atmospheric lifetime and high emission factor [221, 223]. Other common biomass burning tracers include vanillin, sinapaldehyde, syringaldehyde, coniferyl alcohol, as well as syringol, guaiacol, catechol, and their nitrated forms [51, 61, 109, 230, 231]. The characteristics that make a useful tracer are those that aid in its detection, these include: having a high emission factor, long atmospheric lifetime, high fuel specificity, and ease of detection over the rest of the emission matrix [61, 221, 223].

The challenge in the current tracer-based targeted approach, is that while the most commonly used tracers - such as levoglucosan - are biomass burning specific, they are not biomass fuel specific [1, 204, 221]. That is to say, while it is straightforward to differentiate BBE from other combustion sources, it is much more difficult to differentiate BBE from wood versus other biomass types [61, 141]. Nonetheless, there do

exist tracers which are characteristic of certain wood species. For example, vanillin is emitted in much larger quantities from pine wood than oak wood, whereas the opposite occurs for syringaldehyde [61, 141]. However, atmospheric models tend to conflate all BBE as being emitted by wood for simplification purposes, while disregarding other fuel sources [73, 161, 232, 233]. This is presumably due to wood being the biomass fuel with the most well characterized emissions, and the fuel most commonly used within the Western context [61]. Currently, there is a gap of knowledge in the identification of tracers emitted from biomass fuels (such as cow dung) which are commonly used in developing countries [6, 157]. This is why, even for known tracers like levoglucosan, emission factors from understudied fuels such as cow dung have only been reported twice before [1, 204].

1.5.4 Separation-based techniques

1.5.4.1 Gas Chromatography

GC is a separation technique generally used for the analysis of complex sample matrices, or the fast quantitative detection of known compounds [234, 235]. In GC, samples are volatilized and injected into an inert gas mobile phase such as nitrogen, helium, or hydrogen. The mobile phase flows through a heated separation column, typically a long (10-30 m) non-polar coated capillary tube [234, 235]. Compounds will interact with the column coating by varying degrees depending on their physical and chemical properties [235]. For instance, a large non-polar compound will take more time to move through a non-polar column than a small polar molecule. The retention time (t_R) of a given compound through columns of equal length and phase is consistent between instruments, which aids in identification [235]. After separation, the mobile phase containing the sample can be routed to a variety of detectors [234, 235], a MS and a flame ionization detector (FID) are two common options [215, 234, 235]. Due to the separation, the species which make up the sample matrix can be individually detected, preventing interference from their coelution [235].

Detection intensity using a FID is dependent on how efficiently a compound is combusted and ionized by a flame [234–236]. A FID consists of a jet air-hydrogen flame placed beneath an electrode. After eluting from the GC column, electrically charged

single carbon species (CHO^+) are formed by the reaction of oxygen and decomposed organic compounds (due to the flame). CHO^+ then reacts with water to form hydronium ions (H_3O^+) which are detected by the electrode as an electric signal. The intensity of the signal is directly proportional to the number of carbons atoms of the combusted compound [235]. Under ideal conditions, detection limits below 0.5 ng have been achieved as far back as 1958 [236]. Although the resulting GC-FID peak shape can not be used to infer the identity of a compound, the intensity and tR of the peak can [235]. The major benefit of a FID is its non-discriminatory nature and lack of interference from water. Generally, hydrocarbons and most combustible C-H bond containing compounds can be readily detected [235].

When using a MS after separation, as detailed in Section 1.5.1.1 above, a GC is typically coupled to an EI for ionization and a ToF or quadrupole as a mass analyzer for detection [215]. For hard ionization techniques like EI, characterization is contingent on comparison of the detected ion fragment m/z to a known library [215, 237]. This makes the identification of compounds which are not part of a library distinctly challenging.

A GC-MS can be employed for both targeted and untargeted analyses. Throughout this thesis, the characteristic tR and ion fragments are employed to target specific compounds (such as levoglucosan) within the complex BBE matrix. In some instances, compounds underwent pre-treatment such as derivatization to enhance their ionization efficiency, volatility, or to introduce known ion fragments which aid in EI detection.

1.5.4.2 Liquid chromatography mass spectrometry

LC-MS is a separation and characterization technique similar to GC-MS. As the name implies, the mobile phase which transports sample through the column is in the liquid-phase as opposed to the gas-phase [237]. This allows the LC-MS to separate samples which can not be volatilized in a GC-MS, expanding the possible instrumental applications. As a downside, LC-MS peaks are generally not as well resolved as those separated using GC-MS, due in part to dispersion induced band broadening in the column [238].

In the following chapters, LC-MS is used as an exploratory, non-targeted technique. The wide variety of species which can be separated and detected through the technique meshes well with the complex emission matrix of BBE. The soft ionization technique used, electrospray ionization (ESI+ or ESI- depending on the applied charge), can only be adapted to a liquid-phase. ESI volatilizes and ionizes the mobile phase and the sample it carries for direct and continuous measurement by the MS [239, 240]. The benefit of applying ESI to BBE is the wide range of compound classes and molecular weights it is capable of ionizing, as well as the lack of fragmentation in those ions, which facilitates characterization [1, 109, 239, 240].

1.5.4.3 Two-dimensional gas chromatography mass spectrometry

LC- and GC-MS techniques sometimes do not provide sufficient peak resolution to separate complex samples. In this case, it can be helpful to apply a second dimension of separation. GC×GC-MS is an extension of GC-MS. By adding a second dimension of separation (a second column), diverse chemical compounds can be more efficiently resolved [167, 213, 214, 224, 241, 242]. For complex matrices, the separation method is typically the same as in one-dimensional GC-MS, i.e. low-ramping temperature and long time-frame for separation. Using GC×GC-MS, the output from the first column is routed into a second column typically containing a different phase than the first. By doing this, chemical species can be separated by how they interact with two different columns, yielding a two-dimensional separation plot (with time on both axes) [213, 214, 242]. The separation in the second dimension must be fast (in the order of seconds as opposed to minutes), as the instrument continuously injects the output from the first dimension into the second in slices or bands using a modulator, and an injection can not be started until the previous separation has been completed [213, 214]. By coupling the instrument to a MS, molecular compositions for each of the separated compounds can be obtained. This makes GC×GC-MS particularly useful for the analysis of trace compounds in the intricate matrices emitted by biomass burning [107, 167, 224, 241, 243].

Due to the relatively long analysis time of both samples and data, the high upfront and maintenance costs, as well as the expertise required to run the instrument, GC×GC-MS is rarely employed unless necessary. For this reason, although it is an effective

method for characterization and separation, GC×GC-MS has only been adapted to wood BBE analysis recently [107, 167, 224, 241, 243], and has never been applied to other biomass fuels like cow dung.

1.5.5 Uptake measurement techniques

1.5.5.1 Coated wall flow tubes and Knudsen cells

The two most common experimental setups for uptake analyses are coated wall flow tubes and Knudsen cells [26]. For the study of atmospheric dust-pollutant interactions aerosol flow tubes are also common, although beyond the scope of this introduction. As their name implies, coated wall flow tubes consist of a cylindrical glass tube of known internal diameter coated with an adsorptive or absorptive liquid or solid substrate. A constant flow of gas is used to transport a gas-phase sample through the tube. As the gas travels over the tube coating, molecules of the sample will continuously collide and become trapped on the coating surface. The γ is obtained by comparing the concentration of the sample before and after moving through the flow tube [26, 28, 118]. To facilitate that comparison, coated wall flow tubes may contain a movable injector [117, 244, 245]. When fully deployed, the injector bypasses the coated section of the tube completely, preventing uptake. By slowly retracting the injector, the exact exposure time of the sample to the substrate can be controlled without the need for a multitude of flow tubes of different sizes [26, 117, 244, 245]. Knudsen cells follow a similar concept to flow tubes. In this case, the sample to be uptaken is continuously introduced into a vacuum sealed chamber [26]. Instead of being coated on the surface of a tube, the substrate is placed behind a moveable platform or isolation plate. By doing this, uptake can only occur when the isolation plate is open [26]. The pressure inside the Knudsen cell (<10 mTorr) allows for direct coupling to a MS for sample gas quantification and calculation of γ . Additionally, the low pressure causes the mean free path of the gas molecules in the chamber to be larger than to the substrate surface [26]. This means that it is more likely for sample molecules to collide with the substrate than each other, and that therefore, the heterogeneous reaction can be considered the major source of sample loss in the cell [26]. This is especially helpful for highly reactive species such as OH, which are

prone to gas diffusion limitations [246]. The downside however, is that as opposed to a coated wall flow tube, volatile substrates or ambient conditions such as RH can not be simulated while maintaining the pressure required by the Knudsen cell [26].

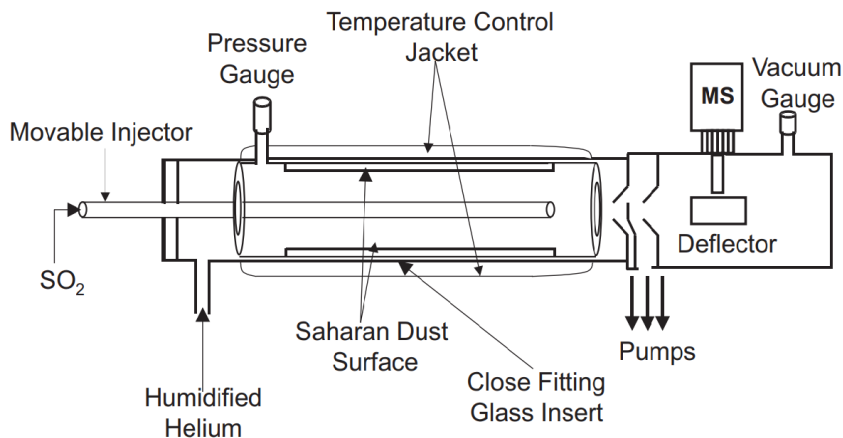


Figure 1.12: Schematic diagram of a coated wall flow tube coupled to a mass spectrometer applied to the uptake of SO_2 on Saharan dust. Figure reprinted with adapted caption under Creative Commons Attribution (CC BY-NC-SA 2.5 CA) from: Adams *et al.* “The uptake of SO_2 on Saharan dust: a flow tube study,” *Atmos. Chem. and Phys.*, vol. 5, pp. 2679-2689, 2005 [245]

1.6 Motivation

The purpose of studying BBE such as particulate matter, BrC, and other BBOA remains to inform on potential risks to health and the environment. It is disappointing then, that our overall understanding of global BBE is not sufficient to appraise those impacts yet [43]. Most of the research being performed on BBE falls into two broad categories, non-targeted and targeted analyses. Still, semi-targeted – rather than targeted – would seem to be a more accurate description of this objective. The semi-targeted studies generally do not focus on single compounds, but rather prefer to emphasize the importance of compound classes or groups, and how these behave as a unit within the atmosphere [109, 217, 224, 226, 227]. Meanwhile, the untargeted studies aim to understand how BBOA such as BrC move and age within the atmosphere, often with the goal of developing models that attempt to classify emissions into systematic categories [124, 164, 247]. Although both methods are popular, there is a definite shift from untargeted to semi-targeted studies in recent years.

The complexity of BBE has been known for a long time. However, it has recently become apparent that overly simplified models are not sufficient to predict BBOA behaviour. Rather, a detailed deconvolution and characterization of the complex emission matrix and the processes which affect it in the atmosphere must inform the creation of simplified models [43, 48, 124, 164]. Nonetheless, the current body of scientific knowledge is missing information on the large variety of different conditions that can affect BBE, leading directly to inaccuracies of modern prediction models and discrepancies between laboratory and field data [48, 158, 247]. This includes both characterization data on the emissions themselves, but also on the atmospheric processes - such as heterogeneous reactions - which affect their evolution after emission [48, 109, 124, 228]. Additionally, while wood fuel emissions are better described than other biomass types, the emissions from fuels such as cow dung - which are uncommon in the Western context - remain largely un-characterized [1, 204, 248, 249]. Therefore, the impacts of dung burning are even more difficult to predict than other biomass types, and often conflated with those of wood in predictive models [73, 250]. Given the rising incidence of wildfires [30, 31], as well as the large amount of people who still rely on biomass for heating and cooking [6], improving our understanding of BBE on a fundamental level should be a priority for both atmospheric and fire scientists, and appropriately, is the motivation for the present thesis.

1.7 Thesis Objectives

The overall goal of this thesis is threefold:

- Firstly, to develop a reproducible method capable of deconvoluting the complex BBE matrix.
- Secondly, to obtain detailed novel molecular data on emissions from a variety of biomass fuels, including fuels commonly used in developing countries, such as cow dung.
- And thirdly, to elucidate some of the unrecognized heterogeneous chemical processes occurring in and on biomass burning aerosol, as well as their impacts on the particle- and gas-phase compositions.

1.8 Thesis Outline

This thesis consists of 5 chapters, Chapter 1 contains a summary of the background of biomass burning emissions, including the current gap in knowledge, the combustion process, the environmental factors which affect emissions in the atmosphere, modern analytical techniques for sampling and emission analysis, as well as some of the specificities of heterogeneous reactions. Specifically, emphasis is placed on why reproducibility and targeted analyses are important in fire research. Chapter 2 reports particulate matter characterization data gathered using LC-MS from wood and cow dung fuels, including particle size distribution and concentration data, light-absorption properties, and novel levoglucosan emission factors. Chapter 3 further expands on the characterization, applying GC×GC-MS to wood and cow dung burning particulate matter for high efficiency separation and detection. Additionally, Chapter 3 reports on the novel use of multivariate statistics to investigate the impacts varying the combustion conditions has on the emission composition. Chapter 4 reinforces the importance of understanding the processes affecting biomass burning emissions in the atmosphere, it describes the reactive heterogeneous uptake of anhydrides to the surface of BBE, and their propensity to form unrecognized compounds with nucleophiles present on that surface. Finally, Chapter 5 summarizes the overall findings of the thesis and explores further research directions.

References

- [1] M. Loebel Roson *et al.*, “Chemical characterization of emissions arising from solid fuel combustion—contrasting wood and cow dung burning,” *ACS Earth and Space Chemistry*, vol. 5, no. 10, pp. 2925–2937, 2021. DOI: 10.1021/acsearthspacechem.1c00268.
- [2] M. Loebel Roson *et al.*, “Unexpected electrophiles in the atmosphere – anhydride nucleophile reactions and uptake to biomass burning emissions,” *Phys. Chem. Chem. Phys.*, 2023. DOI: 10.1039/D3CP01751F.
- [3] J. D. Clark and J. W. K. Harris, “Fire and its roles in early hominid lifeways,” *African Archaeological Review*, vol. 3, no. 1, pp. 3–27, Dec. 1985, ISSN: 1572-9842. DOI: 10.1007/BF01117453. [Online]. Available: <https://doi.org/10.1007/BF01117453>.
- [4] N. Alperson-Afil, “Archaeology of fire: Methodological aspects of reconstructing fire history of prehistoric archaeological sites,” *Earth-Science Reviews*, vol. 113, no. 3, pp. 111–119, 2012, ISSN: 0012-8252. DOI: <https://doi.org/10.1016/j.earscirev.2012.03.012>. [Online]. Available: <https://www.sciencedirect.com/science/article/pii/S0012825212000499>.
- [5] K. Balakrishnan *et al.*, “Air pollution from household solid fuel combustion in india: An overview of exposure and health related information to inform health research priorities,” *Global Health Action*, vol. 4, no. 1, p. 5638, 2011, PMID: 21987631. DOI: 10.3402/gha.v4i0.5638. [Online]. Available: <https://doi.org/10.3402/gha.v4i0.5638>.
- [6] W. H. O. (WHO), “Global household energy database,” 2023. [Online]. Available: <https://www.who.int/data/gho/data/themes/air-pollution/household-air-pollution>.
- [7] J. Popp, S. Kovács, J. Oláh, Z. Divéki, and E. Balázs, “Bioeconomy: Biomass and biomass-based energy supply and demand,” *New Biotechnology*, vol. 60, pp. 76–84, 2021, ISSN: 1871-6784. DOI: <https://doi.org/10.1016/j.nbt.2020.10.004>. [Online]. Available: <https://www.sciencedirect.com/science/article/pii/S1871678420301825>.
- [8] P. McKendry, “Energy production from biomass (part 1): Overview of biomass,” *Bioresource Technology*, vol. 83, no. 1, pp. 37–46, 2002, Reviews Issue, ISSN: 0960-8524. DOI: [https://doi.org/10.1016/S0960-8524\(01\)00118-3](https://doi.org/10.1016/S0960-8524(01)00118-3). [Online]. Available: <https://www.sciencedirect.com/science/article/pii/S0960852401001183>.
- [9] T. C. Bond, D. G. Streets, K. F. Yarber, S. M. Nelson, J.-H. Woo, and Z. Klimont, “A technology-based global inventory of black and organic carbon emissions from combustion,” *Journal of Geophysical Research: Atmospheres*, vol. 109, no. D14, 2004, D14203, 10.1029/2003JD003697. DOI: <https://doi.org/10.1029/2003JD003697>. [Online]. Available: <https://agupubs.onlinelibrary.wiley.com/doi/abs/10.1029/2003JD003697>.

- [10] R. G. Barry and R. J. Chorley, *Atmosphere, weather and climate*, 8th ed. Routledge, 2004, ch. 2,12, pp. 9–32,321–385.
- [11] S. S. Lim *et al.*, “A comparative risk assessment of burden of disease and injury attributable to 67 risk factors and risk factor clusters in 21 regions, 1990–2010: A systematic analysis for the Global Burden of Disease Study 2010,” en, *The Lancet*, vol. 380, no. 9859, pp. 2224–2260, Dec. 2012, ISSN: 01406736. DOI: 10.1016/S0140-6736(12)61766-8. [Online]. Available: <https://linkinghub.elsevier.com/retrieve/pii/S0140673612617668> (visited on 06/25/2021).
- [12] D. W. Dockery *et al.*, “An association between air pollution and mortality in six u.s. cities,” *New England Journal of Medicine*, vol. 329, no. 24, pp. 1753–1759, 1993, PMID: 8179653. DOI: 10.1056/NEJM199312093292401. [Online]. Available: <https://doi.org/10.1056/NEJM199312093292401>.
- [13] J. Liu, D. L. Mauzerall, and L. W. Horowitz, “Evaluating inter-continental transport of fine aerosols:(2) global health impact,” *Atmospheric Environment*, vol. 43, no. 28, pp. 4339–4347, 2009, ISSN: 1352-2310. DOI: <https://doi.org/10.1016/j.atmosenv.2009.05.032>. [Online]. Available: <https://www.sciencedirect.com/science/article/pii/S1352231009004610>.
- [14] C. Samara and D. Voutsas, “Size distribution of airborne particulate matter and associated heavy metals in the roadside environment,” *Chemosphere*, vol. 59, no. 8, pp. 1197–1206, 2005, ISSN: 0045-6535. DOI: <https://doi.org/10.1016/j.chemosphere.2004.11.061>. [Online]. Available: <https://www.sciencedirect.com/science/article/pii/S0045653504011361>.
- [15] Y.-F. Xing, Y.-H. Xu, M.-H. Shi, and Y.-X. Lian, “The impact of PM_{2.5} on the human respiratory system,” en, *J Thorac Dis*, vol. 8, no. 1, E69–74, Jan. 2016.
- [16] C. J. Murray *et al.*, “Global burden of 87 risk factors in 204 countries and territories, 1990–2019: A systematic analysis for the global burden of disease study 2019,” *The lancet*, vol. 396, no. 10258, pp. 1223–1249, 2020.
- [17] M. O. Andreae and P. Merlet, “Emission of trace gases and aerosols from biomass burning,” *Global Biogeochemical Cycles*, vol. 15, no. 4, pp. 955–966, 2001. DOI: <https://doi.org/10.1029/2000GB001382>. [Online]. Available: <https://agupubs.onlinelibrary.wiley.com/doi/abs/10.1029/2000GB001382>.
- [18] M. Pflieger and A. Kroflič, “Acute toxicity of emerging atmospheric pollutants from wood lignin due to biomass burning,” *Journal of Hazardous Materials*, vol. 338, pp. 132–139, 2017, ISSN: 0304-3894. DOI: <https://doi.org/10.1016/j.jhazmat.2017.05.023>. [Online]. Available: <https://www.sciencedirect.com/science/article/pii/S0304389417303667>.
- [19] W. H. Organization *et al.*, “Who global air quality guidelines: Particulate matter (pm_{2.5} and pm₁₀), ozone, nitrogen dioxide, sulfur dioxide and carbon monoxide: Executive summary,” pp. 73–89, 2021.

- [20] and European Environment Agency, M Pinterits, B Ullrich, and E Kampel, *European Union emission inventory report 1990-2020 Under the UNECE Air Convention*. Publications Office of the European Union, 2022. DOI: doi/10.2800/928370.
- [21] M. Lippmann *et al.*, “The u.s. environmental protection agency particulate matter health effects research centers program: A midcourse report of status, progress, and plans.,” *Environmental Health Perspectives*, vol. 111, no. 8, pp. 1074–1092, 2003. DOI: 10.1289/ehp.5750. [Online]. Available: <https://ehp.niehs.nih.gov/doi/abs/10.1289/ehp.5750>.
- [22] A. A. May *et al.*, “Gas-particle partitioning of primary organic aerosol emissions: 3. biomass burning,” *Journal of Geophysical Research: Atmospheres*, vol. 118, no. 19, pp. 11,327–11,338, 2013. DOI: <https://doi.org/10.1002/jgrd.50828>. [Online]. Available: <https://agupubs.onlinelibrary.wiley.com/doi/abs/10.1002/jgrd.50828>.
- [23] M. Hallquist *et al.*, “The formation, properties and impact of secondary organic aerosol: Current and emerging issues,” *Atmospheric Chemistry and Physics*, vol. 9, no. 14, pp. 5155–5236, 2009. DOI: 10.5194/acp-9-5155-2009. [Online]. Available: <https://acp.copernicus.org/articles/9/5155/2009/>.
- [24] M. Kanakidou *et al.*, “Organic aerosol and global climate modelling: A review,” *Atmospheric Chemistry and Physics*, vol. 5, no. 4, pp. 1053–1123, 2005. DOI: 10.5194/acp-5-1053-2005. [Online]. Available: <https://acp.copernicus.org/articles/5/1053/2005/>.
- [25] M. B. Fernandes, J. O. Skjemstad, B. B. Johnson, J. D. Wells, and P. Brooks, “Characterization of carbonaceous combustion residues. i. morphological, elemental and spectroscopic features,” *Chemosphere*, vol. 51, no. 8, pp. 785–795, 2003, ISSN: 0045-6535. DOI: [https://doi.org/10.1016/S0045-6535\(03\)00098-5](https://doi.org/10.1016/S0045-6535(03)00098-5). [Online]. Available: <https://www.sciencedirect.com/science/article/pii/S0045653503000985>.
- [26] C. E. Kolb *et al.*, “An overview of current issues in the uptake of atmospheric trace gases by aerosols and clouds,” *Atmospheric Chemistry and Physics*, vol. 10, no. 21, pp. 10 561–10 605, 2010. DOI: 10.5194/acp-10-10561-2010. [Online]. Available: <https://acp.copernicus.org/articles/10/10561/2010/>.
- [27] V. H. Grassian, “Heterogeneous uptake and reaction of nitrogen oxides and volatile organic compounds on the surface of atmospheric particles including oxides, carbonates, soot and mineral dust: Implications for the chemical balance of the troposphere,” *International Reviews in Physical Chemistry*, vol. 20, no. 3, pp. 467–548, 2001. DOI: 10.1080/01442350110051968. [Online]. Available: <https://doi.org/10.1080/01442350110051968>.
- [28] U. Pöschl, Y. Rudich, and M. Ammann, “Kinetic model framework for aerosol and cloud surface chemistry and gas-particle interactions — part 1: General equations, parameters, and terminology,” *Atmospheric Chemistry and Physics*,

- vol. 7, no. 23, pp. 5989–6023, 2007. DOI: 10.5194/acp-7-5989-2007. [Online]. Available: <https://acp.copernicus.org/articles/7/5989/2007/>.
- [29] T. Xia, M. Kovoichich, and A. Nel, “The role of reactive oxygen species and oxidative stress in mediating particulate matter injury,” en, *Clin Occup Environ Med*, vol. 5, no. 4, pp. 817–836, 2006.
- [30] P. Jain, D. Castellanos-Acuna, S. C. P. Coogan, J. T. Abatzoglou, and M. D. Flannigan, “Observed increases in extreme fire weather driven by atmospheric humidity and temperature,” *Nature Climate Change*, vol. 12, no. 1, pp. 63–70, Jan. 2022, ISSN: 1758-6798. DOI: 10.1038/s41558-021-01224-1. [Online]. Available: <https://doi.org/10.1038/s41558-021-01224-1>.
- [31] A. L. Westerling, “Increasing western us forest wildfire activity: Sensitivity to changes in the timing of spring,” *Philosophical Transactions of the Royal Society B: Biological Sciences*, vol. 371, no. 1696, p. 20150178, 2016. DOI: 10.1098/rstb.2015.0178. [Online]. Available: <https://royalsocietypublishing.org/doi/abs/10.1098/rstb.2015.0178>.
- [32] S. Szopa *et al.*, “Short-lived climate forcers,” in *Climate Change 2021: The Physical Science Basis. Contribution of Working Group I to the Sixth Assessment Report of the Intergovernmental Panel on Climate Change*, V. Masson-Delmotte *et al.*, Eds. Cambridge, United Kingdom and New York, NY, USA: Cambridge University Press, 2021, 817–922. DOI: 10.1017/9781009157896.008.
- [33] “Nasa worldview,” [Online]. Available: <https://worldview.earthdata.nasa.gov/>.
- [34] I. P. on Climate Change, “Anthropogenic and natural radiative forcing,” in *Climate Change 2013 – The Physical Science Basis: Working Group I Contribution to the Fifth Assessment Report of the Intergovernmental Panel on Climate Change*. Cambridge University Press, 2014, 659–740, 923–1055. DOI: 10.1017/CBO9781107415324.018.
- [35] V. Ramanathan and G. Carmichael, “Global and regional climate changes due to black carbon,” *Nature Geoscience*, vol. 1, no. 4, pp. 221–227, Apr. 2008, ISSN: 1752-0908. DOI: 10.1038/ngeo156. [Online]. Available: <https://doi.org/10.1038/ngeo156>.
- [36] R. J. Park, M. J. Kim, J. I. Jeong, D. Youn, and S. Kim, “A contribution of brown carbon aerosol to the aerosol light absorption and its radiative forcing in east asia,” *Atmospheric Environment*, vol. 44, no. 11, pp. 1414–1421, 2010, ISSN: 1352-2310. DOI: <https://doi.org/10.1016/j.atmosenv.2010.01.042>. [Online]. Available: <https://www.sciencedirect.com/science/article/pii/S1352231010001019>.
- [37] Z. Lu *et al.*, “Light absorption properties and radiative effects of primary organic aerosol emissions,” *Environmental Science & Technology*, vol. 49, no. 8, pp. 4868–4877, 2015. DOI: 10.1021/acs.est.5b00211. [Online]. Available: <https://doi.org/10.1021/acs.est.5b00211>.

- [38] I. P. on Climate Change, J. T. Houghton, and W. M. Organization, *IPCC first assessment report*, eng. Geneva: WMO, 1990.
- [39] J. T. Kiehl and B. P. Briegleb, “The relative roles of sulfate aerosols and greenhouse gases in climate forcing,” *Science*, vol. 260, no. 5106, pp. 311–314, 1993. DOI: 10.1126/science.260.5106.311. [Online]. Available: <https://www.science.org/doi/abs/10.1126/science.260.5106.311>.
- [40] S. H. Schneider, “A comment on “climate: The influence of aerosols”,” *Journal of Applied Meteorology and Climatology*, vol. 10, no. 4, pp. 840–841, 1971. DOI: [https://doi.org/10.1175/1520-0450\(1971\)010<0840:ACOTIO>2.0.CO;2](https://doi.org/10.1175/1520-0450(1971)010<0840:ACOTIO>2.0.CO;2). [Online]. Available: https://journals.ametsoc.org/view/journals/apme/10/4/1520-0450_1971_010_0840_acotio_2_0_co_2.xml.
- [41] H. Brown *et al.*, “Biomass burning aerosols in most climate models are too absorbing,” *Nature communications*, vol. 12, no. 1, pp. 1–15, 2021.
- [42] C. E. Stockwell *et al.*, “Nepal ambient monitoring and source testing experiment (namaste): Emissions of trace gases and light-absorbing carbon from wood and dung cooking fires, garbage and crop residue burning, brick kilns, and other sources,” *Atmospheric Chemistry and Physics*, vol. 16, no. 17, pp. 11 043–11 081, 2016. DOI: 10.5194/acp-16-11043-2016. [Online]. Available: <https://acp.copernicus.org/articles/16/11043/2016/>.
- [43] A. Laskin, J. Laskin, and S. A. Nizkorodov, “Chemistry of atmospheric brown carbon,” *Chemical Reviews*, vol. 115, no. 10, pp. 4335–4382, 2015. DOI: 10.1021/cr5006167. [Online]. Available: <https://doi.org/10.1021/cr5006167>.
- [44] M. O. Andreae and A. Gelencsér, “Black carbon or brown carbon? the nature of light-absorbing carbonaceous aerosols,” *Atmospheric Chemistry and Physics*, vol. 6, no. 10, pp. 3131–3148, 2006. DOI: 10.5194/acp-6-3131-2006. [Online]. Available: <https://acp.copernicus.org/articles/6/3131/2006/>.
- [45] N. A. Janssen *et al.*, *Health effects of black carbon*. World Health Organization. Regional Office for Europe, 2012, viii, 86 p.
- [46] J. Hansen, M. Sato, and R. Ruedy, “Radiative forcing and climate response,” *Journal of Geophysical Research: Atmospheres*, vol. 102, no. D6, pp. 6831–6864, 1997. DOI: <https://doi.org/10.1029/96JD03436>. [Online]. Available: <https://agupubs.onlinelibrary.wiley.com/doi/abs/10.1029/96JD03436>.
- [47] T. Novakov and H. Rosen, “The black carbon story: Early history and new perspectives,” en, *Ambio*, vol. 42, no. 7, pp. 840–851, Apr. 2013.
- [48] R. Saleh, “From measurements to models: Toward accurate representation of brown carbon in climate calculations,” *Current Pollution Reports*, vol. 6, no. 2, pp. 90–104, Jun. 2020, ISSN: 2198-6592. DOI: 10.1007/s40726-020-00139-3. [Online]. Available: <https://doi.org/10.1007/s40726-020-00139-3>.

- [49] M. Xie, G. Shen, A. L. Holder, M. D. Hays, and J. J. Jetter, “Light absorption of organic carbon emitted from burning wood, charcoal, and kerosene in household cookstoves,” *Environmental Pollution*, vol. 240, pp. 60–67, 2018, ISSN: 0269-7491. DOI: <https://doi.org/10.1016/j.envpol.2018.04.085>. [Online]. Available: <https://www.sciencedirect.com/science/article/pii/S0269749118303476>.
- [50] Y. Feng, V. Ramanathan, and V. R. Kotamarthi, “Brown carbon: A significant atmospheric absorber of solar radiation?” *Atmospheric Chemistry and Physics*, vol. 13, no. 17, pp. 8607–8621, 2013. DOI: 10.5194/acp-13-8607-2013. [Online]. Available: <https://acp.copernicus.org/articles/13/8607/2013/>.
- [51] Y. Iinuma, O. Böge, R. Gräfe, and H. Herrmann, “Methyl-nitrocatechols: Atmospheric tracer compounds for biomass burning secondary organic aerosols,” *Environmental Science & Technology*, vol. 44, no. 22, pp. 8453–8459, 2010. DOI: 10.1021/es102938a. [Online]. Available: <https://doi.org/10.1021/es102938a>.
- [52] K. M. Updyke, T. B. Nguyen, and S. A. Nizkorodov, “Formation of brown carbon via reactions of ammonia with secondary organic aerosols from biogenic and anthropogenic precursors,” *Atmospheric Environment*, vol. 63, pp. 22–31, 2012, ISSN: 1352-2310. DOI: <https://doi.org/10.1016/j.atmosenv.2012.09.012>. [Online]. Available: <https://www.sciencedirect.com/science/article/pii/S1352231012008710>.
- [53] D. O. De Haan *et al.*, “Brown carbon production in ammonium- or amine-containing aerosol particles by reactive uptake of methylglyoxal and photolytic cloud cycling,” *Environmental Science & Technology*, vol. 51, no. 13, pp. 7458–7466, 2017, PMID: 28562016. DOI: 10.1021/acs.est.7b00159. [Online]. Available: <https://doi.org/10.1021/acs.est.7b00159>.
- [54] C. Li *et al.*, “Formation of secondary brown carbon in biomass burning aerosol proxies through no₃ radical reactions,” *Environmental Science & Technology*, vol. 54, no. 3, pp. 1395–1405, 2020, PMID: 31730747. DOI: 10.1021/acs.est.9b05641. [Online]. Available: <https://doi.org/10.1021/acs.est.9b05641>.
- [55] A. K. Y. Lee *et al.*, “Single-particle characterization of biomass burning organic aerosol (bboa): Evidence for non-uniform mixing of high molecular weight organics and potassium,” *Atmospheric Chemistry and Physics*, vol. 16, no. 9, pp. 5561–5572, 2016. DOI: 10.5194/acp-16-5561-2016. [Online]. Available: <https://acp.copernicus.org/articles/16/5561/2016/>.
- [56] R. Suresh, V. Singh, J. Malik, A. Datta, and R. Pal, “Evaluation of the performance of improved biomass cooking stoves with different solid biomass fuel types,” *Biomass and Bioenergy*, vol. 95, pp. 27–34, 2016, ISSN: 0961-9534. DOI: <https://doi.org/10.1016/j.biombioe.2016.08.002>. [Online]. Available: <https://www.sciencedirect.com/science/article/pii/S0961953416302616>.
- [57] M. A. Johnson *et al.*, “Impacts on household fuel consumption from biomass stove programs in india, nepal, and peru,” *Energy for Sustainable Development*, vol. 17, no. 5, pp. 403–411, 2013, ISSN: 0973-0826. DOI: <https://doi.org/10.1016/j.esd.2013.05.002>.

- 1016/j.esd.2013.04.004. [Online]. Available: <https://www.sciencedirect.com/science/article/pii/S0973082613000343>.
- [58] N. M. Donahue, J. H. Kroll, S. N. Pandis, and A. L. Robinson, “A two-dimensional volatility basis set – part 2: Diagnostics of organic-aerosol evolution,” *Atmospheric Chemistry and Physics*, vol. 12, no. 2, pp. 615–634, 2012. DOI: 10.5194/acp-12-615-2012. [Online]. Available: <https://acp.copernicus.org/articles/12/615/2012/>.
- [59] R. Atkinson, “Atmospheric chemistry of vocs and nox,” *Atmospheric Environment*, vol. 34, no. 12, pp. 2063–2101, 2000, ISSN: 1352-2310. DOI: [https://doi.org/10.1016/S1352-2310\(99\)00460-4](https://doi.org/10.1016/S1352-2310(99)00460-4). [Online]. Available: <https://www.sciencedirect.com/science/article/pii/S1352231099004604>.
- [60] R. Atkinson and J. Arey, “Atmospheric degradation of volatile organic compounds,” *Chemical Reviews*, vol. 103, no. 12, pp. 4605–4638, 2003, PMID: 14664626. DOI: 10.1021/cr0206420. [Online]. Available: <https://doi.org/10.1021/cr0206420>.
- [61] B. R. Simoneit, “Biomass burning — a review of organic tracers for smoke from incomplete combustion,” *Applied Geochemistry*, vol. 17, no. 3, pp. 129–162, 2002, ISSN: 0883-2927. DOI: [https://doi.org/10.1016/S0883-2927\(01\)00061-0](https://doi.org/10.1016/S0883-2927(01)00061-0). [Online]. Available: <https://www.sciencedirect.com/science/article/pii/S0883292701000610>.
- [62] R. K. Chakrabarty *et al.*, “Brown carbon aerosols from burning of boreal peatlands: Microphysical properties, emission factors, and implications for direct radiative forcing,” *Atmospheric Chemistry and Physics*, vol. 16, no. 5, pp. 3033–3040, 2016. DOI: 10.5194/acp-16-3033-2016. [Online]. Available: <https://acp.copernicus.org/articles/16/3033/2016/>.
- [63] W. O. Osburn and T. W. Kensler, “Nrf2 signaling: An adaptive response pathway for protection against environmental toxic insults,” *Mutation Research/Reviews in Mutation Research*, vol. 659, no. 1, pp. 31–39, 2008, Proceedings of the 5th International Conference on Environmental Mutagens in Human Populations (ICEMHP), ISSN: 1383-5742. DOI: <https://doi.org/10.1016/j.mrrev.2007.11.006>. [Online]. Available: <https://www.sciencedirect.com/science/article/pii/S1383574207000695>.
- [64] K. M. Venables, “Low molecular weight chemicals, hypersensitivity, and direct toxicity: The acid anhydrides,” *Occupational and Environmental Medicine*, vol. 46, no. 4, pp. 222–232, 1989, ISSN: 0007-1072. DOI: 10.1136/oem.46.4.222. [Online]. Available: <https://oem.bmj.com/content/46/4/222>.
- [65] V. Feron, H. Til, F. de Vrijer, and P. van Bladeren, “Review : Toxicology of volatile organic compounds in indoor air and strategy for further research,” *Indoor Environment*, vol. 1, no. 2, pp. 69–81, 1992. DOI: 10.1177/1420326X9200100204. [Online]. Available: <https://doi.org/10.1177/1420326X9200100204>.

- [66] X. Shen, Y. Zhao, Z. Chen, and D. Huang, “Heterogeneous reactions of volatile organic compounds in the atmosphere,” *Atmospheric Environment*, vol. 68, pp. 297–314, 2013, ISSN: 1352-2310. DOI: <https://doi.org/10.1016/j.atmosenv.2012.11.027>. [Online]. Available: <https://www.sciencedirect.com/science/article/pii/S1352231012010898>.
- [67] M. Claeys *et al.*, “Formation of secondary organic aerosols through photooxidation of isoprene,” *Science*, vol. 303, no. 5661, pp. 1173–1176, 2004. DOI: [10.1126/science.1092805](https://doi.org/10.1126/science.1092805). [Online]. Available: <https://www.science.org/doi/abs/10.1126/science.1092805>.
- [68] Y. Kanaya *et al.*, “Urban photochemistry in central Tokyo: 2. rates and regimes of oxidant (O₃ + NO₂) production,” *Journal of Geophysical Research: Atmospheres*, vol. 113, no. D6, 2008. DOI: <https://doi.org/10.1029/2007JD008671>. [Online]. Available: <https://agupubs.onlinelibrary.wiley.com/doi/abs/10.1029/2007JD008671>.
- [69] J. Kirkby *et al.*, “Ion-induced nucleation of pure biogenic particles,” *Nature*, vol. 533, no. 7604, pp. 521–526, May 2016.
- [70] J. S. Reid, R. Koppmann, T. F. Eck, and D. P. Eleuterio, “A review of biomass burning emissions part II: Intensive physical properties of biomass burning particles,” *Atmospheric Chemistry and Physics*, vol. 5, no. 3, pp. 799–825, 2005. DOI: [10.5194/acp-5-799-2005](https://doi.org/10.5194/acp-5-799-2005). [Online]. Available: <https://acp.copernicus.org/articles/5/799/2005/>.
- [71] G. Adler, J. M. Flores, A. Abo Rizeq, S. Borrmann, and Y. Rudich, “Chemical, physical, and optical evolution of biomass burning aerosols: A case study,” *Atmospheric Chemistry and Physics*, vol. 11, no. 4, pp. 1491–1503, 2011. DOI: [10.5194/acp-11-1491-2011](https://doi.org/10.5194/acp-11-1491-2011). [Online]. Available: <https://acp.copernicus.org/articles/11/1491/2011/>.
- [72] K. Tsigaridis and M. Kanakidou, “Global modelling of secondary organic aerosol in the troposphere: A sensitivity analysis,” *Atmospheric Chemistry and Physics*, vol. 3, no. 5, pp. 1849–1869, 2003. DOI: [10.5194/acp-3-1849-2003](https://doi.org/10.5194/acp-3-1849-2003). [Online]. Available: <https://acp.copernicus.org/articles/3/1849/2003/>.
- [73] S. R. Freitas *et al.*, “Monitoring the transport of biomass burning emissions in South America,” *Environmental Fluid Mechanics*, vol. 5, no. 1, pp. 135–167, Apr. 2005, ISSN: 1573-1510. DOI: [10.1007/s10652-005-0243-7](https://doi.org/10.1007/s10652-005-0243-7). [Online]. Available: <https://doi.org/10.1007/s10652-005-0243-7>.
- [74] R. F. Pueschel *et al.*, “Vertical transport of anthropogenic soot aerosol into the middle atmosphere,” *Journal of Geophysical Research: Atmospheres*, vol. 105, no. D3, pp. 3727–3736, 2000. DOI: <https://doi.org/10.1029/1999JD900505>. [Online]. Available: <https://agupubs.onlinelibrary.wiley.com/doi/abs/10.1029/1999JD900505>.

- [75] M. G. Lawrence and J. Lelieveld, “Atmospheric pollutant outflow from southern asia: A review,” *Atmospheric Chemistry and Physics*, vol. 10, no. 22, pp. 11 017–11 096, 2010. DOI: 10.5194/acp-10-11017-2010. [Online]. Available: <https://acp.copernicus.org/articles/10/11017/2010/>.
- [76] A. F. Stein, R. R. Draxler, G. D. Rolph, B. J. B. Stunder, M. D. Cohen, and F. Ngan, “Noaa’s hysplit atmospheric transport and dispersion modeling system,” *Bulletin of the American Meteorological Society*, vol. 96, no. 12, pp. 2059–2077, 2015. DOI: <https://doi.org/10.1175/BAMS-D-14-00110.1>. [Online]. Available: <https://journals.ametsoc.org/view/journals/bams/96/12/bams-d-14-00110.1.xml>.
- [77] M. Shiraiwa *et al.*, “Global distribution of particle phase state in atmospheric secondary organic aerosols,” *Nature Communications*, vol. 8, no. 1, p. 15 002, Apr. 2017, ISSN: 2041-1723. DOI: 10.1038/ncomms15002. [Online]. Available: <https://doi.org/10.1038/ncomms15002>.
- [78] K. Li, R. Liu, and C. Sun, “Comparison of anaerobic digestion characteristics and kinetics of four livestock manures with different substrate concentrations,” *Bioresource Technology*, vol. 198, pp. 133–140, 2015, ISSN: 0960-8524. DOI: <https://doi.org/10.1016/j.biortech.2015.08.151>. [Online]. Available: <https://www.sciencedirect.com/science/article/pii/S0960852415012675>.
- [79] B. R. Simoneit and V. Elias, “Detecting organic tracers from biomass burning in the atmosphere,” *Marine Pollution Bulletin*, vol. 42, no. 10, pp. 805–810, 2001, ISSN: 0025-326X. DOI: [https://doi.org/10.1016/S0025-326X\(01\)00094-7](https://doi.org/10.1016/S0025-326X(01)00094-7). [Online]. Available: <https://www.sciencedirect.com/science/article/pii/S0025326X01000947>.
- [80] L. Ganzeveld and J. Lelieveld, “Dry deposition parameterization in a chemistry general circulation model and its influence on the distribution of reactive trace gases,” *Journal of Geophysical Research: Atmospheres*, vol. 100, no. D10, pp. 20 999–21 012, 1995. DOI: <https://doi.org/10.1029/95JD02266>. [Online]. Available: <https://agupubs.onlinelibrary.wiley.com/doi/abs/10.1029/95JD02266>.
- [81] N. A. Esmen and M. Corn, “Residence time of particles in urban air,” *Atmospheric Environment (1967)*, vol. 5, no. 8, pp. 571–578, 1971, ISSN: 0004-6981. DOI: [https://doi.org/10.1016/0004-6981\(71\)90113-2](https://doi.org/10.1016/0004-6981(71)90113-2). [Online]. Available: <https://www.sciencedirect.com/science/article/pii/0004698171901132>.
- [82] C. Textor *et al.*, “Analysis and quantification of the diversities of aerosol life cycles within aerocom,” *Atmospheric Chemistry and Physics*, vol. 6, no. 7, pp. 1777–1813, 2006. DOI: 10.5194/acp-6-1777-2006. [Online]. Available: <https://acp.copernicus.org/articles/6/1777/2006/>.
- [83] J. Pandey and U. Pandey, “Accumulation of heavy metals in dietary vegetables and cultivated soil horizon in organic farming system in relation to atmospheric deposition in a seasonally dry tropical region of india,” *Environmental Monitoring and Assessment*, vol. 148, no. 1, pp. 61–74, Jan. 2009,

- ISSN: 1573-2959. DOI: 10.1007/s10661-007-0139-8. [Online]. Available: <https://doi.org/10.1007/s10661-007-0139-8>.
- [84] A. Lukowski, R. Popek, and P. Karolewski, “Particulate matter on foliage of *betula pendula*, *quercus robur*, and *tilia cordata*: Deposition and eco-physiology,” *Environmental Science and Pollution Research*, vol. 27, no. 10, pp. 10 296–10 307, Apr. 2020, ISSN: 1614-7499. DOI: 10.1007/s11356-020-07672-0. [Online]. Available: <https://doi.org/10.1007/s11356-020-07672-0>.
- [85] K. Nicholson, “A review of particle resuspension,” *Atmospheric Environment (1967)*, vol. 22, no. 12, pp. 2639–2651, 1988, ISSN: 0004-6981. DOI: [https://doi.org/10.1016/0004-6981\(88\)90433-7](https://doi.org/10.1016/0004-6981(88)90433-7). [Online]. Available: <https://www.sciencedirect.com/science/article/pii/0004698188904337>.
- [86] M. Possanzini, P. Buttini, and V. Di Palo, “Characterization of a rural area in terms of dry and wet deposition,” *Science of The Total Environment*, vol. 74, pp. 111–120, 1988, ISSN: 0048-9697. DOI: [https://doi.org/10.1016/0048-9697\(88\)90132-5](https://doi.org/10.1016/0048-9697(88)90132-5). [Online]. Available: <https://www.sciencedirect.com/science/article/pii/0048969788901325>.
- [87] L. A. Barrie, “Scavenging ratios, wet deposition, and in-cloud oxidation: An application to the oxides of sulphur and nitrogen,” *Journal of Geophysical Research: Atmospheres*, vol. 90, no. D3, pp. 5789–5799, 1985. DOI: <https://doi.org/10.1029/JD090iD03p05789>. [Online]. Available: <https://agupubs.onlinelibrary.wiley.com/doi/abs/10.1029/JD090iD03p05789>.
- [88] M. Z. Jacobson, “Development of mixed-phase clouds from multiple aerosol size distributions and the effect of the clouds on aerosol removal,” *Journal of Geophysical Research: Atmospheres*, vol. 108, no. D8, 2003. DOI: <https://doi.org/10.1029/2002JD002691>. [Online]. Available: <https://agupubs.onlinelibrary.wiley.com/doi/abs/10.1029/2002JD002691>.
- [89] R. G. Barry and R. J. Chorley, *Atmosphere, weather and climate*, 8th ed. Routledge, 2004, ch. 3-4, pp. 32–89.
- [90] W. Guelle, Y. J. Balkanski, M. Schulz, F. Dulac, and P. Monfray, “Wet deposition in a global size-dependent aerosol transport model: 1. comparison of a 1 year 210pb simulation with ground measurements,” *Journal of Geophysical Research: Atmospheres*, vol. 103, no. D10, pp. 11 429–11 445, 1998. DOI: <https://doi.org/10.1029/97JD03680>. [Online]. Available: <https://agupubs.onlinelibrary.wiley.com/doi/abs/10.1029/97JD03680>.
- [91] L. Iavorivska, E. W. Boyer, and D. R. DeWalle, “Atmospheric deposition of organic carbon via precipitation,” *Atmospheric Environment*, vol. 146, pp. 153–163, 2016, Acid Rain and its Environmental Effects: Recent Scientific Advances, ISSN: 1352-2310. DOI: <https://doi.org/10.1016/j.atmosenv.2016.06.006>. [Online]. Available: <https://www.sciencedirect.com/science/article/pii/S135223101630437X>.

- [92] Y. Pan *et al.*, “Study on dissolved organic carbon in precipitation in northern china,” *Atmospheric Environment*, vol. 44, no. 19, pp. 2350–2357, 2010, ISSN: 1352-2310. DOI: <https://doi.org/10.1016/j.atmosenv.2010.03.033>. [Online]. Available: <https://www.sciencedirect.com/science/article/pii/S1352231010002591>.
- [93] “Construction of a $1^\circ \times 1^\circ$ fossil fuel emission data set for carbonaceous aerosol and implementation and radiative impact in the echam4 model,” *Journal of Geophysical Research: Atmospheres*, vol. 104, no. D18, pp. 22 137–22 162, 1999. DOI: <https://doi.org/10.1029/1999JD900187>. [Online]. Available: <https://agupubs.onlinelibrary.wiley.com/doi/abs/10.1029/1999JD900187>.
- [94] R. J. Park *et al.*, “Export efficiency of black carbon aerosol in continental outflow: Global implications,” *Journal of Geophysical Research: Atmospheres*, vol. 110, no. D11, 2005. DOI: <https://doi.org/10.1029/2004JD005432>. [Online]. Available: <https://agupubs.onlinelibrary.wiley.com/doi/abs/10.1029/2004JD005432>.
- [95] P. S. Tourinho, V. Kočí, S. Loureiro, and C. A. van Gestel, “Partitioning of chemical contaminants to microplastics: Sorption mechanisms, environmental distribution and effects on toxicity and bioaccumulation,” *Environmental Pollution*, vol. 252, pp. 1246–1256, 2019, ISSN: 0269-7491. DOI: <https://doi.org/10.1016/j.envpol.2019.06.030>. [Online]. Available: <https://www.sciencedirect.com/science/article/pii/S0269749118356744>.
- [96] J. F. Pankow, “An absorption model of gas/particle partitioning of organic compounds in the atmosphere,” *Atmospheric Environment*, vol. 28, no. 2, pp. 185–188, 1994, ISSN: 1352-2310. DOI: [https://doi.org/10.1016/1352-2310\(94\)90093-0](https://doi.org/10.1016/1352-2310(94)90093-0). [Online]. Available: <https://www.sciencedirect.com/science/article/pii/1352231094900930>.
- [97] G. Rao and E. P. Vejerano, “Partitioning of volatile organic compounds to aerosols: A review,” *Chemosphere*, vol. 212, pp. 282–296, 2018, ISSN: 0045-6535. DOI: <https://doi.org/10.1016/j.chemosphere.2018.08.073>. [Online]. Available: <https://www.sciencedirect.com/science/article/pii/S0045653518315534>.
- [98] N. M. Donahue, S. A. Epstein, S. N. Pandis, and A. L. Robinson, “A two-dimensional volatility basis set: 1. organic-aerosol mixing thermodynamics,” *Atmospheric Chemistry and Physics*, vol. 11, no. 7, pp. 3303–3318, 2011. DOI: [10.5194/acp-11-3303-2011](https://doi.org/10.5194/acp-11-3303-2011). [Online]. Available: <https://acp.copernicus.org/articles/11/3303/2011/>.
- [99] D. Mackay and P. J. Leinonen, “Rate of evaporation of low-solubility contaminants from water bodies to atmosphere,” *Environmental Science & Technology*, vol. 9, no. 13, pp. 1178–1180, 1975. DOI: [10.1021/es60111a012](https://doi.org/10.1021/es60111a012). [Online]. Available: <https://doi.org/10.1021/es60111a012>.

- [100] A. Neftel, A. Blatter, R. Hesterberg, and T. Staffelbach, “Measurements of concentration gradients of hno₂ and hno₃ over a semi-natural ecosystem,” *Atmospheric Environment*, vol. 30, no. 17, pp. 3017–3025, 1996, ISSN: 1352-2310. DOI: [https://doi.org/10.1016/1352-2310\(96\)00011-8](https://doi.org/10.1016/1352-2310(96)00011-8). [Online]. Available: <https://www.sciencedirect.com/science/article/pii/S1352231096000118>.
- [101] J. W. Telford and S. K. Chai, “A new aspect of condensation theory,” *pure and applied geophysics*, vol. 118, no. 2, pp. 720–742, Sep. 1980, ISSN: 1420-9136. DOI: 10.1007/BF01593025. [Online]. Available: <https://doi.org/10.1007/BF01593025>.
- [102] T. Novakov and J. E. Penner, “Large contribution of organic aerosols to cloud-condensation-nuclei concentrations,” *Nature*, vol. 365, no. 6449, pp. 823–826, Oct. 1993, ISSN: 1476-4687. DOI: 10.1038/365823a0. [Online]. Available: <https://doi.org/10.1038/365823a0>.
- [103] K. Hämeri *et al.*, “Hygroscopic and ccn properties of aerosol particles in boreal forests,” *Tellus B: Chemical and Physical Meteorology*, vol. 53, no. 4, pp. 359–379, 2001. DOI: 10.3402/tellusb.v53i4.16609. [Online]. Available: <https://doi.org/10.3402/tellusb.v53i4.16609>.
- [104] K. A. Koehler *et al.*, “Cloud condensation nuclei and ice nucleation activity of hydrophobic and hydrophilic soot particles,” *Phys. Chem. Chem. Phys.*, vol. 11, pp. 7906–7920, 36 2009. DOI: 10.1039/B905334B. [Online]. Available: <http://dx.doi.org/10.1039/B905334B>.
- [105] L. Brégonzio-Rozier *et al.*, “Secondary organic aerosol formation from isoprene photooxidation during cloud condensation–evaporation cycles,” *Atmospheric Chemistry and Physics*, vol. 16, no. 3, pp. 1747–1760, 2016. DOI: 10.5194/acp-16-1747-2016. [Online]. Available: <https://acp.copernicus.org/articles/16/1747/2016/>.
- [106] J. H. Kroll and J. H. Seinfeld, “Chemistry of secondary organic aerosol: Formation and evolution of low-volatility organics in the atmosphere,” *Atmospheric Environment*, vol. 42, no. 16, pp. 3593–3624, 2008, ISSN: 1352-2310. DOI: <https://doi.org/10.1016/j.atmosenv.2008.01.003>. [Online]. Available: <https://www.sciencedirect.com/science/article/pii/S1352231008000253>.
- [107] A. T. Ahern *et al.*, “Production of secondary organic aerosol during aging of biomass burning smoke from fresh fuels and its relationship to voc precursors,” *Journal of Geophysical Research: Atmospheres*, vol. 124, no. 6, pp. 3583–3606, 2019. DOI: <https://doi.org/10.1029/2018JD029068>. [Online]. Available: <https://agupubs.onlinelibrary.wiley.com/doi/abs/10.1029/2018JD029068>.
- [108] J. M. Delgado-Saborit, M. S. Alam, K. J. Godri Pollitt, C. Stark, and R. M. Harrison, “Analysis of atmospheric concentrations of quinones and polycyclic aromatic hydrocarbons in vapour and particulate phases,” *Atmospheric Environment*, vol. 77, pp. 974–982, 2013, ISSN: 1352-2310. DOI: <https://doi.org/10.1016/j.atmosenv.2013.05.080>. [Online]. Available: <https://www.sciencedirect.com/science/article/pii/S1352231013004536>.

- [109] P. Lin, L. T. Fleming, S. A. Nizkorodov, J. Laskin, and A. Laskin, “Comprehensive molecular characterization of atmospheric brown carbon by high resolution mass spectrometry with electrospray and atmospheric pressure photoionization,” *Analytical Chemistry*, vol. 90, no. 21, pp. 12 493–12 502, 2018. DOI: 10.1021/acs.analchem.8b02177. [Online]. Available: <https://doi.org/10.1021/acs.analchem.8b02177>.
- [110] V. Samburova *et al.*, “Polycyclic aromatic hydrocarbons in biomass-burning emissions and their contribution to light absorption and aerosol toxicity,” *Science of The Total Environment*, vol. 568, pp. 391–401, 2016, ISSN: 0048-9697. DOI: <https://doi.org/10.1016/j.scitotenv.2016.06.026>. [Online]. Available: <https://www.sciencedirect.com/science/article/pii/S0048969716311974>.
- [111] T. Jokinen *et al.*, “Production of extremely low volatile organic compounds from biogenic emissions: Measured yields and atmospheric implications,” *Proceedings of the National Academy of Sciences*, vol. 112, no. 23, pp. 7123–7128, 2015. DOI: 10.1073/pnas.1423977112. [Online]. Available: <https://www.pnas.org/doi/abs/10.1073/pnas.1423977112>.
- [112] S. Yu, “Role of organic acids (formic, acetic, pyruvic and oxalic) in the formation of cloud condensation nuclei (ccn): A review,” *Atmospheric Research*, vol. 53, no. 4, pp. 185–217, 2000, ISSN: 0169-8095. DOI: [https://doi.org/10.1016/S0169-8095\(00\)00037-5](https://doi.org/10.1016/S0169-8095(00)00037-5). [Online]. Available: <https://www.sciencedirect.com/science/article/pii/S0169809500000375>.
- [113] J. P. Reid *et al.*, “The viscosity of atmospherically relevant organic particles,” *Nature Communications*, vol. 9, no. 1, p. 956, Mar. 2018, ISSN: 2041-1723. DOI: 10.1038/s41467-018-03027-z. [Online]. Available: <https://doi.org/10.1038/s41467-018-03027-z>.
- [114] E. Saukko, H. Kuuluvainen, and A. Virtanen, “A method to resolve the phase state of aerosol particles,” *Atmospheric Measurement Techniques*, vol. 5, no. 1, pp. 259–265, 2012. DOI: 10.5194/amt-5-259-2012. [Online]. Available: <https://amt.copernicus.org/articles/5/259/2012/>.
- [115] L. Renbaum-Wolff *et al.*, “Observations and implications of liquid–liquid phase separation at high relative humidities in secondary organic material produced by α -pinene ozonolysis without inorganic salts,” *Atmospheric Chemistry and Physics*, vol. 16, no. 12, pp. 7969–7979, 2016. DOI: 10.5194/acp-16-7969-2016. [Online]. Available: <https://acp.copernicus.org/articles/16/7969/2016/>.
- [116] Y. Zhang *et al.*, “Effect of the aerosol-phase state on secondary organic aerosol formation from the reactive uptake of isoprene-derived epoxydiols (iepoxy),” *Environmental Science & Technology Letters*, vol. 5, no. 3, pp. 167–174, 2018. DOI: 10.1021/acs.estlett.8b00044. [Online]. Available: <https://doi.org/10.1021/acs.estlett.8b00044>.

- [117] J. Li, S. M. Forrester, and D. A. Knopf, “Heterogeneous oxidation of amorphous organic aerosol surrogates by O_3 , NO_3 , and oh, at typical tropospheric temperatures,” *Atmospheric Chemistry and Physics*, vol. 20, no. 10, pp. 6055–6080, 2020. DOI: 10.5194/acp-20-6055-2020. [Online]. Available: <https://acp.copernicus.org/articles/20/6055/2020/>.
- [118] A. M. Arangio, J. H. Slade, T. Berkemeier, U. Pöschl, D. A. Knopf, and M. Shiraiwa, “Multiphase chemical kinetics of oh radical uptake by molecular organic markers of biomass burning aerosols: Humidity and temperature dependence, surface reaction, and bulk diffusion,” *The Journal of Physical Chemistry A*, vol. 119, no. 19, pp. 4533–4544, 2015, PMID: 25686209. DOI: 10.1021/jp510489z. [Online]. Available: <https://doi.org/10.1021/jp510489z>.
- [119] S. Madronich, “Photodissociation in the atmosphere: 1. actinic flux and the effects of ground reflections and clouds,” *Journal of Geophysical Research: Atmospheres*, vol. 92, no. D8, pp. 9740–9752, 1987. DOI: <https://doi.org/10.1029/JD092iD08p09740>. [Online]. Available: <https://agupubs.onlinelibrary.wiley.com/doi/abs/10.1029/JD092iD08p09740>.
- [120] Y. Matsumi and M. Kawasaki, “Photolysis of atmospheric ozone in the ultraviolet region,” *Chemical Reviews*, vol. 103, no. 12, pp. 4767–4782, 2003, PMID: 14664632. DOI: 10.1021/cr0205255. [Online]. Available: <https://doi.org/10.1021/cr0205255>.
- [121] T. Staffelbach, A. Neftel, B. Stauffer, and D. Jacob, “A record of the atmospheric methane sink from formaldehyde in polar ice cores,” *Nature*, vol. 349, no. 6310, pp. 603–605, Feb. 1991, ISSN: 1476-4687. DOI: 10.1038/349603a0. [Online]. Available: <https://doi.org/10.1038/349603a0>.
- [122] B. Rappenglück, P. K. Dasgupta, M. Leuchner, Q. Li, and W. Luke, “Formaldehyde and its relation to co, pan, and so₂ in the houston-galveston airshed,” *Atmospheric Chemistry and Physics*, vol. 10, no. 5, pp. 2413–2424, 2010. DOI: 10.5194/acp-10-2413-2010. [Online]. Available: <https://acp.copernicus.org/articles/10/2413/2010/>.
- [123] P. Lin, N. Bluvshstein, Y. Rudich, S. A. Nizkorodov, J. Laskin, and A. Laskin, “Molecular chemistry of atmospheric brown carbon inferred from a nationwide biomass burning event,” *Environmental Science & Technology*, vol. 51, no. 20, pp. 11 561–11 570, 2017. DOI: 10.1021/acs.est.7b02276. [Online]. Available: <https://doi.org/10.1021/acs.est.7b02276>.
- [124] L. T. Fleming *et al.*, “Molecular composition and photochemical lifetimes of brown carbon chromophores in biomass burning organic aerosol,” *Atmospheric Chemistry and Physics*, vol. 20, no. 2, pp. 1105–1129, 2020. DOI: 10.5194/acp-20-1105-2020. [Online]. Available: <https://acp.copernicus.org/articles/20/1105/2020/>.

- [125] C. F. Fortenberry, M. J. Walker, Y. Zhang, D. Mitroo, W. H. Brune, and B. J. Williams, “Bulk and molecular-level characterization of laboratory-aged biomass burning organic aerosol from oak leaf and heartwood fuels,” *Atmospheric Chemistry and Physics*, vol. 18, no. 3, pp. 2199–2224, 2018. DOI: 10.5194/acp-18-2199-2018. [Online]. Available: <https://acp.copernicus.org/articles/18/2199/2018/>.
- [126] J. Clayden, N. Greeves, and S. Warren, *Organic chemistry*. Oxford university press, 2012, pp. 107–124, 427–447.
- [127] H. B. Burgi, J. D. Dunitz, and E. Shefter, “Geometrical reaction coordinates. ii. nucleophilic addition to a carbonyl group,” *Journal of the American Chemical Society*, vol. 95, no. 15, pp. 5065–5067, 1973. DOI: 10.1021/ja00796a058. [Online]. Available: <https://doi.org/10.1021/ja00796a058>.
- [128] H. Nemoto, T. Kawamura, and N. Miyoshi, “A highly efficient carbon-carbon bond formation reaction via nucleophilic addition to n-alkylaldimines without acids or metallic species,” *Journal of the American Chemical Society*, vol. 127, no. 42, pp. 14 546–14 547, 2005, PMID: 16231887. DOI: 10.1021/ja054010h. [Online]. Available: <https://doi.org/10.1021/ja054010h>.
- [129] V Grignard, “Mixed organomagnesium combinations and their application in acid, alcohol, and hydrocarbon synthesis,” *Ann. Chim*, vol. 24, pp. 433–490, 1901.
- [130] J. Y. Chen, H. Jiang, S. J. Chen, C. Cullen, C. M. S. Ahmed, and Y.-H. Lin, “Characterization of electrophilicity and oxidative potential of atmospheric carbonyls,” *Environ. Sci.: Processes Impacts*, vol. 21, pp. 856–866, 5 2019. DOI: 10.1039/C9EM00033J. [Online]. Available: <http://dx.doi.org/10.1039/C9EM00033J>.
- [131] J. L. Axson, K. Takahashi, D. O. D. Haan, and V. Vaida, “Gas-phase water-mediated equilibrium between methylglyoxal and its geminal diol,” *Proceedings of the National Academy of Sciences*, vol. 107, no. 15, pp. 6687–6692, 2010. DOI: 10.1073/pnas.0912121107. [Online]. Available: <https://www.pnas.org/doi/abs/10.1073/pnas.0912121107>.
- [132] J. D. Rindelaub *et al.*, “The acid-catalyzed hydrolysis of an α -pinene-derived organic nitrate: Kinetics, products, reaction mechanisms, and atmospheric impact,” *Atmospheric Chemistry and Physics*, vol. 16, no. 23, pp. 15 425–15 432, 2016. DOI: 10.5194/acp-16-15425-2016. [Online]. Available: <https://acp.copernicus.org/articles/16/15425/2016/>.
- [133] M. Takeuchi and N. L. Ng, “Chemical composition and hydrolysis of organic nitrate aerosol formed from hydroxyl and nitrate radical oxidation of α -pinene and β -pinene,” *Atmospheric Chemistry and Physics*, vol. 19, no. 19, pp. 12 749–12 766, 2019. DOI: 10.5194/acp-19-12749-2019. [Online]. Available: <https://acp.copernicus.org/articles/19/12749/2019/>.

- [134] M. N. Chan *et al.*, “Influence of aerosol acidity on the chemical composition of secondary organic aerosol from β -caryophyllene,” *Atmospheric Chemistry and Physics*, vol. 11, no. 4, pp. 1735–1751, 2011. DOI: 10.5194/acp-11-1735-2011. [Online]. Available: <https://acp.copernicus.org/articles/11/1735/2011/>.
- [135] D. J. Jacob and S. C. Wofsy, “Photochemical production of carboxylic acids in a remote continental atmosphere,” in *Acid Deposition at High Elevation Sites*, M. H. Unsworth and D. Fowler, Eds. Dordrecht: Springer Netherlands, 1988, pp. 73–92, ISBN: 978-94-009-3079-7. DOI: 10.1007/978-94-009-3079-7_3. [Online]. Available: https://doi.org/10.1007/978-94-009-3079-7_3.
- [136] K. K. Crahan, D. Hegg, D. S. Covert, and H. Jonsson, “An exploration of aqueous oxalic acid production in the coastal marine atmosphere,” *Atmospheric Environment*, vol. 38, no. 23, pp. 3757–3764, 2004, ISSN: 1352-2310. DOI: <https://doi.org/10.1016/j.atmosenv.2004.04.009>. [Online]. Available: <https://www.sciencedirect.com/science/article/pii/S1352231004003693>.
- [137] Z. C. J. Decker *et al.*, “Novel analysis to quantify plume crosswind heterogeneity applied to biomass burning smoke,” *Environmental Science & Technology*, vol. 55, no. 23, pp. 15 646–15 657, 2021, PMID: 34817984. DOI: 10.1021/acs.est.1c03803. [Online]. Available: <https://doi.org/10.1021/acs.est.1c03803>.
- [138] E. A. Bruns *et al.*, “Characterization of gas-phase organics using proton transfer reaction time-of-flight mass spectrometry: Fresh and aged residential wood combustion emissions,” *Atmospheric Chemistry and Physics*, vol. 17, no. 1, pp. 705–720, 2017. DOI: 10.5194/acp-17-705-2017. [Online]. Available: <https://acp.copernicus.org/articles/17/705/2017/>.
- [139] A. W. H. Chan *et al.*, “Secondary organic aerosol formation from photooxidation of naphthalene and alkylnaphthalenes: Implications for oxidation of intermediate volatility organic compounds (ivocs),” *Atmospheric Chemistry and Physics*, vol. 9, no. 9, pp. 3049–3060, 2009. DOI: 10.5194/acp-9-3049-2009. [Online]. Available: <https://acp.copernicus.org/articles/9/3049/2009/>.
- [140] L. Zhang, Z. Wang, W. Zhang, Y. Liang, and Q. Shi, “Determination of anhydride in atmospheric fine particles by optimized solvent extraction,” *Atmospheric Environment*, vol. 285, p. 119 249, 2022, ISSN: 1352-2310. DOI: <https://doi.org/10.1016/j.atmosenv.2022.119249>. [Online]. Available: <https://www.sciencedirect.com/science/article/pii/S1352231022003144>.
- [141] Y. Iinuma *et al.*, “Source characterization of biomass burning particles: The combustion of selected european conifers, african hardwood, savanna grass, and german and indonesian peat,” *Journal of Geophysical Research: Atmospheres*, vol. 112, no. D8, 2007. DOI: <https://doi.org/10.1029/2006JD007120>. [Online]. Available: <https://agupubs.onlinelibrary.wiley.com/doi/abs/10.1029/2006JD007120>.

- [142] P. L. Cooper and J. P. D. Abbatt, “Heterogeneous interactions of oh and ho₂ radicals with surfaces characteristic of atmospheric particulate matter,” *The Journal of Physical Chemistry*, vol. 100, no. 6, pp. 2249–2254, 1996. DOI: 10.1021/jp952142z. [Online]. Available: <https://doi.org/10.1021/jp952142z>.
- [143] T. Moise and Y. Rudich, “Reactive uptake of ozone by proxies for organic aerosols: Surface versus bulk processes,” *Journal of Geophysical Research: Atmospheres*, vol. 105, no. D11, pp. 14 667–14 676, 2000. DOI: <https://doi.org/10.1029/2000JD900071>. [Online]. Available: <https://agupubs.onlinelibrary.wiley.com/doi/abs/10.1029/2000JD900071>.
- [144] J. D. Hearn and G. D. Smith, “Kinetics and product studies for ozonolysis reactions of organic particles using aerosol cims,” *The Journal of Physical Chemistry A*, vol. 108, no. 45, pp. 10 019–10 029, 2004. DOI: 10.1021/jp0404145. [Online]. Available: <https://doi.org/10.1021/jp0404145>.
- [145] L. Lee and K. Wilson, “The reactive–diffusive length of oh and ozone in model organic aerosols,” *The Journal of Physical Chemistry A*, vol. 120, no. 34, pp. 6800–6812, 2016, PMID: 27509443. DOI: 10.1021/acs.jpca.6b05285. [Online]. Available: <https://doi.org/10.1021/acs.jpca.6b05285>.
- [146] M. M. Galloway *et al.*, “Analysis of photochemical and dark glyoxal uptake: Implications for soa formation,” *Geophysical Research Letters*, vol. 38, no. 17, 2011. DOI: <https://doi.org/10.1029/2011GL048514>. [Online]. Available: <https://agupubs.onlinelibrary.wiley.com/doi/abs/10.1029/2011GL048514>.
- [147] A. Indarto, “Heterogeneous reactions of hono formation from no₂ and hno₃: A review,” *Research on Chemical Intermediates*, vol. 38, no. 3, pp. 1029–1041, Mar. 2012, ISSN: 1568-5675. DOI: 10.1007/s11164-011-0439-z. [Online]. Available: <https://doi.org/10.1007/s11164-011-0439-z>.
- [148] J. Lobert and J. Warnatz, “Emissions from the combustion process in vegetation,” *Fire in the Environment*, vol. 13, pp. 15–37, 1993.
- [149] I. A. of Fire Chiefs, “Basic fire science,” in *Fire investigator: Principles and practice to NFPA 921 and 1033*, 5th ed. Jones and Bartlett Learning, 2018, 21–61.
- [150] A. Thygesen, J. Oddershede, H. Lilholt, A. Bjerre, and K. Ståhl, “On the determination of crystallinity and cellulose content in plant fibres,” *Cellulose*, vol. 12, pp. 563–576, Dec. 2005. DOI: 10.1007/s10570-005-9001-8.
- [151] A. L. Sullivan, “Inside the inferno: Fundamental processes of wildland fire behaviour,” *Current Forestry Reports*, vol. 3, no. 2, pp. 132–149, Jun. 2017, ISSN: 2198-6436. DOI: 10.1007/s40725-017-0057-0. [Online]. Available: <https://doi.org/10.1007/s40725-017-0057-0>.
- [152] J. M. Lobert, D. H. Scharffe, W. M. Hao, and P. J. Crutzen, “Importance of biomass burning in the atmospheric budgets of nitrogen-containing gases,” *Nature*, vol. 346, no. 6284, pp. 552–554, Aug. 1990, ISSN: 1476-4687. DOI: 10.1038/346552a0. [Online]. Available: <https://doi.org/10.1038/346552a0>.

- [153] A. P. Sullivan *et al.*, “Biomass burning markers and residential burning in the winter aircraft campaign,” *Journal of Geophysical Research: Atmospheres*, vol. 124, no. 3, pp. 1846–1861, 2019. DOI: <https://doi.org/10.1029/2017JD028153>. [Online]. Available: <https://agupubs.onlinelibrary.wiley.com/doi/abs/10.1029/2017JD028153>.
- [154] M. O. Andreae, “Biomass burning-its history, use, and distribution and its impact on environmental quality and global climate,” in *Global biomass burning- Atmospheric, climatic, and biospheric implications*, 1991.
- [155] S. K. Akagi *et al.*, “Emission factors for open and domestic biomass burning for use in atmospheric models,” *Atmospheric Chemistry and Physics*, vol. 11, no. 9, pp. 4039–4072, 2011. DOI: 10.5194/acp-11-4039-2011. [Online]. Available: <https://acp.copernicus.org/articles/11/4039/2011/>.
- [156] S. P. Urbanski, “Combustion efficiency and emission factors for wildfire-season fires in mixed conifer forests of the northern rocky mountains, us,” *Atmospheric Chemistry and Physics*, vol. 13, no. 14, pp. 7241–7262, 2013. DOI: 10.5194/acp-13-7241-2013. [Online]. Available: <https://acp.copernicus.org/articles/13/7241/2013/>.
- [157] B. Rooney *et al.*, “Impacts of household sources on air pollution at village and regional scales in india,” *Atmospheric Chemistry and Physics*, vol. 19, no. 11, pp. 7719–7742, 2019. DOI: 10.5194/acp-19-7719-2019. [Online]. Available: <https://acp.copernicus.org/articles/19/7719/2019/>.
- [158] A. L. Hodshire *et al.*, “Aging effects on biomass burning aerosol mass and composition: A critical review of field and laboratory studies,” *Environmental Science & Technology*, vol. 53, no. 17, pp. 10 007–10 022, 2019. DOI: 10.1021/acs.est.9b02588. [Online]. Available: <https://doi.org/10.1021/acs.est.9b02588>.
- [159] Y. H. Kim *et al.*, “Mutagenicity and lung toxicity of smoldering vs. flaming emissions from various biomass fuels: Implications for health effects from wild-land fires,” *Environmental Health Perspectives*, vol. 126, no. 1, p. 017 011, 2018. DOI: 10.1289/EHP2200. [Online]. Available: <https://ehp.niehs.nih.gov/doi/abs/10.1289/EHP2200>.
- [160] Y. H. Kim *et al.*, “The role of fuel type and combustion phase on the toxicity of biomass smoke following inhalation exposure in mice,” *Archives of Toxicology*, vol. 93, no. 6, pp. 1501–1513, Jun. 2019, ISSN: 1432-0738. DOI: 10.1007/s00204-019-02450-5. [Online]. Available: <https://doi.org/10.1007/s00204-019-02450-5>.
- [161] Z. C. J. Decker *et al.*, “Nighttime chemical transformation in biomass burning plumes: A box model analysis initialized with aircraft observations,” *Environmental Science & Technology*, vol. 53, no. 5, pp. 2529–2538, 2019, PMID: 30698424. DOI: 10.1021/acs.est.8b05359. [Online]. Available: <https://doi.org/10.1021/acs.est.8b05359>.

- [162] A. Hecobian *et al.*, “Comparison of chemical characteristics of 495 biomass burning plumes intercepted by the nasa dc-8 aircraft during the arctas/carb-2008 field campaign,” *Atmospheric Chemistry and Physics*, vol. 11, no. 24, pp. 13 325–13 337, 2011. DOI: 10.5194/acp-11-13325-2011. [Online]. Available: <https://acp.copernicus.org/articles/11/13325/2011/>.
- [163] D. J. Jacob *et al.*, “The arctic research of the composition of the troposphere from aircraft and satellites (arctas) mission: Design, execution, and first results,” *Atmospheric Chemistry and Physics*, vol. 10, no. 11, pp. 5191–5212, 2010. DOI: 10.5194/acp-10-5191-2010. [Online]. Available: <https://acp.copernicus.org/articles/10/5191/2010/>.
- [164] M. Müller *et al.*, “In situ measurements and modeling of reactive trace gases in a small biomass burning plume,” *Atmospheric Chemistry and Physics*, vol. 16, no. 6, pp. 3813–3824, 2016. DOI: 10.5194/acp-16-3813-2016. [Online]. Available: <https://acp.copernicus.org/articles/16/3813/2016/>.
- [165] J. Tian *et al.*, “A biomass combustion chamber: Design, evaluation, and a case study of wheat straw combustion emission tests,” *Aerosol and Air Quality Research*, vol. 15, no. 5, pp. 2104–2114, 2015. DOI: 10.4209/aaqr.2015.03.0167. [Online]. Available: <https://doi.org/10.4209/aaqr.2015.03.0167>.
- [166] C. D. McClure, C. Y. Lim, D. H. Hagan, J. H. Kroll, and C. D. Cappa, “Biomass-burning-derived particles from a wide variety of fuels – part 1: Properties of primary particles,” *Atmospheric Chemistry and Physics*, vol. 20, no. 3, pp. 1531–1547, 2020. DOI: 10.5194/acp-20-1531-2020. [Online]. Available: <https://acp.copernicus.org/articles/20/1531/2020/>.
- [167] L. E. Hatch, A. Rivas-Ubach, C. N. Jen, M. Lipton, A. H. Goldstein, and K. C. Barsanti, “Measurements of i/svocs in biomass-burning smoke using solid-phase extraction disks and two-dimensional gas chromatography,” *Atmospheric Chemistry and Physics*, vol. 18, no. 24, pp. 17 801–17 817, 2018. DOI: 10.5194/acp-18-17801-2018. [Online]. Available: <https://acp.copernicus.org/articles/18/17801/2018/>.
- [168] R. P. Pokhrel, J. Gordon, M. N. Fiddler, and S. Bililign, “Determination of emission factors of pollutants from biomass burning of african fuels in laboratory measurements,” *Journal of Geophysical Research: Atmospheres*, vol. 126, no. 20, e2021JD034731, 2021, e2021JD034731 2021JD034731. DOI: <https://doi.org/10.1029/2021JD034731>. [Online]. Available: <https://agupubs.onlinelibrary.wiley.com/doi/abs/10.1029/2021JD034731>.
- [169] E. Sarpong, D. Smith, R. Pokhrel, M. N. Fiddler, and S. Bililign, “Refractive indices of biomass burning aerosols obtained from african biomass fuels using rdg approximation,” *Atmosphere*, vol. 11, no. 1, 2020, ISSN: 2073-4433. DOI: 10.3390/atmos11010062. [Online]. Available: <https://www.mdpi.com/2073-4433/11/1/62>.

- [170] R. P. Pokhrel, J. Gordon, M. N. Fiddler, and S. Bililign, “Impact of combustion conditions on physical and morphological properties of biomass burning aerosol,” *Aerosol Science and Technology*, vol. 55, no. 1, pp. 80–91, 2021. DOI: 10.1080/02786826.2020.1822512. [Online]. Available: <https://doi.org/10.1080/02786826.2020.1822512>.
- [171] R. J. Yokelson, T. J. Christian, T. G. Karl, and A. Guenther, “The tropical forest and fire emissions experiment: Laboratory fire measurements and synthesis of campaign data,” *Atmospheric Chemistry and Physics*, vol. 8, no. 13, pp. 3509–3527, 2008. DOI: 10.5194/acp-8-3509-2008. [Online]. Available: <https://acp.copernicus.org/articles/8/3509/2008/>.
- [172] M. F. S. Laboratory, “Experimental fire studied in the fire lab’s combustion chamber,” [Online]. Available: <https://firelab.org/image-gallery>.
- [173] M. Fawaz, A. Avery, T. B. Onasch, L. R. Williams, and T. C. Bond, “Technical note: Pyrolysis principles explain time-resolved organic aerosol release from biomass burning,” *Atmospheric Chemistry and Physics*, vol. 21, no. 20, pp. 15 605–15 618, 2021. DOI: 10.5194/acp-21-15605-2021. [Online]. Available: <https://acp.copernicus.org/articles/21/15605/2021/>.
- [174] S. JIMÉNEZ and J. BALLESTER, “Particulate matter formation and emission in the combustion of different pulverized biomass fuels,” *Combustion Science and Technology*, vol. 178, no. 4, pp. 655–683, 2006. DOI: 10.1080/00102200500241248. [Online]. Available: <https://doi.org/10.1080/00102200500241248>.
- [175] S. Jiménez and J. Ballester, “Formation of alkali sulphate aerosols in biomass combustion,” *Fuel*, vol. 86, no. 4, pp. 486–493, 2007, ISSN: 0016-2361. DOI: <https://doi.org/10.1016/j.fuel.2006.08.005>. [Online]. Available: <https://www.sciencedirect.com/science/article/pii/S0016236106003127>.
- [176] S. Jennings, “The mean free path in air,” *Journal of Aerosol Science*, vol. 19, no. 2, pp. 159–166, 1988, ISSN: 0021-8502. DOI: [https://doi.org/10.1016/0021-8502\(88\)90219-4](https://doi.org/10.1016/0021-8502(88)90219-4). [Online]. Available: <https://www.sciencedirect.com/science/article/pii/0021850288902194>.
- [177] S.-H. Hong and J. Winter, “Size dependence of optical properties and internal structure of plasma grown carbonaceous nanoparticles studied by in situ Rayleigh-Mie scattering ellipsometry,” *Journal of Applied Physics*, vol. 100, no. 6, Sep. 2006, 064303, ISSN: 0021-8979. DOI: 10.1063/1.2338132. [Online]. Available: <https://doi.org/10.1063/1.2338132>.
- [178] R. G. Pinnick, J. M. Rosen, and D. J. Hofmann, “Measured light-scattering properties of individual aerosol particles compared to mie scattering theory,” *Appl. Opt.*, vol. 12, no. 1, pp. 37–41, Jan. 1973. DOI: 10.1364/AO.12.000037. [Online]. Available: <https://opg.optica.org/ao/abstract.cfm?URI=ao-12-1-37>.

- [179] I. Tegen and A. A. Lacis, “Modeling of particle size distribution and its influence on the radiative properties of mineral dust aerosol,” *Journal of Geophysical Research: Atmospheres*, vol. 101, no. D14, pp. 19 237–19 244, 1996. DOI: <https://doi.org/10.1029/95JD03610>. [Online]. Available: <https://agupubs.onlinelibrary.wiley.com/doi/abs/10.1029/95JD03610>.
- [180] S.-S. Park, S. Y. Sim, M.-S. Bae, and J. J. Schauer, “Size distribution of water-soluble components in particulate matter emitted from biomass burning,” *Atmospheric Environment*, vol. 73, pp. 62–72, 2013, ISSN: 1352-2310. DOI: <https://doi.org/10.1016/j.atmosenv.2013.03.025>. [Online]. Available: <https://www.sciencedirect.com/science/article/pii/S135223101300201X>.
- [181] P. J. Silva, D.-Y. Liu, C. A. Noble, and K. A. Prather, “Size and chemical characterization of individual particles resulting from biomass burning of local southern california species,” *Environmental Science & Technology*, vol. 33, no. 18, pp. 3068–3076, 1999. DOI: 10.1021/es980544p. [Online]. Available: <https://doi.org/10.1021/es980544p>.
- [182] J. Rissler *et al.*, “Size distribution and hygroscopic properties of aerosol particles from dry-season biomass burning in amazonia,” *Atmospheric Chemistry and Physics*, vol. 6, no. 2, pp. 471–491, 2006. DOI: 10.5194/acp-6-471-2006. [Online]. Available: <https://acp.copernicus.org/articles/6/471/2006/>.
- [183] P. A. Baron, “Calibration and use of the aerodynamic particle sizer (aps 3300),” *Aerosol Science and Technology*, vol. 5, no. 1, pp. 55–67, 1986. DOI: 10.1080/02786828608959076. [Online]. Available: <https://doi.org/10.1080/02786828608959076>.
- [184] T. M. Peters and D. Leith, “Concentration measurement and counting efficiency of the aerodynamic particle sizer 3321,” *Journal of Aerosol Science*, vol. 34, no. 5, pp. 627–634, 2003, ISSN: 0021-8502. DOI: [https://doi.org/10.1016/S0021-8502\(03\)00030-2](https://doi.org/10.1016/S0021-8502(03)00030-2). [Online]. Available: <https://www.sciencedirect.com/science/article/pii/S0021850203000302>.
- [185] C. Sioutas, “Evaluation of the measurement performance of the scanning mobility particle sizer and aerodynamic particle sizer,” *Aerosol Science and Technology*, vol. 30, no. 1, pp. 84–92, 1999. DOI: 10.1080/027868299304903. [Online]. Available: <https://doi.org/10.1080/027868299304903>.
- [186] B. T. Chen, Y. S. Cheng, and H. C. Yeh, “Performance of a tsi aerodynamic particle sizer,” *Aerosol Science and Technology*, vol. 4, no. 1, pp. 89–97, 1985. DOI: 10.1080/02786828508959041. [Online]. Available: <https://doi.org/10.1080/02786828508959041>.
- [187] J. D. Yanosky, P. L. Williams, and D. L. MacIntosh, “A comparison of two direct-reading aerosol monitors with the federal reference method for pm_{2.5} in indoor air,” *Atmospheric Environment*, vol. 36, no. 1, pp. 107–113, 2002, ISSN: 1352-2310. DOI: [https://doi.org/10.1016/S1352-2310\(01\)00422-8](https://doi.org/10.1016/S1352-2310(01)00422-8). [Online]. Available: <https://www.sciencedirect.com/science/article/pii/S1352231001004228>.

- [188] S. Shen, P. A. Jaques, Y. Zhu, M. D. Geller, and C. Sioutas, “Evaluation of the smps-aps system as a continuous monitor for measuring pm_{2.5}, pm₁₀ and coarse (pm_{2.5}-10) concentrations,” *Atmospheric Environment*, vol. 36, no. 24, pp. 3939–3950, 2002, ISSN: 1352-2310. DOI: [https://doi.org/10.1016/S1352-2310\(02\)00330-8](https://doi.org/10.1016/S1352-2310(02)00330-8). [Online]. Available: <https://www.sciencedirect.com/science/article/pii/S1352231002003308>.
- [189] J. P. Shi, R. M. Harrison, and D. Evans, “Comparison of ambient particle surface area measurement by epiphaniometer and smps/aps,” *Atmospheric Environment*, vol. 35, no. 35, pp. 6193–6200, 2001, ISSN: 1352-2310. DOI: [https://doi.org/10.1016/S1352-2310\(01\)00382-X](https://doi.org/10.1016/S1352-2310(01)00382-X). [Online]. Available: <https://www.sciencedirect.com/science/article/pii/S135223100100382X>.
- [190] B. Sarangi, S. G. Aggarwal, D. Sinha, and P. K. Gupta, “Aerosol effective density measurement using scanning mobility particle sizer and quartz crystal microbalance with the estimation of involved uncertainty,” *Atmospheric Measurement Techniques*, vol. 9, no. 3, pp. 859–875, 2016. DOI: 10.5194/amt-9-859-2016. [Online]. Available: <https://amt.copernicus.org/articles/9/859/2016/>.
- [191] T. Incorporated, *Scanning mobility particle sizer model 3938 spec sheet us*, 2022.
- [192] P. H. McMurry, X. Wang, K. Park, and K. Ehara, “The relationship between mass and mobility for atmospheric particles: A new technique for measuring particle density,” *Aerosol Science and Technology*, vol. 36, no. 2, pp. 227–238, 2002. DOI: 10.1080/027868202753504083. [Online]. Available: <https://doi.org/10.1080/027868202753504083>.
- [193] B. Y. Liu and D. Y. Pui, “A submicron aerosol standard and the primary, absolute calibration of the condensation nuclei counter,” *Journal of Colloid and Interface Science*, vol. 47, no. 1, pp. 155–171, 1974, ISSN: 0021-9797. DOI: [https://doi.org/10.1016/0021-9797\(74\)90090-3](https://doi.org/10.1016/0021-9797(74)90090-3). [Online]. Available: <https://www.sciencedirect.com/science/article/pii/0021979774900903>.
- [194] J. L. Hand and S. M. Kreidenweis, “A new method for retrieving particle refractive index and effective density from aerosol size distribution data,” *Aerosol Science and Technology*, vol. 36, no. 10, pp. 1012–1026, 2002. DOI: 10.1080/02786820290092276. [Online]. Available: <https://doi.org/10.1080/02786820290092276>.
- [195] M. M. Maricq, D. H. Podsiadlik, and R. E. Chase, “Size distributions of motor vehicle exhaust pm: A comparison between elpi and smps measurements,” *Aerosol Science and Technology*, vol. 33, no. 3, pp. 239–260, 2000. DOI: 10.1080/027868200416231. [Online]. Available: <https://doi.org/10.1080/027868200416231>.
- [196] G. Buonanno, M. Dell’Isola, L. Stabile, and A. Viola, “Uncertainty budget of the smps-aps system in the measurement of pm₁, pm_{2.5}, and pm₁₀,” *Aerosol Science and Technology*, vol. 43, no. 11, pp. 1130–1141, 2009. DOI:

- 10.1080/02786820903204078. [Online]. Available: <https://doi.org/10.1080/02786820903204078>.
- [197] E. Mikhailov, S. Vlasenko, S. T. Martin, T. Koop, and U. Pöschl, “Amorphous and crystalline aerosol particles interacting with water vapor: Conceptual framework and experimental evidence for restructuring, phase transitions and kinetic limitations,” *Atmospheric Chemistry and Physics*, vol. 9, no. 24, pp. 9491–9522, 2009. DOI: 10.5194/acp-9-9491-2009. [Online]. Available: <https://acp.copernicus.org/articles/9/9491/2009/>.
- [198] M. Shiraiwa, M. Ammann, T. Koop, and U. Pöschl, “Gas uptake and chemical aging of semisolid organic aerosol particles,” *Proceedings of the National Academy of Sciences*, vol. 108, no. 27, pp. 11 003–11 008, 2011. DOI: 10.1073/pnas.1103045108. [Online]. Available: <https://www.pnas.org/doi/abs/10.1073/pnas.1103045108>.
- [199] L. Renbaum-Wolff *et al.*, “Viscosity of α -pinene secondary organic material and implications for particle growth and reactivity,” *Proceedings of the National Academy of Sciences*, vol. 110, no. 20, pp. 8014–8019, 2013. DOI: 10.1073/pnas.1219548110. [Online]. Available: <https://www.pnas.org/doi/abs/10.1073/pnas.1219548110>.
- [200] A. M. Maclean *et al.*, “Humidity-dependent viscosity of secondary organic aerosol from ozonolysis of β -caryophyllene: Measurements, predictions, and implications,” *ACS Earth and Space Chemistry*, vol. 5, no. 2, pp. 305–318, 2021. DOI: 10.1021/acsearthspacechem.0c00296. [Online]. Available: <https://doi.org/10.1021/acsearthspacechem.0c00296>.
- [201] M. L. Hinks *et al.*, “Effect of viscosity on photodegradation rates in complex secondary organic aerosol materials,” *Phys. Chem. Chem. Phys.*, vol. 18, pp. 8785–8793, 13 2016. DOI: 10.1039/C5CP05226B. [Online]. Available: <http://dx.doi.org/10.1039/C5CP05226B>.
- [202] A. Laskin, J. S. Smith, and J. Laskin, “Molecular characterization of nitrogen-containing organic compounds in biomass burning aerosols using high-resolution mass spectrometry,” *Environmental Science & Technology*, vol. 43, no. 10, pp. 3764–3771, 2009, PMID: 19544885. DOI: 10.1021/es803456n. [Online]. Available: <https://doi.org/10.1021/es803456n>.
- [203] P. Lin *et al.*, “Molecular characterization of brown carbon in biomass burning aerosol particles,” *Environmental Science & Technology*, vol. 50, no. 21, pp. 11 815–11 824, 2016. DOI: 10.1021/acs.est.6b03024. [Online]. Available: <https://doi.org/10.1021/acs.est.6b03024>.
- [204] R. J. Sheesley, J. J. Schauer, Z. Chowdhury, G. R. Cass, and B. R. Simoneit, “Characterization of organic aerosols emitted from the combustion of biomass indigenous to south asia,” *Journal of Geophysical Research: Atmospheres*, vol. 108, no. D9, 2003, 4285, 10.1029/2002JD002981.

- [205] I. J. George and J. P. D. Abbatt, “Heterogeneous oxidation of atmospheric aerosol particles by gas-phase radicals,” *Nature Chemistry*, vol. 2, no. 9, pp. 713–722, Sep. 2010, ISSN: 1755-4349. DOI: 10.1038/nchem.806. [Online]. Available: <https://doi.org/10.1038/nchem.806>.
- [206] R. Volkamer *et al.*, “Secondary organic aerosol formation from anthropogenic air pollution: Rapid and higher than expected,” *Geophysical Research Letters*, vol. 33, no. 17, 2006. DOI: <https://doi.org/10.1029/2006GL026899>. [Online]. Available: <https://agupubs.onlinelibrary.wiley.com/doi/abs/10.1029/2006GL026899>.
- [207] M. Canagaratna *et al.*, “Chemical and microphysical characterization of ambient aerosols with the aerodyne aerosol mass spectrometer,” *Mass Spectrometry Reviews*, vol. 26, no. 2, pp. 185–222, 2007. DOI: <https://doi.org/10.1002/mas.20115>. [Online]. Available: <https://analyticalsciencejournals.onlinelibrary.wiley.com/doi/abs/10.1002/mas.20115>.
- [208] J. T. Jayne *et al.*, “Development of an aerosol mass spectrometer for size and composition analysis of submicron particles,” *Aerosol Science and Technology*, vol. 33, no. 1-2, pp. 49–70, 2000. DOI: 10.1080/027868200410840. [Online]. Available: <https://doi.org/10.1080/027868200410840>.
- [209] W. Lindinger, A. Hansel, and A. Jordan, “On-line monitoring of volatile organic compounds at pptv levels by means of proton-transfer-reaction mass spectrometry (ptr-ms) medical applications, food control and environmental research,” *International Journal of Mass Spectrometry and Ion Processes*, vol. 173, no. 3, pp. 191–241, 1998, ISSN: 0168-1176. DOI: [https://doi.org/10.1016/S0168-1176\(97\)00281-4](https://doi.org/10.1016/S0168-1176(97)00281-4). [Online]. Available: <https://www.sciencedirect.com/science/article/pii/S0168117697002814>.
- [210] C. N. Hewitt, S. Hayward, and A. Tani, “The application of proton transfer reaction-mass spectrometry (ptr-ms) to the monitoring and analysis of volatile organic compounds in the atmosphere,” *J. Environ. Monit.*, vol. 5, pp. 1–7, 1 2003. DOI: 10.1039/B204712H. [Online]. Available: <http://dx.doi.org/10.1039/B204712H>.
- [211] R. S. Blake, P. S. Monks, and A. M. Ellis, “Proton-transfer reaction mass spectrometry,” *Chemical Reviews*, vol. 109, no. 3, pp. 861–896, 2009, PMID: 19215144. DOI: 10.1021/cr800364q. [Online]. Available: <https://doi.org/10.1021/cr800364q>.
- [212] R. Holzinger, J. Williams, F. Herrmann, J. Lelieveld, N. M. Donahue, and T. Röckmann, “Aerosol analysis using a thermal-desorption proton-transfer-reaction mass spectrometer (td-ptr-ms): A new approach to study processing of organic aerosols,” *Atmospheric Chemistry and Physics*, vol. 10, no. 5, pp. 2257–2267, 2010. DOI: 10.5194/acp-10-2257-2010. [Online]. Available: <https://acp.copernicus.org/articles/10/2257/2010/>.

- [213] J. Dallüge, J. Beens, and U. A. Brinkman, “Comprehensive two-dimensional gas chromatography: A powerful and versatile analytical tool,” *Journal of Chromatography A*, vol. 1000, no. 1, pp. 69–108, 2003, A Century of Chromatography 1903-2003, ISSN: 0021-9673. DOI: [https://doi.org/10.1016/S0021-9673\(03\)00242-5](https://doi.org/10.1016/S0021-9673(03)00242-5). [Online]. Available: <https://www.sciencedirect.com/science/article/pii/S0021967303002425>.
- [214] P. Marriott and R. Shellie, “Principles and applications of comprehensive two-dimensional gas chromatography,” *TrAC Trends in Analytical Chemistry*, vol. 21, no. 9, pp. 573–583, 2002, ISSN: 0165-9936. DOI: [https://doi.org/10.1016/S0165-9936\(02\)00814-2](https://doi.org/10.1016/S0165-9936(02)00814-2). [Online]. Available: <https://www.sciencedirect.com/science/article/pii/S0165993602008142>.
- [215] R. L. Grob and E. F. Barry, *Modern practice of gas chromatography*. John Wiley & Sons, 2004, ch. 7, pp. 339–403.
- [216] W. Wardencki, “Problems with the determination of environmental sulphur compounds by gas chromatography,” *Journal of Chromatography A*, vol. 793, no. 1, pp. 1–19, 1998, ISSN: 0021-9673. DOI: [https://doi.org/10.1016/S0021-9673\(97\)00997-7](https://doi.org/10.1016/S0021-9673(97)00997-7). [Online]. Available: <https://www.sciencedirect.com/science/article/pii/S0021967397009977>.
- [217] Z. Yang, N. T. Tsona, C. George, and L. Du, “Nitrogen-containing compounds enhance light absorption of aromatic-derived brown carbon,” *Environmental Science & Technology*, vol. 56, no. 7, pp. 4005–4016, 2022, PMID: 35192318. DOI: 10.1021/acs.est.1c08794. [Online]. Available: <https://doi.org/10.1021/acs.est.1c08794>.
- [218] K. S. Chow, X. H. H. Huang, and J. Z. Yu, “Quantification of nitroaromatic compounds in atmospheric fine particulate matter in hong kong over 3 years: Field measurement evidence for secondary formation derived from biomass burning emissions,” *Environmental Chemistry*, vol. 13, no. 4, pp. 665–673, 2016. DOI: 10.1071/EN15174. [Online]. Available: <https://doi.org/10.1071/EN15174>.
- [219] A. R. Koss *et al.*, “Non-methane organic gas emissions from biomass burning: Identification, quantification, and emission factors from ptr-tof during the firex 2016 laboratory experiment,” *Atmospheric Chemistry and Physics*, vol. 18, no. 5, pp. 3299–3319, 2018. DOI: 10.5194/acp-18-3299-2018. [Online]. Available: <https://acp.copernicus.org/articles/18/3299/2018/>.
- [220] M. C. Jacobson, H. C. Hansson, K. J. Noone, and R. J. Charlson, “Organic atmospheric aerosols: Review and state of the science,” *Reviews of Geophysics*, vol. 38, no. 2, pp. 267–294, 2000. DOI: <https://doi.org/10.1029/1998RG000045>. [Online]. Available: <https://agupubs.onlinelibrary.wiley.com/doi/abs/10.1029/1998RG000045>.

- [221] H. Bhattarai *et al.*, “Levoglucosan as a tracer of biomass burning: Recent progress and perspectives,” *Atmospheric Research*, vol. 220, pp. 20–33, 2019, ISSN: 0169-8095. DOI: <https://doi.org/10.1016/j.atmosres.2019.01.004>. [Online]. Available: <https://www.sciencedirect.com/science/article/pii/S0169809518311098>.
- [222] A. P. Sullivan *et al.*, “A method for smoke marker measurements and its potential application for determining the contribution of biomass burning from wild-fires and prescribed fires to ambient pm2.5 organic carbon,” *Journal of Geophysical Research: Atmospheres*, vol. 113, no. D22, 2008. DOI: <https://doi.org/10.1029/2008JD010216>. [Online]. Available: <https://agupubs.onlinelibrary.wiley.com/doi/abs/10.1029/2008JD010216>.
- [223] B. Simoneit *et al.*, “Levoglucosan, a tracer for cellulose in biomass burning and atmospheric particles,” *Atmospheric Environment*, vol. 33, no. 2, pp. 173–182, 1999, ISSN: 1352-2310. DOI: [https://doi.org/10.1016/S1352-2310\(98\)00145-9](https://doi.org/10.1016/S1352-2310(98)00145-9). [Online]. Available: <https://www.sciencedirect.com/science/article/pii/S1352231098001459>.
- [224] Y. Huo *et al.*, “Chemical fingerprinting of hulis in particulate matters emitted from residential coal and biomass combustion,” *Environmental Science & Technology*, vol. 55, no. 6, pp. 3593–3603, 2021, PMID: 33656861. DOI: 10.1021/acs.est.0c08518. [Online]. Available: <https://doi.org/10.1021/acs.est.0c08518>.
- [225] H. Wang *et al.*, “Source profiles of volatile organic compounds from biomass burning in yangtze river delta, china,” *Aerosol and Air Quality Research*, vol. 14, no. 3, pp. 818–828, 2014. DOI: 10.4209/aaqr.2013.05.0174. [Online]. Available: <https://doi.org/10.4209/aaqr.2013.05.0174>.
- [226] A. Bertrand *et al.*, “Evolution of the chemical fingerprint of biomass burning organic aerosol during aging,” *Atmospheric Chemistry and Physics*, vol. 18, no. 10, pp. 7607–7624, 2018. DOI: 10.5194/acp-18-7607-2018. [Online]. Available: <https://acp.copernicus.org/articles/18/7607/2018/>.
- [227] C. Warneke *et al.*, “An important contribution to springtime arctic aerosol from biomass burning in russia,” *Geophysical Research Letters*, vol. 37, no. 1, 2010. DOI: <https://doi.org/10.1029/2009GL041816>. [Online]. Available: <https://agupubs.onlinelibrary.wiley.com/doi/abs/10.1029/2009GL041816>.
- [228] K. Sekimoto *et al.*, “High- and low-temperature pyrolysis profiles describe volatile organic compound emissions from western us wildfire fuels,” *Atmospheric Chemistry and Physics*, vol. 18, no. 13, pp. 9263–9281, 2018. DOI: 10.5194/acp-18-9263-2018. [Online]. Available: <https://acp.copernicus.org/articles/18/9263/2018/>.
- [229] C. Y. Lim *et al.*, “Secondary organic aerosol formation from the laboratory oxidation of biomass burning emissions,” *Atmospheric Chemistry and Physics*, vol. 19, no. 19, pp. 12 797–12 809, 2019. DOI: 10.5194/acp-19-12797-2019. [Online]. Available: <https://acp.copernicus.org/articles/19/12797/2019/>.

- [230] W. Li *et al.*, “Tracers from biomass burning emissions and identification of biomass burning,” *Atmosphere*, vol. 12, no. 11, 2021, ISSN: 2073-4433. DOI: 10.3390/atmos12111401. [Online]. Available: <https://www.mdpi.com/2073-4433/12/11/1401>.
- [231] C. E. Stockwell, P. R. Veres, J. Williams, and R. J. Yokelson, “Characterization of biomass burning emissions from cooking fires, peat, crop residue, and other fuels with high-resolution proton-transfer-reaction time-of-flight mass spectrometry,” *Atmospheric Chemistry and Physics*, vol. 15, no. 2, pp. 845–865, 2015. DOI: 10.5194/acp-15-845-2015. [Online]. Available: <https://acp.copernicus.org/articles/15/845/2015/>.
- [232] K. E. Pickering *et al.*, “Convective transport of biomass burning emissions over Brazil during TRACE A,” *Journal of Geophysical Research: Atmospheres*, vol. 101, no. D19, pp. 23 993–24 012, 1996. DOI: <https://doi.org/10.1029/96JD00346>. [Online]. Available: <https://agupubs.onlinelibrary.wiley.com/doi/abs/10.1029/96JD00346>.
- [233] J. S. Fu *et al.*, “Evaluating the influences of biomass burning during 2006 base-asia: A regional chemical transport modeling,” *Atmospheric Chemistry and Physics*, vol. 12, no. 9, pp. 3837–3855, 2012. DOI: 10.5194/acp-12-3837-2012. [Online]. Available: <https://acp.copernicus.org/articles/12/3837/2012/>.
- [234] K. D. Bartle and P. Myers, “History of gas chromatography,” *TrAC Trends in Analytical Chemistry*, vol. 21, no. 9, pp. 547–557, 2002, ISSN: 0165-9936. DOI: [https://doi.org/10.1016/S0165-9936\(02\)00806-3](https://doi.org/10.1016/S0165-9936(02)00806-3). [Online]. Available: <https://www.sciencedirect.com/science/article/pii/S0165993602008063>.
- [235] R. L. Grob and E. F. Barry, *Modern practice of gas chromatography*. John Wiley & Sons, 2004, ch. 2-3,6, pp. 25–193,277–339.
- [236] I. G. McWILLIAM and R. A. DEWAR, “Flame ionization detector for gas chromatography,” *Nature*, vol. 181, no. 4611, pp. 760–760, Mar. 1958, ISSN: 1476-4687. DOI: 10.1038/181760a0. [Online]. Available: <https://doi.org/10.1038/181760a0>.
- [237] W. M. Niessen, *Liquid chromatography-mass spectrometry*. CRC press, 2006, ch. 1-2, pp. 3–53.
- [238] F. Gritti and G. Guiochon, “Mass transfer kinetics, band broadening and column efficiency,” *Journal of Chromatography A*, vol. 1221, pp. 2–40, 2012, Editors’ Choice VI, ISSN: 0021-9673. DOI: <https://doi.org/10.1016/j.chroma.2011.04.058>. [Online]. Available: <https://www.sciencedirect.com/science/article/pii/S0021967311005681>.
- [239] W. Niessen and A. Tinke, “Liquid chromatography-mass spectrometry general principles and instrumentation,” *Journal of Chromatography A*, vol. 703, no. 1, pp. 37–57, 1995, ISSN: 0021-9673. DOI: [https://doi.org/10.1016/0021-9673\(94\)01198-N](https://doi.org/10.1016/0021-9673(94)01198-N). [Online]. Available: <https://www.sciencedirect.com/science/article/pii/002196739401198N>.

- [240] S. Banerjee and S. Mazumdar, “Electrospray ionization mass spectrometry: A technique to access the information beyond the molecular weight of the analyte,” *International Journal of Analytical Chemistry*, vol. 2012, p. 282574, Mar. 2012, ISSN: 1687-8760. DOI: 10.1155/2012/282574. [Online]. Available: <https://doi.org/10.1155/2012/282574>.
- [241] L. E. Hatch, W. Luo, J. F. Pankow, R. J. Yokelson, C. E. Stockwell, and K. C. Barsanti, “Identification and quantification of gaseous organic compounds emitted from biomass burning using two-dimensional gas chromatography–time-of-flight mass spectrometry,” *Atmospheric Chemistry and Physics*, vol. 15, no. 4, pp. 1865–1899, 2015. DOI: 10.5194/acp-15-1865-2015. [Online]. Available: <https://acp.copernicus.org/articles/15/1865/2015/>.
- [242] W. Welthagen, J. Schnelle-Kreis, and R. Zimmermann, “Search criteria and rules for comprehensive two-dimensional gas chromatography–time-of-flight mass spectrometry analysis of airborne particulate matter,” *Journal of Chromatography A*, vol. 1019, no. 1, pp. 233–249, 2003, First International Symposium on Comprehensive Multidimensional Gas Chromatography, ISSN: 0021-9673. DOI: <https://doi.org/10.1016/j.chroma.2003.08.053>. [Online]. Available: <https://www.sciencedirect.com/science/article/pii/S0021967303015498>.
- [243] C. N. Jen *et al.*, “Speciated and total emission factors of particulate organics from burning western us wildland fuels and their dependence on combustion efficiency,” *Atmospheric Chemistry and Physics*, vol. 19, no. 2, pp. 1013–1026, 2019. DOI: 10.5194/acp-19-1013-2019. [Online]. Available: <https://acp.copernicus.org/articles/19/1013/2019/>.
- [244] M. Abou-Ghanem *et al.*, “Significant variability in the photocatalytic activity of natural titanium-containing minerals: Implications for understanding and predicting atmospheric mineral dust photochemistry,” *Environmental Science & Technology*, vol. 54, no. 21, pp. 13 509–13 516, 2020, PMID: 33058682. DOI: 10.1021/acs.est.0c05861. [Online]. Available: <https://doi.org/10.1021/acs.est.0c05861>.
- [245] J. W. Adams, D. Rodriguez, and R. A. Cox, “The uptake of so₂ on saharan dust: A flow tube study,” *Atmospheric Chemistry and Physics*, vol. 5, no. 10, pp. 2679–2689, 2005. DOI: 10.5194/acp-5-2679-2005. [Online]. Available: <https://acp.copernicus.org/articles/5/2679/2005/>.
- [246] Y. Liu, A. V. Ivanov, and M. J. Molina, “Temperature dependence of oh diffusion in air and he,” *Geophysical Research Letters*, vol. 36, no. 3, 2009. DOI: <https://doi.org/10.1029/2008GL036170>. [Online]. Available: <https://agupubs.onlinelibrary.wiley.com/doi/abs/10.1029/2008GL036170>.
- [247] J. Fast *et al.*, “Evaluating simulated primary anthropogenic and biomass burning organic aerosols during milagro: Implications for assessing treatments of secondary organic aerosols,” *Atmospheric Chemistry and Physics*, vol. 9, no. 16, pp. 6191–6215, 2009. DOI: 10.5194/acp-9-6191-2009. [Online]. Available: <https://acp.copernicus.org/articles/9/6191/2009/>.

- [248] V. Choudhary, M. Loebel Roson, X. Guo, T. Gautam, T. Gupta, and R. Zhao, “Aqueous-phase photochemical oxidation of water-soluble brown carbon aerosols arising from solid biomass fuel burning,” *Environ. Sci.: Atmos.*, pp. –, 2023. DOI: 10.1039/D2EA00151A. [Online]. Available: <http://dx.doi.org/10.1039/D2EA00151A>.
- [249] L. T. Fleming *et al.*, “Emissions from village cookstoves in haryana, india, and their potential impacts on air quality,” *Atmospheric Chemistry and Physics*, vol. 18, no. 20, pp. 15 169–15 182, 2018. DOI: 10.5194/acp-18-15169-2018. [Online]. Available: <https://acp.copernicus.org/articles/18/15169/2018/>.
- [250] M. Mouton *et al.*, “The hygroscopic properties of biomass burning aerosol from eucalyptus and cow dung under different combustion conditions,” *Aerosol Science and Technology*, vol. 0, no. 0, pp. 1–13, 2023. DOI: 10.1080/02786826.2023.2198587. [Online]. Available: <https://doi.org/10.1080/02786826.2023.2198587>.

Chapter 2

Chemical Characterization of Emissions Arising from Solid Fuel Combustion - Contrasting Wood and Cow Dung Burning

Reprinted with permission and minor formatting changes from its original publication as:

M. Loebel Roson, R. Duruisseau-Kuntz, M. Wang, K. Klimchuk, R. J. Abel, J. J. Harynuk, and R. Zhao, “Chemical characterization of emissions arising from solid fuel combustion—contrasting wood and cow dung burning,” *ACS Earth and Space Chemistry*, vol. 5, no. 10, pp. 2925–2937, 2021. DOI: 10.1021/acsearthspacechem.1c00268. Copyright 2021 American Chemical Society.

2.1 Introduction

The burning of biomass is a major source of particulate matter, or aerosol, which affects both the air quality and Earth’s climate [251–254]. Air-quality-related morbidity is one of the leading causes of death worldwide [255]. In particular, household combustion of solid fuels (wood, coal, agriculture waste, animal waste, and any other combustible solid) is a leading cause of premature death on the global scale [11, 256]. Fires also contribute to positive atmospheric radiative forcing – the difference in sunlight absorbed versus reflected by the atmosphere – by releasing aerosols in the form of black and brown carbon (BC and BrC, respectively) [44, 50, 257, 258].

Behind BC, BrC is the second-most important light-absorbing aerosol in the atmosphere [36, 37]. Biomass burning represents the bulk of all BrC aerosol emissions [9, 258, 259]. BrC is emitted during incomplete combustion, such as when cooking using solid fuels with insufficient airflow [44]. BrC typically absorbs light in the UV and near-visible spectrum, which gives plumes their characteristic brown colour [44]. Although BC has been studied extensively, understanding of the optical properties of BrC arising from biomass burning, particularly solid fuel burning, is lacking [42, 44, 55, 158, 257, 260]. Consequently, BrC is still referred to as a scattering aerosol in some climate forcing models as opposed to an absorbing one [36, 41, 55].

Health outcomes associated with exposure to fire emissions worsen when less-refined fuels are burned. This effect is compounded further in an indoor setting, as exposure rises [261, 262]. Such burning conditions are prevalent in middle- and low-income countries. In 2000, only 22% of Indian households had access to clean (refined) fuels for cooking. This number rose to about 40% by 2016 both in India and globally, with liquid fuels, gaseous fuels, or electricity seeing more widespread use. Still, only about 14% of households in Sub-Saharan Africa had access to clean fuel for cooking at the time [6]. Poor access to clean fuels leads households in these regions to rely heavily on biomass such as wood or animal waste as fuel. With such widespread use, identifying and characterizing emissions from solid fuels and their effects on both climate and health is imperative.

Biomass burning emissions are notoriously difficult to characterize [43, 44, 123, 158, 203, 263, 264]. Nevertheless, numerous studies have examined the emissions of wood

fires in the past [123, 158, 203, 265]. As a result, emissions from wood burning are better-defined than for other biomass types. Fuels that are not used in Western countries are not studied as often, and therefore the impacts of their emissions can not currently be predicted. Omitting fuels from studies because they are not considered Western-relevant creates a standard of dubious environmental equity. Quantitative prediction of the climate and health impacts of emissions from biomass burning requires accurate chemical information [42, 43, 261]. Among solid fuels other than wood, cow dung is commonly used in India and Sub-Saharan Africa for cooking and heating [6, 157]. Dung burning has been shown to emit highly oxidizing particulate matter, with probable adverse health effects [261, 266]. Considering the challenge in characterization and how little-to-no cow manure is used as fuel in Western countries, it is not surprising that few studies have reported on its emissions [204, 249, 261, 262, 266–268].

The challenge associated with characterizing biomass burning aerosol is related to the variability in composition of biomass burning emissions. The exact nature of these emissions will depend on fluctuating parameters, such as fuel types, local air flow, fuel morphology, and composition [44, 158, 264, 266]. As a result, controlling parameters that affect emission composition is of high importance for characterization. A combination of targeted and untargeted analyses are required to provide a comprehensive understanding of biomass burning.

Targeted identification and quantification of tracer compounds is often employed for burn source apportionment and impact prediction [61, 79, 221, 223, 265]. Levoglucosan is a by-product of the pyrolysis of cellulose and one such tracer [221, 223]. It is targeted as a tracer for wood smoke due to the magnitude of its emission and its relatively long atmospheric lifetime [61, 221, 223]. Cellulose content varies between plant species, [150] directly influencing the amount of levoglucosan emitted from different fuel types [61, 204, 269]. As far as the authors are aware, only a single study has reported the emission factor of levoglucosan from dung burning [204]. While there exist tracers, such as coprostanol [204], universal to most types of higher animal faeces, a biomass burning tracer with a well-defined emission factor, and specific to cow dung, has not been identified as of time of writing. Identification of such a tracer would facilitate dung-burning source apportionment, understanding of emission toxicity, and

propensity to undergo subsequent atmospheric chemistry. Discovery of unrecognized tracer compounds can be achieved only through non-targeted analyses; in which the compounds of interest have not yet been catalogued in the literature.

Herein, we provide fundamental chemical information for biomass fuels, with an overall aim to identify the differences between wood and cow dung, and the connection between fuel composition and subsequent emissions. Specifically, we include light absorptive features, chemical signature identification, and emission factors from levoglucosan and its isomers. Our work represents the first in-depth laboratory analysis of emissions from cow dung burning.

2.2 Materials and Methods

2.2.1 Solid Fuels

Three types of fuels are used in this study: firewood, dried cow dung from a local Canadian farm (CAD), and cow dung cakes purchased from India (IND). Pictures of wood (b), CAD (c), and IND (d) biomass are provided in Figure 2.1. The firewood sample was collected from Lodgepole Pine (*Pinus Contorta*) and was purchased from a local store. The CAD sample was collected from Mattheis Ranch, an experimental farm managed by the Rangeland Research Institute of the University of Alberta. The CAD were naturally dried on the pasture. The IND samples were purchased through a major online shopping platform. The samples were manufactured in India, advertised as “pure cow dung” for spiritual and ritual activities. All samples were stored in a laboratory fume hood prior to analysis. CAD samples were further dried using a desiccator.

2.2.2 Elemental Analysis of Solid Fuels

To obtain insights into the composition of each fuel type used, elemental analyses were conducted using a Thermo Flash 2000 CHNS-O elemental analyzer following a method similar to that in Shabbar and Janajreh [270]. Biomass samples were separately ground inside a ZM 200 Retsch centrifugal mill. The ground samples were then combusted at 1000 °C inside the elemental analyzer. Using a known amount of pure oxygen, the carbon, hydrogen, nitrogen, and sulphur were converted to CO₂,

H₂O, NO_x, and SO₂, respectively, with NO_x being further converted to N₂. The gases were then transferred to a chromatographic column for separation and detection using a thermal conductivity detector. The peak area of each gas was used to obtain the percentage content of each element in the original biomass samples. Measurements for each sample were automatically taken in triplicate by the instrument.

2.2.3 Solid Fuel Burning and Sample Collection

Combustion of solid fuels was conducted in a home-built apparatus, illustrated in Figure 2.1(a). The entire apparatus is placed inside a fume hood to ensure safety. Biomass samples were heated to 500 °C inside a quartz tube ($\frac{1}{2}$ inch i.d.) contained in a Carbolite E-series tube furnace. A constant flow of 0.2 slpm air controlled using a mass flow controller was provided through an airtight 1" Ultra-Torr Vacuum Fitting sold by Swagelok Inc. upstream of the quartz tube. The quartz tube outlet was open to ambient surroundings. A stainless-steel tube ($\frac{1}{4}$ inch o.d.) inserted through the quartz tube outlet led to a stainless filter holder and subsequently to the house vacuum. The house vacuum resulted in a suction flow rate of approximately 60 lpm. As the biomass samples were heated inside the quartz tube, their emissions were carried downstream by the air flow into the stainless-steel tube and further towards the filter holder to be gathered on the surface of a quartz or glass filter. The temperature ramp for the tube furnace was set to 100 °C/min up to 500 °C, starting from room temperature at ~20 °C. The temperature inside the tube furnace was measured using a type K thermocouple, which indicated 500 °C was reached after 4.9 min (Figure 2.2). Total suspended particles were gathered on filters throughout the ramping process and for 10 minutes after reaching 500 °C.

Given that the air supply through the tube furnace was 0.2 slpm and the suction flow through the filter was 60 lpm, emissions collected on the filter were substantially diluted by the room air. Filters were kept frozen at -20 °C and were analyzed within three months of sampling. No decay is expected within this time frame, although the chemistry happening on frozen filters has not been previously studied. For selected experiments, a scanning mobility particle sizer (SMPS) was connected to the quartz tube outlet by way of a t-junction before the filter holder to observe particle size and concentration. Airflow to the SMPS was diluted by a factor of ten by a second

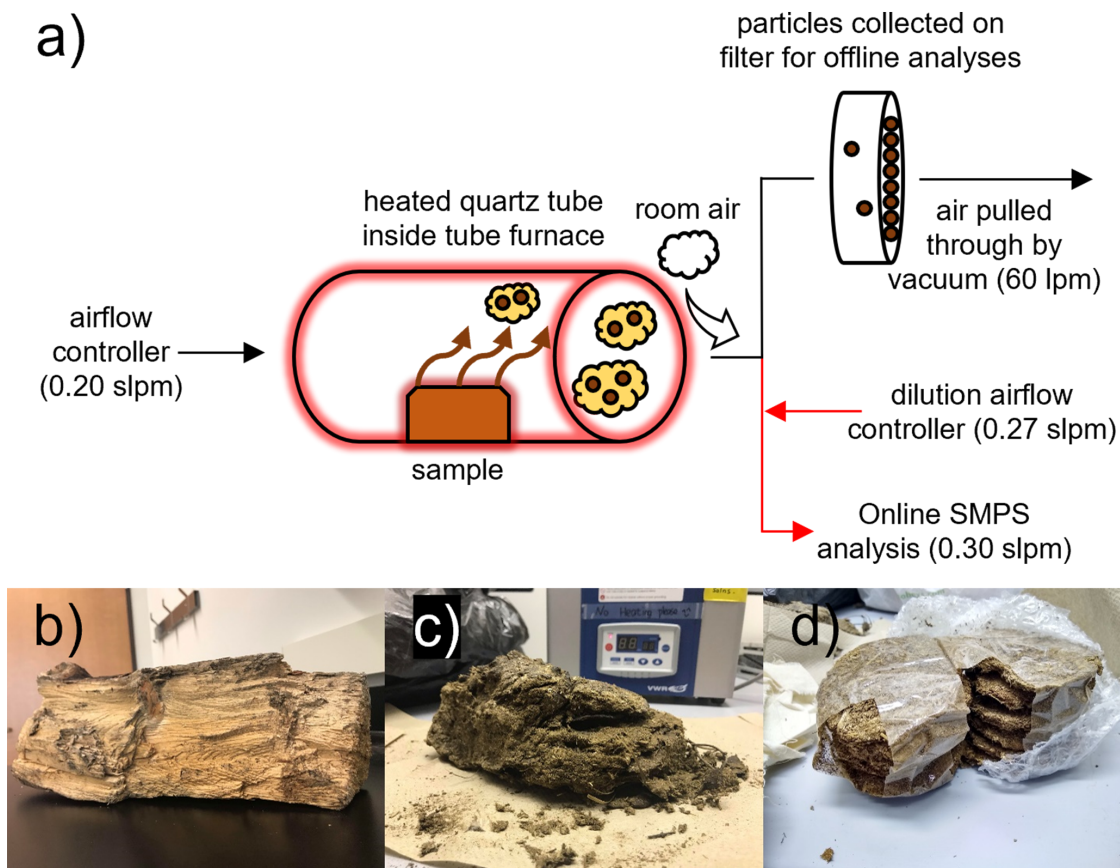


Figure 2.1: Schematic Diagram of Tube Furnace Setup (a) and Pictures of Wood (b), CAD (c), and IND (d) Biomass Fuels.

mass flow controller. The SMPS is a TSI Inc. unit including a model 3080 classifier, a 3081 differential mobility analyzer, and a 3776 particle counter. The instrument was set to scan particles between 15 nm to 670 nm every 2 min for 1 h, with a size resolution of 64 channels/decade of particle diameter. To derive particle mass concentrations, all particles were assumed to be spherical with a uniform density of 1.2 g/mL. Each sample filter was cut into 4 equally sized fractions and further extracted in water or acetonitrile (ACN) by stirring for 40 min. All the filters were pre-cleaned by heating at 600 °C for 4 h. The filter holder was cleaned with solvent (methanol) between each combustion experiment. Similarly, the quartz tube was cleaned between each combustion experiment by heating to 600 °C. The cleanliness of the quartz cylinder and the filter holder was confirmed by heating the tube itself with no sample present, which did not result in aerosol emissions. Blank filters were collected by performing the same procedure, confirming the lack of emissions from

the apparatus in the absence of a sample.

2.2.4 Quantification of Levoglucosan using GC-MS

Levoglucosan in the filter extracts was quantified using gas chromatography mass spectrometry (GC-MS). Levoglucosan was silylated to improve its chromatographic response [271]. As an internal standard, 500 μg of methyl- β -D-xylopyranoside were added to small portions cut from each filter. Filters were then extracted in 2 mL of DCM:MeOH (2:1 by volume) for 1 hour in a bath sonicator. A recovery of 74% was determined by spiking blank filters with a known concentration of levoglucosan and methyl- β -D-xylopyranoside, and extracting them in the same manner. Filter extracts were filtered into vials with a 0.2 μm PTFE syringe filter and dried completely under a stream of nitrogen. 200 μL of pyridine and 200 μL of N,O-Bis(trimethylsilyl)trifluoroacetamide were added to the dried extracts as per previous studies [271], and the vials shaken vigorously by hand. The vials were then placed in a water bath at 80 $^{\circ}\text{C}$ for 2 hours to allow for sufficient time for derivatization. Solutions were then cooled for 30 minutes before drying. Finally, the dried and derivatized samples were redissolved in GC grade DCM before GC-MS analysis. The derivatization mechanism is provided in Figure A.1.

Quantification of levoglucosan was achieved through calibration using standard solutions. Calibration standards were prepared by serially diluting a stock solution of levoglucosan, 1.85 mM in DCM. The internal standard was added by spiking 0.305 mM of methyl- β -D-xylopyranoside into each of the levoglucosan standards. The completeness of derivatization was confirmed from the absence of a GC-MS peak attributed to incompletely derived levoglucosan, with a mass to charge (m/z) of 116 [272]. The levoglucosan measurements were conducted on a single quadrupole GC-MS instrument model 7890A GC with a 7683B autosampler and a 5975C MSD from Agilent Technologies. A HP-5 Column with a (5%-phenyl)-methylpolysiloxane phase, helium carrier gas and a 10:1 split injection were used for separation. The GC heating parameters were as follows: 1 mL/min flow rate. Initial temperature set to 65 $^{\circ}\text{C}$ with a 2 min hold. Ramping at a rate of 6 $^{\circ}\text{C}/\text{min}$ to 300 $^{\circ}\text{C}$ followed by a 10 min hold, totalling to a 51 min runtime.

2.2.5 Total Organic Carbon (TOC) and Total Nitrogen (TN) Measurements

TOC and TN content of the biomass emissions were measured using a Shimadzu TOC-L CPH Analyzer with a Total Nitrogen Unit [273]. Filters for these analyses were extracted in water, as required by the instruments. Organic carbon was measured using the non-purgeable organic carbon (NPOC) method. The NPOC procedure involves removing the inorganic carbon fraction by purging the extracted sample with an inert gas. Organic carbon left in the sample after sparging is then converted to CO₂ and detected using a non-dispersive infrared detector. The NPOC method is a more accurate method for TOC analysis than the Total Carbon/Inorganic Carbon method. However, some volatile organic compounds may be lost during purging, leading to an underestimation of TOC content [274, 275]. TN was obtained by combusting the samples to form NO_x, which was then reacted with ozone to form NO₂ in an excited state. Photons emitted by the NO₂ were then quantified as nitrogen using a chemiluminescence detector.

2.2.6 Characterization of Light Absorption

Light-absorption measurements were taken on a Hewlett Packard 8453 UV-VIS Spectrophotometer. The filter extracts were diluted by a factor of 5-10 to allow reliable UV-Vis measurement between 300 and 500 nm. Absorption was measured by holding individual extracts in a standard 1 cm quartz cuvette and scanning through wavelengths from 190-800 nm. Filters for this analysis were extracted in water, such that the UV-Vis data can be combined with the TOC/TN data which also represents the water-soluble fraction, to obtain the mass absorption coefficient (MAC). MAC represents a mass-normalized absorption parameter of BrC, calculated using Eqn 2.1 [276]:

$$MAC_{(\lambda)} = \frac{A_{(\lambda)} \times \ln(10)}{B \times C_{\text{mass}}} \quad (2.1)$$

Where $A(\lambda)$ is the base-10 log of absorbance at a given wavelength, $B(\text{cm})$ the path length, and $C_{\text{mass}}(\text{mg/L})$ the mass of absorbing organic matter. C_{mass} was calculated

using the previously obtained TOC values (available in Table 2) converted to organic matter mass with an organic mass-to-carbon ratio of 1.5, as per Russell [277] and Hoffer *et al.* [278].

2.2.7 Non-Targeted Organic Analysis with LC-MS

Biomass combustion samples are most commonly extracted in water, ACN, methanol, or mixtures of multiple solvents [109]. It has been shown that organic solvents can dissolve a larger fraction of organic species present in samples from biomass burning [109]. For our non-targeted analysis, we extracted the filter samples in ACN to maximize the number of extractable analytes. The extracts were filtered into vials using 0.2 μm PTFE syringe filters, prior to liquid chromatography-mass spectrometry (LC-MS) analysis. An Agilent Technologies 6220 oaTOF was used to obtain high-resolution measurements.

Positive and Negative Electrospray Ionization (ESI+ and ESI- respectively) were employed as ionization techniques. ESI+ and ESI- are “soft” ionization techniques which are well suited to identify molecules without extensive fragmentation. Positive or negative refers to the voltage applied to the molecules by the ESI source and the mechanism by which the species are ionized. The applied voltage ultimately determines the classes of compounds that can be detected by the mass spectrometer. In ESI+ mode, compounds capable of accepting a proton(s) will be ionized and detected as $[\text{M}+\text{H}]^+$. Alternatively, oxygenated compounds can form ion clusters with background NH_4^+ and Na^+ [279]. Conversely in ESI-, only species which can lose an acidic proton(s) are detectable (e.g., carboxylic acids and phenols). Neither ionization mode can detect all compound classes present in biomass burning emissions. ESI+ and ESI- were used in tandem to provide a broader identification of compound classes.

Separation was performed on a Luna Omega 3 μm Polar C18 100 \AA Column (150 x 2.1 mm) purchased from Phenomenex Inc. A binary mobile phase system was used, consisting of water (Solvent A) and ACN (Solvent B) both buffered with 0.05% formic acid and delivered at a constant flow rate of 0.3 mL/min. The initial mobile phase composition was 90% A and 10% B. This composition was held for the first minute of the run. Following, B was ramped up to 20% from 1 to 3 min, followed by a ramp

up to 95% from 3 to 26 min, and a 3 min hold before returning to 10% B over 1 min. LC-MS data were analyzed using MassHunter software (v. B.07.00). The peak threshold was set to 2.5% of the largest peak observed for a given sample. Candidate elemental formulae were filtered using limits on the allowed number of each element as follows: C - 3 to 60, H - 0 to 120, N - 0 to 3, and O - 0 to 30. Elements such as F, K, P, S, and Cl were disregarded as they exponentially increased the number of possible elemental combinations, leading to improbable chemical compositions being assigned by the software. MassHunter data was then transferred to MATLAB software (v. R2019a) for a refined analysis using a custom written script. Briefly, unrealistic compositions were excluded based on their mass accuracy (>5 ppm) and double bond equivalence, with $[M+H]^+$ or $[M-H]^-$ as potential ion fragments. The final output consisted of chemical compositions for over 100 of the major peaks for each of the fuels.

2.3 Results and discussion

2.3.1 Elemental Composition of Solid Fuels

Mean elemental composition of each of the biomass samples is given in Table 2.1. Exact elemental composition is variable between wood species [280]. Nonetheless, our results agree with those observed for other pine species in previous studies [280–282]. As seen from Table 2.1, C, H, and O comprise the vast majority of the fuel mass, assuming that the remaining fraction of elemental composition is attributable to O. The most distinct difference between fuel types is in the nitrogen content. The two dung samples contain 1.0 and 0.7% of nitrogen, while wood is below the detection limit. Nitrogen is an important component in the formation of amino acids, the basic components of proteins, which may account for the higher nitrogen content in dung vs. wood.

Studies on dung composition usually focus on the components that improve its use as a fertilizer. In an agricultural context, elements available for plant uptake are the most relevant. Thus, a significant portion of the studies report the concentration of organic carbon and nitrogen, as well as available phosphorus and potassium, amongst others [283–287]. The reported concentrations vary significantly between studies, a

Table 2.1: Mean Elemental Composition of Ground Biomass \pm Standard Deviation.

Biomass	Weight (mg)	%N	%C	%H	%S
Wood	1.75 ± 0.034	<0.1	48.1 ± 0.12	5.96 ± 0.029	<0.2
IND	1.78 ± 0.14	0.703 ± 0.0091	41.1 ± 0.036	5.02 ± 0.026	<0.2
CAD	1.82 ± 0.021	1.01 ± 0.0044	43.7 ± 0.0082	5.47 ± 0.038	<0.2

n = 3 for each biomass type.

result of the composition's dependence on the diet of the animal in question [283, 284]. Total nitrogen and carbon content have been reported in the range of 9-70 g/kg and 380-460 g/kg respectively [285, 286]. The carbon content of both CAD and IND observed in Table 2.1 agrees with these ranges. On the other hand, the total nitrogen content in CAD and IND are near the lower end of these concentrations. Still, the relative proximity of our wood composition results to existing literature supports the validity of our determination of cow dung composition.

2.3.2 Combustion Process

The evolution of large amounts of smoke began about 3 minutes into the heating program for each of the samples, when temperatures neared 300 °C. This is consistent with initial stages of pyrolysis and thermal decomposition [288]. The observed smoke began as grey in color, turning and remaining a brown-yellowish color throughout most of the burn; evidence of the large emissions of light absorbing BrC. For select samples, the size and concentration of the emitted particulate matter was investigated throughout the heating process. The SMPS data from an experiment burning IND is presented in Figure 2.2 as an example. Wood (Figure A.2) and CAD burning (Figure A.3) are available in our Supporting Information.

As can be seen in Figure 2.2, particle emission begins between 3-6 minutes into the heating process, with the largest quantity of particles being emitted early on at the 4-6 minute mark, when the temperature reaches its maximum. At the peak of particle emission, the particle mass concentration translates to 1.6 mg/m^3 , assuming a particle density of 1.2 g/ml. However, this mass concentration is likely an underestimate, given that some particles were larger than the maximum size range detectable

using the SMPS employed here (661.2 nm). While the particle concentration started declining from this point, the median particle size remained at approximately 200 nm throughout the burning experiment. Particles are detected by the SMPS up to 50 minutes after the start of the temperature program, long after the heating process is complete.

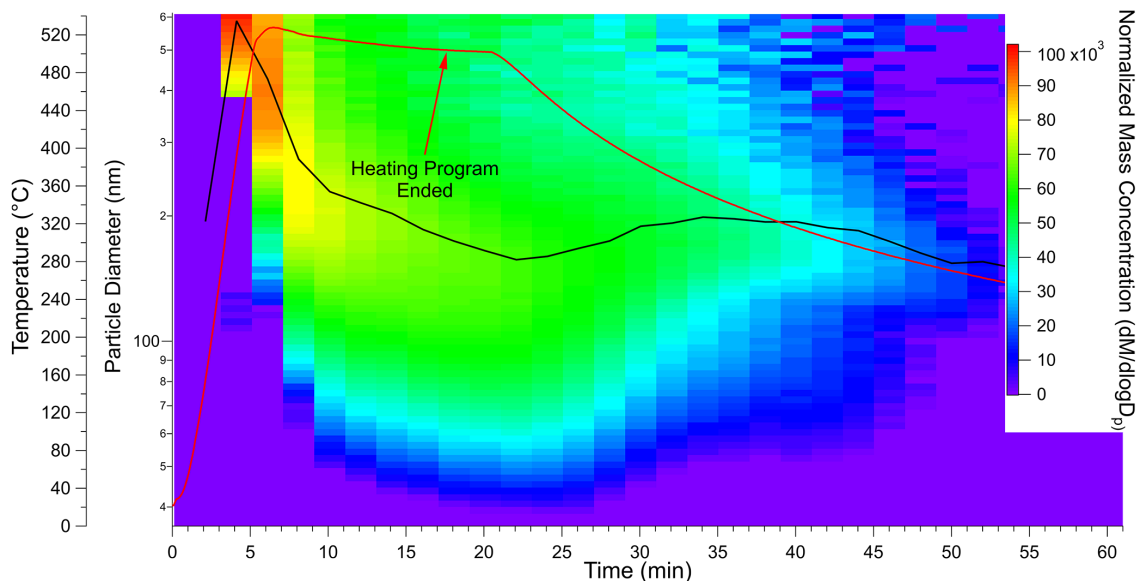


Figure 2.2: Normalized mass concentration ($dM/d\log D_p$) and particle diameter (nm) of biomass burning emissions throughout the IND heating process. The heatmap represents the particle mass concentration (dM) in $\mu g/m^3$ normalized by the number of channels per decade of particle resolution ($d\log D_p$) of the instrument. The black line represents the median particle diameter. The red line represents the temperature measured throughout the heating process using a thermocouple inside the quartz tube.

Some particle evolution at the end of the heating program is to be expected as the tube furnace retains heat well, especially while the quartz tube is present. Still, the continued particle emission is evidence of an ongoing smouldering process, visually confirmed by the appearance of the biofuel inside the furnace. Venkataraman and Rao [266] have previously investigated particle emissions from wood and dung from cooking stoves commonly employed in India. Their findings indicate that dung burning leads to significantly more particles than wood burning. Venkataraman and Rao [266] have also shown that - in traditional mud-based Indian stoves - less particles are emitted as the combustion temperature increases. Although the experimental setup was very different, this effect was not observed within our study. However, the

applied 60 lpm vacuum at the outlet of the tube furnace was much larger than the 0.30 slpm pull of the SMPS. As the pull of the SMPS varied between analyses, providing a similar dilution through the second mass flow controller - Figure 2.1(a) - was challenging. As a consequence, the particle concentration values presented in Figure 2.2, Figure A.2, and Figure A.3 are not comparable between each other. Nonetheless, the median particle diameter should be relatively unaffected by minor variations in the vacuum provided by the SMPS, and was very similar between each of the fuels. Overall, the median particle diameters observed are slightly higher than reported in other studies using similar fuels [289–293]. This is an expected consequence of the relatively low air flow and temperature provided to the tube furnace. Alternatively, the flow differential at the t-junction could cause smaller particles to be more easily deflected by the higher 60 lpm vacuum flow. This would lead to an underestimation of particles with smaller diameter.

2.3.3 Total Organic Carbon and Total Nitrogen

Table 2.2 lists the observed TOC and TN for each of the biomass filter extracts in water. Detection is therefore contingent on the emissions being soluble in water. Triplicate measurements were made for each of the three fuel types with mean measurements and standard deviations reported. A blank filter extracted in water resulted in negligible TOC and TN concentrations compared to those detected from filter samples, i.e., <1.8 mg/L and <0.14 mg/L, respectively. As can be seen from Table 2.2, the TOC and TN are highly variable between samples, reflecting the variation in the mass of fuel burned and the quantity of particles collected on filters. The TN/TOC ratio was consistent between samples of the same type regardless of differences in the mass of sample or loading of the filter. The TN/TOC ratio of the two dung samples are much higher than that of the wood sample. This trend mirrors the results of elemental analysis presented in Table 2.1, implying that the higher nitrogen content in the dung samples resulted in higher TN values in their emissions.

Table 2.2: Total Organic Carbon and Total Nitrogen Content of each Biomass. Mean \pm Standard Deviation.

Biomass ($n = 3$)	TOC (mg/L)	TN (mg/L)	TN/TOC
Wood	411 (± 139)	0.978 (± 0.358)	$(2.38 (\pm 1.18)) \times 10^{-3}$
IND	262 (± 124)	16.3 (± 8.07)	$(6.23 (\pm 4.26)) \times 10^{-2}$
CAD	137 (± 47.6)	8.32 (± 2.33)	$(6.06 (\pm 2.70)) \times 10^{-2}$

2.3.4 UV-Vis Absorption of Filter Extracts and Mass Absorption Coefficients

The water-soluble organic compounds extracted from our filter samples exhibited absorptive features typical to BrC; i.e., highly wavelength-dependent absorption that increases exponentially towards the shorter wavelength [43]. Both Pandey *et al.* [267] and Fleming *et al.* [249] have previously reported MAC for dung-cake and fuel-wood burned in traditional Indian cook stoves. Summarily, Pandey *et al.* analyzed non-extracted fuel-wood filters under direct UV, showing organic carbon MAC values ranging from $\sim 1.0 \times 10^4 \text{ cm}^2/\text{g}$ to $\sim 8.0 \times 10^4 \text{ cm}^2/\text{g}$ at 350 nm (95% CI around the mean). Cow dung filters similarly show $\sim 1.7 \times 10^4 \text{ cm}^2/\text{g}$ to $\sim 6.5 \times 10^4 \text{ cm}^2/\text{g}$ at the same wavelength and confidence interval. The variation between measurements lessens when moving towards higher wavelengths. Likewise, Fleming *et al.* show - for the organic extractable fraction of biomass filters - MACs of $\sim 2.8 \times 10^4 \text{ cm}^2/\text{g}$ to $\sim 7 \times 10^4 \text{ cm}^2/\text{g}$ for brushwood and $\sim 1.7 \times 10^4 \text{ cm}^2/\text{g}$ to $\sim 3.7 \times 10^4 \text{ cm}^2/\text{g}$ for cow dung at 350 nm. In their study, the wide range in MAC values obtained for identical fuels is attributed to extraction efficiency and sampling flow rate errors. The variation between their measurements also decreases at higher wavelengths. Fleming *et al.* also indicate that nonpolar polycyclic aromatic hydrocarbons (PAHs) may account for up to 40% of the total absorbance of sagebrush biomass burning organic aerosol. PAHs are largely undetectable by the LC-MS methods used in our work [294]. Their impacts however, can still be predicted by studying their light-absorptive properties. Figure 2.3 represents the calculated MAC of the water-soluble organic compounds emitted from each fuel type. A replicate measurement was performed for each fuel

type, and the MAC values were found to be highly reproducible within fuel classes, see Figure A.4. As can be seen in Figure 2.3, the MACs observed here, i.e., ranging between 8.0×10^3 and 1.1×10^4 cm^2/g at 350 nm, are lower than the range reported in previous studies [249, 267, 295]. We posit that water extraction may have resulted in less chromophores being detected in our study, compared to the literature, in which organic solvents were used. Alternatively, the low MAC values obtained in our study may be a result of the current burning setup, in which the entire plume is collected on the filter without much space for controlled dilution.

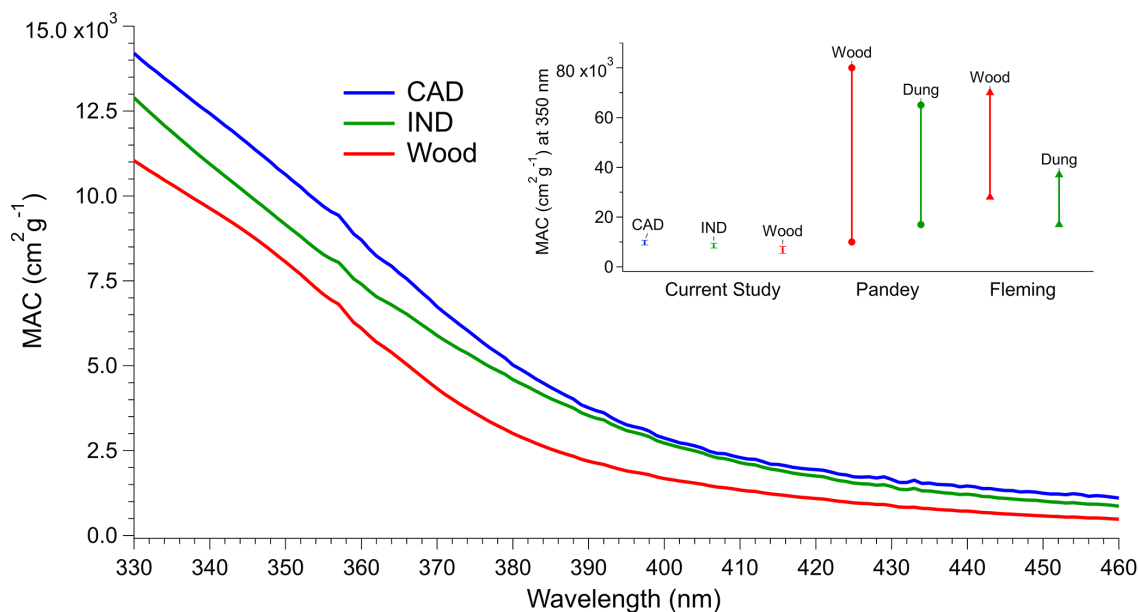


Figure 2.3: Mass Absorption Coefficient (MAC) of water soluble fraction of emissions from the three types of biomass fuels. The sub window contains biomass MACs obtained in the current study as well as values reported by Pandey *et al.* [267] and Fleming *et al.* [249] at 350 nm.

It has been shown that semi-volatile organic compounds (SVOCs) may undergo partitioning to the particle-phase when the aerosol load is high; i.e., near the emission source [296]. Extensive amounts of non-absorbing SVOCs collected in our filter samples may result in a higher TOC value; and thus smaller MAC values. Investigations of the impact of particle dilution on the observed chemical composition is an important topic beyond the scope of the current work. Future studies should revisit the optical properties of dung emissions with setups that allow for variable, controlled particle dilution.

Interestingly, both CAD and IND show higher MAC values than wood, especially in the visible range (Figure 2.3). This is an indication that water-extractable chromophores from dung burning could be as strong light absorbers as those emitted from wood. As such, we investigate the composition of these emissions through LC-MS further in this work.

2.3.5 Emission Factors of Levoglucosan and its Structural Isomers

A representative GC-MS chromatogram of the three biomass fuels is shown in Figure 2.4. Individual spectra are available in Section A.1.4. The peak at 21.65 min is attributed to the fully silylated levoglucosan, as confirmed by its mass spectrum (inset). The fragmentation pattern exhibited excellent agreement (>80% match, Figure A.8) with the NISTMS library (2017) and literature [297]. The peak at 21.05 is attributed to the internal standard, methyl- β -D-xylopyranoside. Other significant peaks include galactosan and mannosan (structural isomers of levoglucosan) at 20.85 and 21.25 min, respectively [297]. Overall, the wood samples exhibit by far the largest levoglucosan peak, while IND extracts contained a considerable amount, about 25% compared to wood, and CAD about 10% of the amount in wood.

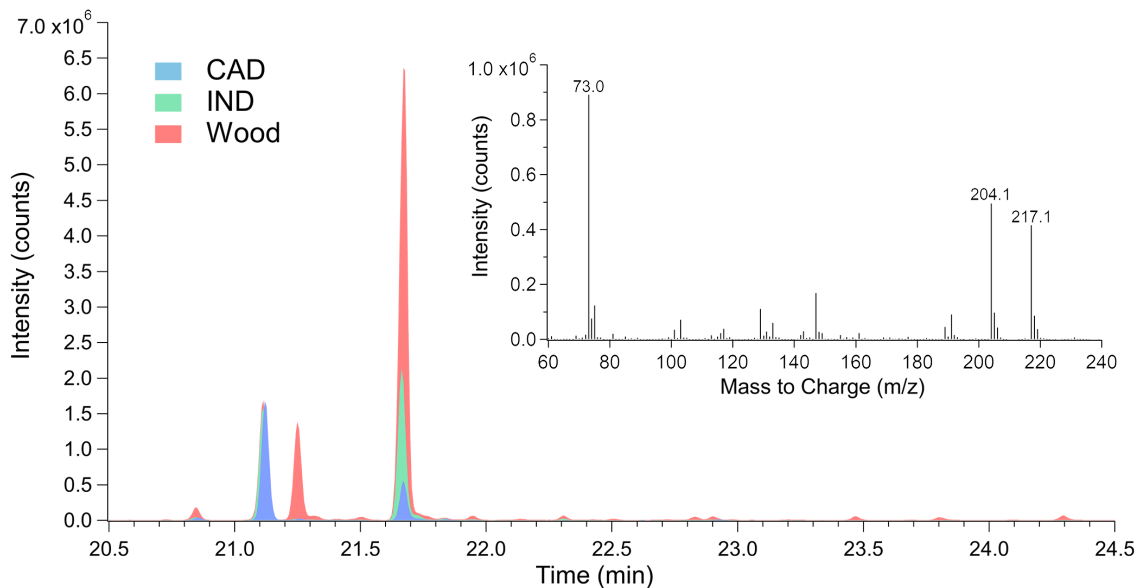


Figure 2.4: GC-MS chromatogram of biomass burning filter extracts.

Table 2.3 lists the observed levoglucosan emission factors for each of the biomass fuels.

All measurements were repeated four times with the means and standard deviations reported. Here, emission factor is defined as the ratio between the amount of levoglucosan detected in filter samples and the mass of fuel burned. The emission factor from wood burning was observed to be an order of magnitude larger than that from CAD and approximately a factor of five larger than that from IND. Even though the fuels were heated inside a well-controlled environment, a large amount of variation in levoglucosan emissions was still observed between IND and CAD samples, represented by a relative standard deviation of 25% and 53%, respectively. Despite the variation observed in our samples, the emission factor of wood burning is still significantly larger than the two dung samples. The two dung samples, which were collected via completely distinct routes, exhibit emission factors consistent to each other. This is an indication that the emission factor of levoglucosan from dung burning may be universally smaller than that from wood.

Table 2.3: Mean Levoglucosan and Isomer Emission Factors \pm Standard Deviation.

Biomass ($n = 4$)	Levo. (mg/g)	Mannosan (mg/g)	Galactosan (mg/g)	Levo./ Mann.	Levo./ Gala.
Wood	14 ± 1.9	3.5 ± 1.2	0.77 ± 0.19	4.2	20
IND	3.0 ± 0.76	0.044 ± 0.018	0.098 ± 0.042	68	31
CAD	1.2 ± 0.64	0.055 ± 0.040	0.097 ± 0.058	22	12

Levoglucosan is a byproduct of cellulose pyrolysis with a high emission factor and a long atmospheric lifetime [61, 221, 223]. These properties make it an ideal tracer for wood biomass burning and source apportionment. Despite this, levoglucosan emission factors from dung remain equivocal. As far as the authors are aware, only Sheesley *et al.* [204] have previously reported on the subject, listing emission factors of 19.1 ± 3.6 ($\mu\text{g mg}^{-1}$) for levoglucosan and 0.65 ± 0.12 ($\mu\text{g mg}^{-1}$) for mannosan. Galactosan emission factors from dung remain unreported. To identify whether the quantity of levoglucosan emitted by dung burning versus wood is significant, we investigated the emission factors of each of the biomass types. Cellulose content is variable between plant species, lodgepole pine wood consists of about 49% cellulose [298]. Cow dung also contains variable amounts of cellulose, in the form of undigested plant matter

dependent on the animal’s diet. Previous studies have placed this content at about 24% [299–301].

Despite its wide use as a tracer, identifying whether levoglucosan was emitted from wood burning versus other biomass sources is currently improbable without accompanying galactosan and mannosan ratios [221]. This means that the impacts of dung burning based on wood levoglucosan measurements are underestimated due to levoglucosan’s lower emission factor from dung. Work by Sheesley *et al.* [204] corroborates this, showing a 2.0% levoglucosan fraction emitted from the combustion of cow dung patties, as opposed to 15% from pine wood within the same study.

Emission factors for galactosan and mannosan were measured by their GC-MS peak intensity using the same method as levoglucosan. Results from this analysis can be found in Table 2.3. These measurement are based on the assumption that levoglucosan and its isomers have similar response factors, as has been previously shown [302].

Pyrolysis of hemicellulose is a likely contributor to mannosan and galactosan content in biomass burning emissions [223]. Similarly to cellulose, hemicellulose content is predicted to vary between plant species. As a result, galactosan and mannosan emissions will also fluctuate with fuel type burned [204]. Their ratios with respect to levoglucosan have been employed for source apportionment in the past [303–306]. The levoglucosan to mannosan (L/M) ratio has been used to differentiate burns from varying wood species. The ratio of levoglucosan to galactosan (L/G) is less commonly employed, presumably due to the lower emission factor of galactosan from wood in comparison to mannosan. However, the L/G ratio has been used to identify wood versus leaf emissions in the past [303, 307].

Currently, L/G ratio has not yet been reported for dung burning exclusively. As can be seen in Table 2.3, the L/M of wood falls in line with expected values for softwood [303, 307, 308]. However, the L/G ratio observed is higher than previously reported for lodgepole pine burning emissions [308], and charred pine [309]. The ratio of mannosan to galactosan (M/G) decreases from hardwood to softwood to brushwood to “greener” biomasses [204, 303, 304, 308, 310]. Our observations for M/G of cow dung match previously published data for rice straw burning [204, 304]. Rice straw is regularly used as animal feed in India. Presumably, the diet of the cows is directly

impacting the hemicellulose content of the dung, leading to similar emissions during burning.

2.3.6 Non-Targeted Organic Analysis with LC-MS

Figure 2.5(a) lists the number of formulas observed among all three biomass fuels in ESI- and ESI+ mode between three separate burns. CHN, CHON, and CHO refer to the elemental composition of the observed species, e.g., a compound classified as CHON contains only carbon, hydrogen, oxygen, and nitrogen atoms. Overall, 369 species with differing molecular formulae were detected in ESI+ mode and 189 in ESI- mode. By the number of species obtained, ESI+ ionizes nitrogen containing species more efficiently than ESI-, which detects a larger number of CHO compounds. IND accounts for 209 of the unique species detected in ESI+ mode, followed by Wood at 81, and CAD with 79. This trend is not sustained in ESI- mode.

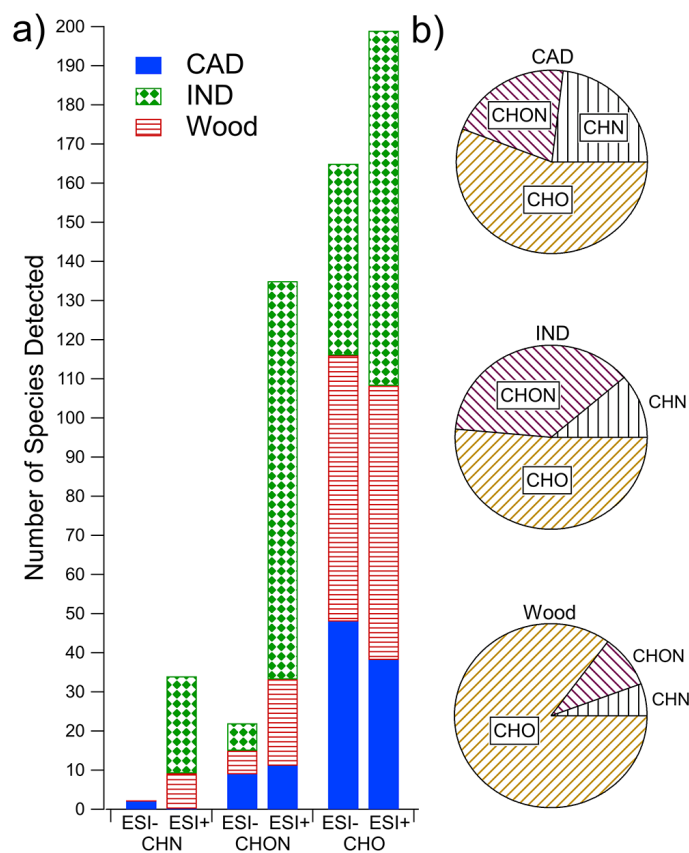


Figure 2.5: Species detected in emissions from each fuel by LC-MS in ESI- and ESI+, by number (a). The intensity-weighted breakdown of CHN, CHON, and CHO compounds detected by the ESI+ mode are presented in (b).

Of the 189 species detected in ESI-, 74 were attributed to Wood, 59 to CAD, and 56 to IND. In ESI- mode, all fuel emissions show around 96% content of CHO compounds when normalized by the intensity of the detections, with variations of $\pm 2\%$ depending on the fuel. For ESI+ mode, fuel emission content normalized by intensity is available in Figure 2.5(b). The fraction of CHO compounds is consistent between burns. Despite this, we observe discrepancies between CHN and CHON content among replicate experiments. Nonetheless, the sum of N-containing species - CHN and CHON - persists between measurements, only their intensities relative to each other vary.

Generally, the total fraction of nitrogen-containing species is much larger in the two dung samples than that in wood. This trend is consistent both with our own results from elemental analysis and TOC/TN measurement (Table 2.1, 2.2) and previous literature [249]. Combining two independent methods, TOC/TN and LC-MS, our study makes a strong suggestion that the higher nitrogen content in dung burning emissions is a universal trend. The higher nitrogen content in emitted particles is likely arising from the larger elemental fraction of N in the fuels themselves.

2.3.7 Major Peaks Detected

Figure 2.6 represents a typical base peak chromatogram (BPC) collected by ESI-. Each of the biomass extracts are overlaid to facilitate visualization. Individual spectra are available in Section A.1.6. A blank filter collected by heating the furnace without any fuel in the quartz tube did not result in any significant signals. MassHunter identified over 100 major peaks from an initial screening process. All major peaks and the majority of low intensity peaks are reproducible between different wood sample burns

CAD and IND chromatograms remain consistent when the concentration of the extracted particulate matter is kept along the same order of magnitude. If the extracts are diluted, peaks beyond 13 min are typically undetectable. These peaks are usually attributed to chemical formulae $>C_{13}$. We are confident in our assignments as all major peaks elute before this time, and both MassHunter and MATLAB were able to assign consistent elemental compositions for these peaks. Most major peaks are also consistent between biomass samples, as can be seen between 2 and 10 min in

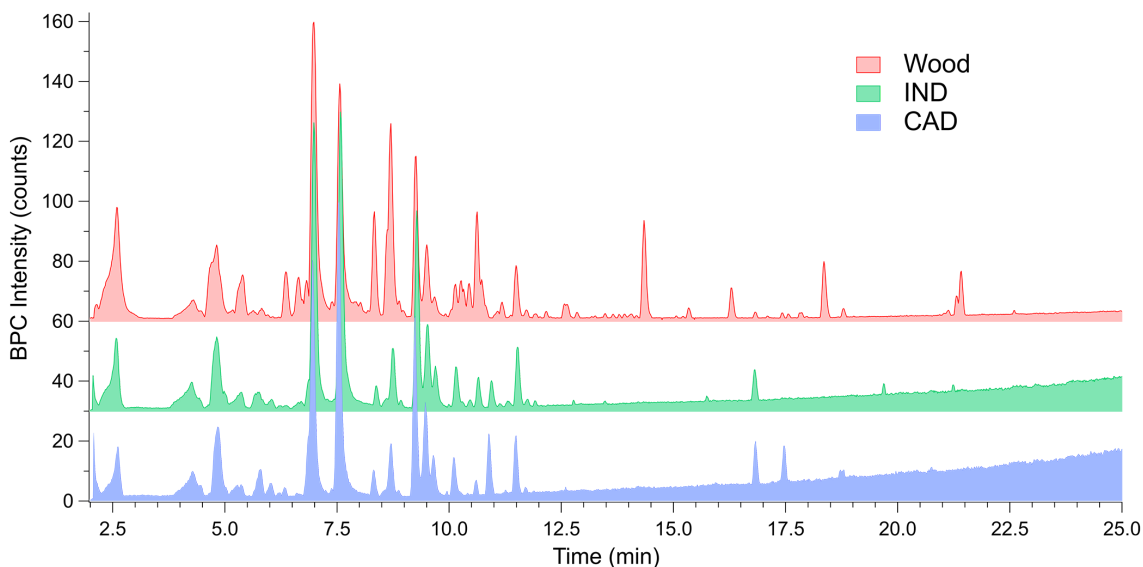


Figure 2.6: ESI- LC-MS Base Peak Chromatogram (BPC) of biomass burning emissions. IND and Wood spectra offset by 30 and 60 counts respectively.

Figure 2.6. These peaks are typically attributed to chemical formulas containing C6 to C10 with a double bond equivalence of 4 or 5, which are likely monoaromatic phenolic compounds common to the burning of any fuel type. Nevertheless, we observed substantial variation for the low intensity peaks between chromatograms of the same biomass only in ESI+.

Figure 2.7 represents the BPCs and total ion chromatograms (TICs) collected in ESI+ mode. The TICs demonstrate how they are typically overtaken by the tremendous number of low intensity species in the extracts. Individual spectra are available in Section A.1.7. Overall, ESI+ BPCs follow the same broad characteristics as their ESI- counterparts. Most major peaks between biomass samples and peaks throughout the wood and CAD replicates are consistent. However, we observe variations between distinct IND samples present only in ESI+ mode, even when the results for these same samples are consistent in ESI- mode. We assume this disparity is caused by the significantly larger variety and quantity of compounds ionized in ESI+ mode.

It is noteworthy that we identified ESI+ peaks that are consistently observable in IND and CAD, but absent in wood (i.e., Retention Time (t_R) = 8.0 and 9.8 min). These peaks were assigned a m/z of 154.0624 and 168.0781 respectively, and were of particular interest for tracer identification. These mass to charge ratios likely

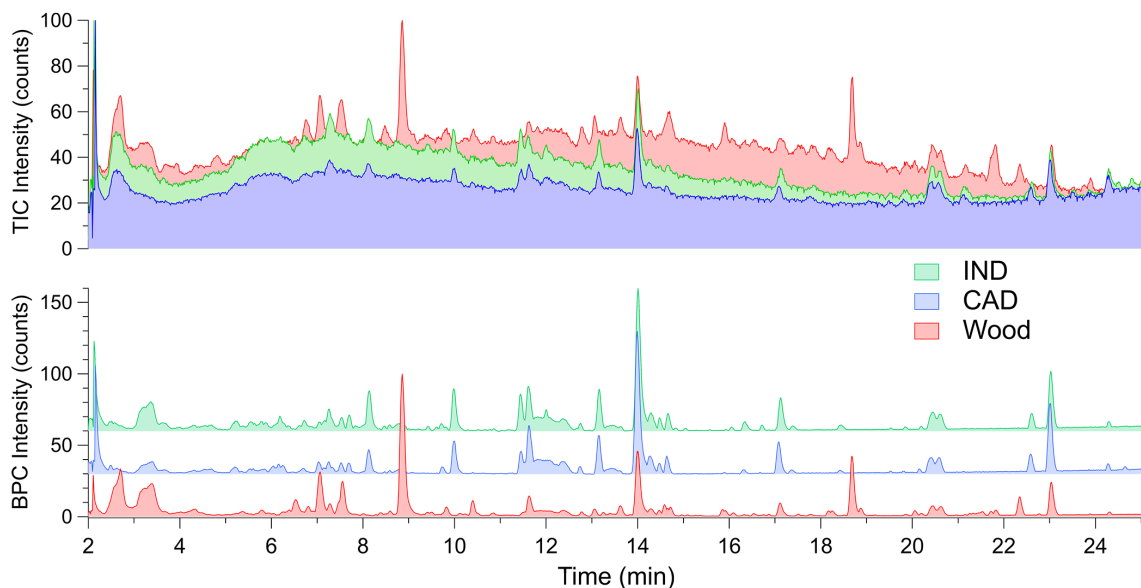


Figure 2.7: Total Ion Chromatogram (TIC)(a) and Base Peak Chromatogram (BPC)(b) ESI+ LC-MS chromatograms of biomass burning emissions. CAD and IND spectra in base peak chromatogram are offset by 30 and 60 counts respectively.

correspond to syringol and methylsyringol. Syringol and methylsyringol are known wood biomass burning tracers that are not emitted from the burning of pine wood [269]. This exemplifies the importance of emission source awareness, as an appropriate tracer must be matched to the biomass that emits it. The potential dung tracers 5β -stigmastanol, coprostanol and cholestanol described by Sheesley *et al.* [204] were not detected in either ionization mode in IND or CAD.

2.3.8 Detailed MS Assignments

Both Lin *et al.* [109] and Fleming *et al.* [249] have performed comprehensive investigations of particulate matter emissions from biomass burning [109, 124, 249]. The former by using a flame stack as part of the FIREX campaign, the latter using two traditional Indian cook stoves. Here, we compare their observations with emissions from our custom tube furnace setup, see Figure 2.1(a).

Table A.1 lists the top 100 chemical species detected through ESI+ unique to CAD and IND fuels, in order of intensity. Molecular formula assignments are based on proximity between the m/z calculated by MassHunter and theoretical m/z . Columns 3. and 6. ‘Prev. Rep.’ list whether a compound has been identified in the aforemen-

tioned Fleming *et al.* [249] study as unique to dung samples (1), common to wood and dung samples (2), or not detected (0).

Of the 100 most intense detections, 24 are consistent with Fleming *et al.* 17 of these 24 matching assignments are asserted to be common to brushwood and dung [249]. Nonetheless, these species were only detected within dung burning emissions in this work. This agreement is reasonable considering the differences in procedure, burning conditions, and sample compositions between the studies.

2.3.9 Targeted Analysis of Representative Biomass Burning Compounds

A series of standard chemicals - vanillin ($t_R = 6.9$), 4-nitrocatechol ($t_R = 7.4$), coniferyl aldehyde ($t_R = 8.7$), sinapaldehyde ($t_R = 9.1$), and 4-nitroguaiacol ($t_R = 10.2$) - were evaluated using the same method to provide more insight into the detected peaks and to ensure correct assignment by the MassHunter software. A mixture of the compounds dissolved in water, containing 100 μM of each standard, was analyzed with the same parameters as the biomass burning extracts. These compounds were chosen as they represent classes of chemical species previously observed in biomass burning plumes [51, 221, 311]. All compounds were accurately identified by our method in the standard mixture in both ionization modes. Results from the standard analysis are available in Table A.2 and Table A.3.

ESI- mode generally shows greater sensitivity over ESI+ due to its higher ionization efficiency [312, 313]. Interestingly, the detection sensitivities of nitrophenols (4-nitroguaiacol and 4-nitrocatechol) are three orders of magnitude higher in ESI- than those in ESI+. We presume that the lack of detection of these nitrophenols in ESI+ mode is due to their inability to accept protons and form $[\text{M}+\text{H}]^+$. This observation provides important insights into the identity of nitrogen-containing species. Based on the concentration of standards used, the concentration of individual nitrophenols in the filter extracts are in the sub- μM range. This explains why CHON and CHN containing compounds represent a minor fraction of detected peaks in ESI- mode, even though the ionization mode is highly sensitive towards nitrophenols. This also implies that the majority of CHN and CHON peaks detected by ESI+ mode are not attributed to nitrophenols but unidentified nitrogen-containing species.

Our results are consistent with observations in a few previous studies, which showed that freshly emitted biomass burning aerosol contained a small nitrophenol content [203], and that nitrophenols present in biomass burning plumes are likely formed during atmospheric processing [117]. Phenolic compounds containing an aldehyde group, i.e., vanillin, sinapaldehyde, and coniferyl aldehyde, were detected by both ESI- and ESI+ with relatively similar sensitivities.

Vanillin, a lignin degradation product, was the most abundant chemical species detected in ESI- mode, and the only compound detected in both ionization modes in all biomass samples. Vanillin being detected in all samples is due to its high concentration in biomass burning emissions, one of the reasons it has been employed as a tracer compound [51, 221]. We found that the vanillin concentrations in wood samples are consistently higher than those in dung samples, demonstrated by both of our ESI- and ESI+ data (Section A.1.7). The difference between these two concentrations is not a factor of the number of particles emitted by the fuels. Normalizing the mass of particles collected on the filter by the mass of the sample burned yields similar results for each fuel, between 30 and 50 mg of particles collected per gram of fuel burned. Vanillin concentrations in the emissions are therefore correlated to the lignin content of the samples.

2.3.10 Implication and Conclusion

This work provides a comprehensive laboratory based analysis of dung biomass burning emissions in comparison to wood. Additionally, our study of particle evolution, levoglucosan emission factors, MAC, and in-depth MS analysis serves to demonstrate the viability and improved reproducibility provided by a tube furnace for laboratory experiments. For each of these analyses, our observations are in general agreement with established literature. We observe that dung burning leads to equal or higher MAC than wood burning for the water-extractable fraction. TOC and TN analysis of that same fraction corroborates the MAC results, as the TN/TOC ratio of dung samples is much higher than wood. These observations are consistent even when accounting for potential underestimation in TOC content as a result of the purging procedure. A higher TN/TOC corresponds to a greater number of nitrogen containing species, which generally display enhanced light absorptive properties [43, 314].

Dung burning emissions having a MAC akin to wood is particularly relevant towards regions of the world without access to clean fuels. Dung emissions could have climatic impacts equal to or greater than wood burning while being - through necessity - employed without consideration for their deleterious effects.

Biomass burning mass spectra are highly complex and are - beyond a few major peaks - dominated by low intensity chemical species. The major peaks are common among all fuel types tested and are likely arising from phenolic compounds. Identification of a reliable tracer compound for dung burning was challenging, as the differences between wood and the dung samples were represented by numerous minor peaks, mostly those detected by ESI+.

Despite the complexity of samples, our study highlighted a few key differences between the chemical composition of wood and those of dung samples. These differences all originate from characteristics of the fuels themselves, including cellulose content, lignin content, and the amount of nitrogen. The emission factors of levoglucosan from IND and CAD were observed to be lower than that from wood by a factor of 4.7 and 12, respectively. Given dung's lower content of cellulose - the precursor of levoglucosan during pyrolysis - the low emission factor of levoglucosan is likely universal for a wide variety of dung samples. This observation has strong implications for source apportionment. If the same emission factor is assumed for both wood and dung, a receptor chemical balance model will likely underestimate the amount of dung emissions and their impact on air quality and climate. The L/G ratio observed here for IND burning benefits future emission source apportionments. The lignin content of wood is larger than that of dung, which has likely resulted in a larger amount of lignin degradation products in the wood sample. The most representative example was vanillin, which was approximately an order of magnitude more abundant in wood samples.

Finally, a consistently higher nitrogen content was observed in dung samples, as per the elemental fraction of the fuels, the TN/TOC ratio in the water extract, and nitrogen-containing peaks detected by LC-MS. This observation again points to nitrogen-containing species being the most significant difference between wood and dung samples. Our results indicate that the majority of nitrogen-containing species detected, especially those detected in ESI+ mode, are not nitrophenols but other

unidentified species. The nitrogen-containing fraction of dung emissions is particularly relevant towards their unknown health and climate effects and the identification of a tracer compound.

The tube furnace is capable of precisely reproducing burning conditions. Despite this, it is not adapted to accurately simulate a fire as it would happen in the environment. Using a tube furnace in a laboratory setting will still require field measurements to confirm observations. However, field measurements can be inconsistent due to the large amount of variation the burning conditions bestow the emissions. While accounting for “real” airflows, mixing ratios, temperature profiles and fuel morphologies using a tube furnace is challenging, its use allows for a reduction in the variability all of these factors cause.

Studies of dung emissions remain few and far between considering the commonality of its use and the potential ramifications of its enhanced complexity. Further studies should focus on the nitrogen-containing compounds present in dung burning emissions, as they represent the major point of distinction between wood and dung. To achieve such objectives, advanced separation, MS with higher mass resolution, and a greater variety of ionization modes should be employed. Certain aspects of such an effort are currently underway within our group.

2.4 Acknowledgements

The authors thank the Rangeland Research Institute of the University of Alberta for providing biomass samples, the U of Alberta MS Facility for their assistance with GC-MS and LC-MS, the Department of Chemistry Glass Shop for manufacturing the quartz tube, the U of Alberta Natural Resources Analytical Laboratory for support with TOC and TN analyses, Dr. Wolfgang Jäger for SMPS use, Dr. Gregory Kiema for providing access to a centrifugal mill, Dr. Sheref Mansy and Tania Gautam for UV-Vis use, and Dr. Wayne Moffat for assistance with elemental analyses. The authors also thank NSERC and the U of Alberta for financial support.

Funding

This research was supported by the Natural Sciences and Engineering Research Council of Canada (Award Number: RGPIN-2018-03814) and the University of Alberta.

2.5 Supporting Information

Additional experimental details, including derivatization mechanism, standard and replicate analyses, and compound characterization data.

References

- [1] M. Loebel Roson *et al.*, “Chemical characterization of emissions arising from solid fuel combustion—contrasting wood and cow dung burning,” *ACS Earth and Space Chemistry*, vol. 5, no. 10, pp. 2925–2937, 2021. DOI: 10.1021/acsearthspacechem.1c00268.
- [6] W. H. O. (WHO), “Global household energy database,” 2023. [Online]. Available: <https://www.who.int/data/gho/data/themes/air-pollution/household-air-pollution>.
- [9] T. C. Bond, D. G. Streets, K. F. Yarber, S. M. Nelson, J.-H. Woo, and Z. Klimont, “A technology-based global inventory of black and organic carbon emissions from combustion,” *Journal of Geophysical Research: Atmospheres*, vol. 109, no. D14, 2004, D14203, 10.1029/2003JD003697. DOI: <https://doi.org/10.1029/2003JD003697>. [Online]. Available: <https://agupubs.onlinelibrary.wiley.com/doi/abs/10.1029/2003JD003697>.
- [11] S. S. Lim *et al.*, “A comparative risk assessment of burden of disease and injury attributable to 67 risk factors and risk factor clusters in 21 regions, 1990–2010: A systematic analysis for the Global Burden of Disease Study 2010,” en, *The Lancet*, vol. 380, no. 9859, pp. 2224–2260, Dec. 2012, ISSN: 01406736. DOI: 10.1016/S0140-6736(12)61766-8. [Online]. Available: <https://linkinghub.elsevier.com/retrieve/pii/S0140673612617668> (visited on 06/25/2021).
- [36] R. J. Park, M. J. Kim, J. I. Jeong, D. Youn, and S. Kim, “A contribution of brown carbon aerosol to the aerosol light absorption and its radiative forcing in east asia,” *Atmospheric Environment*, vol. 44, no. 11, pp. 1414–1421, 2010, ISSN: 1352-2310. DOI: <https://doi.org/10.1016/j.atmosenv.2010.01.042>. [Online]. Available: <https://www.sciencedirect.com/science/article/pii/S1352231010001019>.
- [37] Z. Lu *et al.*, “Light absorption properties and radiative effects of primary organic aerosol emissions,” *Environmental Science & Technology*, vol. 49, no. 8, pp. 4868–4877, 2015. DOI: 10.1021/acs.est.5b00211. [Online]. Available: <https://doi.org/10.1021/acs.est.5b00211>.
- [41] H. Brown *et al.*, “Biomass burning aerosols in most climate models are too absorbing,” *Nature communications*, vol. 12, no. 1, pp. 1–15, 2021.
- [42] C. E. Stockwell *et al.*, “Nepal ambient monitoring and source testing experiment (namaste): Emissions of trace gases and light-absorbing carbon from wood and dung cooking fires, garbage and crop residue burning, brick kilns, and other sources,” *Atmospheric Chemistry and Physics*, vol. 16, no. 17, pp. 11 043–11 081, 2016. DOI: 10.5194/acp-16-11043-2016. [Online]. Available: <https://acp.copernicus.org/articles/16/11043/2016/>.
- [43] A. Laskin, J. Laskin, and S. A. Nizkorodov, “Chemistry of atmospheric brown carbon,” *Chemical Reviews*, vol. 115, no. 10, pp. 4335–4382, 2015. DOI: 10.1021/cr5006167. [Online]. Available: <https://doi.org/10.1021/cr5006167>.

- [44] M. O. Andreae and A. Gelencsér, “Black carbon or brown carbon? the nature of light-absorbing carbonaceous aerosols,” *Atmospheric Chemistry and Physics*, vol. 6, no. 10, pp. 3131–3148, 2006. DOI: 10.5194/acp-6-3131-2006. [Online]. Available: <https://acp.copernicus.org/articles/6/3131/2006/>.
- [50] Y. Feng, V. Ramanathan, and V. R. Kotamarthi, “Brown carbon: A significant atmospheric absorber of solar radiation?” *Atmospheric Chemistry and Physics*, vol. 13, no. 17, pp. 8607–8621, 2013. DOI: 10.5194/acp-13-8607-2013. [Online]. Available: <https://acp.copernicus.org/articles/13/8607/2013/>.
- [51] Y. Iinuma, O. Böge, R. Gräfe, and H. Herrmann, “Methyl-nitrocatechols: Atmospheric tracer compounds for biomass burning secondary organic aerosols,” *Environmental Science & Technology*, vol. 44, no. 22, pp. 8453–8459, 2010. DOI: 10.1021/es102938a. [Online]. Available: <https://doi.org/10.1021/es102938a>.
- [55] A. K. Y. Lee *et al.*, “Single-particle characterization of biomass burning organic aerosol (bboa): Evidence for non-uniform mixing of high molecular weight organics and potassium,” *Atmospheric Chemistry and Physics*, vol. 16, no. 9, pp. 5561–5572, 2016. DOI: 10.5194/acp-16-5561-2016. [Online]. Available: <https://acp.copernicus.org/articles/16/5561/2016/>.
- [61] B. R. Simoneit, “Biomass burning — a review of organic tracers for smoke from incomplete combustion,” *Applied Geochemistry*, vol. 17, no. 3, pp. 129–162, 2002, ISSN: 0883-2927. DOI: [https://doi.org/10.1016/S0883-2927\(01\)00061-0](https://doi.org/10.1016/S0883-2927(01)00061-0). [Online]. Available: <https://www.sciencedirect.com/science/article/pii/S0883292701000610>.
- [79] B. R. Simoneit and V. Elias, “Detecting organic tracers from biomass burning in the atmosphere,” *Marine Pollution Bulletin*, vol. 42, no. 10, pp. 805–810, 2001, ISSN: 0025-326X. DOI: [https://doi.org/10.1016/S0025-326X\(01\)00094-7](https://doi.org/10.1016/S0025-326X(01)00094-7). [Online]. Available: <https://www.sciencedirect.com/science/article/pii/S0025326X01000947>.
- [109] P. Lin, L. T. Fleming, S. A. Nizkorodov, J. Laskin, and A. Laskin, “Comprehensive molecular characterization of atmospheric brown carbon by high resolution mass spectrometry with electrospray and atmospheric pressure photoionization,” *Analytical Chemistry*, vol. 90, no. 21, pp. 12493–12502, 2018. DOI: 10.1021/acs.analchem.8b02177. [Online]. Available: <https://doi.org/10.1021/acs.analchem.8b02177>.
- [117] J. Li, S. M. Forrester, and D. A. Knopf, “Heterogeneous oxidation of amorphous organic aerosol surrogates by O_3 , NO_3 , and oh, at typical tropospheric temperatures,” *Atmospheric Chemistry and Physics*, vol. 20, no. 10, pp. 6055–6080, 2020. DOI: 10.5194/acp-20-6055-2020. [Online]. Available: <https://acp.copernicus.org/articles/20/6055/2020/>.
- [123] P. Lin, N. Bluvshstein, Y. Rudich, S. A. Nizkorodov, J. Laskin, and A. Laskin, “Molecular chemistry of atmospheric brown carbon inferred from a nationwide biomass burning event,” *Environmental Science & Technology*, vol. 51, no. 20,

- pp. 11 561–11 570, 2017. DOI: 10.1021/acs.est.7b02276. [Online]. Available: <https://doi.org/10.1021/acs.est.7b02276>.
- [124] L. T. Fleming *et al.*, “Molecular composition and photochemical lifetimes of brown carbon chromophores in biomass burning organic aerosol,” *Atmospheric Chemistry and Physics*, vol. 20, no. 2, pp. 1105–1129, 2020. DOI: 10.5194/acp-20-1105-2020. [Online]. Available: <https://acp.copernicus.org/articles/20/1105/2020/>.
- [150] A. Thygesen, J. Oddershede, H. Lilholt, A. Bjerre, and K. Ståhl, “On the determination of crystallinity and cellulose content in plant fibres,” *Cellulose*, vol. 12, pp. 563–576, Dec. 2005. DOI: 10.1007/s10570-005-9001-8.
- [157] B. Rooney *et al.*, “Impacts of household sources on air pollution at village and regional scales in india,” *Atmospheric Chemistry and Physics*, vol. 19, no. 11, pp. 7719–7742, 2019. DOI: 10.5194/acp-19-7719-2019. [Online]. Available: <https://acp.copernicus.org/articles/19/7719/2019/>.
- [158] A. L. Hodshire *et al.*, “Aging effects on biomass burning aerosol mass and composition: A critical review of field and laboratory studies,” *Environmental Science & Technology*, vol. 53, no. 17, pp. 10 007–10 022, 2019. DOI: 10.1021/acs.est.9b02588. [Online]. Available: <https://doi.org/10.1021/acs.est.9b02588>.
- [203] P. Lin *et al.*, “Molecular characterization of brown carbon in biomass burning aerosol particles,” *Environmental Science & Technology*, vol. 50, no. 21, pp. 11 815–11 824, 2016. DOI: 10.1021/acs.est.6b03024. [Online]. Available: <https://doi.org/10.1021/acs.est.6b03024>.
- [204] R. J. Sheesley, J. J. Schauer, Z. Chowdhury, G. R. Cass, and B. R. Simoneit, “Characterization of organic aerosols emitted from the combustion of biomass indigenous to south asia,” *Journal of Geophysical Research: Atmospheres*, vol. 108, no. D9, 2003, 4285, 10.1029/2002JD002981.
- [221] H. Bhattarai *et al.*, “Levoglucosan as a tracer of biomass burning: Recent progress and perspectives,” *Atmospheric Research*, vol. 220, pp. 20–33, 2019, ISSN: 0169-8095. DOI: <https://doi.org/10.1016/j.atmosres.2019.01.004>. [Online]. Available: <https://www.sciencedirect.com/science/article/pii/S0169809518311098>.
- [223] B. Simoneit *et al.*, “Levoglucosan, a tracer for cellulose in biomass burning and atmospheric particles,” *Atmospheric Environment*, vol. 33, no. 2, pp. 173–182, 1999, ISSN: 1352-2310. DOI: [https://doi.org/10.1016/S1352-2310\(98\)00145-9](https://doi.org/10.1016/S1352-2310(98)00145-9). [Online]. Available: <https://www.sciencedirect.com/science/article/pii/S1352231098001459>.
- [249] L. T. Fleming *et al.*, “Emissions from village cookstoves in haryana, india, and their potential impacts on air quality,” *Atmospheric Chemistry and Physics*, vol. 18, no. 20, pp. 15 169–15 182, 2018. DOI: 10.5194/acp-18-15169-2018. [Online]. Available: <https://acp.copernicus.org/articles/18/15169/2018/>.

- [251] G. G. Pfister, C. Wiedinmyer, and L. K. Emmons, “Impacts of the fall 2007 california wildfires on surface ozone: Integrating local observations with global model simulations,” *Geophysical Research Letters*, vol. 35, no. 19, 2008, L19814, 10.1029/2008GL034747. DOI: <https://doi.org/10.1029/2008GL034747>. [Online]. Available: <https://agupubs.onlinelibrary.wiley.com/doi/abs/10.1029/2008GL034747>.
- [252] B. Langmann, B. Duncan, C. Textor, J. Trentmann, and G. R. van der Werf, “Vegetation fire emissions and their impact on air pollution and climate,” *Atmospheric Environment*, vol. 43, no. 1, pp. 107–116, 2009, ISSN: 1352-2310. DOI: <https://doi.org/10.1016/j.atmosenv.2008.09.047>. [Online]. Available: <https://www.sciencedirect.com/science/article/pii/S135223100800900X>.
- [253] R. J. Yokelson *et al.*, “Coupling field and laboratory measurements to estimate the emission factors of identified and unidentified trace gases for prescribed fires,” *Atmospheric Chemistry and Physics*, vol. 13, no. 1, pp. 89–116, 2013. DOI: 10.5194/acp-13-89-2013. [Online]. Available: <https://acp.copernicus.org/articles/13/89/2013/>.
- [254] R. Cordell *et al.*, “Evaluation of biomass burning across north west europe and its impact on air quality,” *Atmospheric Environment*, vol. 141, pp. 276–286, 2016, ISSN: 1352-2310. DOI: <https://doi.org/10.1016/j.atmosenv.2016.06.065>. [Online]. Available: <https://www.sciencedirect.com/science/article/pii/S1352231016304988>.
- [255] “Health effects institute. state of global air 2020,”
- [256] C. J. L. Murray *et al.*, “Global burden of 87 risk factors in 204 countries and territories, 1990–2019: A systematic analysis for the Global Burden of Disease Study 2019,” *The Lancet*, vol. 396, no. 10258, pp. 1223–1249, Oct. 2020, ISSN: 01406736. DOI: 10.1016/S0140-6736(20)30752-2. [Online]. Available: <https://linkinghub.elsevier.com/retrieve/pii/S0140673620307522> (visited on 06/25/2021).
- [257] H. Lukács *et al.*, “Seasonal trends and possible sources of brown carbon based on 2-year aerosol measurements at six sites in europe,” *Journal of Geophysical Research*, vol. 112, Sep. 2007, D23S18, 10.1029/2006JD008151. DOI: 10.1029/2006JD008151.
- [258] T. Kirchstetter, T. Novakov, and P. Hobbs, “Evidence that the spectral dependence of light absorption by aerosols is affected by organic carbon,” *Journal of Geophysical Research Atmospheres*, vol. 109, pp. 21208–, Nov. 2004, D21208, 10.1029/2004JD004999. DOI: 10.1029/2004JD004999.
- [259] R. A. Washenfelder *et al.*, “Biomass burning dominates brown carbon absorption in the rural southeastern united states,” *Geophysical Research Letters*, vol. 42, no. 2, pp. 653–664, 2015, 10.1002/2014GL062444. DOI: <https://doi.org/10.1002/2014GL062444>. [Online]. Available: <https://agupubs.onlinelibrary.wiley.com/doi/abs/10.1002/2014GL062444>.

- [260] J. P. S. Wong, A. Nenes, and R. J. Weber, “Changes in light absorptivity of molecular weight separated brown carbon due to photolytic aging,” *Environmental Science & Technology*, vol. 51, no. 15, pp. 8414–8421, 2017. DOI: 10.1021/acs.est.7b01739. [Online]. Available: <https://doi.org/10.1021/acs.est.7b01739>.
- [261] I. S. Mudway, S. T. Duggan, C. Venkataraman, G. Habib, F. J. Kelly, and J. Grigg, “Combustion of dried animal dung as biofuel results in the generation of highly redox active fine particulates,” *Particle and Fibre Toxicology*, vol. 2, no. 1, p. 6, 2005, ISSN: 17438977. DOI: 10.1186/1743-8977-2-6. [Online]. Available: <http://particleandfibretoxicology.biomedcentral.com/articles/10.1186/1743-8977-2-6> (visited on 06/25/2021).
- [262] D. Park *et al.*, “Emission Characteristics of Particulate Matter and Volatile Organic Compounds in Cow Dung Combustion,” en, *Environmental Science & Technology*, vol. 47, no. 22, pp. 12 952–12 957, Nov. 2013, ISSN: 0013-936X, 1520-5851. DOI: 10.1021/es402822e. [Online]. Available: <https://pubs.acs.org/doi/10.1021/es402822e> (visited on 06/25/2021).
- [263] M. D. Jolleys *et al.*, “Characterizing the aging of biomass burning organic aerosol by use of mixing ratios: A meta-analysis of four regions,” *Environmental Science & Technology*, vol. 46, no. 24, pp. 13 093–13 102, 2012. DOI: 10.1021/es302386v. [Online]. Available: <https://doi.org/10.1021/es302386v>.
- [264] J. Martinsson *et al.*, “Impacts of combustion conditions and photochemical processing on the light absorption of biomass combustion aerosol,” *Environmental science & technology*, vol. 49, Nov. 2015. DOI: 10.1021/acs.est.5b03205.
- [265] B. R. T. Simoneit, W. F. Rogge, M. A. Mazurek, L. J. Standley, L. M. Hildemann, and G. R. Cass, “Lignin pyrolysis products, lignans, and resin acids as specific tracers of plant classes in emissions from biomass combustion,” *Environmental Science & Technology*, vol. 27, no. 12, pp. 2533–2541, 1993. DOI: 10.1021/es00048a034. [Online]. Available: <https://doi.org/10.1021/es00048a034>.
- [266] C. Venkataraman and G. U. M. Rao, “Emission factors of carbon monoxide and size-resolved aerosols from biofuel combustion,” *Environmental Science & Technology*, vol. 35, no. 10, pp. 2100–2107, 2001. DOI: 10.1021/es001603d. [Online]. Available: <https://doi.org/10.1021/es001603d>.
- [267] A. Pandey, S. Pervez, and R. K. Chakrabarty, “Filter-based measurements of uv–vis mass absorption cross sections of organic carbon aerosol from residential biomass combustion: Preliminary findings and sources of uncertainty,” *Journal of Quantitative Spectroscopy and Radiative Transfer*, vol. 182, pp. 296–304, 2016, ISSN: 0022-4073. DOI: <https://doi.org/10.1016/j.jqsrt.2016.06.023>. [Online]. Available: <https://www.sciencedirect.com/science/article/pii/S0022407316300796>.

- [268] M. O. Andreae, “Emission of trace gases and aerosols from biomass burning – an updated assessment,” *Atmospheric Chemistry and Physics*, vol. 19, no. 13, pp. 8523–8546, 2019. DOI: 10.5194/acp-19-8523-2019. [Online]. Available: <https://acp.copernicus.org/articles/19/8523/2019/>.
- [269] J. J. Schauer, M. J. Kleeman, G. R. Cass, and B. R. T. Simoneit, “Measurement of emissions from air pollution sources. 3. c1-c29 organic compounds from fireplace combustion of wood,” *Environmental Science & Technology*, vol. 35, no. 9, pp. 1716–1728, 2001. DOI: 10.1021/es001331e. [Online]. Available: <https://doi.org/10.1021/es001331e>.
- [270] S. Shabbar and I. Janajreh, “Thermodynamic equilibrium analysis of coal gasification using gibbs energy minimization method,” *Energy Conversion and Management*, vol. 65, pp. 755–763, 2013, ISSN: 0196-8904. DOI: <https://doi.org/10.1016/j.enconman.2012.02.032>. [Online]. Available: <https://www.sciencedirect.com/science/article/pii/S0196890412001501>.
- [271] Z. Zdráhal, J. Oliveira, R. Vermeylen, M. Claeys, and W. Maenhaut, “Improved method for quantifying levoglucosan and related monosaccharide anhydrides in atmospheric aerosols and application to samples from urban and tropical locations,” *Environmental Science & Technology*, vol. 36, no. 4, pp. 747–753, 2002. DOI: 10.1021/es015619v. [Online]. Available: <https://doi.org/10.1021/es015619v>.
- [272] D. Fabbri, G. Chiavari, S. Prati, I. Vassura, and M. Vangelista, “Gas chromatography/mass spectrometric characterisation of pyrolysis/silylation products of glucose and cellulose,” *Rapid Communications in Mass Spectrometry*, vol. 16, no. 24, pp. 2349–2355, 2002. DOI: <https://doi.org/10.1002/rm.856>. [Online]. Available: <https://analyticalsciencejournals.onlinelibrary.wiley.com/doi/abs/10.1002/rm.856>.
- [273] K. Yang and B. Xing, “Adsorption of fulvic acid by carbon nanotubes from water,” *Environmental Pollution*, vol. 157, no. 4, pp. 1095–1100, 2009, ISSN: 0269-7491. DOI: <https://doi.org/10.1016/j.envpol.2008.11.007>. [Online]. Available: <https://www.sciencedirect.com/science/article/pii/S0269749108005964>.
- [274] B. Wallace, M. Purcell, and J. Furlong, “Total organic carbon analysis as a precursor to disinfection byproducts in potable water: Oxidation technique considerations,” *J. Environ. Monit.*, vol. 4, pp. 35–42, 1 2002. DOI: 10.1039/B106049J. [Online]. Available: <http://dx.doi.org/10.1039/B106049J>.
- [275] I. Bisutti, I. Hilke, and M. Raessler, “Determination of total organic carbon – an overview of current methods,” *TrAC Trends in Analytical Chemistry*, vol. 23, no. 10, pp. 716–726, 2004, ISSN: 0165-9936. DOI: <https://doi.org/10.1016/j.trac.2004.09.003>. [Online]. Available: <https://www.sciencedirect.com/science/article/pii/S0165993604030535>.

- [276] R. Zhao, A. K. Y. Lee, L. Huang, X. Li, F. Yang, and J. P. D. Abbatt, “Photochemical processing of aqueous atmospheric brown carbon,” *Atmospheric Chemistry and Physics*, vol. 15, no. 11, pp. 6087–6100, 2015. DOI: 10.5194/acp-15-6087-2015. [Online]. Available: <https://acp.copernicus.org/articles/15/6087/2015/>.
- [277] L. M. Russell, “Aerosol organic-mass-to-organic-carbon ratio measurements,” *Environmental Science & Technology*, vol. 37, no. 13, pp. 2982–2987, 2003. DOI: 10.1021/es026123w. [Online]. Available: <https://doi.org/10.1021/es026123w>.
- [278] A. Hoffer *et al.*, “Optical properties of humic-like substances (hulis) in biomass-burning aerosols,” *Atmospheric Chemistry and Physics*, vol. 6, no. 11, pp. 3563–3570, 2006. DOI: 10.5194/acp-6-3563-2006. [Online]. Available: <https://acp.copernicus.org/articles/6/3563/2006/>.
- [279] R. Zhao, C. M. Kenseth, Y. Huang, N. F. Dalleska, and J. H. Seinfeld, “Iodometry-assisted liquid chromatography electrospray ionization mass spectrometry for analysis of organic peroxides: An application to atmospheric secondary organic aerosol,” *Environmental Science & Technology*, vol. 52, no. 4, pp. 2108–2117, 2018, PMID: 29370527. DOI: 10.1021/acs.est.7b04863. [Online]. Available: <https://doi.org/10.1021/acs.est.7b04863>.
- [280] R. C. Pettersen, “The chemical composition of wood,” in *The Chemistry of Solid Wood*, ch. 2, pp. 57–126. DOI: 10.1021/ba-1984-0207.ch002. [Online]. Available: <https://pubs.acs.org/doi/abs/10.1021/ba-1984-0207.ch002>.
- [281] G. N. Inari, M. Pétrissans, A. Pétrissans, and P. Gérardin, “Elemental composition of wood as a potential marker to evaluate heat treatment intensity,” *Polymer Degradation and Stability*, vol. 94, no. 3, pp. 365–368, 2009, ISSN: 0141-3910. DOI: <https://doi.org/10.1016/j.polymdegradstab.2008.12.003>. [Online]. Available: <https://www.sciencedirect.com/science/article/pii/S0141391008004023>.
- [282] A. Mohareb, P. Sirmah, M. Pétrissans, and P. Gérardin, “Effect of heat treatment intensity on wood chemical composition and decay durability of *Pinus patula*,” in *European Journal of Wood and Wood Products*, vol. 70, no. 4, pp. 519–524, Jul. 2012, ISSN: 0018-3768, 1436-736X. DOI: 10.1007/s00107-011-0582-7. [Online]. Available: <http://link.springer.com/10.1007/s00107-011-0582-7> (visited on 05/26/2021).
- [283] M. Choudhary, L. Bailey, and C. Grant, “Review of the use of swine manure in crop production: Effects on yield and composition and on soil and water quality,” *Waste Management & Research*, vol. 14, no. 6, pp. 581–595, 1996. DOI: 10.1177/0734242X9601400606. [Online]. Available: <https://doi.org/10.1177/0734242X9601400606>.
- [284] P. Sørensen, M. R. Weisbjerg, and P. Lund, “Dietary effects on the composition and plant utilization of nitrogen in dairy cattle manure,” *The Journal of Agricultural Science*, vol. 141, no. 1, pp. 79–91, 2003. DOI: 10.1017/S0021859603003368.

- [285] T. S. Griffin, Z. He, and C. W. Honeycutt, “Manure composition affects net transformation of nitrogen from dairy manures,” en, *Plant and Soil*, vol. 273, no. 1-2, pp. 29–38, Jun. 2005, ISSN: 0032-079X, 1573-5036. DOI: 10.1007/s11104-004-6473-5. [Online]. Available: <http://link.springer.com/10.1007/s11104-004-6473-5> (visited on 06/28/2021).
- [286] S. H. Han, J. Y. An, J. Hwang, S. B. Kim, and B. B. Park, “The effects of organic manure and chemical fertilizer on the growth and nutrient concentrations of yellow poplar (*liriodendron tulipifera* lin.) in a nursery system,” *Forest Science and Technology*, vol. 12, no. 3, pp. 137–143, 2016. DOI: 10.1080/21580103.2015.1135827. [Online]. Available: <https://doi.org/10.1080/21580103.2015.1135827>.
- [287] J. Huang *et al.*, “Chemical structures and characteristics of animal manures and composts during composting and assessment of maturity indices,” en, *PLOS ONE*, vol. 12, no. 6, J. Mao, Ed., e0178110, Jun. 2017, ISSN: 1932-6203. DOI: 10.1371/journal.pone.0178110. [Online]. Available: <https://dx.plos.org/10.1371/journal.pone.0178110> (visited on 05/28/2021).
- [288] F.-X. Collard and J. Blin, “A review on pyrolysis of biomass constituents: Mechanisms and composition of the products obtained from the conversion of cellulose, hemicelluloses and lignin,” *Renewable and Sustainable Energy Reviews*, vol. 38, pp. 594–608, 2014, ISSN: 1364-0321. DOI: <https://doi.org/10.1016/j.rser.2014.06.013>. [Online]. Available: <https://www.sciencedirect.com/science/article/pii/S136403211400450X>.
- [289] J. R. Laing, D. A. Jaffe, and J. R. Hee, “Physical and optical properties of aged biomass burning aerosol from wildfires in siberia and the western usa at the mt. bachelor observatory,” *Atmospheric Chemistry and Physics*, vol. 16, no. 23, pp. 15 185–15 197, 2016. DOI: 10.5194/acp-16-15185-2016. [Online]. Available: <https://acp.copernicus.org/articles/16/15185/2016/>.
- [290] K. M. Sakamoto, J. D. Allan, H. Coe, J. W. Taylor, T. J. Duck, and J. R. Pierce, “Aged boreal biomass-burning aerosol size distributions from bortas 2011,” *Atmospheric Chemistry and Physics*, vol. 15, no. 4, pp. 1633–1646, 2015. DOI: 10.5194/acp-15-1633-2015. [Online]. Available: <https://acp.copernicus.org/articles/15/1633/2015/>.
- [291] S. Janhäll, M. O. Andreae, and U. Pöschl, “Biomass burning aerosol emissions from vegetation fires: Particle number and mass emission factors and size distributions,” *Atmospheric Chemistry and Physics*, vol. 10, no. 3, pp. 1427–1439, 2010. DOI: 10.5194/acp-10-1427-2010. [Online]. Available: <https://acp.copernicus.org/articles/10/1427/2010/>.
- [292] M. D. Hays, P. M. Fine, C. D. Geron, M. J. Kleeman, and B. K. Gullett, “Open burning of agricultural biomass: Physical and chemical properties of particle-phase emissions,” *Atmospheric Environment*, vol. 39, no. 36, pp. 6747–6764, 2005, ISSN: 1352-2310. DOI: <https://doi.org/10.1016/j.atmosenv.2005.07.072>. [Online]. Available: <https://www.sciencedirect.com/science/article/pii/S1352231005007247>.

- [293] A. Y. P. Wardoyo, L. Morawska, Z. D. Ristovski, and J. Marsh, “Quantification of particle number and mass emission factors from combustion of queensland trees,” *Environmental Science & Technology*, vol. 40, no. 18, pp. 5696–5703, 2006, PMID: 17007128. DOI: 10.1021/es0609497. [Online]. Available: <https://doi.org/10.1021/es0609497>.
- [294] A. P. Bruins, “Mechanistic aspects of electrospray ionization,” *Journal of Chromatography A*, vol. 794, no. 1, pp. 345–357, 1998, ISSN: 0021-9673. DOI: [https://doi.org/10.1016/S0021-9673\(97\)01110-2](https://doi.org/10.1016/S0021-9673(97)01110-2). [Online]. Available: <https://www.sciencedirect.com/science/article/pii/S0021967397011102>.
- [295] Y. Chen and T. C. Bond, “Light absorption by organic carbon from wood combustion,” *Atmospheric Chemistry and Physics*, vol. 10, no. 4, pp. 1773–1787, 2010. DOI: 10.5194/acp-10-1773-2010. [Online]. Available: <https://acp.copernicus.org/articles/10/1773/2010/>.
- [296] A. L. Robinson *et al.*, “Rethinking organic aerosols: Semivolatile emissions and photochemical aging,” *Science*, vol. 315, no. 5816, pp. 1259–1262, 2007, ISSN: 0036-8075. DOI: 10.1126/science.1133061. [Online]. Available: <https://science.sciencemag.org/content/315/5816/1259>.
- [297] C.-L. Hsu, C.-Y. Cheng, C.-T. Lee, and W.-H. Ding, “Derivatization procedures and determination of levoglucosan and related monosaccharide anhydrides in atmospheric aerosols by gas chromatography–mass spectrometry,” *Talanta*, vol. 72, no. 1, pp. 199–205, 2007, ISSN: 0039-9140. DOI: <https://doi.org/10.1016/j.talanta.2006.10.018>. [Online]. Available: <https://www.sciencedirect.com/science/article/pii/S0039914006006898>.
- [298] I. Sable *et al.*, “Properties of wood and pulp fibers from lodgepole pine (*pinus contorta*) as compared to scots pine (*pinus sylvestris*),” *BioResources*, vol. 7, no. 2, pp. 1771–1783, 2012, ISSN: 1930-2126. [Online]. Available: https://ojs.cnr.ncsu.edu/index.php/BioRes/article/view/BioRes_07_2_1771_Sable_GJVIVT_Props_Wood_Pulp_Fibers_Pines.
- [299] Z. Wen, W. Liao, and S. Chen, “Hydrolysis of animal manure lignocellulosics for reducing sugar production,” *Bioresource Technology*, vol. 91, no. 1, pp. 31–39, 2004, ISSN: 0960-8524. DOI: [https://doi.org/10.1016/S0960-8524\(03\)00166-4](https://doi.org/10.1016/S0960-8524(03)00166-4). [Online]. Available: <https://www.sciencedirect.com/science/article/pii/S0960852403001664>.
- [300] W. Liao, Y. Liu, C. Liu, Z. Wen, and S. Chen, “Acid hydrolysis of fibers from dairy manure,” *Bioresource Technology*, vol. 97, no. 14, pp. 1687–1695, 2006, ISSN: 0960-8524. DOI: <https://doi.org/10.1016/j.biortech.2005.07.028>. [Online]. Available: <https://www.sciencedirect.com/science/article/pii/S096085240500369X>.
- [301] P. Kumar, D. M. Barrett, M. J. Delwiche, and P. Stroeve, “Methods for pretreatment of lignocellulosic biomass for efficient hydrolysis and biofuel production,” *Industrial & Engineering Chemistry Research*, vol. 48, no. 8, pp. 3713–

- 3729, 2009. DOI: 10.1021/ie801542g. [Online]. Available: <https://doi.org/10.1021/ie801542g>.
- [302] A. Piazzalunga, P. Fermo, V. Bernardoni, R. Vecchi, G. Valli, and M. A. D. Gregorio, “A simplified method for levoglucosan quantification in wintertime atmospheric particulate matter by high performance anion-exchange chromatography coupled with pulsed amperometric detection,” *International Journal of Environmental Analytical Chemistry*, vol. 90, no. 12, pp. 934–947, 2010. DOI: 10.1080/03067310903023619. [Online]. Available: <https://doi.org/10.1080/03067310903023619>.
- [303] C. Schmidl *et al.*, “Chemical characterisation of particle emissions from burning leaves,” *Atmospheric Environment*, vol. 42, no. 40, pp. 9070–9079, 2008, ISSN: 1352-2310. DOI: <https://doi.org/10.1016/j.atmosenv.2008.09.010>. [Online]. Available: <https://www.sciencedirect.com/science/article/pii/S1352231008008406>.
- [304] G. Engling, J. J. Lee, Y.-W. Tsai, S.-C. C. Lung, C. C.-K. Chou, and C.-Y. Chan, “Size-resolved anhydrosugar composition in smoke aerosol from controlled field burning of rice straw,” *Aerosol Science and Technology*, vol. 43, no. 7, pp. 662–672, 2009. DOI: 10.1080/02786820902825113. [Online]. Available: <https://doi.org/10.1080/02786820902825113>.
- [305] X. Sang, Z. Zhang, C. Chan, and G. Engling, “Source categories and contribution of biomass smoke to organic aerosol over the southeastern tibetan plateau,” *Atmospheric Environment*, vol. 78, pp. 113–123, 2013, ISSN: 1352-2310. DOI: <https://doi.org/10.1016/j.atmosenv.2012.12.012>. [Online]. Available: <https://www.sciencedirect.com/science/article/pii/S1352231012011624>.
- [306] R. Urban, C. Alves, A. Allen, A. Cardoso, M. Queiroz, and M. Campos, “Sugar markers in aerosol particles from an agro-industrial region in brazil,” *Atmospheric Environment*, vol. 90, pp. 106–112, 2014, ISSN: 1352-2310. DOI: <https://doi.org/10.1016/j.atmosenv.2014.03.034>. [Online]. Available: <https://www.sciencedirect.com/science/article/pii/S135223101400209X>.
- [307] Y. Cheng *et al.*, “Biomass burning contribution to beijing aerosol,” *Atmospheric Chemistry and Physics*, vol. 13, no. 15, pp. 7765–7781, 2013. DOI: 10.5194/acp-13-7765-2013. [Online]. Available: <https://acp.copernicus.org/articles/13/7765/2013/>.
- [308] P. M. Medeiros and B. R. T. Simoneit, “Source profiles of organic compounds emitted upon combustion of green vegetation from temperate climate forests,” *Environmental Science & Technology*, vol. 42, no. 22, pp. 8310–8316, 2008. DOI: 10.1021/es801533b. [Online]. Available: <https://doi.org/10.1021/es801533b>.
- [309] A. Otto, R. Gondokusumo, and M. J. Simpson, “Characterization and quantification of biomarkers from biomass burning at a recent wildfire site in northern alberta, canada,” *Applied Geochemistry*, vol. 21, no. 1, pp. 166–183, 2006, ISSN: 0883-2927. DOI: <https://doi.org/10.1016/j.apgeochem.2005.09.007>.

- [Online]. Available: <https://www.sciencedirect.com/science/article/pii/S0883292705002003>.
- [310] C. Schmidl *et al.*, “Chemical characterisation of fine particle emissions from wood stove combustion of common woods growing in mid-european alpine regions,” *Atmospheric Environment*, vol. 42, no. 1, pp. 126–141, 2008, ISSN: 1352-2310. DOI: <https://doi.org/10.1016/j.atmosenv.2007.09.028>. [Online]. Available: <https://www.sciencedirect.com/science/article/pii/S1352231007008047>.
- [311] M. Brege, M. Paglione, S. Gilardoni, S. Decesari, M. C. Facchini, and L. R. Mazzoleni, “Molecular insights on aging and aqueous-phase processing from ambient biomass burning emissions-influenced po valley fog and aerosol,” *Atmospheric Chemistry and Physics*, vol. 18, no. 17, pp. 13197–13214, 2018. DOI: 10.5194/acp-18-13197-2018. [Online]. Available: <https://acp.copernicus.org/articles/18/13197/2018/>.
- [312] A. Krueve, K. Kaupmees, J. Liigand, and I. Leito, “Negative electrospray ionization via deprotonation: Predicting the ionization efficiency,” *Analytical Chemistry*, vol. 86, no. 10, pp. 4822–4830, 2014. DOI: 10.1021/ac404066v. [Online]. Available: <https://doi.org/10.1021/ac404066v>.
- [313] P. Liigand *et al.*, “Think negative: Finding the best electrospray ionization/ms mode for your analyte,” *Analytical Chemistry*, vol. 89, no. 11, pp. 5665–5668, 2017. DOI: 10.1021/acs.analchem.7b00096. [Online]. Available: <https://doi.org/10.1021/acs.analchem.7b00096>.
- [314] M. Xie, X. Chen, M. D. Hays, and A. L. Holder, “Composition and light absorption of n-containing aromatic compounds in organic aerosols from laboratory biomass burning,” *Atmospheric Chemistry and Physics*, vol. 19, no. 5, pp. 2899–2915, 2019. DOI: 10.5194/acp-19-2899-2019. [Online]. Available: <https://acp.copernicus.org/articles/19/2899/2019/>.

Chapter 3

Comprehensive Two-Dimensional Gas Chromatographic Analysis of Biomass Burning Emissions

Contributions: This chapter was written by Max Loebel Roson, with feedback and review by Dr. Ran Zhao.

3.1 Introduction

Biomass burning is a major source of climate and health affecting aerosol [32, 34, 36, 44]. BBE affect the Earth’s radiative balance by absorbing or reflecting light [9, 34, 35]. From a health perspective, particulate matter emitted during a burn can - due to its size - penetrate deep into the lungs, from where it can be transferred and impact the cardiovascular system [11, 16]. Within this context, biomass refers to biological matter, including vegetation such as wood, grass, and leaves, as well as agricultural and animal residue [8]. Wildfires are the major driver of biomass burning in the environment, they are predicted to rise in both incidence and severity as climate change proceeds [30, 31]. However, biomass burning is also a major global source of energy [7], particularly so in developing countries which rely on it for cooking and heating [5, 6, 157]. In regions where wood biomass is not widely available, households may rely on alternative fuels such as animal dung for combustion [157, 204].

As a result of its widespread use, biomass burning is believed to be responsible for up to 90% of global combustion OA emissions [9, 22–24]. Of those emissions, BrC is the second most light-absorptive component [32, 34, 36, 37]. The dominant fraction of BrC is composed of organic compounds which absorb light strongly in the ultraviolet and low-visible spectrum, with unpredictable climate effects [43, 48, 50]. While the major emission components are similar between burns, there is significant variability in the vast quantity of low-intensity compounds emitted during the combustion of biomass [43, 107, 156]. These varied, often unsaturated and nitrogen-containing compounds are believed to be largely responsible for the light-absorbing properties of BBOA [43, 109, 124]. On the other hand, part of the variability in emission composition is attributed to changes in burning conditions, which even in a laboratory setting are challenging to consistently reproduce [158, 165]. Modifying the fuel density, morphology, moisture content, and heating temperature will all affect the emission characteristics [9, 44, 48, 158]. For instance, BrC compounds are emitted more readily during incomplete combustion, when insufficient airflow or temperature is available to drive a flame [43, 56, 57]. To complicate things further, different types of biomass have distinct compound emission factors under equal burning conditions. For example, oak and pine wood emit syringaldehyde - a biomass burning tracer -

at different concentrations during combustion [61, 141]. As might be expected, more dissimilar fuels (such as wood and animal dung) are expected to have more disparate emissions [1, 141, 204]. Yet, emissions from distinct fuels are treated uniformly by climate models, usually under the assumption that the biomass which originated them is wood [73, 157, 161, 232, 233].

In addition to the complexity of reproducing burns, it is also challenging to separately identify compounds from the biomass burning emission matrix. Analytical techniques such as LC- and GC-MS can have difficulties isolating and detecting compounds from the bulk [1, 315–317]. This has not prevented a large body of research from employing these techniques to success [109, 124, 125, 217–219, 249]. However, difficulties associated with identifying the mixed low-intensity fraction of BBE remain ubiquitous. In recent years, strides in the development of GC×GC-MS techniques have allowed the analysis of samples which were previously considered too complex to efficiently separate [315, 318, 319]. Despite this, few studies have reported on the analysis of wood burning emissions using GC×GC-MS [107, 167, 224, 241, 243], and as far as the author is aware, none have on cow dung burning emissions.

Herein, I report preliminary compositional data obtained using thermal desorption two-dimensional gas chromatography-time of flight mass spectrometry (TD-GC×GC-ToF-MS) from wood and cow dung biomass particulate matter gathered under three separate burning conditions: 500 °C and slow air flow, as well as 500 and 700 °C and fast air flow. These conditions correspond to varying levels of combustion efficiency, which directly impact the nature of the collected emissions [48, 158]. In particular, I sought to determine which heating conditions have the most influence on the emission composition, whether the changes in emission composition translate into differences in unsaturation or nitrogen content, and if those differences are fuel specific. These questions were explored using two approaches, firstly by way of manual trend analysis of the GC×GC-MS molecular composition data, and secondly through automated principal component analysis (PCA). PCA is a statistical testing method particularly helpful in deconvoluting complex chemical data, as well as identifying variables in a group of samples which may otherwise appear too similar to differentiate. With regards to the combustion method, some of the reproducibility concerns typically associated with fire experiments are bypassed using a tube furnace, which is capable

of consistently and uniformly heating samples. At the time of publication of this thesis, for the first time, biomass burning particulate matter generated using a tube furnace, as well as cow dung burning emissions, are studied under GC×GC-MS and analyzed using PCA.

3.2 Materials and methods

3.2.1 Sample combustion and collection

The sampling procedure has been previously described in detail in Chapter 2 Section 2.2.3 of this thesis. Briefly, wood, Canadian cow dung (CAD), and Indian cow dung (IND) were separately placed in a quartz inset tube inside a tube furnace. A mass flow controller set to 0.2 or 10 slpm regulates the amount of air flowing through the tube and over the biomass sample. The tube furnace uniformly heats the quartz tube at a ramping rate of 100 °C/min up to 500 or 700 °C, corresponding to pyrolysis and flaming combustion respectively. Modifying the flow rate and heating parameters allows for the sampling of a variety of emission profiles. By for example broadly simulating the inefficient combustion conditions encountered in traditional biomass cook stoves or low-intensity wildfires [157, 320]. A filter holder containing a pre-baked quartz filter (Whatman QM-A, 4.7 cm in diameter) gathers the BBE downstream of the furnace. A vacuum ensures the entirety the emissions pass through the filter. A total of 27 filters were sampled, corresponding to 3 separate burns per biomass fuel under the following conditions: 10 slpm and 700 °C, 10 slpm and 500 °C, as well as 0.2 slpm and 500 °C. Instrumental filter blanks were collected under the same heating conditions, without biomass in the quartz tube. Following sampling, the filters were stored in a freezer at -20 °C prior to analysis.

3.2.2 Thermal desorption and GC×GC-MS analysis

1/8" filter punches were loaded inside individual glass thermal desorption (TD) tubes in a TD100-xr (Marques International) before injection into the GC×GC-ToF-MS (Agilent 7890 GC). Punches were collected approximately halfway between the center-point and outer-edge of each filter. Filter punch loading was calculated based on the surface area and loading of the original filter. Calculated punch loadings ranged

from 0.68-4.1 μg , with the range between burns of equal conditions being 0.60 μg on average. Glass wool was positioned before and after each filter punch in the TD tubes to prevent injection of unwanted material. The TD tubes were heated to 300 $^{\circ}\text{C}$ for 15 min to remove (desorb) the BBE gathered on their surface. A cold trap held at -25 $^{\circ}\text{C}$ focuses the desorbed emissions before injection into the GC \times GC-MS instrument. A quantifiable GC \times GC-MS signal was not observed in TD tubes heated a second time, ensuring complete desorption. The GC \times GC-MS parameters were as follows: 100% polydimethylsiloxane column in the first dimension (Rtx-1, 31 m \times 250 μm), and 50% phenyl 50% dimethylsiloxane in the second (Rxi-17, 5 m \times 250 μm), 70 eV electron impact, 2.3 second modulation time, split flow of 1/153, 0.73 mL/min flow rate, initial GC temperature held at 40 $^{\circ}\text{C}$ for 4 min, 5 $^{\circ}\text{C}/\text{min}$ ramp to 300 $^{\circ}\text{C}$ and hold for 10 min, totalling to a 66 min separation and 81 min analysis time.

3.2.3 Peak detection

Before PCA, the GC \times GC-ToF-MS data was processed through ImageJ (v.3.2.1) to obtain the peak volume, tR, and identity of each compound. Only peaks with a height 3 \times larger than the signal-to-noise ratio and a minimum width of 50 counts were integrated and identified. Compounds were identified through library search (NIST), with a minimum match and reverse match factor of 500. Identities of select compounds were manually confirmed by correlating their retention index (RI) to a series of linear alkane standards of increasing carbon number (C6-C27), analyzed using the same GC \times GC-MS method.

3.2.4 Feature selection

After peak detection, data containing the peak volume for all compounds common and unique to each sample was analyzed using a custom cluster resolution feature selection Matlab algorithm (MATLAB[®] R2020b v.9.9.0.1467703). The algorithm has been described in detail in Armstrong *et al.* -[321]. Briefly, during the feature selection process, each sample was manually assigned a classification according to its biomass type, temperature, and flow rate parameters. The Matlab algorithm interprets the classes and identifies significant features (according to the peak volume of each compound across the classes) for PCA. Based on the cluster resolution metric,

the selected features are those whose linear combination returns the most separation between each of the classes in PCA (i.e. the compounds that differentiate each class most significantly) [321, 322]. This process was repeated once per group of classifications. For example, once to draft a PCA plot of both biomass type and flow rate (Figure 3.7), and one time each for PCA plots of only biomass type or heating temperature (Figures 3.5 and 3.6). Without selecting significant features, PCA can be inaccurate due to the numerous species present in BBE [321]. As a result, only peaks found to be significant by the cluster resolution feature selection algorithm were further analyzed through PCA.

3.2.5 Principal component analysis

PCA was performed using the Matlab PLS_Toolbox (Eigenvector Research Inc., v.9.2.1). In each case, the number of principal components (PC) selected for the analysis were those suggested by the toolbox (3 or more across all samples). The PC % represents which percentage of the variance among all classifications can be explained by that PC. The higher the score (correlation) of a sample along a PC axis, the more that PC explains the variance in that sample. Across all analyses, no PCs with a variance below 7.0% were used.

3.2.5.1 Concepts and definitions

PCA is a statistical testing method designed to deconvolute complex samples [322]. PCA takes each of the mathematical components from a series of samples and extracts the variables which are correlated and anti-correlated with each sample. The output is a series of PC, ordered by the variance between the samples each component explains, with the highest being PC 1 [321, 322]. Typically, each PC is associated with one or more feature of the samples.

In atmospheric science, PCA is commonly applied to source apportionment aerosol. For example, Song *et al.* employed PCA to distinguish the contribution of different sources to PM_{2.5} in Beijing [323]. Similarly, Choi *et al.* used PCA to deconvolute and identify major pollution sources and VOCs in 500 individual airborne samples obtained from the upper troposphere and analyzed using GC [324]. More recently, Ravindra *et al.* monitored known air pollutants at 8 Indian sites, PCA was applied by the authors to

identify which pollutants impact air quality most significantly at each location, finding that rural sites are strongly affected by biomass burning [325]. On the other hand, Wang *et al.* approached the issue from a different angle, applying PCA to investigate the base elemental composition of crop and dung biomass before combustion. The authors use PCA to correlate the elemental composition of the samples between each other and estimate their potential as fuels (by for example finding PCs associated with oxygen or nitrogen content) [326]. Nonetheless, PCA has not been previously applied in a laboratory setting to specifically identify and distinguish the burn products from different types of biomass, such as peat, cow dung, hardwood, softwood, and others [327].

As purely mathematical constructs, PC do not necessarily have to reflect a specific property or parameter of the samples being analyzed [327]. With complex matrices like BBE, PCs can be particularly challenging to identify due to the inherent imprecision of the combustion process, which causes multiple variables (morphology, moisture content, air flow, etc.) to jointly contribute to each PC [322]. Additionally, PCA requires a large sample size for accurate classification. And furthermore, studies ideally need to be repeated to ensure the PCA results can be replicated [326, 327]. Following is a list common terms and definitions used throughout the PCA discussion.

- Classification/Classes: Refers to the groups each sample is manually assigned before feature selection. A classification of 500 °C includes all samples gathered at that temperature, disregarding biomass type or flow rate. Each entry in the legend of a PCA plot is a separate classification.
- Principal component (PC): Obtained after PCA and plotted under score or correlation axes (x,y,z), PCs are the group of features which explain the highest % of variability between the samples under the defined classifications.
- Feature: Variables found to be significant towards a given classification. Here, features are chemical compounds identified through the GC×GC-MS analysis followed by the cluster resolution feature selection algorithm. During the PCA, features may be correlated, unaffected by, or anti-correlated with one or more PCs.

- Parameter: Used here as combustion variable, i.e., heating temperature, flow rate, and biomass type. A classification may contain one or more parameters.
- Clustering: Used in the context of a PCA plot to mean visual concentration or agglomeration of samples of the same class. Clustering is an indication of accurate classification and feature selection.
- Dispersion: Used in the context of a PCA plot to mean visual spread of samples of the same class. Dispersion is an indication of low sampling precision or inaccurate classification.
- Differentiation/Separation: Used in the context of a PCA plot to mean visual dissociation between classes. Differentiation indicates whether the variability in the defined classes is explained by the different PCs.

Herein, PCA is applied to aid in sample differentiation. PCs are automatically selected by the PLS toolbox based on the relative peak volumes of the feature selected compounds present in each sample. These PCs are expected to be a direct representation of the burning conditions used during the collection of the samples. Ideally, high % variability PCs, coupled to sample clustering and good differentiation between sample classes on the PCA plots will indicate which burning conditions have the most impact on the emission composition [322].

3.3 Results and discussion

3.3.1 GC×GC-ToF-MS Results

Figure 3.1 displays a typical GC×GC-ToF-MS wood chromatogram. The circles indicate the integrated peaks, each representing a detected compound. The tR on the x-axis represents the amount of time each compound is retained on the first column. Every 2.3 seconds, the eluent exiting the first column is modulated and injected into a second column (also called the second dimension) with a different stationary phase. The y-axis represents the amount of time each compound is retained in the second dimension. The benefit of this approach is that compounds with equal tR in the first dimension (which would appear as overlapping peaks in single column LC

or GC) can be separated in the second dimension. Also, information gleaned from their relative position on either axis can hint at their molecular composition. By analyzing a series of linear alkane standards of increasing carbon number (C6-C27) and known RI, each peak in the chromatogram can be assigned a specific RI relative to its position to the nearest alkane standard. Once the peaks are identified through database-matching, the calculated peak RI can be manually compared to the RI of the compound identified in the database. If the two RI values do not match, it is possible that the automatic database identification is erroneous. Using both the molecular fragments and RI improves the chances of accurate identification. However, not all compounds in a given database have known RIs.

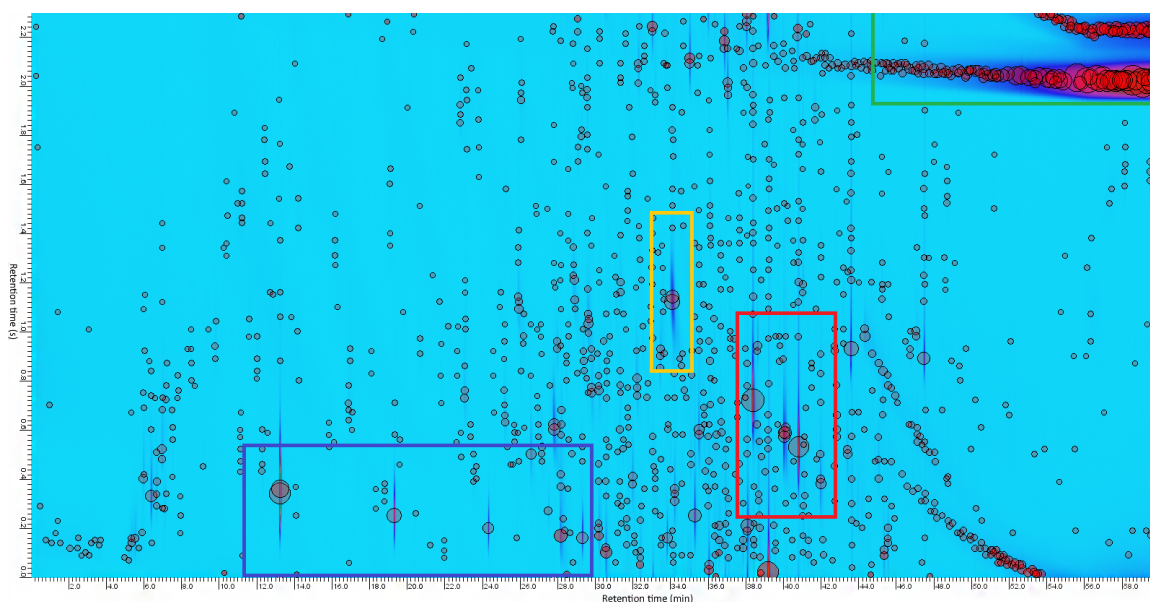


Figure 3.1: Two-dimensional gas chromatography time of flight mass spectrometry (GC×GC-ToF-MS) chromatogram of wood biomass burning particulate matter gathered at 500 °C and 0.2 slpm of airflow. The yellow square represents levoglucosan. The red square displays a series of syringaldehyde-like compounds of increasing molecular mass. The blue and green squares represent interferences from the glass wool and column bleed respectively. An enlarged version of this figure is available in the Supporting Information (B.1.1)

As can be seen in Figure 3.1, chromatograms contain hundreds of separate detections of varying intensities. The peak integration settings have a purposefully low threshold to maximise the number of detections. Compounds with similar structures will generally align themselves in gradients of increasing molecular weight. For instance,

the five compounds with highest peak volume in the red square area of Figure 3.1 correspond to: acetosyringone ($C_{10}H_{12}O_4$), 4-allyl syringol ($C_{11}H_{14}O_3$), sinapyl alcohol ($C_{11}H_{14}O_4$), syringylacetone ($C_{12}H_{16}O_4$), and syringaresinol ($C_{22}H_{26}O_8$), all of which are common structural, decomposition, or BBE plant components [141, 328, 329]. Syringaresinol is believed to form through protein coupling of sinapyl alcohol [328]. To illustrate the benefits of using RI, syringaresinol is the only one of these compounds with a RI (3655) that does not match the predicted value for the peak (1858). This indicates that the structural assignment is possibly inaccurate. Although accurate identification is still pending, it is likely this peak instead represents a compound of around half the C number and with a similar fragment spectrum as syringaresinol not found within the NIST database.

CAD and IND chromatograms contain the same major features, with generally lower volume peaks and more spread out integrations. The biomass burning tracer levoglucosan (yellow square) is visible across all chromatograms, irrespective of biomass type or heating parameters. The large high intensity area in the top right occurs in every chromatogram as a result of siloxane compounds bleeding from the column coating. Similarly, the high-volume equidistant peaks in the blue area represent interference from the glass wool surrounding the filter punch in the TD tube.

The GC \times GC-MS peak volume and molecular data obtained from ImageJ were exported and deconvoluted using Matlab. Figure 3.2 displays the double bond equivalent (DBE), carbon number, and nitrogen number of each of the 994 detected compounds across all 27 biomass samples after deconvolution. If markers overlap, the compound with the larger nitrogen number is preferentially shown, if the nitrogen number is equal between the two compounds, the peak volume is also summed. The DBE is a measure of the unsaturation of each compound, and is calculated using Eqn 3.1 [330, 331]:

$$DBE = C + 1 - \frac{H}{2} - \frac{X}{2} + \frac{N}{2} \quad (3.1)$$

Where C, H, X, and N are the number of carbon, hydrogen, halogen, and nitrogen atoms in the compound respectively. A compound with a DBE of 2 contains two double bonds or rings, a ring and a double bond, or a single triple bond.

As shown in Figure 3.2, a higher DBE and a lower carbon number is associated with

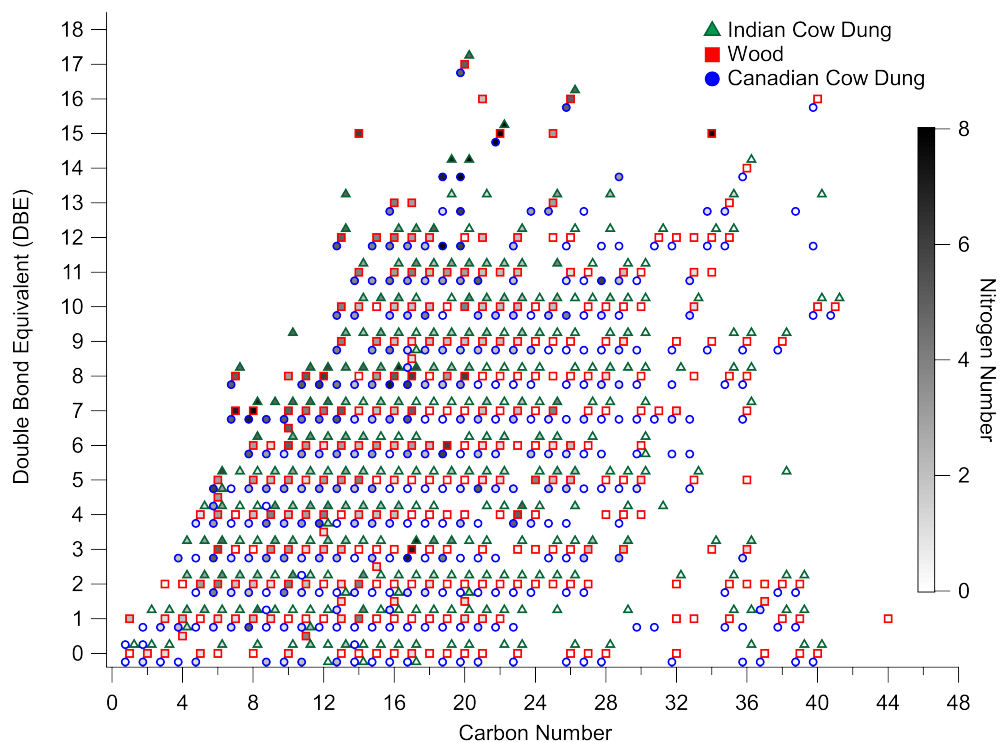


Figure 3.2: Double bond equivalent (DBE) and carbon number obtained from the combustion of Indian cow dung (IND) (green triangles, offset by -0.25 counts on the x- and y-axis), wood (red squares), and Canadian cow dung (CAD) (blue circles, offset by 0.25 counts on the x- and y-axis) biomass. The marker shading represents the number of nitrogen atoms detected in each compound.

a higher nitrogen content. This is consistent with previously reported studies on the subject [332–334]. The emissions from each of the biomass fuels appear highly uniform, with only occasional detections seeming to be specific to each biomass. Considering the total number of species detected, it is not unexpected that most positions in the plot are occupied. While featuring only the unique detections produces a more visually parsable plot, it does not yield any obvious DBE or carbon and nitrogen number trends. However, if the species are plotted by whether they are unique to each flow rate used during the combustion, the differences become more striking. For example, Figure 3.3 shows the compounds unique to IND samples combusted at 500 °C under 0.2 slpm and 10 slpm of air flow.

In total, 117 compounds were found to be unique to the 10 slpm samples and 191 to the 0.2 slpm of air flow. Here, the high DBE region is overtaken by higher peak volume compounds occurring only under low air flow rate, corresponding to inefficient burning

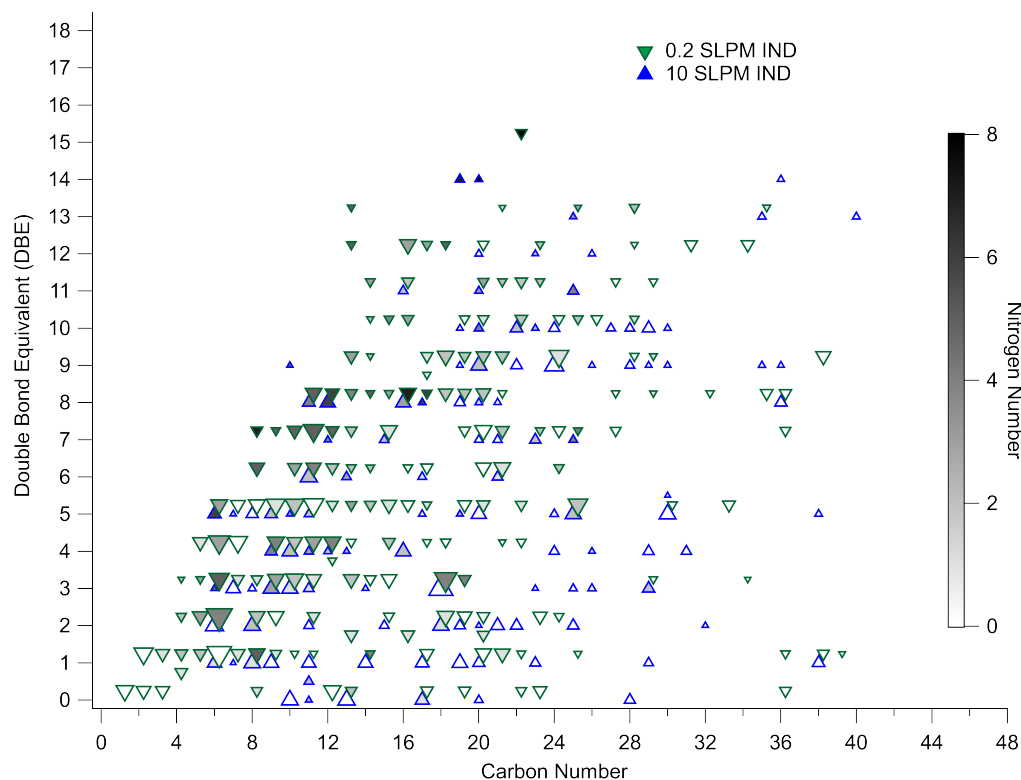


Figure 3.3: Double bond equivalence (DBE) and carbon number obtained from the combustion of Indian cow dung (IND) samples at 500 °C using 0.2 (green triangles) and 10 (blue triangles, offset on the x- and y-axis by 0.25 counts) slpm of air, unique detections only. The marker shading represents the number of nitrogen atoms detected in each compound. The size of the markers indicates the logarithmic peak volume of each compound, normalized by the average loading mass of each filter punch class. The peak volumes of a compound that appears multiple times at a given flow rate are summed. $n = 3$ for each flow rate.

conditions. These unsaturated nitrogen containing compounds are likely responsible for the more significant BrC-like light-absorptive properties observed for dung samples in my previous study [1].

Plots with sample characteristics other than DBE have similar complexities to those shown previously in Figure 3.2. For example, Figure 3.4 (A) displays the H/C and O/C ratios, as well as the number of nitrogen atoms for the compounds found to be unique in each biomass fuel. During a burn, larger molecules are fragmented into smaller components more readily as combustion efficiency is enhanced [61]. Ideally, H/C versus O/C plots display linear oxygenation or methyl group loss trends as a result of this fragmentation. However, no obvious linear trends due to fuel type can be

observed in Figure 3.4 (A). The average number of nitrogen atoms among the unique species were 0.515, 0.596, and 0.595, for wood, IND, and CAD respectively. Since the the dung fuels contain significantly more nitrogen than wood before combustion [1, 326], it is surprising that the dung emission samples do not display the same magnitude of nitrogen differentiation. Presumably, the largest fraction of nitrogen containing compounds emitted during the combustion is common to all fuels. And by extension, only a small part of the elemental nitrogen fuel composition is translated into unique emissions during the combustion process.

Figure 3.4 (B) displays the H/C and O/C ratios, as well as the number of nitrogen atoms for compounds found to be unique among the 0.2 and 10 slpm IND emissions.

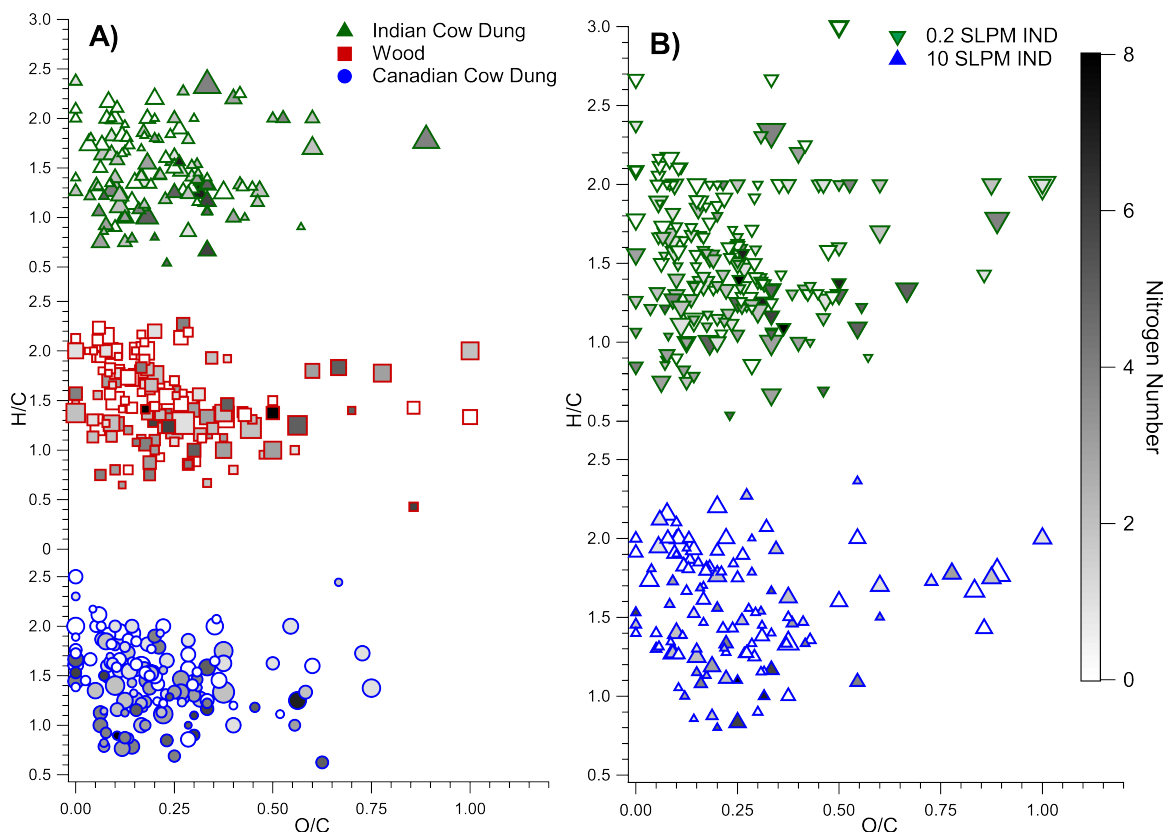


Figure 3.4: Hydrogen to carbon (H/C) and oxygen to carbon (O/C) ratio obtained from: **A**), species unique to the combustion of Indian cow dung (green triangles), wood (red squares), and Canadian cow dung (blue circles) biomass, and **B**), the combustion of Indian cow dung (IND) at 500 °C using 0.2 (downwards green triangles) and 10 (upwards blue triangles) slpm of air. The interior marker shading represents the number of nitrogen atoms identified in each detection. The size of the markers indicates the logarithmic peak volume of each compound.

Again, the trends observed in Figure 3.3 are repeated here. The compounds unique to 0.2 slpm IND are more numerous, generally have a larger peak volume, and contain a higher number of nitrogen atoms on average (1.66 for 0.2 slpm, and 1.21 for 10 slpm). This is further confirmation that the inefficient burning conditions are leading to the formation of more nitrogen containing species. Specifically, the linear increasing O/C for the 0.2 slpm IND sample at an H/C of 2 corresponds to oxygenated benzene and heterocyclic compounds, some of which contain pyrrole, imidazole, thiazole, or furan fragments. Furans have known deleterious health effects [335, 336], while thiazole compounds such as benzothiazole and its derivatives have been recently identified as health-affecting [337]. Presumably, inefficient burning conditions will also release more of these health-affecting components. However, since Figure 3.4 (B) only displays unique species, there is also the possibility that other biomass types and flow conditions also contain furan or thiazole groups, and simply do not contain the specific compounds observed in 0.2 slpm IND.

3.3.2 Principal component analysis

Figure 3.5 displays a 3 dimensional PCA plot of each of the samples classified by biomass type. A positive score on the PC 1 axis indicates a given sample is positively correlated with PC 1. As can be seen in Figure 3.5, a PCA classified by biomass type yields very little clustering with the exception of the blanks. Nonetheless, PC 1 explains up to 31.95% of the variance in the samples. This indicates that although biomass type is a significant driver of variance among the samples, it is not the determining factor in differentiating those samples, as evidenced by the lack of marker clustering. Likely, other factors (temperature, flow rate, or more) are responsible for the position of each of the markers in the PCA plot. For instance, the three light blue markers in the top right corner of the plot are the only wood samples gathered at 500 °C and 0.2 slpm.

Whether other properties are responsible for the differences observed in Figure 3.5 can be studied by classifying the samples differently before feature selection. For example, Figure 3.6 displays a similar PCA plot classified by the tube furnace temperature each of the samples was heated to, 0.2 slpm samples non-inclusive. Here, there is more obvious differentiation between the two heating temperatures and a better quadrant

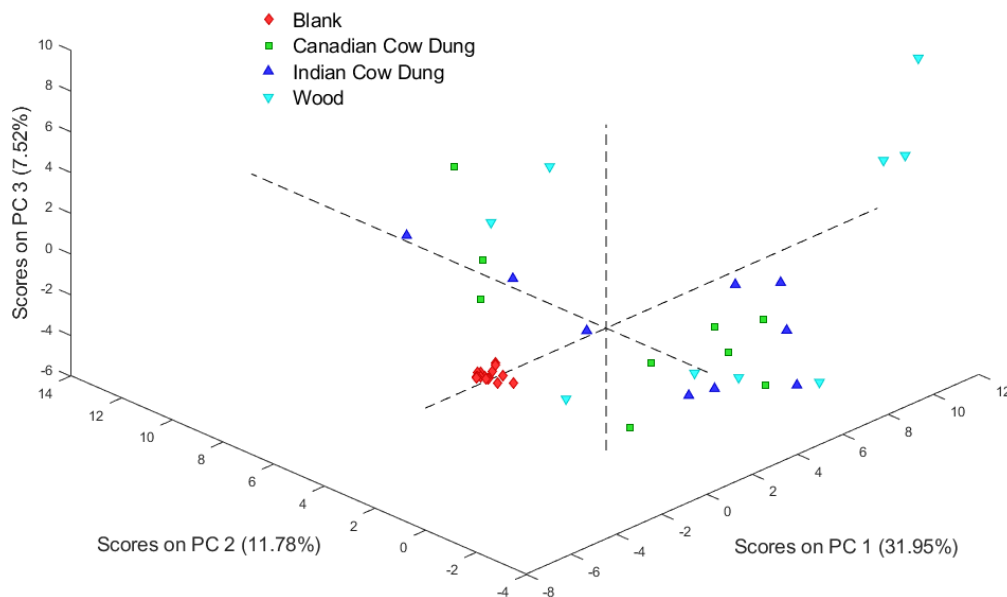


Figure 3.5: Principal component analysis (PCA) of biomass burning emissions after feature selection and classification by biomass fuel type.

dispersion along the PCA plot. However, there is still a significant spread for the 500 °C class and an apparent outlier along the PC 3 axis for the 700 °C class. The lack of clustering could be an indication that no single PC can explain the variance observed between the 500 °C samples. This effect is not entirely unexpected considering that lower heating temperatures are associated with pyrolysis and smouldering conditions, both of which release a larger array of compound classes during the heating process [154]. This larger compound variety could be responsible for the spread in the 500 °C samples in Figure 3.6.

Classification by flow rate yields similar results, with good differentiation between classes and similar spread for the samples gathered under 0.2 slpm of airflow. However, there is substantial clustering in the samples classified as 10 slpm. Presumably, the higher supply of oxygen during the heating process enhances the combustion efficiency, leading to more consistently similar emissions. In either case, these results corroborate the effects observed in Figures 3.3 and 3.4 (B). Throughout the PCAs, the blanks are well clustered and differentiated among all analyses no matter the classification chosen, with one exception; if the Matlab feature selection algorithm is not performed before PCA, the majority of the samples cluster and overlap the blanks, yielding no significant differentiation.

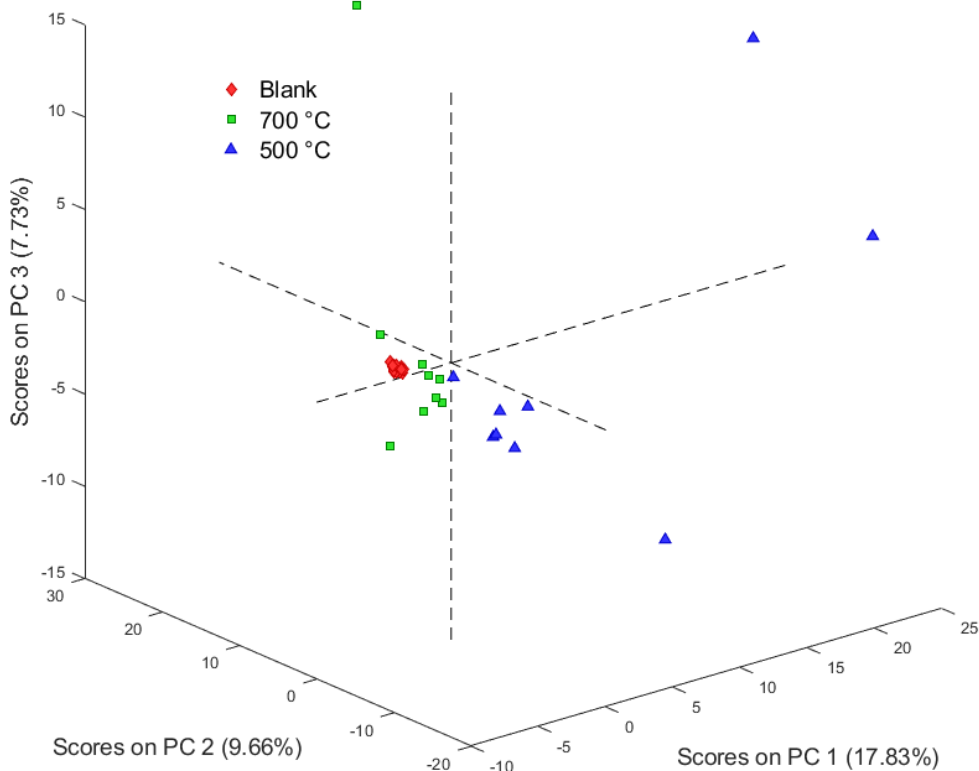


Figure 3.6: Principal component analysis (PCA) of biomass burning emissions after feature selection and classification by heating temperature at 10 slpm.

Similarly, the more distinct classifications are selected, the higher the number of significant variables identified by the feature selection algorithm. Having too many significant variables can cause the PCA to fail to identify enough PCs to explain the variability in the samples. For instance, adding a separate classification for each of the 9 potential parameter combinations (i.e. wood 500 °C and 0.2 slpm, wood 500 °C and 10 slpm, wood 700 °C and 10 slpm, and so on for each other biomass fuel) leads to every single compounds in the samples being selected as significant by the feature selection algorithm. This effect can be avoided by simply obtaining more samples of each classification, or by classifying the samples according to only one or two parameters, as shown in Figures 3.5 and 3.6.

Nonetheless, it can still be helpful to add granularity in the classifications so long as enough variability is explained by each PC. Since temperature and flow rate appear to cause the most clustering, PCA with separate classifications for both of these parameters was performed further. As can be seen in Figure 3.7, separating the heating

temperatures by the flow rate used yields better clustering for the majority of the samples. The high dispersion among the 500 °C 0.2 slpm samples is presumably due to the inefficient heating parameters, which may cause the emission of more varied molecules. Alternatively, it is also possible that biomass fuel type has more significance in dictating emission properties during inefficient pyrolysis, whereas efficient combustion produces more uniform emissions.

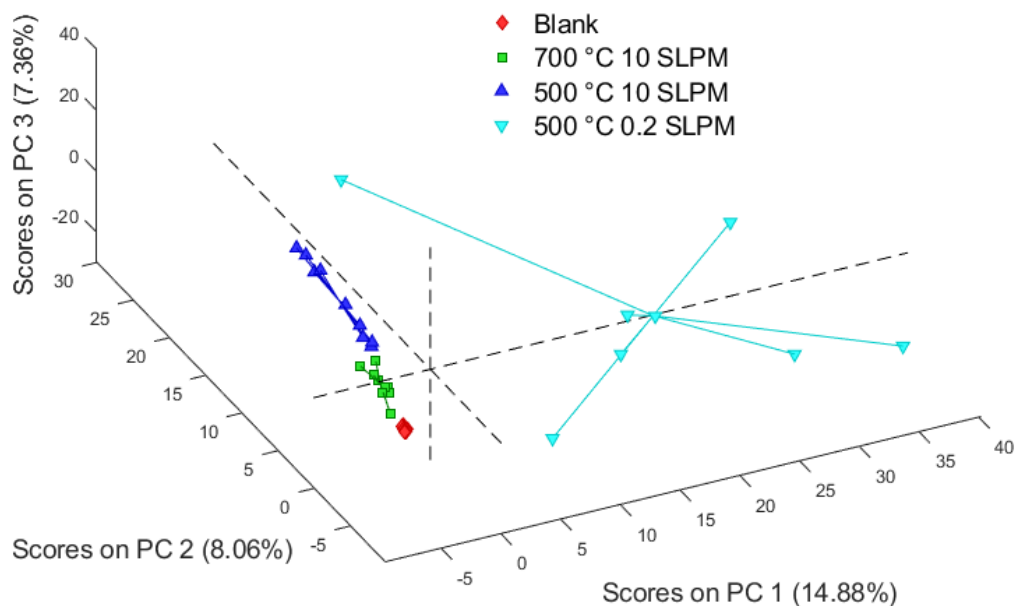


Figure 3.7: Principal component analysis (PCA) of biomass burning emissions after feature selection and classification by flow rate and heating temperature. The point at which the lines from each marker meet indicates the average score for all samples of that classification.

Overall, the PCA plots indicate that each of the parameters (biomass type, temperature, and flow rate), all drive the emission of specific compound features. While features originated by the type of biomass burned tend to explain a higher % of the variability, it is flow rate and temperature which cluster and characterize the emissions most significantly. Appropriately, samples gathered under inefficient burning conditions appear to have more diverse compositions, corroborating the results from Section 3.3.1.

3.4 Conclusion and future work

This work represents the first investigation of emissions from cow dung combustion using GC×GC-MS, and the first application of PCA to the study cow dung burning emissions at the time this thesis was published. We found that under the parameters studied the major driver of differentiation in emission composition were flow rate and temperature during the combustion, rather than biomass type. Specifically, the composition of the emissions was more variable under inefficient burning conditions. At lower flow rates and temperatures, the emissions become more unsaturated, containing a higher number of nitrogen atoms and heterocyclic features which are typical of BrC compounds. This has implications for their capacity to absorb light after emission into the atmosphere, as well as their potential health effects. Although the base composition of dung biomass fuels has been shown to contain a larger fraction of nitrogen over wood [1, 280, 285, 326], this did not translate into the emission of nitrogen containing compounds specific to cow dung biomass. Rather, a higher number of nitrogen containing compounds common to all biomass types are emitted from cow dung fuels, particularly so under low flow rate conditions.

PCA for the deconvolution of BBE shows promising results. Ideally, the PCA data shown in this chapter should be validated by analyzing additional samples in the future. While the classifications presented here are enough to differentiate some sample parameters (such as temperature and flow rate), there is not sufficient data for more granular differentiation (such as the simultaneous effect of temperature, flow rate, and biomass type). With more accurate classifications, the PC and features which drive the variability in the samples could be ascertained. This would allow the identification of individual compounds emitted by different biomass types under specific combustion conditions. Optimistically, these compounds might serve as tracers for source apportionment of dung biomass burning events, or to better constrain the degree of combustion efficiency of the burn which originated them.

References

- [1] M. Loebel Roson *et al.*, “Chemical characterization of emissions arising from solid fuel combustion—contrasting wood and cow dung burning,” *ACS Earth and Space Chemistry*, vol. 5, no. 10, pp. 2925–2937, 2021. DOI: 10.1021/acsearthspacechem.1c00268.
- [5] K. Balakrishnan *et al.*, “Air pollution from household solid fuel combustion in india: An overview of exposure and health related information to inform health research priorities,” *Global Health Action*, vol. 4, no. 1, p. 5638, 2011, PMID: 21987631. DOI: 10.3402/gha.v4i0.5638. [Online]. Available: <https://doi.org/10.3402/gha.v4i0.5638>.
- [6] W. H. O. (WHO), “Global household energy database,” 2023. [Online]. Available: <https://www.who.int/data/gho/data/themes/air-pollution/household-air-pollution>.
- [7] J. Popp, S. Kovács, J. Oláh, Z. Divéki, and E. Balázs, “Bioeconomy: Biomass and biomass-based energy supply and demand,” *New Biotechnology*, vol. 60, pp. 76–84, 2021, ISSN: 1871-6784. DOI: <https://doi.org/10.1016/j.nbt.2020.10.004>. [Online]. Available: <https://www.sciencedirect.com/science/article/pii/S1871678420301825>.
- [8] P. McKendry, “Energy production from biomass (part 1): Overview of biomass,” *Bioresource Technology*, vol. 83, no. 1, pp. 37–46, 2002, Reviews Issue, ISSN: 0960-8524. DOI: [https://doi.org/10.1016/S0960-8524\(01\)00118-3](https://doi.org/10.1016/S0960-8524(01)00118-3). [Online]. Available: <https://www.sciencedirect.com/science/article/pii/S0960852401001183>.
- [9] T. C. Bond, D. G. Streets, K. F. Yarber, S. M. Nelson, J.-H. Woo, and Z. Klimont, “A technology-based global inventory of black and organic carbon emissions from combustion,” *Journal of Geophysical Research: Atmospheres*, vol. 109, no. D14, 2004, D14203, 10.1029/2003JD003697. DOI: <https://doi.org/10.1029/2003JD003697>. [Online]. Available: <https://agupubs.onlinelibrary.wiley.com/doi/abs/10.1029/2003JD003697>.
- [11] S. S. Lim *et al.*, “A comparative risk assessment of burden of disease and injury attributable to 67 risk factors and risk factor clusters in 21 regions, 1990–2010: A systematic analysis for the Global Burden of Disease Study 2010,” en, *The Lancet*, vol. 380, no. 9859, pp. 2224–2260, Dec. 2012, ISSN: 01406736. DOI: 10.1016/S0140-6736(12)61766-8. [Online]. Available: <https://linkinghub.elsevier.com/retrieve/pii/S0140673612617668> (visited on 06/25/2021).
- [16] C. J. Murray *et al.*, “Global burden of 87 risk factors in 204 countries and territories, 1990–2019: A systematic analysis for the global burden of disease study 2019,” *The lancet*, vol. 396, no. 10258, pp. 1223–1249, 2020.

- [22] A. A. May *et al.*, “Gas-particle partitioning of primary organic aerosol emissions: 3. biomass burning,” *Journal of Geophysical Research: Atmospheres*, vol. 118, no. 19, pp. 11,327–11,338, 2013. DOI: <https://doi.org/10.1002/jgrd.50828>. [Online]. Available: <https://agupubs.onlinelibrary.wiley.com/doi/abs/10.1002/jgrd.50828>.
- [23] M. Hallquist *et al.*, “The formation, properties and impact of secondary organic aerosol: Current and emerging issues,” *Atmospheric Chemistry and Physics*, vol. 9, no. 14, pp. 5155–5236, 2009. DOI: 10.5194/acp-9-5155-2009. [Online]. Available: <https://acp.copernicus.org/articles/9/5155/2009/>.
- [24] M. Kanakidou *et al.*, “Organic aerosol and global climate modelling: A review,” *Atmospheric Chemistry and Physics*, vol. 5, no. 4, pp. 1053–1123, 2005. DOI: 10.5194/acp-5-1053-2005. [Online]. Available: <https://acp.copernicus.org/articles/5/1053/2005/>.
- [30] P. Jain, D. Castellanos-Acuna, S. C. P. Coogan, J. T. Abatzoglou, and M. D. Flannigan, “Observed increases in extreme fire weather driven by atmospheric humidity and temperature,” *Nature Climate Change*, vol. 12, no. 1, pp. 63–70, Jan. 2022, ISSN: 1758-6798. DOI: 10.1038/s41558-021-01224-1. [Online]. Available: <https://doi.org/10.1038/s41558-021-01224-1>.
- [31] A. L. Westerling, “Increasing western us forest wildfire activity: Sensitivity to changes in the timing of spring,” *Philosophical Transactions of the Royal Society B: Biological Sciences*, vol. 371, no. 1696, p. 20150178, 2016. DOI: 10.1098/rstb.2015.0178. [Online]. Available: <https://royalsocietypublishing.org/doi/abs/10.1098/rstb.2015.0178>.
- [32] S. Szopa *et al.*, “Short-lived climate forcers,” in *Climate Change 2021: The Physical Science Basis. Contribution of Working Group I to the Sixth Assessment Report of the Intergovernmental Panel on Climate Change*, V. Masson-Delmotte *et al.*, Eds. Cambridge, United Kingdom and New York, NY, USA: Cambridge University Press, 2021, 817–922. DOI: 10.1017/9781009157896.008.
- [34] I. P. on Climate Change, “Anthropogenic and natural radiative forcing,” in *Climate Change 2013 – The Physical Science Basis: Working Group I Contribution to the Fifth Assessment Report of the Intergovernmental Panel on Climate Change*. Cambridge University Press, 2014, 659–740, 923–1055. DOI: 10.1017/CBO9781107415324.018.
- [35] V. Ramanathan and G. Carmichael, “Global and regional climate changes due to black carbon,” *Nature Geoscience*, vol. 1, no. 4, pp. 221–227, Apr. 2008, ISSN: 1752-0908. DOI: 10.1038/ngeo156. [Online]. Available: <https://doi.org/10.1038/ngeo156>.
- [36] R. J. Park, M. J. Kim, J. I. Jeong, D. Youn, and S. Kim, “A contribution of brown carbon aerosol to the aerosol light absorption and its radiative forcing in east asia,” *Atmospheric Environment*, vol. 44, no. 11, pp. 1414–1421, 2010, ISSN: 1352-2310. DOI: <https://doi.org/10.1016/j.atmosenv.2010.01.042>.

- [Online]. Available: <https://www.sciencedirect.com/science/article/pii/S1352231010001019>.
- [37] Z. Lu *et al.*, “Light absorption properties and radiative effects of primary organic aerosol emissions,” *Environmental Science & Technology*, vol. 49, no. 8, pp. 4868–4877, 2015. DOI: 10.1021/acs.est.5b00211. [Online]. Available: <https://doi.org/10.1021/acs.est.5b00211>.
- [43] A. Laskin, J. Laskin, and S. A. Nizkorodov, “Chemistry of atmospheric brown carbon,” *Chemical Reviews*, vol. 115, no. 10, pp. 4335–4382, 2015. DOI: 10.1021/cr5006167. [Online]. Available: <https://doi.org/10.1021/cr5006167>.
- [44] M. O. Andreae and A. Gelencsér, “Black carbon or brown carbon? the nature of light-absorbing carbonaceous aerosols,” *Atmospheric Chemistry and Physics*, vol. 6, no. 10, pp. 3131–3148, 2006. DOI: 10.5194/acp-6-3131-2006. [Online]. Available: <https://acp.copernicus.org/articles/6/3131/2006/>.
- [48] R. Saleh, “From measurements to models: Toward accurate representation of brown carbon in climate calculations,” *Current Pollution Reports*, vol. 6, no. 2, pp. 90–104, Jun. 2020, ISSN: 2198-6592. DOI: 10.1007/s40726-020-00139-3. [Online]. Available: <https://doi.org/10.1007/s40726-020-00139-3>.
- [50] Y. Feng, V. Ramanathan, and V. R. Kotamarthi, “Brown carbon: A significant atmospheric absorber of solar radiation?” *Atmospheric Chemistry and Physics*, vol. 13, no. 17, pp. 8607–8621, 2013. DOI: 10.5194/acp-13-8607-2013. [Online]. Available: <https://acp.copernicus.org/articles/13/8607/2013/>.
- [56] R. Suresh, V. Singh, J. Malik, A. Datta, and R. Pal, “Evaluation of the performance of improved biomass cooking stoves with different solid biomass fuel types,” *Biomass and Bioenergy*, vol. 95, pp. 27–34, 2016, ISSN: 0961-9534. DOI: <https://doi.org/10.1016/j.biombioe.2016.08.002>. [Online]. Available: <https://www.sciencedirect.com/science/article/pii/S0961953416302616>.
- [57] M. A. Johnson *et al.*, “Impacts on household fuel consumption from biomass stove programs in india, nepal, and peru,” *Energy for Sustainable Development*, vol. 17, no. 5, pp. 403–411, 2013, ISSN: 0973-0826. DOI: <https://doi.org/10.1016/j.esd.2013.04.004>. [Online]. Available: <https://www.sciencedirect.com/science/article/pii/S0973082613000343>.
- [61] B. R. Simoneit, “Biomass burning — a review of organic tracers for smoke from incomplete combustion,” *Applied Geochemistry*, vol. 17, no. 3, pp. 129–162, 2002, ISSN: 0883-2927. DOI: [https://doi.org/10.1016/S0883-2927\(01\)00061-0](https://doi.org/10.1016/S0883-2927(01)00061-0). [Online]. Available: <https://www.sciencedirect.com/science/article/pii/S0883292701000610>.
- [73] S. R. Freitas *et al.*, “Monitoring the transport of biomass burning emissions in south america,” *Environmental Fluid Mechanics*, vol. 5, no. 1, pp. 135–167, Apr. 2005, ISSN: 1573-1510. DOI: 10.1007/s10652-005-0243-7. [Online]. Available: <https://doi.org/10.1007/s10652-005-0243-7>.

- [107] A. T. Ahern *et al.*, “Production of secondary organic aerosol during aging of biomass burning smoke from fresh fuels and its relationship to voc precursors,” *Journal of Geophysical Research: Atmospheres*, vol. 124, no. 6, pp. 3583–3606, 2019. DOI: <https://doi.org/10.1029/2018JD029068>. [Online]. Available: <https://agupubs.onlinelibrary.wiley.com/doi/abs/10.1029/2018JD029068>.
- [109] P. Lin, L. T. Fleming, S. A. Nizkorodov, J. Laskin, and A. Laskin, “Comprehensive molecular characterization of atmospheric brown carbon by high resolution mass spectrometry with electrospray and atmospheric pressure photoionization,” *Analytical Chemistry*, vol. 90, no. 21, pp. 12 493–12 502, 2018. DOI: [10.1021/acs.analchem.8b02177](https://doi.org/10.1021/acs.analchem.8b02177). [Online]. Available: <https://doi.org/10.1021/acs.analchem.8b02177>.
- [124] L. T. Fleming *et al.*, “Molecular composition and photochemical lifetimes of brown carbon chromophores in biomass burning organic aerosol,” *Atmospheric Chemistry and Physics*, vol. 20, no. 2, pp. 1105–1129, 2020. DOI: [10.5194/acp-20-1105-2020](https://doi.org/10.5194/acp-20-1105-2020). [Online]. Available: <https://acp.copernicus.org/articles/20/1105/2020/>.
- [125] C. F. Fortenberry, M. J. Walker, Y. Zhang, D. Mitroo, W. H. Brune, and B. J. Williams, “Bulk and molecular-level characterization of laboratory-aged biomass burning organic aerosol from oak leaf and heartwood fuels,” *Atmospheric Chemistry and Physics*, vol. 18, no. 3, pp. 2199–2224, 2018. DOI: [10.5194/acp-18-2199-2018](https://doi.org/10.5194/acp-18-2199-2018). [Online]. Available: <https://acp.copernicus.org/articles/18/2199/2018/>.
- [141] Y. Iinuma *et al.*, “Source characterization of biomass burning particles: The combustion of selected european conifers, african hardwood, savanna grass, and german and indonesian peat,” *Journal of Geophysical Research: Atmospheres*, vol. 112, no. D8, 2007. DOI: <https://doi.org/10.1029/2006JD007120>. [Online]. Available: <https://agupubs.onlinelibrary.wiley.com/doi/abs/10.1029/2006JD007120>.
- [154] M. O. Andreae, “Biomass burning-its history, use, and distribution and its impact on environmental quality and global climate,” in *Global biomass burning- Atmospheric, climatic, and biospheric implications*, 1991.
- [156] S. P. Urbanski, “Combustion efficiency and emission factors for wildfire-season fires in mixed conifer forests of the northern rocky mountains, us,” *Atmospheric Chemistry and Physics*, vol. 13, no. 14, pp. 7241–7262, 2013. DOI: [10.5194/acp-13-7241-2013](https://doi.org/10.5194/acp-13-7241-2013). [Online]. Available: <https://acp.copernicus.org/articles/13/7241/2013/>.
- [157] B. Rooney *et al.*, “Impacts of household sources on air pollution at village and regional scales in india,” *Atmospheric Chemistry and Physics*, vol. 19, no. 11, pp. 7719–7742, 2019. DOI: [10.5194/acp-19-7719-2019](https://doi.org/10.5194/acp-19-7719-2019). [Online]. Available: <https://acp.copernicus.org/articles/19/7719/2019/>.

- [158] A. L. Hodshire *et al.*, “Aging effects on biomass burning aerosol mass and composition: A critical review of field and laboratory studies,” *Environmental Science & Technology*, vol. 53, no. 17, pp. 10 007–10 022, 2019. DOI: 10.1021/acs.est.9b02588. [Online]. Available: <https://doi.org/10.1021/acs.est.9b02588>.
- [161] Z. C. J. Decker *et al.*, “Nighttime chemical transformation in biomass burning plumes: A box model analysis initialized with aircraft observations,” *Environmental Science & Technology*, vol. 53, no. 5, pp. 2529–2538, 2019, PMID: 30698424. DOI: 10.1021/acs.est.8b05359. [Online]. Available: <https://doi.org/10.1021/acs.est.8b05359>.
- [165] J. Tian *et al.*, “A biomass combustion chamber: Design, evaluation, and a case study of wheat straw combustion emission tests,” *Aerosol and Air Quality Research*, vol. 15, no. 5, pp. 2104–2114, 2015. DOI: 10.4209/aaqr.2015.03.0167. [Online]. Available: <https://doi.org/10.4209/aaqr.2015.03.0167>.
- [167] L. E. Hatch, A. Rivas-Ubach, C. N. Jen, M. Lipton, A. H. Goldstein, and K. C. Barsanti, “Measurements of i/svocs in biomass-burning smoke using solid-phase extraction disks and two-dimensional gas chromatography,” *Atmospheric Chemistry and Physics*, vol. 18, no. 24, pp. 17 801–17 817, 2018. DOI: 10.5194/acp-18-17801-2018. [Online]. Available: <https://acp.copernicus.org/articles/18/17801/2018/>.
- [204] R. J. Sheesley, J. J. Schauer, Z. Chowdhury, G. R. Cass, and B. R. Simoneit, “Characterization of organic aerosols emitted from the combustion of biomass indigenous to south asia,” *Journal of Geophysical Research: Atmospheres*, vol. 108, no. D9, 2003, 4285, 10.1029/2002JD002981.
- [217] Z. Yang, N. T. Tsona, C. George, and L. Du, “Nitrogen-containing compounds enhance light absorption of aromatic-derived brown carbon,” *Environmental Science & Technology*, vol. 56, no. 7, pp. 4005–4016, 2022, PMID: 35192318. DOI: 10.1021/acs.est.1c08794. [Online]. Available: <https://doi.org/10.1021/acs.est.1c08794>.
- [218] K. S. Chow, X. H. H. Huang, and J. Z. Yu, “Quantification of nitroaromatic compounds in atmospheric fine particulate matter in hong kong over 3 years: Field measurement evidence for secondary formation derived from biomass burning emissions,” *Environmental Chemistry*, vol. 13, no. 4, pp. 665–673, 2016. DOI: 10.1071/EN15174. [Online]. Available: <https://doi.org/10.1071/EN15174>.
- [219] A. R. Koss *et al.*, “Non-methane organic gas emissions from biomass burning: Identification, quantification, and emission factors from ptr-tof during the firex 2016 laboratory experiment,” *Atmospheric Chemistry and Physics*, vol. 18, no. 5, pp. 3299–3319, 2018. DOI: 10.5194/acp-18-3299-2018. [Online]. Available: <https://acp.copernicus.org/articles/18/3299/2018/>.

- [224] Y. Huo *et al.*, “Chemical fingerprinting of hulis in particulate matters emitted from residential coal and biomass combustion,” *Environmental Science & Technology*, vol. 55, no. 6, pp. 3593–3603, 2021, PMID: 33656861. DOI: 10.1021/acs.est.0c08518. [Online]. Available: <https://doi.org/10.1021/acs.est.0c08518>.
- [232] K. E. Pickering *et al.*, “Convective transport of biomass burning emissions over brazil during trace a,” *Journal of Geophysical Research: Atmospheres*, vol. 101, no. D19, pp. 23 993–24 012, 1996. DOI: <https://doi.org/10.1029/96JD00346>. [Online]. Available: <https://agupubs.onlinelibrary.wiley.com/doi/abs/10.1029/96JD00346>.
- [233] J. S. Fu *et al.*, “Evaluating the influences of biomass burning during 2006 base-asia: A regional chemical transport modeling,” *Atmospheric Chemistry and Physics*, vol. 12, no. 9, pp. 3837–3855, 2012. DOI: 10.5194/acp-12-3837-2012. [Online]. Available: <https://acp.copernicus.org/articles/12/3837/2012/>.
- [241] L. E. Hatch, W. Luo, J. F. Pankow, R. J. Yokelson, C. E. Stockwell, and K. C. Barsanti, “Identification and quantification of gaseous organic compounds emitted from biomass burning using two-dimensional gas chromatography–time-of-flight mass spectrometry,” *Atmospheric Chemistry and Physics*, vol. 15, no. 4, pp. 1865–1899, 2015. DOI: 10.5194/acp-15-1865-2015. [Online]. Available: <https://acp.copernicus.org/articles/15/1865/2015/>.
- [243] C. N. Jen *et al.*, “Speciated and total emission factors of particulate organics from burning western us wildland fuels and their dependence on combustion efficiency,” *Atmospheric Chemistry and Physics*, vol. 19, no. 2, pp. 1013–1026, 2019. DOI: 10.5194/acp-19-1013-2019. [Online]. Available: <https://acp.copernicus.org/articles/19/1013/2019/>.
- [249] L. T. Fleming *et al.*, “Emissions from village cookstoves in haryana, india, and their potential impacts on air quality,” *Atmospheric Chemistry and Physics*, vol. 18, no. 20, pp. 15 169–15 182, 2018. DOI: 10.5194/acp-18-15169-2018. [Online]. Available: <https://acp.copernicus.org/articles/18/15169/2018/>.
- [280] R. C. Pettersen, “The chemical composition of wood,” in *The Chemistry of Solid Wood*, ch. 2, pp. 57–126. DOI: 10.1021/ba-1984-0207.ch002. [Online]. Available: <https://pubs.acs.org/doi/abs/10.1021/ba-1984-0207.ch002>.
- [285] T. S. Griffin, Z. He, and C. W. Honeycutt, “Manure composition affects net transformation of nitrogen from dairy manures,” in *Plant and Soil*, vol. 273, no. 1-2, pp. 29–38, Jun. 2005, ISSN: 0032-079X, 1573-5036. DOI: 10.1007/s11104-004-6473-5. [Online]. Available: <http://link.springer.com/10.1007/s11104-004-6473-5> (visited on 06/28/2021).
- [315] E. A. Higgins Keppler, C. L. Jenkins, T. J. Davis, and H. D. Bean, “Advances in the application of comprehensive two-dimensional gas chromatography in metabolomics,” *TrAC Trends in Analytical Chemistry*, vol. 109, pp. 275–286, 2018, ISSN: 0165-9936. DOI: <https://doi.org/10.1016/j.trac.2018.10.015>. [Online]. Available: <https://www.sciencedirect.com/science/article/pii/S0165993618300633>.

- [316] Y. Gloaguen, J. A. Kirwan, and D. Beule, “Deep learning-assisted peak curation for large-scale lc-ms metabolomics,” *Analytical Chemistry*, vol. 94, no. 12, pp. 4930–4937, 2022, PMID: 35290737. DOI: 10.1021/acs.analchem.1c02220. [Online]. Available: <https://doi.org/10.1021/acs.analchem.1c02220>.
- [317] N. Schauer *et al.*, “Gc–ms libraries for the rapid identification of metabolites in complex biological samples,” *FEBS Letters*, vol. 579, no. 6, pp. 1332–1337, 2005, ISSN: 0014-5793. DOI: <https://doi.org/10.1016/j.febslet.2005.01.029>. [Online]. Available: <https://www.sciencedirect.com/science/article/pii/S0014579305001183>.
- [318] S. L. Nam, A. P. de la Mata, and J. J. Harynuk, “Automated screening and filtering scripts for gc×gc-tofms metabolomics data,” *Separations*, vol. 8, no. 6, 2021, ISSN: 2297-8739. DOI: 10.3390/separations8060084. [Online]. Available: <https://www.mdpi.com/2297-8739/8/6/84>.
- [319] G. S. Groenewold *et al.*, “Pyrolysis two-dimensional gc-ms of miscanthus biomass: Quantitative measurement using an internal standard method,” *Energy & Fuels*, vol. 31, no. 2, pp. 1620–1630, 2017. DOI: 10.1021/acs.energyfuels.6b02645. [Online]. Available: <https://doi.org/10.1021/acs.energyfuels.6b02645>.
- [320] S. P. Urbanski, W. M. Hao, and S. Baker, “Chapter 4 chemical composition of wildland fire emissions,” in *Wildland Fires and Air Pollution*, ser. Developments in Environmental Science, A. Bytnerowicz, M. J. Arbaugh, A. R. Riebau, and C. Andersen, Eds., vol. 8, Elsevier, 2008, pp. 79–107. DOI: [https://doi.org/10.1016/S1474-8177\(08\)00004-1](https://doi.org/10.1016/S1474-8177(08)00004-1). [Online]. Available: <https://www.sciencedirect.com/science/article/pii/S1474817708000041>.
- [321] M. S. Armstrong, A. P. de la Mata, and J. J. Harynuk, “An efficient and accurate numerical determination of the cluster resolution metric in two dimensions,” *Journal of Chemometrics*, vol. 35, no. 7-8, e3346, 2021. DOI: <https://doi.org/10.1002/cem.3346>. [Online]. Available: <https://analyticalsciencejournals.onlinelibrary.wiley.com/doi/abs/10.1002/cem.3346>.
- [322] N. A. Sinkov and J. J. Harynuk, “Cluster resolution: A metric for automated, objective and optimized feature selection in chemometric modeling,” *Talanta*, vol. 83, no. 4, pp. 1079–1087, 2011, Enhancing Chemical Separations with Chemometric Data Analysis, ISSN: 0039-9140. DOI: <https://doi.org/10.1016/j.talanta.2010.10.025>. [Online]. Available: <https://www.sciencedirect.com/science/article/pii/S0039914010008210>.
- [323] Y. Song, S. Xie, Y. Zhang, L. Zeng, L. G. Salmon, and M. Zheng, “Source apportionment of pm2.5 in beijing using principal component analysis/absolute principal component scores and unmix,” *Science of The Total Environment*, vol. 372, no. 1, pp. 278–286, 2006, ISSN: 0048-9697. DOI: <https://doi.org/10.1016/j.scitotenv.2006.08.041>. [Online]. Available: <https://www.sciencedirect.com/science/article/pii/S0048969706006760>.

- [324] Y. Choi *et al.*, “Survey of whole air data from the second airborne biomass burning and lightning experiment using principal component analysis,” *Journal of Geophysical Research: Atmospheres*, vol. 108, no. D5, 2003. DOI: <https://doi.org/10.1029/2002JD002841>. [Online]. Available: <https://agupubs.onlinelibrary.wiley.com/doi/abs/10.1029/2002JD002841>.
- [325] K. Ravindra, T. Singh, V. Singh, S. Chintalapati, G. Beig, and S. Mor, “Understanding the influence of summer biomass burning on air quality in north india: Eight cities field campaign study,” *Science of The Total Environment*, vol. 861, p. 160 361, 2023, ISSN: 0048-9697. DOI: <https://doi.org/10.1016/j.scitotenv.2022.160361>. [Online]. Available: <https://www.sciencedirect.com/science/article/pii/S0048969722074630>.
- [326] M. Wang *et al.*, “To distinguish the primary characteristics of agro-waste biomass by the principal component analysis: An investigation in east china,” *Waste Management*, vol. 90, pp. 100–120, 2019, ISSN: 0956-053X. DOI: <https://doi.org/10.1016/j.wasman.2019.04.046>. [Online]. Available: <https://www.sciencedirect.com/science/article/pii/S0956053X19302594>.
- [327] W. Li *et al.*, “Tracers from biomass burning emissions and identification of biomass burning,” *Atmosphere*, vol. 12, no. 11, 2021, ISSN: 2073-4433. DOI: [10.3390/atmos12111401](https://doi.org/10.3390/atmos12111401). [Online]. Available: <https://www.mdpi.com/2073-4433/12/11/1401>.
- [328] N. G. Lewis and L. B. Davin, “1.25 - lignans: Biosynthesis and function,” in *Comprehensive Natural Products Chemistry*, S. D. Barton, K. Nakanishi, and O. Meth-Cohn, Eds., Oxford: Pergamon, 1999, pp. 639–712, ISBN: 978-0-08-091283-7. DOI: <https://doi.org/10.1016/B978-0-08-091283-7.00027-8>. [Online]. Available: <https://www.sciencedirect.com/science/article/pii/B9780080912837000278>.
- [329] J. del Río, M. Speranza, A. Gutiérrez, M. Martínez, and A. Martínez, “Lignin attack during eucalypt wood decay by selected basidiomycetes: A py-gc/ms study,” *Journal of Analytical and Applied Pyrolysis*, vol. 64, no. 2, pp. 421–431, 2002, ISSN: 0165-2370. DOI: [https://doi.org/10.1016/S0165-2370\(02\)00043-8](https://doi.org/10.1016/S0165-2370(02)00043-8). [Online]. Available: <https://www.sciencedirect.com/science/article/pii/S0165237002000438>.
- [330] E. Bae, J.-G. Na, S. H. Chung, H. S. Kim, and S. Kim, “Identification of about 30000 chemical components in shale oils by electrospray ionization (esi) and atmospheric pressure photoionization (appi) coupled with 15 t fourier transform ion cyclotron resonance mass spectrometry (ft-icr ms) and a comparison to conventional oil,” *Energy & Fuels*, vol. 24, no. 4, pp. 2563–2569, 2010. DOI: [10.1021/ef100060b](https://doi.org/10.1021/ef100060b). [Online]. Available: <https://doi.org/10.1021/ef100060b>.
- [331] B. P. Koch and T. Dittmar, “From mass to structure: An aromaticity index for high-resolution mass data of natural organic matter,” *Rapid Communications in Mass Spectrometry*, vol. 20, no. 5, pp. 926–932, 2006. DOI: <https://doi.org/10.1002/rcm.2386>. [Online]. Available: <https://analyticalsciencejournals.onlinelibrary.wiley.com/doi/abs/10.1002/rcm.2386>.

- [332] H. Tong *et al.*, “Molecular composition of organic aerosols at urban background and road tunnel sites using ultra-high resolution mass spectrometry,” *Faraday Discuss.*, vol. 189, pp. 51–68, 0 2016. DOI: 10.1039/C5FD00206K. [Online]. Available: <http://dx.doi.org/10.1039/C5FD00206K>.
- [333] J.-H. Park, Z. B. Babar, S. J. Baek, H. S. Kim, and H.-J. Lim, “Effects of nox on the molecular composition of secondary organic aerosol formed by the ozonolysis and photooxidation of α -pinene,” *Atmospheric Environment*, vol. 166, pp. 263–275, 2017, ISSN: 1352-2310. DOI: <https://doi.org/10.1016/j.atmosenv.2017.07.022>. [Online]. Available: <https://www.sciencedirect.com/science/article/pii/S1352231017304636>.
- [334] Y. Wei, T. Cao, and J. E. Thompson, “The chemical evolution & physical properties of organic aerosol: A molecular structure based approach,” *Atmospheric Environment*, vol. 62, pp. 199–207, 2012, ISSN: 1352-2310. DOI: <https://doi.org/10.1016/j.atmosenv.2012.08.029>. [Online]. Available: <https://www.sciencedirect.com/science/article/pii/S1352231012008011>.
- [335] K. O. Johansson *et al.*, “Formation and emission of large furans and oxygenated hydrocarbons from flames,” *Proceedings of the National Academy of Sciences*, vol. 113, no. 30, pp. 8374–8379, 2016. DOI: 10.1073/pnas.1604772113. [Online]. Available: <https://www.pnas.org/doi/abs/10.1073/pnas.1604772113>.
- [336] S. Rowat, “Incinerator toxic emissions: A brief summary of human health effects with a note on regulatory control,” *Medical Hypotheses*, vol. 52, no. 5, pp. 389–396, 1999, ISSN: 0306-9877. DOI: <https://doi.org/10.1054/mehy.1994.0675>. [Online]. Available: <https://www.sciencedirect.com/science/article/pii/S030698778470675X>.
- [337] X. Liao *et al.*, “Contamination profiles and health impact of benzothiazole and its derivatives in pm2.5 in typical chinese cities,” *Science of The Total Environment*, vol. 755, p. 142617, 2021, ISSN: 0048-9697. DOI: <https://doi.org/10.1016/j.scitotenv.2020.142617>. [Online]. Available: <https://www.sciencedirect.com/science/article/pii/S0048969720361465>.

Chapter 4

Unexpected Electrophiles in the Atmosphere - Anhydride Nucleophile Reactions and Uptake to Biomass Burning Emissions

Reproduced with minor formatting changes from its original publication as:

M. Loebel Roson, M. Abou-Ghanem, E. Kim, S. Wu, D. Long, S. A. Styler, and R. Zhao, “Unexpected electrophiles in the atmosphere – anhydride nucleophile reactions and uptake to biomass burning emissions,” *Phys. Chem. Chem. Phys.*, 2023. DOI: 10.1039/D3CP01751F. With permission from the Royal Society of Chemistry.

4.1 Introduction

As a source of both environment- and health-affecting emissions, biomass burning has garnered considerable focus over the past few decades [11, 16, 155, 268, 338]. Much of this attention has been focused on identifying the effects and evolution of biomass burning emissions in the atmosphere [70, 155, 339]. Additional efforts have been directed towards deconvoluting the composition of the emissions themselves, as it is highly variable between burns and likely responsible for its harmful effects [11, 16]; however, the fluctuating emission composition makes identification efforts considerably more difficult. While the commonly - and relatively high abundance - emitted compounds are well established (such as cellulose and hemicellulose decomposition products), the largest fraction represented by numerous low-intensity species, is not [1, 42, 43, 123, 141, 155, 340]. Convoluting things further, primary organic aerosol will physically and chemically evolve in the atmosphere. Through reactions occurring inside particles, as well as interactions with gas-phase molecules, its composition and effects are additionally modified [67, 106, 248, 341–343].

Recent studies have demonstrated that photochemical processing of biomass burn plumes in the atmosphere leads to the formation of anhydrides through aromatic oxidation and furan chemistry [137, 344–348]. Specifically, maleic and phthalic anhydride represent two significant primary emissions from the combustion of biomass [138]. Without taking their eventual formation in the atmosphere into consideration, the emission factors of maleic and phthalic anhydride (50 ± 30 and 19 ± 9 mg kg⁻¹ from beech wood respectively [138]) can surpass those of other significant tracer species. For instance, the emission factor of syringol (20 ± 30 mg kg⁻¹), vanillin (10 ± 10 mg kg⁻¹), and guaiacol (40 ± 50 mg kg⁻¹) have been found to be inferior under the same burning conditions, although highly variable between burns [138].

Ordinarily, reactive anhydrides such as maleic or phthalic anhydride would be expected to swiftly decay once emitted into the atmosphere through hydration into their acid form [139, 140, 349, 350]. As a result, both maleic and phthalic acid have been previously detected as a fraction of particulate matter [139, 140, 351–353]. Observation of acids suggests the occurrence of anhydride condensed-phase chemistry [354]. However, atmospherically relevant anhydrides are too volatile to be found in

the condensed-phase. The effective saturated mass concentration (C^*) of maleic and phthalic anhydride estimated using Donahue *et al.*'s two-dimensional volatility basis set are 0.237 and 18.8 g m⁻³ at 300 K respectively under ideal conditions (activity coefficient = 1) [98]. This means that the vast majority of anhydride molecules are presumably found in the vapour-phase and are unlikely to partition into the particle-phase under typical ambient aerosol loading (0.1-20 μg m⁻³) [98, 207, 355]. Therefore, it is reasonable to expect that maleic and phthalic anhydride must undergo transformation prior to partitioning, and that unrecognized processes are bringing the gas-phase anhydrides in contact with condensed-phase components. In fact, it has been suggested that a condensed-phase is likely required for some acid anhydrides to hydrolyze [139, 140], and that there are multiple pathways for the formation of particle-phase phthalic acid [354].

As part of a burn plume, anhydrides have been shown to remain stable over several days [348]. While traveling inside a plume or bound to particulate matter, anhydrides can be shielded from environmental effects that would typically degrade them, such as moisture or sunlight [356, 357]. Due to this increased atmospheric lifetime, anhydrides have been considered as potential tracers for aged biomass burning plumes [348], which have historically been source apportioned by atmospheric modelers using species such as levoglucosan [61, 221, 223]. Exposure to maleic and phthalic anhydride is a known cause of pulmonary, eye, and skin irritation [64]. While electrophiles can also increase the incidence of cancer by reacting with DNA [63], this effect has not been studied for anhydrides specifically.

In solvents, electrophilic anhydrides readily react with an assortment of nucleophiles. The mechanism for the acid catalyzed nucleophilic addition of water to an acid anhydride is depicted in Figure 4.1, ester and amide formation paths shortened [358]. The acid catalyzed path is favoured in the atmosphere, where the majority of available water is acidic in nature [359]. Similarly to Figure 4.1, heterocyclic anhydrides such as maleic and phthalic anhydride also hydrolyze under addition of water, forming instead dicarboxylic acids with higher molecular weight than their precursors. Correspondingly, they may also react with alcohol and amine containing nucleophiles to form products which contain both a carboxylic acid functional group in addition to an ester or amide group respectively.

With greater mass and inhibited volatility, these compounds are likely to contribute to secondary organic aerosol, enhancing the impact of biomass burning on air quality and climate [43, 77]. However, since the composition of biomass burning particulate matter has not been fully established, the identity of these nucleophiles, the outcome of their reaction with anhydrides, and their ultimate environmental fate remains largely unknown and unpredictable. Nonetheless, to react with particle-bound nucleophilic species, anhydrides need to first be uptaken to the surface of biomass burning particulate matter. Heterogeneous uptake of gas-phase species by particulate matter is an important consideration in atmospheric research, as it has been shown to impact particle optical and cloud forming capabilities, as well as the distribution of gas-phase species in the atmosphere [26]. Carbonaceous particles such as those emitted from biomass burning have a significant surface area to size ratio [25], which promotes uptake as both a physical (through absorption and adsorption, also known as bulk and surface accommodation respectively) and chemical process (through which the species react with the substrate itself, also known as reactive uptake) [26–28, 96, 143]. However, to our best knowledge, the uptake of anhydrides to particulate matter, including that arising from biomass burning, has never been studied. Identifying and quantifying the propensity for uptake anhydrides possess is imperative towards understanding their reactions on the surface of biomass burning particulate matter. And ultimately, determining whether these processes are forming distinct product classes, in addition to the fate of compounds anhydrides readily react with.

Herein, we posit that anhydrides are unrecognized and environmentally relevant electrophiles in the atmosphere, and have conducted a series of laboratory experiments to assess this hypothesis. In particular, we aimed to examine whether anhydrides would react with nucleophiles emitted from biomass burning, and how variable conditions would affect this reaction. Firstly, in a controlled liquid environment to assess the reversibility of the reaction, the stability of any formed products, the role of water, and the potential for competition with hydrolysis. Following, we sought to determine whether gas-phase anhydrides would be capable of accessing nucleophiles present in biomass burning emissions to produce similar products. To this end, we quantify the reactive uptake of phthalic anhydride on biomass burning films. We demonstrate

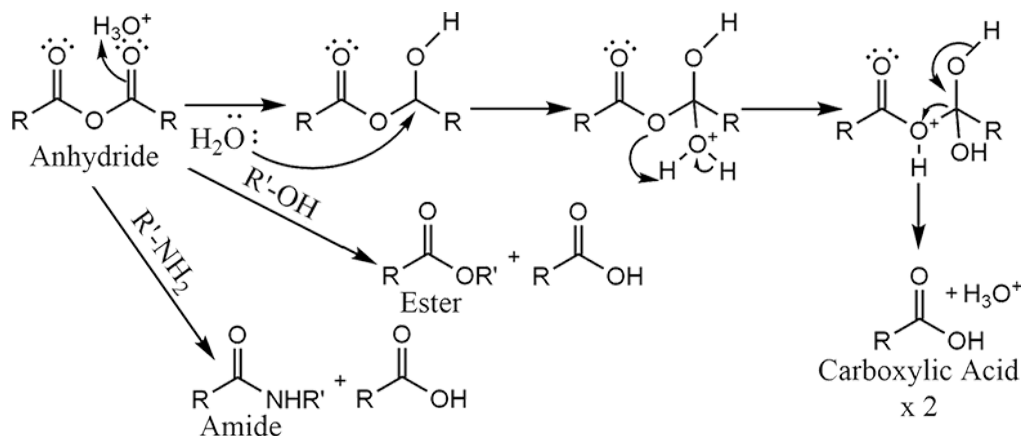


Figure 4.1: Acid catalyzed acid anhydride nucleophilic addition reaction, alcohol and amine driven additions are simplified.

that anhydrides emitted from biomass burning readily react with a variety of chemical species - including levoglucosan, a major biomass burning tracer - present in biomass burning emissions; and form low-volatility, water-stable products. These properties, coupled with their propensity to be strongly uptaken by biomass burning emissions, may make anhydrides significant model compounds to probe gas-phase interactions at the surface of biomass burning emissions in the future.

4.2 Materials and Methods

4.2.1 Choice of Anhydrides and Nucleophiles

Anhydrides are significant contributors of total emissions from biomass burning [347]. Maleic (99% purity, purchased from Sigma Aldrich) and phthalic anhydride (99+% A.C.S Reagent, Sigma Aldrich) were chosen as two of the major anhydrides observed in biomass burning emissions [138, 347]. Maleic anhydride is the end product of furan chemistry [347], while phthalic anhydride mostly forms through oxidation of naphthalene [138]. Phthalic anhydride is a precursor for phthalic acid [138, 347], which has been identified as a secondary organic aerosol constituent of aged biomass burning emissions [360, 361], and suggested as a proxy for the contribution of secondary organic aerosol to ambient samples [362–364]. The chosen nucleophilic species (referred to further as nucleophiles) represent only a few of the major emissions from biomass burning, and were selected due to their previous detection in Loebel Roson *et al.*[1].

Levoglucozan (99%, Sigma Aldrich), coniferyl aldehyde (98%, Sigma Aldrich), anisyl alcohol (98%, Sigma Aldrich), and vanillin (99%, ReagentPlus, Sigma Aldrich) are all common biomass burning tracers which represent a variety of functional groups and molecular properties [61, 141, 223, 351, 365]. Histidine (99%, ReagentPlus, Sigma Aldrich) is an essential amino acid present in animal dung, which is used as fuel for cooking and heating in numerous developing countries [157]. Additionally, to study the interactions between anhydrides and nucleophiles extrinsic to biomass burning emissions, a few species of anthropogenic origin were also studied. These species included aniline, chosen as the simplest aromatic amine ($\geq 99.5\%$, A.C.S Reagent, Sigma Aldrich), and triethylene glycol, as a highly oxygenated volatile organic compound (99%, ReagentPlus, Sigma Aldrich).

4.2.2 Nucleophilic Addition in the Condensed-Phase

To test the propensity of anhydrides to undergo nucleophilic addition reactions in the condensed-phase, a series of fundamental analyses were performed in solvents. The atmospheric condensed phases can be highly variable in their water contents. Organic aerosol can have minimal liquid water content under dry conditions, while cloud and fog are made of aqueous droplets. With high water availability, it is possible for the anhydride hydrolysis to take precedence over other nucleophilic addition reactions. As such, solutions were prepared in water and acetonitrile (ACN), with differing fractions of each solvent ranging from 0 to 99% (v/v) water. ACN was employed as an aprotic solvent that does not react with anhydrides. The stability of anhydrides in protic and aprotic solvents were examined using proton nuclear magnetic resonance (^1H NMR) spectroscopy. Each standard was dissolved to a concentration of 1 mM in both deuterated water (protic) and deuterated chloroform (aprotic), for a total of 8 samples per analysis. Each sample was spiked with a known concentration (0.5 mM) of dimethyl sulfoxide to act as an internal standard for chemical shift calibration and quantification, and analyzed after resting overnight. ^1H NMR chemical shift spectra are included in the Supplementary Information (C.1.1).

The nucleophiles and anhydrides were separately dissolved - in water and ACN respectively - to avoid premature formation of the acid. Following, maleic or phthalic anhydride dissolved in ACN were added to an aliquot of each nucleophile standard.

In each solution, the final concentration of the nucleophile and the anhydride was 0.8 mM and 0.08 mM respectively. To evaluate the stability of the formed products, solutions were left to rest enclosed under room light and temperature for up to a week after mixing. Liquid Chromatography Mass Spectrometry (LC-MS) injections of each solution were performed after 24 hours and 1 week. Solutions were separated on a Luna Omega 3 μm Polar C18 100 Å column (150×2.1 mm) purchased from Phenomenex Inc. The mobile phase consisted of 50% water and 50% ACN, both buffered with 0.05% formic acid, and kept isocratic throughout the 8 min separation. Negative electrospray ionization mode (ESI-) was used for ionization as it consistently yielded higher product signals over positive electrospray ionization (ESI+). Ion detection was conducted on a linear ion trap mass spectrometer (model LTQ XL, Thermo Scientific). LC-MS data were analyzed on the Thermo Scientific FreeStyle software (v. 1.7.73.12)

4.2.3 Uptake Experiments

Uptake of reactive gaseous species can be monitored by a few methods as outlined in Kolb *et al.*[26]. In its simplest form, uptake is measured as the difference in initial versus final gas-phase mixing ratio of a compound of interest after passing through an absorptive or adsorptive device, typically a coated flow tube or Knudsen cell of known dimensions [26]. The uptake setup is depicted below in Figure 4.2. Two mass flow controllers (MFCs) are used to adjust the flow of dry zero air through the system. The first MFC adjusts the airflow through a glass cell containing 0.03-0.04 g of a solid anhydride. Gas-phase anhydride is continuously generated as the air flow causes steady vaporization of anhydride molecules. This MFC therefore modulates the quantity of gas-phase anhydride flowing through the glass tubes. The second MFC regulates the humidity of the total airflow by flowing zero air through a water bubbler. The ratio of humidified to dry air dictates the final relative humidity (RH) of the total airflow, which is monitored using an RH and temperature sensor before the Gas Chromatography Flame Ionisation Detection (GC-FID) inlet.

As can be seen in Figure 4.2, the anhydride initially flows through an uncoated glass tube into the GC-FID. A gas sampling valve inside the GC inlet port samples the anhydride continuously. Detection is achieved with the following parameters: Split

injection 6:1, 100 °C injection temperature, 250 °C FID temperature, oven initial temperature set to 60 °C and held for 0.2 min, ramp rate set to 125 °C per min up to 150 °C and held for 0.2 min for a total run time of 1.250 min. A RTX-5 capillary column (7 m, 0.32 mm I.D., 0.25 μ m film thickness, Thermo Scientific, CA) was used for separation. Including the time needed for the instrument to cool down between runs, an anhydride peak signal is obtained every 2.7 min.

Stabilization of the anhydride GC-FID signal typically occurs over the course of \sim 2 hours and is measured using the height of the signal peak. The stabilized gas-phase concentration was estimated using the water bubbler under a differing experimental setup and is described in the Supplementary Information (C.1.2). Once stabilized, the flow is switched through the first three way valve to a tube coated with biomass burning emissions, the collection and coating of which are described in following sections. The uptake of anhydride is derived by measuring the decrease in the GC-FID signal relative to the initial signal over the course of 2 hours, when the signal approaches steady-state. After this point, the flow is once again switched to the uncoated tube for 2 more hours, totaling to a 6 hour experimental run time. RH and temperature are measured before and after each experiment by diverting the flow through a sensor, no significant changes in RH or temperature were observed within this time frame.

To date, gas-phase phthalic anhydride ambient air measurements have not been reported, while maleic anhydride concentrations are sparsely reported [137, 347, 366]. Lee *et al.* have performed ambient particle measurements showing variable concentrations of phthalic anhydride of $\sim 49.9 \pm 47.7$ ng m⁻³ [367]. The lack of ambient data is in part due to the anhydride concentration being negligible after plume dissipation, combined with requiring high resolution instrumentation for their detection which is typically not employed for routine analyses. Instead, anhydrides are usually detected as part of the complex plumes emitted after burn events, when their concentrations spike. The predicted phthalic anhydride mixing ratio within our system is 4-10 ppb, which is closely associated with previous reports of \sim 1-2 ppb for maleic anhydride in aged burn plumes [137, 347, 366]. However, the mixing ratio of maleic anhydride was estimated to be 2-7 ppm, lowering this concentration while maintaining reproducibility was challenging due to its high volatility. For this reason, only phthalic anhydride

uptake coefficients are reported following. Nevertheless, maleic anhydride is expected to uptake more strongly than phthalic anhydride, and is still employed for alternative experiments in the previous and following sections.

By modifying the composition of the coated tube, the mass loading, RH effect, as well as coating with an uncoated tube (blank), an unreactive material (linoleic acid), or with an anhydride reactive one (dopant) were all studied.

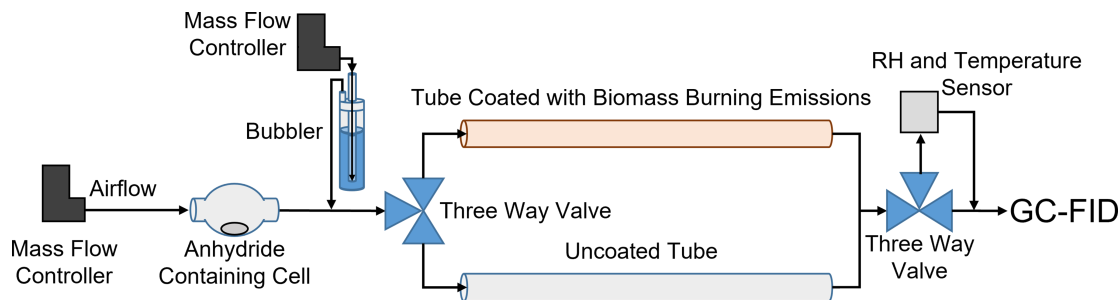


Figure 4.2: Anhydride uptake experimental setup.

4.2.4 Coating Material Collection and Solid Fuel Burning

Samples were collected as previously described in Loebel Roson *et al.* [1]. Briefly, a tube furnace was used to reproducibly burn and collect wood (lodgepole pine) biomass burning emissions at 500 °C under 0.2 slpm of air on pre-baked 0.22 μm pore size quartz fiber filters. These conditions are representative of inefficient low temperature combustion and pyrolysis. After collection, whole filters were extracted in 10 or 20 mL of ACN using a magnetic stirrer for 40 minutes. To ensure homogeneity of the coating material, a composite sample, combining 4 filter extracts of separate burns, was employed for the coated tube uptake experiments. The exact burn parameters and filter loading information can be found in the Supplementary Information (Table C.2). In addition to the biomass burning materials, we have also used linoleic acid as a coating material in selected experiments. Linoleic acid serves as a surrogate for an unreactive coating towards which anhydrides should display only physical uptake, it has been employed in a number of previous studies [144, 368–371].

4.2.5 Tube Coating

Before uptake, glass tubes (200 mm long, 9.50 mm inner diameter) were coated with the filter extracts described above. To ensure uniform coating, the glass tubes were placed on a rotating hot dog roller (Nostalgia HDR8RR Retro Hot Dog Warmer 8) with the heating plate disabled. A pre-defined volume (0.6 to 7.2 mL) of extract was slowly pipetted into the rotating tube. This volume was used to calculate the mass loading of the coating. For select experiments, a dopant - usually a strong nucleophile (e.g., levoglucosan) - was also pipetted into the rotating tube. The dopant serves to modify the uptake properties of the coating and promote the formation of the anhydride nucleophile product. A constant flow of dry air was blown through the revolving tube to remove the ACN solvent. As the tubes rotate, the extracts are uniformly coated along their inner surface. After 30 minutes, at which point the liquid appears visually removed, the rotation function of the roller was disabled.

Our biomass burning materials represent primary organic components collected directly from the source, which contain a substantial quantity of semivolatile organic compounds. In the atmosphere, these semivolatile species are expected to undergo partitioning into the gas-phase following plume dilution [26]. To ensure the removal of semivolatile organic compounds from the coating, the tubes were then rested with continued airflow for 24 hours before the uptake experiments were performed. Tube loading mass was back-calculated under the assumption that the entirety of the filter particulate matter was extracted into the liquid matrix and that the fraction of removed semivolatile organic compounds is the same between coatings.

4.2.6 LC-MS Analysis of the Coating Material

After performing the uptake experiments, each of the glass tubes were washed with 5 mL of ACN to remove the coated material. For select tubes, this material was recovered and diluted into LC-MS vials for analysis. Maleic and phthalic anhydride standards were used to confirm the presence of the anhydride, and detected as their corresponding acids using LC-MS. Separation, detection, and data analysis were performed as described in Section 4.2.2.

4.2.7 Uptake Calculations

Based on the uptake experiments, the uptake coefficients (γ) of the two anhydrides to biomass burning materials were calculated. The obtained γ is the net probability a molecule will be uptaken by a surface after colliding with it [28, 372, 373]. It is the most common parameter used for a wide range of reactive gaseous species [26]. In this work, the uptake was obtained using the peak signal of the anhydride of interest detected through GC-FID, under the assumption that the GC-FID signal is proportional to the gas-phase concentration of the anhydride. The surface area available for uptake is approximated by the geometric surface area of the tube, which is assumed to be uniformly coated due to the coloration of the film. The effective uptake (γ_{eff}) values are normalized by the average gas kinetic flux and are determined as described by Knopf, Poeschl and Shiraiwa (KPS Method) [374], using Eqn (4.1):

$$\gamma_{eff,X} = \frac{D_{tube}}{\omega_x t} \ln\left(\frac{[X]_{g,0}}{[X]_g}\right) \quad (4.1)$$

Where D_{tube} is the diameter of the tube, t the residence time inside the flow tube, and $[X]_{g,0}$ and $[X]_g$ the initial and final gas-phase concentration respectively, which we substitute here with the initial and final GC-FID signal. The molecular velocity (ω_x) can be calculated using Eqn (4.2)[375]:

$$\omega_x = \sqrt{\frac{8RT}{\pi m}} \quad (4.2)$$

Where, R is the ideal gas constant (8.3145 J K⁻¹ mol⁻¹), m the molar mass of particles (0.1481 kg/mol for phthalic anhydride), and T the temperature (296.15 K).

The KPS method corrects for the establishment of concentration gradients as a result of flow entrance effects into the coated tubes, which may cause overestimation of γ [117, 374].

To derive which parameters limit the uptake mechanism of a specific species it is useful to identify the gas flow regime occurring inside the flow tube, which is described by the Knudsen number (Kn_x) [28, 374]. Air flow through the uptake tube was found to be laminar using the Reynolds number (Re) and established after less than 1

cm of tube length [176]. Under laminar flow, the uptake mechanism is driven by molecular diffusion depending on the flow regime [374]. In turn, there are typically three possible flow regimes [28]. The flow of a given species from the gas-phase to the surface is limited either only by surface interactions (free-molecule regime, when $Kn_x \gg 1$), by gas-phase diffusion (continuum regime, when $Kn_x \ll 1$) or by both gas-phase diffusion and uptake (transition regime, $\gamma \approx 1$ or if $Kn_x \ll 1$ and $Kn_x/\gamma \approx 1$) [28, 374]. Consequently, the flow of the anhydride in the experimental setup is usually limited by gas-phase diffusion ($Kn_x \ll 1$). However, heavily loaded tubes can approach the transition regime and therefore be limited by both gas-phase diffusion and uptake ($Kn_x \ll 1$ and $Kn_x/\gamma \sim 2$). Under either of these conditions, the effective uptake was corrected for diffusion effects (obtaining γ) by using the Kn_x and Sherwood (Sh_w) numbers as per KPS, as shown in Eqns (4.3-4.6) [374, 376]. Calculations for each of the parameters and their experimental values are included in the Supplementary Information (Table C.3).

$$\lambda_x = \frac{3D_{g,x}}{\omega_x} \quad (4.3)$$

$D_{g,x}$ is obtained for each anhydride as described by Tang *et al.* [375].

$$Kn_x = \frac{2\lambda_x}{D_{tube}} \quad (4.4)$$

$$N_{Shw}^{eff} = 3.6568 + \frac{A}{z^* + B} \quad (4.5)$$

A and B are constants (0.0978 and 0.0154 respectively) [374], the dimensional axial distance (z^*) for the flow tube setup was calculated to be 0.651.

$$\gamma_x = \frac{\gamma_{eff,X}}{1 - \gamma_{eff,X} \frac{3}{2N_{Shw}^{eff} Kn_x}} \quad (4.6)$$

Both γ_{eff} and γ describe the net movement of anhydride from the gas-phase to the coated tube surface. γ however, is normalized (corrected) by the actual surface collision flux rather than the average gas kinetic flux [28]. Herein, the KPS factor typically corrected the γ_{eff} values by ~ 5 -12%, with the highest corrections being 20 and 21% for the two most heavily loaded tubes.

4.3 Results and discussion

4.3.1 Fundamental Investigation of Nucleophilic Addition

4.3.1.1 Anhydrides in Protic and Aprotic Solvents - NMR Characterization

To verify that anhydrides are both fully hydrolyzed in water and remain stable in aprotic environment, we characterized the formation of their acid counterparts in different solvents using ^1H NMR. Throughout the NMR experiments, a distinct acid peak was observed for all samples, except for the anhydride samples dissolved in deuterated chloroform, an aprotic solvent. Complete hydrolysis of the anhydride was confirmed by the lack of an anhydride peak in the deuterated water samples, as well as the acid peak intensity for all samples being analogous. Additional details for this experiment, including nuclear magnetic resonance peaks, are available in the Supplementary Information (C.1.1).

4.3.1.2 Reaction Confirmation using LC-MS

As electrophiles, anhydrides have a predisposition towards reacting with nucleophilic species. Significant tracers emitted from biomass burning - such as vanillin and levoglucosan - are nucleophiles and can be reactive towards anhydrides. As a basis for the uptake and degradation experiments, the formation of an anhydride and nucleophile product was first probed in an aprotic solvent. Table 4.1 lists the product peaks (anhydride + nucleophile) of species observed using LC-MS after mixing each anhydride with a variety of nucleophiles dissolved in ACN.

Both maleic and phthalic anhydride consistently form products with the majority of nucleophiles studied here. This reaction involves a hydrolysis-like ring opening of the anhydride and addition of the nucleophile to form a higher molecular mass product, which appears to be independent of the anhydride used. Likely due to its higher ionization efficiency, product peaks of maleic anhydride displayed ~ 10 times the peak area of phthalic. Maleic and phthalic anhydride were found to react with biomass burning atmospheric tracers such as levoglucosan, syringaldehyde, anisyl alcohol, and vanillin. The m/z of all the products were equivalent to the combined molecular mass of the anhydride and the corresponding nucleophile (see Supplementary Information

(Figure C.9) for predicted structures). The list presented in Table 4.1 is nonexhaustive, and our results suggest that a wider spectrum of compounds in actual biomass burning plumes are likely reactive to anhydrides. Certain nucleophiles, such as aniline and levoglucosan, do not contain any acidic protons and are not detectable by ESI- themselves. The fact that the products are detectable suggests the presence of an acidic functional group (i.e., carboxyl group), which is in agreement with the general reaction scheme and supports our structural assignment. Markedly, all products had a higher detection signal in ESI- as opposed to ESI+, with the exception of the maleic anhydride coniferyl aldehyde product. After observing these reactions in ACN, whether anhydrides can react with nucleophiles of biomass burning origin in water - a protic solvent - and whether the products of such a reaction are stable is explored further.

Table 4.1: Maleic (M) or phthalic (P) anhydride nucleophile reaction products detected using LC-MS. In each instance, the listed product peak mass to charges (m/z) were those that yielded the highest intensity LC-MS signals.

Nucleophile	Anhydride	Product Peak (m/z)
Anisyl alcohol	Both	236 (M) and 286 (P)
Coniferyl aldehyde	M	276 (M)
Histidine	Both	253 (M) and 303 (P)
Levoglucosan	Both	260 (M) and 310 (P)
Vanillin	Both	250 (M) and 300 (P)
Aniline*	Both	190 (M) and 241 (P)
Triethylene glycol*	Both	248 (M) and 298 (P)

*Compounds not detected in biomass burning emissions in Loebel Roson *et al.*[1]

4.3.1.3 Reaction Competition and Product Stability in Water

Since anhydrides fully hydrolyze when dissolved in water, the potential for competition between hydrolysis and the anhydride nucleophile reaction was explored further. Depending on local atmospheric conditions, biomass burning emissions are subjected to a spectrum of relative humidities [43, 77, 359, 374]. Water can impact reactions at the surface and bulk of the particle-phase, and through hydrolysis - along with

photolysis and oxidation - is one of the main mechanisms leading to the decomposition of certain chemical species in the atmosphere [279]. To study whether the size of the water fraction hinders the formation of the anhydride nucleophile product and if that product is stable in water over time, the evolution of the product was tracked in increasing fractions of water in ACN, as described in Section 4.2.2. By comparing the relative area of the product peak over each injection, whether the product is forming or decaying is determined. Anisyl alcohol, levoglucosan and vanillin were selected as nucleophiles for this analysis, as they each represent significant biomass burning tracers [61, 141, 351]. Data for maleic anhydride and vanillin, as well as for phthalic anhydride and levoglucosan are presented in Figure 4.3. Data for other anhydride nucleophile products is available in the Supplementary Information (C.1.7). Anisyl alcohol followed a similar trend to levoglucosan curves in Figure 4.3, albeit with an even higher product signal intensity.

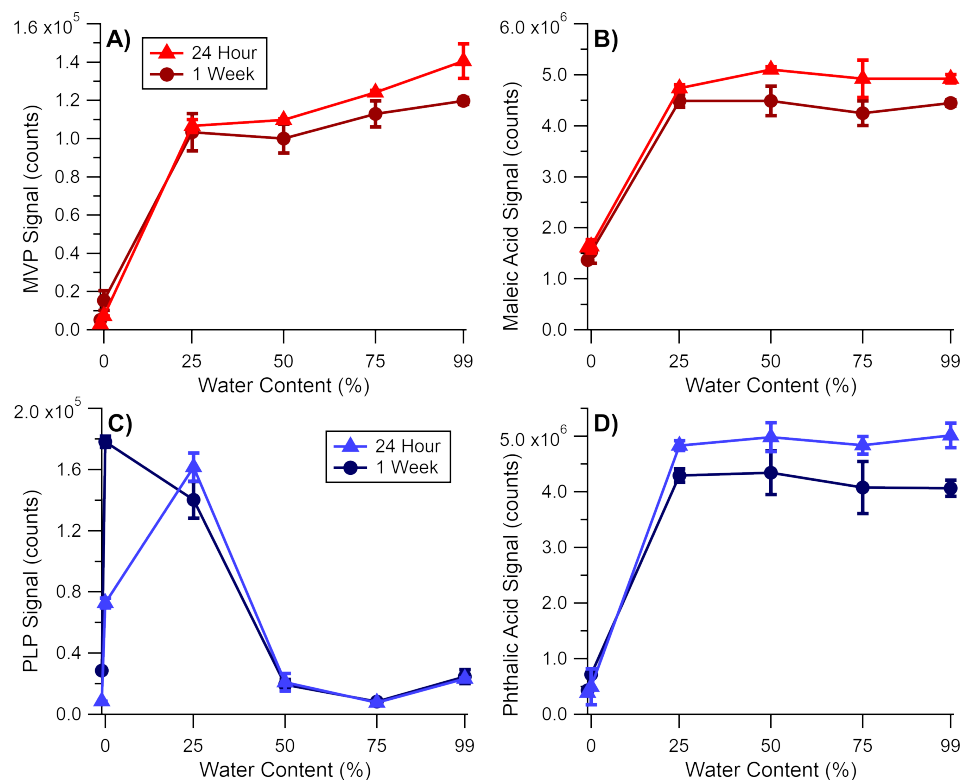


Figure 4.3: LC-MS peak area signals obtained from increasing fractions of water in acetonitrile (ACN) after the 24 hour and 1 week-long analysis period for A) Maleic anhydride vanillin product (MVP), B) Maleic acid, C) Phthalic anhydride levoglucosan product (PLP), D) Phthalic acid. Error bars represent the range between duplicate experiments.

As displayed in Figure 4.3, anhydride hydrolysis becomes dominant when the water content exceeds 25%. This is illustrated by the sharp rise in acid signals - i.e., maleic acid (Figure 4.3B) and phthalic acid (Figure 4.3D), which the previously reported NMR analysis also corroborates. On the other hand, the evolution of the nucleophile product follows a non-linear trend. This indicates that the presence of water is playing a more complex role in its formation. For both the maleic anhydride vanillin product (MVP) (Figure 4.3A) and phthalic anhydride levoglucosan product (PLP) (Figure 4.3C) systems, up to 25% water facilitated the formation of the products. As can be seen in Figure 4.1A, a proton must migrate from the nucleophile to the newly formed carboxylic group. Likely, water may act as a proton carrier during the nucleophilic addition, resulting in the enhanced product formation observed in Figures 4.3A and 4.3C. Specifically for 4.3C, 1% water is enough to initiate proton transfer and the formation of PLP - albeit at a much slower rate - leading to a maxima over 1 week. The acid catalyzed reaction path (Figure 4.1B) is also promoted with an increased water fraction, as more acidic protons become available.

Opposing trends were observed between the two experimental systems after increasing the water fraction beyond 25%. The PLP intensity diminishes at higher water contents, indicating that hydrolysis competes over the nucleophilic addition. Simultaneously, the MVP signal exhibits a continuous enhancement with water content. This trend is likely an interplay of multiple factors, including the reactivity of the anhydride, the nucleophilicity of vanillin, and their concentrations relative to each other in the solution. Nonetheless, we were unable to identify the exact reason for this observation within the MVP system.

These experiments also gauge the stability of the products in water. As shown in Figures 4.3A and 4.3C, the product signals exhibited minimal (<10%) reduction over a 1 week time frame. A decrease of the same magnitude was observed for the acids (Figures 4.3B and 4.3D), indicating the decline might be due to changes in instrumental sensitivity between analyses. In either case, the products remain stable in water once formed. This confirms that the anhydride nucleophilic addition reaction is irreversible. Overall, our observations indicate that water serves to facilitate the nucleophilic addition to anhydrides when it does not represent the majority of the medium. This corresponds to dry atmospheric conditions under which liquid water in

aerosol is scarce and dependent on ambient relative humidity and the hygroscopicity of the aerosol itself [377]. When water becomes abundant, hydrolysis eventually overtakes the nucleophilic addition. However, our results also demonstrate that certain nucleophiles can still react under such conditions, and form products that are stable and do not decompose in water. Since anhydrides and nucleophiles must come into contact to react, the controlled liquid environment used in these experiments facilitates observing their reaction. While this is useful as a proof of principle, the drastic changes in solvent composition make detailed determinations of the reaction mechanisms challenging, which we accordingly do not pursue further. Instead, knowing that anhydride nucleophile reaction proceeds readily in the presence of water, we investigate following whether gas-phase anhydrides similarly interact with nucleophiles in biomass burning emissions. In the next section, we explore whether anhydrides are susceptible to surface and bulk uptake on biomass burning films, as this interaction might explain one of the pathways by which highly volatile non-polar anhydrides are partitioned to the particle-phase in burn plumes.

4.3.2 Uptake of Anhydrides to Biomass Burning Material

4.3.2.1 Uptake of Phthalic Anhydride

Figure 4.4 depicts a typical phthalic anhydride uptake experiment. The top panel displays a single phthalic anhydride GC-FID chromatogram, while each point on the bottom chromatogram represents the height of the anhydride peak measured in real time by the GC-FID, as exemplified by the green marker in each panel. Each uptake experiment was divided into three regions as described in the experimental section, represented by the shaded areas in the figure. Initially, the anhydride equilibrates throughout the uncoated tube over the course of ~ 100 minutes (gray shade). After equilibration, a three-way valve is switched, and the anhydride is flown through the coated tube (red shade). The GC-FID signal begins decreasing over the course of a single injection (2.7 min) and usually reaches a minimum after 6-8 injections (16.2-21.6 min). From here, the signal begins slowly increasing as the surface of the tube is saturated with anhydride. Once the anhydride flow is switched back to the uncoated tube (gray shade), it re-equilibrates over a further 100 min. The film

coating the tube (composed of the organic extractable fraction of biomass burning particulate matter, including various nucleophiles) interacts with the electrophilic anhydride vapour flowing through the tube. These conditions are entirely distinct from the liquid bulk reactions explored in Section 4.3.1.3, and more representative of what vapour-phase anhydrides might experience as part of a burn plume. Here, when 0% RH air is used to flow the anhydride through the tubes, water trapped in the film is likely the only proton carrier facilitating the anhydride nucleophile reaction. Under these conditions (non-polar anhydrides partitioning into a polar matrix), the mass-based activity coefficient for both anhydrides would be > 1 (non-ideal). Therefore, C^* would be even higher than under ideal conditions, driving the anhydride further into the vapour-phase [98, 355].

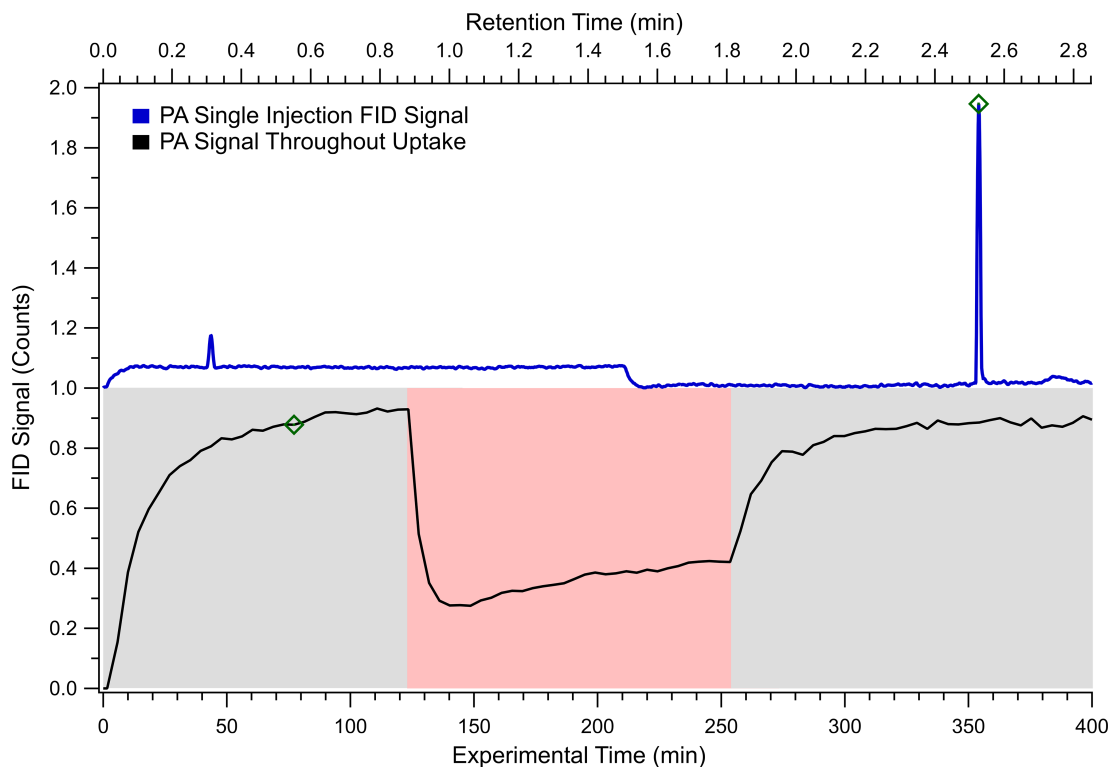


Figure 4.4: Phthalic anhydride (PA) uptake experiment. The top blue curve represents a typical GC-FID PA peak vertically offset by 1 count, taken at 2.7 min intervals throughout the experiment and from which the bottom uptake graph is constructed. The bottom gray and red shaded areas represent the anhydride flowing through the uncoated and coated tubes respectively, γ is calculated over the length of the red area. The green marker on the bottom graph indicates the time at which the top peak is taken.

γ can be calculated for different positions of the uptake curve. As the largest uptake occurs during the initial switch to the coated tube, γ determined by the difference between the initial and final GC-FID signals yields initial uptake. γ calculated over the entire experiment, i.e., over the entirety of the red shaded area in Figure 4.4, represents the averaged uptake. Unless specified otherwise, all γ values reported denote the average uptake. The molecular mass of an uptaken trace gas strongly influences the speed and degree of uptake [375]. As relatively large molecules - over the more commonly studied gas-phase oxidants OH, O₃ and NO₃ [117, 374] - maleic and phthalic anhydride are expected to follow a slower uptake profile with reduced average uptake.

It is worth noting that γ is theoretically unaffected by the gas-phase concentration of the uptaken trace-gas as it simply measures the difference between the initial and final concentrations of a gas after passing over a coated material. However, should the gas-phase concentration of the trace-gas be too high, or conversely, insufficient coating material (reactive sites) be available for uptake, γ may be over or underestimated. While the shape of the uptake curves is usually consistent, γ coefficients available in literature have a wide range of values due to the variable experimental conditions and correction methods [117, 374, 378–381]. For example, in liquid coated reactive uptake setups, the concentration of the liquid will directly affect its total capacity for uptake when diffusion into the bulk is unlimited [378]. This phenomenon occurs when the number of reactive sites in the bulk are the limiting factor for uptake, and is observed here as the loading mass of the coated tubes is changed (see Section 4.3.3.1 - Mass Dependence). The shape of the phthalic uptake curve in Figure 4.4 is consistent with uptake experiments reported on in previous ozone studies [117, 244, 374, 381, 382]. However, the uptake efficiency here appears to lessen over the course of the experiment, likely as a result of the consumption of available reactive sites (nucleophiles) in the coating. Notably, removing the electrophile source after uptake to the coated tube leads to no significant re-emission of anhydride from the coating, as determined by the GC-FID anhydride signal decay rate.

Table 4.2 lists the γ obtained as a function of the loading mass of the coatings. Also included are experiments with coated linoleic acid and variable RH, covered in sections 4.3.3.2 and 4.3.3.3, respectively. As can be seen in Table 4.2, uptake is

driven by the quantity of coating applied to the tube, which directly correlates to the mass concentration of particles emitted from the burn. Therefore, it is reasonable to expect burns which emit a larger number of particles - such as large scale wildfires - to promote the uptake of anhydrides. The limited range of uptake values can be explained by the morphology of the uptake setup and the low diffusivity of phthalic anhydride. The comparatively low airflow and long tube length promote slow uptake and deposition of the anhydride on the sides of the glass tubes whether a coating is present or not [117]. This causes uncoated tubes to have ~ 6 times less uptake than the most heavily loaded ones.

Table 4.2: Range of γ values obtained for phthalic anhydride during uptake as loading mass is decreased under variable relative humidity (RH).

Loading Mass (g)	Replicates	RH (%)	Uptake (γ) ($\times 10^{-6}$)
0.0127	2	0	10.87 - 11.44
0.0042	3	0	5.77 - 6.98
0.0032	3	0	5.44 - 6.55
0.0032	2	24	5.50 - 5.66
0.0032	3	47	5.24 - 6.49
0.0021	2	0	4.05 - 4.51
0.0011	2	0	2.63 - 2.69
0	3	0	1.07 - 2.43
0.0168*	1	0	1.78
0.0017*	1	0	1.85

*Tubes coated with linoleic acid

4.3.3 Evidence of Reactive Uptake

Differentiating between reactive and non-reactive uptake is challenging, as experimentally both types lower the relative concentration of gas-phase species being uptaken, yielding γ_{eff} coefficients. This is in part due to physical accommodation process being a pre-requisite for reactive uptake to occur. Nevertheless, physical and reactive uptake each modify the chemical composition of the uptake substrate in distinct ways.

Reactive uptake can be reversible or irreversible, and has been shown to alter the properties of both the gas-phase species being uptaken as well as the uptake substrate itself [26, 118]. For example, particulate matter emitted from biomass burning can act as a surface for the condensation of semivolatile species in the atmosphere [118]. As such, identifying whether anhydride reactive uptake is occurring and whether the products of such a reaction are stable is of high importance towards predicting their impacts.

We posit that significant reactive uptake is occurring on the biomass burning coating for the following reasons, each of which is expanded upon in their respective sections below.

- 1) A tube coated with the same loading mass of linoleic acid, towards which anhydrides are nonreactive, did not show significant uptake and no dependence on mass loading.
- 2) Products of the reaction of anhydrides and common biomass burning species (such as levoglucosan) were identified in tube coating extracts after uptake, and were shown to increase in concentration when the tubes were doped with the nucleophilic precursors.
- 3) A more reactive coating, from which semivolatile species were not removed before uptake, showed significantly higher γ .

4.3.3.1 Mass Dependence

Uptake is partially driven by the quantity of material loaded on the glass tubes, as can be seen in Figure 4.5 and Table 4.2. Loading mass represents the mass of particles originally collected on the quartz filters before extraction, except for the linoleic acid data-points, where it represents the mass of linoleic acid used for coating.

In either case, γ increases relatively linearly as the tubes are loaded with more material. A coating that covers the entirety of the glass tube - the surface area of which can not increase further - can only expand in depth as it is further loaded. Since γ increases with tube loading, uptake must be spurred by the transfer of the anhydride to the bulk of the coating. This is additional evidence of the reactive uptake process outlined in the previous sections. The divergence from linearity can be explained by the increasing resistance the coating thickness imposes on the uptake process and

the depletion of readily available reactive sites (nucleophilic species). As nucleophiles nearer to the surface are consumed first, the anhydride must travel deeper into the coating, creating a concentration gradient.

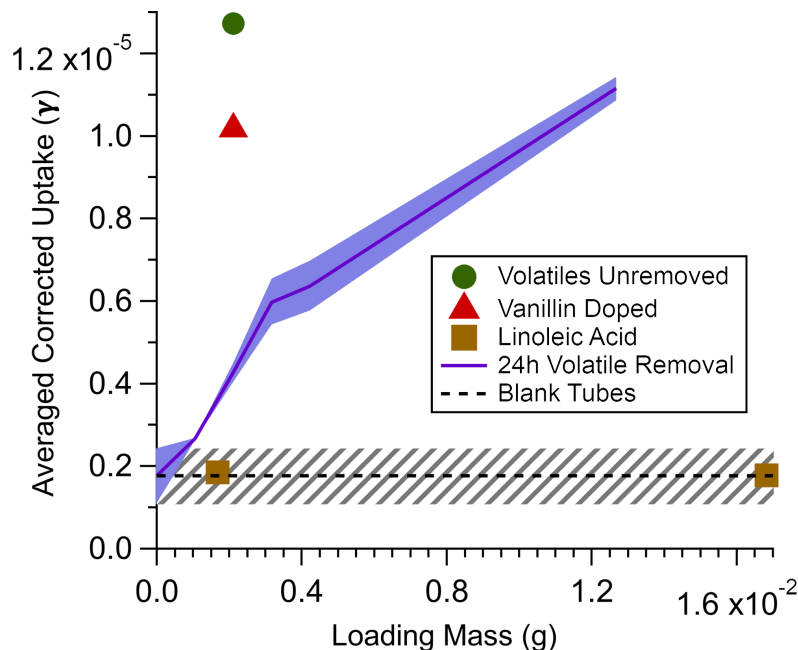


Figure 4.5: Range of γ values obtained for phthalic anhydride on tubes coated with biomass burning material as a function of loading mass of the coating. Each data point represents the averaged γ values obtained over 2 hours of uptake at a relative humidity of 0. The shaded blue area depicts the range of γ values observed from tubes which underwent 24 hours of semivolatile removal. The green dot portrays the γ obtained from a tube which did not go through the semivolatile removal procedure. The red triangle represents the γ from a tube in which 0.0167 g of vanillin were dissolved during the coating process, in addition to the biomass burning material. The brown squares illustrate the γ obtained from tubes coated with linoleic acid, an unreactive material. The dashed line indicates the average γ obtained for uncoated (blank) tubes.

4.3.3.2 Linoleic Acid

To investigate whether the uptake process was purely physical or reactive, γ was also measured using tubes coated with linoleic acid, represented by the brown markers in Figure 4.5. Emitted from cooking processes, long chain unsaturated fatty acids such as oleic and linoleic acid have been previously used for model heterogeneous oxidation studies within an atmospheric context [144, 368–371].

Under a purely physical - adsorptive or absorptive - process, we can assume for

comparison with the reactive biomass burning coating, that linoleic acid will either physically align itself along the surface of the tube in a single layer formation. That is to say, as a coating with no depth, in which case only adsorption would be possible. Or more realistically, that the linoleic acid coating does have depth, in which case both adsorption and absorption - also known as surface and bulk accommodation - are possible [26, 28, 143]. In either case, were the uptake on biomass burning emission coated tubes purely a physical process, then γ for linoleic acid should - with similar coating distribution - have a comparable uptake trend to it. However, as can be seen in Figure 4.5 no significant anhydride uptake to linoleic acid was observed over the loading mass range used for the biomass burning emissions. Therefore, we posit that the uptake is not only dependent on the physical properties of the biomass layer, but rather a chemically reactive process between the anhydride and the coating. This is further confirmed by both the effect removal of the volatile organic species had on γ (green dot), and the shape of the uptake curve in Figure 4.4.

4.3.3.3 Removal of Semivolatile Species

The presence of nucleophiles in biomass burning material is suspected to enhance the reactive uptake of anhydrides. Presumably, species which contain phenolic functional groups can serve as nucleophiles in the biomass burning substrate, and therefore heighten uptake. Due to their volatility, low-medium molecular weight phenolic species typically partition into the gas-phase following plume dilution [26]. As a result of the sampling setup, the tube furnace may condense semivolatile species on the surface of the filter which would typically remain in the gas-phase. Semivolatile removal time after coating was found to have a distinct impact on γ . The initial versus final GC-FID signal for phthalic anhydride flowing through a coated tube was found to experience a threefold reduction in γ after 24 hours of semivolatile removal, as displayed by the green dot in Figure 4.5. A similar trend was observed for maleic anhydride. The difference in uptake can be explained by the stripping of more semivolatile organic compounds from the coating over time. These species would usually provide additional sites for anhydride compounds to react with, but are instead removed under continued air flow, and therefore lower the overall reactive potential of the coating. Additionally, removal of the semivolatiles is likely to lower

the overall volatility of the coating, increasing its viscosity, and inhibiting uptake. Unsurprisingly, more freshly emitted biomass burning particulate matter is more reactive towards electrophiles such as anhydrides. Within the atmospheric context, freshly emitted biomass burning plumes which still contain semivolatile organic compounds will be more susceptible to reactive uptake, and therefore modification by anhydrides. Note that we cannot track the mass of semivolatiles lost during the 24 hour removal process, and thus assume that it is a minor fraction of the total biomass burning coating material. If the semivolatiles comprised a substantial fraction of the total mass, the data point (green circle) shown in Figure 4.5 would be underestimating the loading mass.

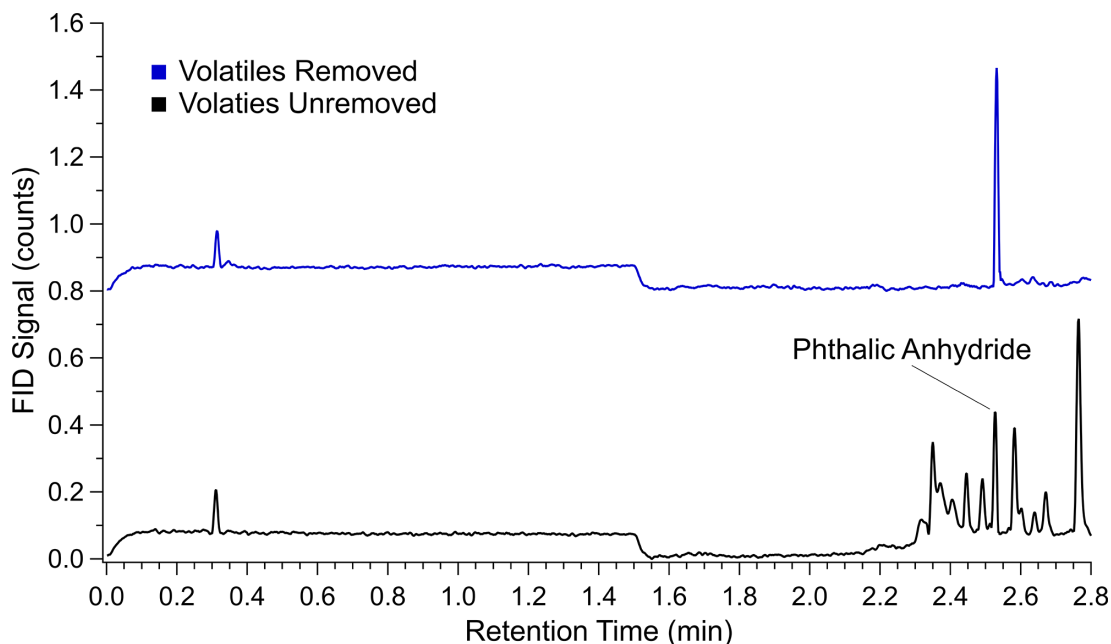


Figure 4.6: GC-FID phthalic anhydride chromatogram of a tube rested under continued airflow for 24 hours versus a tube from which semivolatile species were not removed. The top peak signal is offset by 0.8 counts.

Interestingly, a few of these semivolatile species appear as unique GC-FID peaks when tubes which have not gone through the removal process are used for uptake. Figure 4.6 displays the phthalic anhydride GC-FID peaks obtained for a tube which has undergone the 24 hour removal process, and one which has not. Unsurprisingly, the unremoved coated tube continuously off-gasses volatile species from its surface throughout the uptake experiments. At the same time, the 24 hour removed tube

displays only a single sharp peak, corresponding to phthalic anhydride. The peaks in Figure 4.6 represent only the species which are capable of eluting through the GC column in less than 2.8 minutes. Likely, there are numerous other peaks which could be observed beyond this retention time in the unremoved tubes.

4.3.3.4 Presence of Uptake Products - Tube Doping Experiments

To confirm the anhydrides react with the biomass coating, the tube coating was extracted from the surface after performing the uptake experiments and analyzed using LC-MS. By spiking (doping) the tubes with commercially available nucleophilic precursors during the coating process, we further confirm the identity of the detections using LC-MS. Characterization is necessary as the biomass emission extracts are highly concentrated in a variety of chemically diverse compounds [1, 248]. Despite separation through LC-MS, this environment makes it challenging to confirm the identity of a given product (using only the mass to charge ratio), without chemical standards. However, many of the species emitted from biomass burning either do not have commercially available standards or have not yet been identified. By doping, the surface concentration of the nucleophile is significantly higher, which promotes its reaction with the anhydride. Consequently, this results in the signal intensity of the obtained LC-MS reaction product peak - between the anhydride and the nucleophile - to also increase, confirming its identity within the complex extracts. This is further supported by doped tubes through which no anhydride is flown (containing the nucleophile but no uptaken anhydride), lacking the product peak.

Figure 4.7 displays the mass spectra gathered from two tubes coated with biomass burning emissions and doped with levoglucosan. One of the coated tubes underwent maleic anhydride uptake while the other did not. The TICs were gathered over a 2 min time range, and include the elution time of maleic anhydride, levoglucosan, and the maleic anhydride levoglucosan product (MLP). As can be seen in Figure 4.7, only the tube exposed to maleic anhydride displays peaks at mass to charges (m/z) of 115 (maleic anhydride detected as maleic acid), 259 (MLP), and 519 (MLP dimer). Notably, extractions were completed in an aprotic solvent (ACN), while the uptake was performed using air of 0% RH. As per the experiments in Section 4.3.1.3, formation of MLP is expected to increase further with moderate water availability.

A similar trend to that of the initial reactivity experiments was observed in this section, i.e. maleic and phthalic anhydride react with nucleophiles present in biomass burning emissions. Both biomass burning matrix intrinsic nucleophilic compounds with high emission factors (levoglucosan and vanillin) and matrix extrinsic anthropogenic nucleophilic compounds (aniline) were used as dopants. In either case, products corresponding to a mass to charge ratio of the anhydride plus nucleophile were detected. In each instance, the product mass to charge ratio obtained after doping matched the one observed during the reactivity experiments. The signal intensity of the maleic anhydride products was significantly higher than the phthalic ones in all cases, likely due to its higher gas-phase concentration during uptake. Formation of the products as anhydride is surface - and likely also bulk - accommodated on the tube coating, is further evidence of a reactive uptake process.

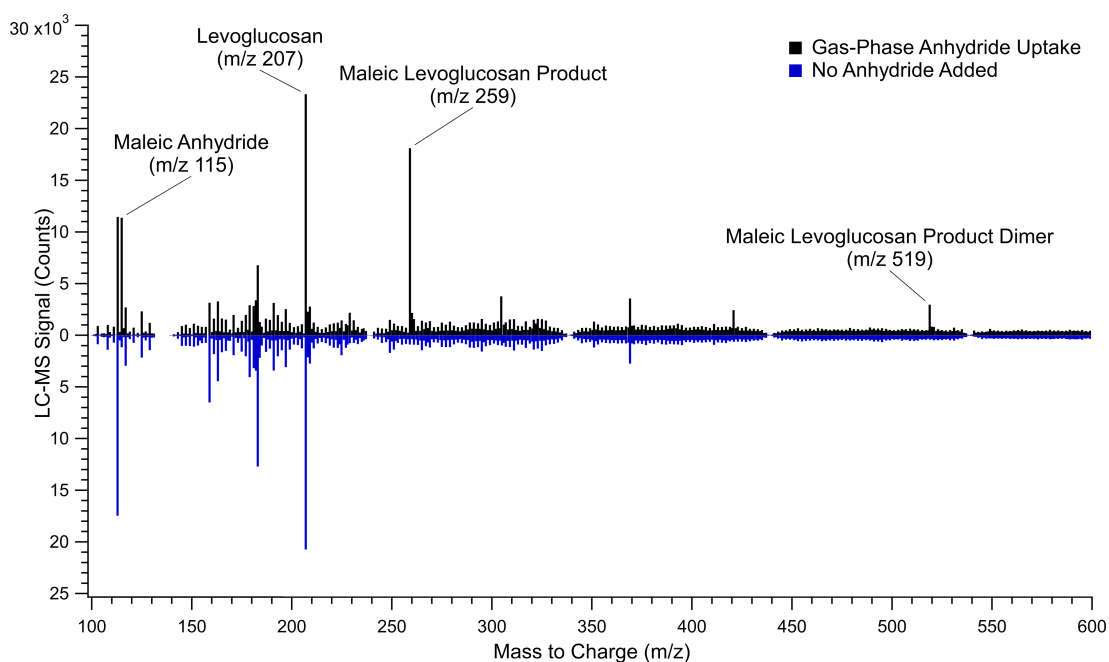


Figure 4.7: Maleic anhydride levoglucosan product negative electrospray ionization (ESI-) total ion chromatogram (TIC) mass spectra. The top spectrum is gathered from a levoglucosan doped tube through which gas-phase anhydride was flown. The mirrored blue bottom spectrum tube was prepared under the same conditions, without the anhydride uptake step.

4.3.4 Additional Factors Affecting the Uptake - Relative Humidity

Relative humidity is an important consideration for atmospheric studies, as it affects the environmental fate, physical properties, and uptake potential of many chemical species. Organic aerosol particles in the atmosphere will change phase state between liquid and solid depending on local RH and temperature [77]. With regards to uptake, RH can decrease the viscosity of the uptake substrate, facilitating the movement of species into the bulk, which usually enhances the uptake [118, 383]. More unusually, RH has also been found to hinder uptake in some systems. For example, Goldberger *et al.* have previously reported that γ of N_2O_5 to biomass burning aerosol emitted from longleaf pine needles is inhibited at higher RH, albeit only slightly [384].

Here, uptake is expected to increase with RH, as lower viscosity improves anhydride transfer into the biomass burning coating. Further, as described in Section 4.3.1.3, water can either facilitate the nucleophilic addition, or react with the anhydrides through hydrolysis directly. Surprisingly, using air of either 0, 24, or 47% RH at room temperature was found to have no significant impact on γ , as can be seen in Table 4.2. Although a different system, a non-impact of RH has been previously reported for other gas-phase species. For example, under dark conditions, RH has no meaningful impact on steady-state uptake of ozone to a benzophenone film [143, 381]. As covered in the experimental methods, the particles that make up the biomass burning coating are collected a few cm downstream of the tube furnace and represent primary emissions. A large fraction of freshly emitted biomass burning aerosol is made up of almost hydrophobic particles, which typically lose their hydrophobicity as they are aged and transported in the atmosphere [117, 182]. During the tube coating process, dry air is used to remove semivolatiles and avoid hydrolysis-driven aging. It is likely that the hydrophobicity of the coating prevents the humidity in the air from lowering its viscosity over the ~ 6 h time frame of the experiments, which nullifies the effect of RH on the uptake. Alternatively, water which is not removed during the tube coating process may instead be trapped as part of the biomass burning film. These small concentrations of water may be sufficient to promote the anhydride nucleophile reaction, just as 1% water had an considerable impact during the bulk experiments

in Section 4.3.1.3.

4.4 Conclusions

Using maleic and phthalic anhydride - compounds present in biomass burning plumes - this study provides novel insights into anhydride chemistry and its implications towards the atmosphere. Our results show that anhydrides can react with a wide spectrum of hydroxy and amino containing nucleophiles, corroborating established literature [358, 385]. For the first time however, we demonstrate the reactivity of anhydrides towards atmospherically relevant nucleophiles, and that therefore, anhydrides may be a hitherto unrecognized class of electrophiles with atmospheric relevance.

Given the abundance of water in the atmospheric environment, it likely represents anhydrides' most dominant reaction partner, leading to the formation of their corresponding acids. However, our results show that reactions with other nucleophiles are possible even in the presence of water. In particular, lower water contents ($\sim 25\%$) facilitated the nucleophilic reaction.

The chemistry of the anhydride can affect their own atmospheric fate as well as the composition of aerosol they come into contact with. We show, using a coated wall flow tube setup, that anhydrides reactively uptake to biomass burning films and influence its composition.

In addition, we show that the reaction is irreversible, and that therefore, reactive uptake to aerosol can serve as a sink for gas-phase anhydrides. The extent of this sink is dependent on the availability of nucleophilic species in the particle-phase, as the uptake coefficient (γ) increased with tube loading mass. This effect is exacerbated by the ability of anhydrides to move from the surface into the bulk of the particle-phase, where they may interact with additional fresher nucleophiles. Anhydrides have previously been considered as potential tracers for biomass burning [347, 348]. However, their uptake properties combined with the non-discriminatory reactivity likely makes them a poor choice of tracer.

In addition to the uptake studies, products arising from the reaction between anhydrides and nucleophiles were monitored using LC-MS. Consistently, product peaks

corresponding to ester and amide species which contain carboxylic groups were detected. Formation of such products has a few important atmospheric implications. Firstly, their enhanced molecular weight coupled to the added functional groups make them less volatile than their anhydride and nucleophile precursors. As mentioned in the Introduction, the anhydrides would be present entirely in the gas-phase under ambient conditions, the observed products are however much more likely to be in the particle-phase. Based on our observations of their stability over a week-long time frame, these products are likely to persist in the particle-phase and contribute to secondary organic aerosol, with knock-on climate and health effects. Secondly, this reaction does not require solar radiation or the presence of free radicals, which indicates that the reaction could proceed during day and nighttime. Thirdly, by reacting with compounds present in biomass burning aerosol, anhydrides may mask the “real” emission factor of nucleophiles. A symptom which may worsen as more anhydrides form through plume aging over time. This is potentially concerning for nucleophiles used as tracers, the concentration of which are used for source apportionment [61, 221, 223]. This effect would be more significant for anhydrides with emission factors higher than the nucleophile they react with. For example, while emissions factors of phthalic anhydride and vanillin are comparable [138, 141], levoglucosan molecules greatly outnumber anhydrides inside a fresh burn plume [141], likely rendering the masking of levoglucosan minimal. Such variability makes obtaining an accurate representation of both the reactions happening inside a plume, and their impacts, challenging.

As climate change proceeds, wildfire incidence and severity is expected to intensify [30]. Understanding chemical reactions leading to the continuous transformation of biomass burning emissions represents an area of significant interest and uncertainty. In this work, we investigated the fundamental chemistry and behavior of anhydrides, showing that they can potentially contribute to the chemical evolution of this type of emission. Future studies should focus on elucidating the complexity of the heterogeneous-phase further, both as a physical and chemical process.

4.5 Author Contributions

Max Loebel Roson: Conceptualization, Methodology, Investigation, Visualization, Writing - Original Draft, **Maya Abou-Ghanem:** Resources, Validation, **Erica Kim:** Formal Analysis, **Shuang Wu:** Resources, **Dylan Long:** Resources, **Sarah A. Styler:** Supervision, **Ran Zhao:** Supervision, Writing - Review & Editing, Funding acquisition.

4.6 Conflicts of interest

There are no conflicts to declare.

4.7 Acknowledgements

The authors thank the University of Alberta Department of Chemistry Glass Shop for manufacturing the quartz and glass tubes and the University of Alberta Department of Chemistry NMR Facility for their assistance in NMR measurements. The authors also thank NSERC and the University of Alberta for financial support. This research was performed while co-author Maya Abou-Ghanem held an NRC Research Associateship award at NOAA Chemical Sciences Laboratory. This research project was partially supported by the Government of Canada's Climate Action and Awareness Fund, Canada Foundation for Innovation (Project Number 38334), and NSERC Discovery Grant (RGPIN2018-03814).

4.8 Supporting Information

Additional experimental details, including NMR plots, gas-phase anhydride determination, LC-MS chromatograms, burn and uptake parameters, standard and replicate analyses, and nucleophile product data. See DOI: 10.1039/cXCP00000x/

References

- [1] M. Loebel Roson *et al.*, “Chemical characterization of emissions arising from solid fuel combustion—contrasting wood and cow dung burning,” *ACS Earth and Space Chemistry*, vol. 5, no. 10, pp. 2925–2937, 2021. DOI: 10.1021/acsearthspacechem.1c00268.
- [2] M. Loebel Roson *et al.*, “Unexpected electrophiles in the atmosphere – anhydride nucleophile reactions and uptake to biomass burning emissions,” *Phys. Chem. Chem. Phys.*, 2023. DOI: 10.1039/D3CP01751F.
- [11] S. S. Lim *et al.*, “A comparative risk assessment of burden of disease and injury attributable to 67 risk factors and risk factor clusters in 21 regions, 1990–2010: A systematic analysis for the Global Burden of Disease Study 2010,” en, *The Lancet*, vol. 380, no. 9859, pp. 2224–2260, Dec. 2012, ISSN: 01406736. DOI: 10.1016/S0140-6736(12)61766-8. [Online]. Available: <https://linkinghub.elsevier.com/retrieve/pii/S0140673612617668> (visited on 06/25/2021).
- [16] C. J. Murray *et al.*, “Global burden of 87 risk factors in 204 countries and territories, 1990–2019: A systematic analysis for the global burden of disease study 2019,” *The lancet*, vol. 396, no. 10258, pp. 1223–1249, 2020.
- [25] M. B. Fernandes, J. O. Skjemstad, B. B. Johnson, J. D. Wells, and P. Brooks, “Characterization of carbonaceous combustion residues. i. morphological, elemental and spectroscopic features,” *Chemosphere*, vol. 51, no. 8, pp. 785–795, 2003, ISSN: 0045-6535. DOI: [https://doi.org/10.1016/S0045-6535\(03\)00098-5](https://doi.org/10.1016/S0045-6535(03)00098-5). [Online]. Available: <https://www.sciencedirect.com/science/article/pii/S0045653503000985>.
- [26] C. E. Kolb *et al.*, “An overview of current issues in the uptake of atmospheric trace gases by aerosols and clouds,” *Atmospheric Chemistry and Physics*, vol. 10, no. 21, pp. 10 561–10 605, 2010. DOI: 10.5194/acp-10-10561-2010. [Online]. Available: <https://acp.copernicus.org/articles/10/10561/2010/>.
- [27] V. H. Grassian, “Heterogeneous uptake and reaction of nitrogen oxides and volatile organic compounds on the surface of atmospheric particles including oxides, carbonates, soot and mineral dust: Implications for the chemical balance of the troposphere,” *International Reviews in Physical Chemistry*, vol. 20, no. 3, pp. 467–548, 2001. DOI: 10.1080/01442350110051968. [Online]. Available: <https://doi.org/10.1080/01442350110051968>.
- [28] U. Pöschl, Y. Rudich, and M. Ammann, “Kinetic model framework for aerosol and cloud surface chemistry and gas-particle interactions — part 1: General equations, parameters, and terminology,” *Atmospheric Chemistry and Physics*, vol. 7, no. 23, pp. 5989–6023, 2007. DOI: 10.5194/acp-7-5989-2007. [Online]. Available: <https://acp.copernicus.org/articles/7/5989/2007/>.

- [30] P. Jain, D. Castellanos-Acuna, S. C. P. Coogan, J. T. Abatzoglou, and M. D. Flannigan, “Observed increases in extreme fire weather driven by atmospheric humidity and temperature,” *Nature Climate Change*, vol. 12, no. 1, pp. 63–70, Jan. 2022, ISSN: 1758-6798. DOI: 10.1038/s41558-021-01224-1. [Online]. Available: <https://doi.org/10.1038/s41558-021-01224-1>.
- [42] C. E. Stockwell *et al.*, “Nepal ambient monitoring and source testing experiment (namaste): Emissions of trace gases and light-absorbing carbon from wood and dung cooking fires, garbage and crop residue burning, brick kilns, and other sources,” *Atmospheric Chemistry and Physics*, vol. 16, no. 17, pp. 11 043–11 081, 2016. DOI: 10.5194/acp-16-11043-2016. [Online]. Available: <https://acp.copernicus.org/articles/16/11043/2016/>.
- [43] A. Laskin, J. Laskin, and S. A. Nizkorodov, “Chemistry of atmospheric brown carbon,” *Chemical Reviews*, vol. 115, no. 10, pp. 4335–4382, 2015. DOI: 10.1021/cr5006167. [Online]. Available: <https://doi.org/10.1021/cr5006167>.
- [61] B. R. Simoneit, “Biomass burning — a review of organic tracers for smoke from incomplete combustion,” *Applied Geochemistry*, vol. 17, no. 3, pp. 129–162, 2002, ISSN: 0883-2927. DOI: [https://doi.org/10.1016/S0883-2927\(01\)00061-0](https://doi.org/10.1016/S0883-2927(01)00061-0). [Online]. Available: <https://www.sciencedirect.com/science/article/pii/S0883292701000610>.
- [63] W. O. Osburn and T. W. Kensler, “Nrf2 signaling: An adaptive response pathway for protection against environmental toxic insults,” *Mutation Research/Reviews in Mutation Research*, vol. 659, no. 1, pp. 31–39, 2008, Proceedings of the 5th International Conference on Environmental Mutagens in Human Populations (ICEMHP), ISSN: 1383-5742. DOI: <https://doi.org/10.1016/j.mrrev.2007.11.006>. [Online]. Available: <https://www.sciencedirect.com/science/article/pii/S1383574207000695>.
- [64] K. M. Venables, “Low molecular weight chemicals, hypersensitivity, and direct toxicity: The acid anhydrides,” *Occupational and Environmental Medicine*, vol. 46, no. 4, pp. 222–232, 1989, ISSN: 0007-1072. DOI: 10.1136/oem.46.4.222. [Online]. Available: <https://oem.bmj.com/content/46/4/222>.
- [67] M. Claeys *et al.*, “Formation of secondary organic aerosols through photooxidation of isoprene,” *Science*, vol. 303, no. 5661, pp. 1173–1176, 2004. DOI: 10.1126/science.1092805. [Online]. Available: <https://www.science.org/doi/abs/10.1126/science.1092805>.
- [70] J. S. Reid, R. Koppmann, T. F. Eck, and D. P. Eleuterio, “A review of biomass burning emissions part ii: Intensive physical properties of biomass burning particles,” *Atmospheric Chemistry and Physics*, vol. 5, no. 3, pp. 799–825, 2005. DOI: 10.5194/acp-5-799-2005. [Online]. Available: <https://acp.copernicus.org/articles/5/799/2005/>.

- [77] M. Shiraiwa *et al.*, “Global distribution of particle phase state in atmospheric secondary organic aerosols,” *Nature Communications*, vol. 8, no. 1, p. 15 002, Apr. 2017, ISSN: 2041-1723. DOI: 10.1038/ncomms15002. [Online]. Available: <https://doi.org/10.1038/ncomms15002>.
- [96] J. F. Pankow, “An absorption model of gas/particle partitioning of organic compounds in the atmosphere,” *Atmospheric Environment*, vol. 28, no. 2, pp. 185–188, 1994, ISSN: 1352-2310. DOI: [https://doi.org/10.1016/1352-2310\(94\)90093-0](https://doi.org/10.1016/1352-2310(94)90093-0). [Online]. Available: <https://www.sciencedirect.com/science/article/pii/S1352231094900930>.
- [98] N. M. Donahue, S. A. Epstein, S. N. Pandis, and A. L. Robinson, “A two-dimensional volatility basis set: 1. organic-aerosol mixing thermodynamics,” *Atmospheric Chemistry and Physics*, vol. 11, no. 7, pp. 3303–3318, 2011. DOI: 10.5194/acp-11-3303-2011. [Online]. Available: <https://acp.copernicus.org/articles/11/3303/2011/>.
- [106] J. H. Kroll and J. H. Seinfeld, “Chemistry of secondary organic aerosol: Formation and evolution of low-volatility organics in the atmosphere,” *Atmospheric Environment*, vol. 42, no. 16, pp. 3593–3624, 2008, ISSN: 1352-2310. DOI: <https://doi.org/10.1016/j.atmosenv.2008.01.003>. [Online]. Available: <https://www.sciencedirect.com/science/article/pii/S1352231008000253>.
- [117] J. Li, S. M. Forrester, and D. A. Knopf, “Heterogeneous oxidation of amorphous organic aerosol surrogates by O_3 , NO_3 , and oh, at typical tropospheric temperatures,” *Atmospheric Chemistry and Physics*, vol. 20, no. 10, pp. 6055–6080, 2020. DOI: 10.5194/acp-20-6055-2020. [Online]. Available: <https://acp.copernicus.org/articles/20/6055/2020/>.
- [118] A. M. Arangio, J. H. Slade, T. Berkemeier, U. Pöschl, D. A. Knopf, and M. Shiraiwa, “Multiphase chemical kinetics of oh radical uptake by molecular organic markers of biomass burning aerosols: Humidity and temperature dependence, surface reaction, and bulk diffusion,” *The Journal of Physical Chemistry A*, vol. 119, no. 19, pp. 4533–4544, 2015, PMID: 25686209. DOI: 10.1021/jp510489z. [Online]. Available: <https://doi.org/10.1021/jp510489z>.
- [123] P. Lin, N. Bluvshstein, Y. Rudich, S. A. Nizkorodov, J. Laskin, and A. Laskin, “Molecular chemistry of atmospheric brown carbon inferred from a nationwide biomass burning event,” *Environmental Science & Technology*, vol. 51, no. 20, pp. 11 561–11 570, 2017. DOI: 10.1021/acs.est.7b02276. [Online]. Available: <https://doi.org/10.1021/acs.est.7b02276>.
- [137] Z. C. J. Decker *et al.*, “Novel analysis to quantify plume crosswind heterogeneity applied to biomass burning smoke,” *Environmental Science & Technology*, vol. 55, no. 23, pp. 15 646–15 657, 2021, PMID: 34817984. DOI: 10.1021/acs.est.1c03803. [Online]. Available: <https://doi.org/10.1021/acs.est.1c03803>.

- [138] E. A. Bruns *et al.*, “Characterization of gas-phase organics using proton transfer reaction time-of-flight mass spectrometry: Fresh and aged residential wood combustion emissions,” *Atmospheric Chemistry and Physics*, vol. 17, no. 1, pp. 705–720, 2017. DOI: 10.5194/acp-17-705-2017. [Online]. Available: <https://acp.copernicus.org/articles/17/705/2017/>.
- [139] A. W. H. Chan *et al.*, “Secondary organic aerosol formation from photooxidation of naphthalene and alkylnaphthalenes: Implications for oxidation of intermediate volatility organic compounds (ivocs),” *Atmospheric Chemistry and Physics*, vol. 9, no. 9, pp. 3049–3060, 2009. DOI: 10.5194/acp-9-3049-2009. [Online]. Available: <https://acp.copernicus.org/articles/9/3049/2009/>.
- [140] L. Zhang, Z. Wang, W. Zhang, Y. Liang, and Q. Shi, “Determination of anhydride in atmospheric fine particles by optimized solvent extraction,” *Atmospheric Environment*, vol. 285, p. 119 249, 2022, ISSN: 1352-2310. DOI: <https://doi.org/10.1016/j.atmosenv.2022.119249>. [Online]. Available: <https://www.sciencedirect.com/science/article/pii/S1352231022003144>.
- [141] Y. Iinuma *et al.*, “Source characterization of biomass burning particles: The combustion of selected european conifers, african hardwood, savanna grass, and german and indonesian peat,” *Journal of Geophysical Research: Atmospheres*, vol. 112, no. D8, 2007. DOI: <https://doi.org/10.1029/2006JD007120>. [Online]. Available: <https://agupubs.onlinelibrary.wiley.com/doi/abs/10.1029/2006JD007120>.
- [143] T. Moise and Y. Rudich, “Reactive uptake of ozone by proxies for organic aerosols: Surface versus bulk processes,” *Journal of Geophysical Research: Atmospheres*, vol. 105, no. D11, pp. 14 667–14 676, 2000. DOI: <https://doi.org/10.1029/2000JD900071>. [Online]. Available: <https://agupubs.onlinelibrary.wiley.com/doi/abs/10.1029/2000JD900071>.
- [144] J. D. Hearn and G. D. Smith, “Kinetics and product studies for ozonolysis reactions of organic particles using aerosol cims,” *The Journal of Physical Chemistry A*, vol. 108, no. 45, pp. 10 019–10 029, 2004. DOI: 10.1021/jp0404145. [Online]. Available: <https://doi.org/10.1021/jp0404145>.
- [155] S. K. Akagi *et al.*, “Emission factors for open and domestic biomass burning for use in atmospheric models,” *Atmospheric Chemistry and Physics*, vol. 11, no. 9, pp. 4039–4072, 2011. DOI: 10.5194/acp-11-4039-2011. [Online]. Available: <https://acp.copernicus.org/articles/11/4039/2011/>.
- [157] B. Rooney *et al.*, “Impacts of household sources on air pollution at village and regional scales in india,” *Atmospheric Chemistry and Physics*, vol. 19, no. 11, pp. 7719–7742, 2019. DOI: 10.5194/acp-19-7719-2019. [Online]. Available: <https://acp.copernicus.org/articles/19/7719/2019/>.
- [176] S. Jennings, “The mean free path in air,” *Journal of Aerosol Science*, vol. 19, no. 2, pp. 159–166, 1988, ISSN: 0021-8502. DOI: [https://doi.org/10.1016/0021-8502\(88\)90219-4](https://doi.org/10.1016/0021-8502(88)90219-4). [Online]. Available: <https://www.sciencedirect.com/science/article/pii/0021850288902194>.

- [182] J. Rissler *et al.*, “Size distribution and hygroscopic properties of aerosol particles from dry-season biomass burning in amazonia,” *Atmospheric Chemistry and Physics*, vol. 6, no. 2, pp. 471–491, 2006. DOI: 10.5194/acp-6-471-2006. [Online]. Available: <https://acp.copernicus.org/articles/6/471/2006/>.
- [207] M. Canagaratna *et al.*, “Chemical and microphysical characterization of ambient aerosols with the aerodyne aerosol mass spectrometer,” *Mass Spectrometry Reviews*, vol. 26, no. 2, pp. 185–222, 2007. DOI: <https://doi.org/10.1002/mas.20115>. [Online]. Available: <https://analyticalsciencejournals.onlinelibrary.wiley.com/doi/abs/10.1002/mas.20115>.
- [221] H. Bhattarai *et al.*, “Levoglucosan as a tracer of biomass burning: Recent progress and perspectives,” *Atmospheric Research*, vol. 220, pp. 20–33, 2019, ISSN: 0169-8095. DOI: <https://doi.org/10.1016/j.atmosres.2019.01.004>. [Online]. Available: <https://www.sciencedirect.com/science/article/pii/S0169809518311098>.
- [223] B. Simoneit *et al.*, “Levoglucosan, a tracer for cellulose in biomass burning and atmospheric particles,” *Atmospheric Environment*, vol. 33, no. 2, pp. 173–182, 1999, ISSN: 1352-2310. DOI: [https://doi.org/10.1016/S1352-2310\(98\)00145-9](https://doi.org/10.1016/S1352-2310(98)00145-9). [Online]. Available: <https://www.sciencedirect.com/science/article/pii/S1352231098001459>.
- [244] M. Abou-Ghanem *et al.*, “Significant variability in the photocatalytic activity of natural titanium-containing minerals: Implications for understanding and predicting atmospheric mineral dust photochemistry,” *Environmental Science & Technology*, vol. 54, no. 21, pp. 13 509–13 516, 2020, PMID: 33058682. DOI: 10.1021/acs.est.0c05861. [Online]. Available: <https://doi.org/10.1021/acs.est.0c05861>.
- [248] V. Choudhary, M. Loebel Roson, X. Guo, T. Gautam, T. Gupta, and R. Zhao, “Aqueous-phase photochemical oxidation of water-soluble brown carbon aerosols arising from solid biomass fuel burning,” *Environ. Sci.: Atmos.*, pp. –, 2023. DOI: 10.1039/D2EA00151A. [Online]. Available: <http://dx.doi.org/10.1039/D2EA00151A>.
- [268] M. O. Andreae, “Emission of trace gases and aerosols from biomass burning – an updated assessment,” *Atmospheric Chemistry and Physics*, vol. 19, no. 13, pp. 8523–8546, 2019. DOI: 10.5194/acp-19-8523-2019. [Online]. Available: <https://acp.copernicus.org/articles/19/8523/2019/>.
- [279] R. Zhao, C. M. Kenseth, Y. Huang, N. F. Dalleska, and J. H. Seinfeld, “Iodometry-assisted liquid chromatography electrospray ionization mass spectrometry for analysis of organic peroxides: An application to atmospheric secondary organic aerosol,” *Environmental Science & Technology*, vol. 52, no. 4, pp. 2108–2117, 2018, PMID: 29370527. DOI: 10.1021/acs.est.7b04863. [Online]. Available: <https://doi.org/10.1021/acs.est.7b04863>.

- [338] J. Chen *et al.*, “A review of biomass burning: Emissions and impacts on air quality, health and climate in china,” *Science of The Total Environment*, vol. 579, pp. 1000–1034, 2017, ISSN: 0048-9697. DOI: <https://doi.org/10.1016/j.scitotenv.2016.11.025>. [Online]. Available: <https://www.sciencedirect.com/science/article/pii/S0048969716324561>.
- [339] V. Vakkari *et al.*, “Rapid changes in biomass burning aerosols by atmospheric oxidation,” *Geophysical Research Letters*, vol. 41, no. 7, pp. 2644–2651, 2014. DOI: <https://doi.org/10.1002/2014GL059396>. [Online]. Available: <https://agupubs.onlinelibrary.wiley.com/doi/abs/10.1002/2014GL059396>.
- [340] M. Claeys *et al.*, “Chemical characterisation of humic-like substances from urban, rural and tropical biomass burning environments using liquid chromatography with uv/vis photodiode array detection and electrospray ionisation mass spectrometry,” *Environmental Chemistry*, vol. 9, no. 3, pp. 273–284, 2012. DOI: 10.1071/EN11163. [Online]. Available: <https://doi.org/10.1071/EN11163>.
- [341] S. N. Pandis, R. A. Harley, G. R. Cass, and J. H. Seinfeld, “Secondary organic aerosol formation and transport,” *Atmospheric Environment. Part A. General Topics*, vol. 26, no. 13, pp. 2269–2282, 1992, ISSN: 0960-1686. DOI: [https://doi.org/10.1016/0960-1686\(92\)90358-R](https://doi.org/10.1016/0960-1686(92)90358-R). [Online]. Available: <https://www.sciencedirect.com/science/article/pii/096016869290358R>.
- [342] P. J. Ziemann and R. Atkinson, “Kinetics, products, and mechanisms of secondary organic aerosol formation,” *Chem. Soc. Rev.*, vol. 41, pp. 6582–6605, 19 2012. DOI: 10.1039/C2CS35122F. [Online]. Available: <http://dx.doi.org/10.1039/C2CS35122F>.
- [343] V. Choudhary, T. Gupta, and R. Zhao, “Evolution of brown carbon aerosols during atmospheric long-range transport in the south asian outflow and himalayan cryosphere,” *ACS Earth and Space Chemistry*, vol. 6, no. 10, pp. 2335–2347, 2022. DOI: 10.1021/acsearthspacechem.2c00047. [Online]. Available: <https://doi.org/10.1021/acsearthspacechem.2c00047>.
- [344] B. Yuan, A. R. Koss, C. Warneke, M. Coggon, K. Sekimoto, and J. A. de Gouw, “Proton-transfer-reaction mass spectrometry: Applications in atmospheric sciences,” *Chemical Reviews*, vol. 117, no. 21, pp. 13 187–13 229, 2017, PMID: 28976748. DOI: 10.1021/acs.chemrev.7b00325. [Online]. Available: <https://doi.org/10.1021/acs.chemrev.7b00325>.
- [345] A. Bierbach, I. Barnes, K. H. Becker, and E. Wiesen, “Atmospheric chemistry of unsaturated carbonyls: Butenedial, 4-oxo-2-pentenal, 3-hexene-2, 5-dione, maleic anhydride, 3h-furan-2-one, and 5-methyl-3h-furan-2-one,” *Environmental science & technology*, vol. 28, no. 4, pp. 715–729, 1994.
- [346] L. Wang *et al.*, “Source characterization of volatile organic compounds measured by proton-transfer-reaction time-of-flight mass spectrometers in delhi, india,” *Atmospheric Chemistry and Physics*, vol. 20, no. 16, pp. 9753–9770, 2020. DOI: 10.5194/acp-20-9753-2020. [Online]. Available: <https://acp.copernicus.org/articles/20/9753/2020/>.

- [347] M. M. Coggon *et al.*, “Oh chemistry of non-methane organic gases (nmogs) emitted from laboratory and ambient biomass burning smoke: Evaluating the influence of furans and oxygenated aromatics on ozone and secondary nmog formation,” *Atmospheric Chemistry and Physics*, vol. 19, no. 23, pp. 14 875–14 899, 2019. DOI: 10.5194/acp-19-14875-2019. [Online]. Available: <https://acp.copernicus.org/articles/19/14875/2019/>.
- [348] P. S. Rickly *et al.*, “Influence of wildfire on urban ozone: An observationally constrained box modeling study at a site in the colorado front range,” *Environmental Science & Technology*, vol. 57, no. 3, pp. 1257–1267, 2023, PMID: 36607321. DOI: 10.1021/acs.est.2c06157. [Online]. Available: <https://doi.org/10.1021/acs.est.2c06157>.
- [349] A. C. D. Rivett and N. V. Sidgwick, “Clvii.—the rate of hydration of acid anhydrides: Succinic, methylsuccinic, itaconic, maleic, citraconic, and phthalic,” *J. Chem. Soc., Trans.*, vol. 97, pp. 1677–1686, 0 1910. DOI: 10.1039/CT9109701677. [Online]. Available: <http://dx.doi.org/10.1039/CT9109701677>.
- [350] J. Rosenfeld and C. Murphy, “Hydrolysis study of organic acid anhydrides by differential thermal analysis—ii: Maleic anhydride and trimellitic anhydride,” *Talanta*, vol. 14, no. 1, pp. 91–96, 1967, ISSN: 0039-9140. DOI: [https://doi.org/10.1016/0039-9140\(67\)80050-X](https://doi.org/10.1016/0039-9140(67)80050-X). [Online]. Available: <https://www.sciencedirect.com/science/article/pii/003991406780050X>.
- [351] B. R. T. Simoneit *et al.*, “Composition and major sources of organic compounds of aerosol particulate matter sampled during the ace-asia campaign,” *Journal of Geophysical Research: Atmospheres*, vol. 109, no. D19, 2004. DOI: <https://doi.org/10.1029/2004JD004598>. [Online]. Available: <https://agupubs.onlinelibrary.wiley.com/doi/abs/10.1029/2004JD004598>.
- [352] K. E. Kautzman *et al.*, “Chemical composition of gas- and aerosol-phase products from the photooxidation of naphthalene,” *The Journal of Physical Chemistry A*, vol. 114, no. 2, pp. 913–934, 2010, PMID: 19904975. DOI: 10.1021/jp908530s. [Online]. Available: <https://doi.org/10.1021/jp908530s>.
- [353] T. E. Kleindienst, M. Jaoui, M. Lewandowski, J. H. Offenberg, and K. S. Docherty, “The formation of soa and chemical tracer compounds from the photooxidation of naphthalene and its methyl analogs in the presence and absence of nitrogen oxides,” *Atmospheric Chemistry and Physics*, vol. 12, no. 18, pp. 8711–8726, 2012. DOI: 10.5194/acp-12-8711-2012. [Online]. Available: <https://acp.copernicus.org/articles/12/8711/2012/>.
- [354] Y. Zhao *et al.*, “Insights into secondary organic aerosol formation mechanisms from measured gas/particle partitioning of specific organic tracer compounds,” *Environmental Science & Technology*, vol. 47, no. 8, pp. 3781–3787, 2013, PMID: 23448102. DOI: 10.1021/es304587x. [Online]. Available: <https://doi.org/10.1021/es304587x>.

- [355] A. A. May, R. Saleh, C. J. Hennigan, N. M. Donahue, and A. L. Robinson, “Volatility of organic molecular markers used for source apportionment analysis: Measurements and implications for atmospheric lifetime,” *Environmental Science & Technology*, vol. 46, no. 22, pp. 12 435–12 444, 2012, PMID: 23013599. DOI: 10.1021/es302276t. [Online]. Available: <https://doi.org/10.1021/es302276t>.
- [356] M. Shrivastava *et al.*, “Global long-range transport and lung cancer risk from polycyclic aromatic hydrocarbons shielded by coatings of organic aerosol,” *Proceedings of the National Academy of Sciences*, vol. 114, no. 6, pp. 1246–1251, 2017. DOI: 10.1073/pnas.1618475114. [Online]. Available: <https://www.pnas.org/doi/abs/10.1073/pnas.1618475114>.
- [357] Q. Mu *et al.*, “Temperature effect on phase state and reactivity controls atmospheric multiphase chemistry and transport of pahs,” *Science Advances*, vol. 4, no. 3, eaap7314, 2018. DOI: 10.1126/sciadv.aap7314. [Online]. Available: <https://www.science.org/doi/abs/10.1126/sciadv.aap7314>.
- [358] Y. Chen, P. McDaid, and L. Deng, “Asymmetric alcoholysis of cyclic anhydrides,” *Chemical Reviews*, vol. 103, no. 8, pp. 2965–2984, 2003, PMID: 12914488. DOI: 10.1021/cr020037x. [Online]. Available: <https://doi.org/10.1021/cr020037x>.
- [359] H. O. T. Pye *et al.*, “The acidity of atmospheric particles and clouds,” *Atmospheric Chemistry and Physics*, vol. 20, no. 8, pp. 4809–4888, 2020. DOI: 10.5194/acp-20-4809-2020. [Online]. Available: <https://acp.copernicus.org/articles/20/4809/2020/>.
- [360] J. Park, A. L. Gomez, M. L. Walser, A. Lin, and S. A. Nizkorodov, “Ozonolysis and photolysis of alkene-terminated self-assembled monolayers on quartz nanoparticles: Implications for photochemical aging of organic aerosol particles,” *Phys. Chem. Chem. Phys.*, vol. 8, pp. 2506–2512, 21 2006. DOI: 10.1039/B602704K. [Online]. Available: <http://dx.doi.org/10.1039/B602704K>.
- [361] J. He, B. Zielinska, and R. Balasubramanian, “Composition of semi-volatile organic compounds in the urban atmosphere of singapore: Influence of biomass burning,” *Atmospheric Chemistry and Physics*, vol. 10, no. 23, pp. 11 401–11 413, 2010. DOI: 10.5194/acp-10-11401-2010. [Online]. Available: <https://acp.copernicus.org/articles/10/11401/2010/>.
- [362] J. J. Schauer, M. P. Fraser, G. R. Cass, and B. R. T. Simoneit, “Source reconciliation of atmospheric gas-phase and particle-phase pollutants during a severe photochemical smog episode,” *Environmental Science & Technology*, vol. 36, no. 17, pp. 3806–3814, 2002, PMID: 12322754. DOI: 10.1021/es011458j. [Online]. Available: <https://doi.org/10.1021/es011458j>.
- [363] P. M. Fine, B. Chakrabarti, M. Krudysz, J. J. Schauer, and C. Sioutas, “Diurnal variations of individual organic compound constituents of ultrafine and accumulation mode particulate matter in the los angeles basin,” *Environmental Science & Technology*, vol. 38, no. 5, pp. 1296–1304, 2004, PMID:

15046329. DOI: 10.1021/es0348389. [Online]. Available: <https://doi.org/10.1021/es0348389>.
- [364] Y.-L. Zhang, K. Kawamura, T. Watanabe, S. Hatakeyama, A. Takami, and W. Wang, “New directions: Need for better understanding of source and formation process of phthalic acid in aerosols as inferred from aircraft observations over china,” *Atmospheric Environment*, vol. 140, pp. 147–149, 2016, ISSN: 1352-2310. DOI: <https://doi.org/10.1016/j.atmosenv.2016.05.058>. [Online]. Available: <https://www.sciencedirect.com/science/article/pii/S135223101630406X>.
- [365] D. Hoffmann, Y. Iinuma, and H. Herrmann, “Development of a method for fast analysis of phenolic molecular markers in biomass burning particles using high performance liquid chromatography/atmospheric pressure chemical ionisation mass spectrometry,” *Journal of Chromatography A*, vol. 1143, no. 1, pp. 168–175, 2007, ISSN: 0021-9673. DOI: <https://doi.org/10.1016/j.chroma.2007.01.035>. [Online]. Available: <https://www.sciencedirect.com/science/article/pii/S0021967307000726>.
- [366] A. P. Mouat, C. Paton-Walsh, J. B. Simmons, J. Ramirez-Gamboa, D. W. T. Griffith, and J. Kaiser, “Measurement report: Observations of long-lived volatile organic compounds from the 2019–2020 australian wildfires during the coala campaign,” *Atmospheric Chemistry and Physics*, vol. 22, no. 17, pp. 11 033–11 047, 2022. DOI: 10.5194/acp-22-11033-2022. [Online]. Available: <https://acp.copernicus.org/articles/22/11033/2022/>.
- [367] J. Y. Lee, D. A. Lane, J. B. Heo, S.-M. Yi, and Y. P. Kim, “Quantification and seasonal pattern of atmospheric reaction products of gas phase pahs in pm2.5,” *Atmospheric Environment*, vol. 55, pp. 17–25, 2012, ISSN: 1352-2310. DOI: <https://doi.org/10.1016/j.atmosenv.2012.03.007>. [Online]. Available: <https://www.sciencedirect.com/science/article/pii/S1352231012002397>.
- [368] G. D. Smith, E. Woods, C. L. DeForest, T. Baer, and R. E. Miller, “Reactive uptake of ozone by oleic acid aerosol particles: Application of single-particle mass spectrometry to heterogeneous reaction kinetics,” *The Journal of Physical Chemistry A*, vol. 106, no. 35, pp. 8085–8095, 2002. DOI: 10.1021/jp020527t. [Online]. Available: <https://doi.org/10.1021/jp020527t>.
- [369] S. Gross, R. Iannone, S. Xiao, and A. K. Bertram, “Reactive uptake studies of no3 and n2o5 on alkenoic acid, alkanoate, and polyalcohol substrates to probe nighttime aerosol chemistry,” *Phys. Chem. Chem. Phys.*, vol. 11, pp. 7792–7803, 36 2009. DOI: 10.1039/B904741G. [Online]. Available: <http://dx.doi.org/10.1039/B904741G>.
- [370] T. Nah, S. H. Kessler, K. E. Daumit, J. H. Kroll, S. R. Leone, and K. R. Wilson, “Influence of molecular structure and chemical functionality on the heterogeneous oh-initiated oxidation of unsaturated organic particles,” *The Journal of Physical Chemistry A*, vol. 118, no. 23, pp. 4106–4119, 2014, PMID: 24840787. DOI: 10.1021/jp502666g. [Online]. Available: <https://doi.org/10.1021/jp502666g>.

- [371] T. Berkemeier, A. Mishra, C. Mattei, A. J. Huisman, U. K. Krieger, and U. Pöschl, “Ozonolysis of oleic acid aerosol revisited: Multiphase chemical kinetics and reaction mechanisms,” *ACS Earth and Space Chemistry*, vol. 5, no. 12, pp. 3313–3323, 2021. DOI: 10.1021/acsearthspacechem.1c00232. [Online]. Available: <https://doi.org/10.1021/acsearthspacechem.1c00232>.
- [372] J. N. Crowley *et al.*, “Evaluated kinetic and photochemical data for atmospheric chemistry: Volume v – heterogeneous reactions on solid substrates,” *Atmospheric Chemistry and Physics*, vol. 10, no. 18, pp. 9059–9223, 2010. DOI: 10.5194/acp-10-9059-2010. [Online]. Available: <https://acp.copernicus.org/articles/10/9059/2010/>.
- [373] F. A. Houle, W. D. Hinsberg, and K. R. Wilson, “Oxidation of a model alkane aerosol by oh radical: The emergent nature of reactive uptake,” *Phys. Chem. Chem. Phys.*, vol. 17, pp. 4412–4423, 6 2015. DOI: 10.1039/C4CP05093B. [Online]. Available: <http://dx.doi.org/10.1039/C4CP05093B>.
- [374] D. A. Knopf, U. Pöschl, and M. Shiraiwa, “Radial diffusion and penetration of gas molecules and aerosol particles through laminar flow reactors, denuders, and sampling tubes,” *Analytical Chemistry*, vol. 87, no. 7, pp. 3746–3754, 2015, PMID: 25744622. DOI: 10.1021/ac5042395. [Online]. Available: <https://doi.org/10.1021/ac5042395>.
- [375] M. J. Tang, M. Shiraiwa, U. Pöschl, R. A. Cox, and M. Kalberer, “Compilation and evaluation of gas phase diffusion coefficients of reactive trace gases in the atmosphere: Volume 2. diffusivities of organic compounds, pressure-normalised mean free paths, and average knudsen numbers for gas uptake calculations,” *Atmospheric Chemistry and Physics*, vol. 15, no. 10, pp. 5585–5598, 2015. DOI: 10.5194/acp-15-5585-2015. [Online]. Available: <https://acp.copernicus.org/articles/15/5585/2015/>.
- [376] N. FUCHS and A. SUTUGIN, “High-dispersed aerosols,” in *Topics in Current Aerosol Research*, ser. International Reviews in Aerosol Physics and Chemistry, G. HIDY and J. BROCK, Eds., Pergamon, 1971, p. 1. DOI: <https://doi.org/10.1016/B978-0-08-016674-2.50006-6>. [Online]. Available: <https://www.sciencedirect.com/science/article/pii/B9780080166742500066>.
- [377] R. Zhao *et al.*, “The role of water in organic aerosol multiphase chemistry: Focus on partitioning and reactivity,” in *Advances in Atmospheric Chemistry*. World Scientific Publishing, Feb. 2017, ch. 2, pp. 95–184. DOI: 10.1142/9789813147355_0002. [Online]. Available: https://www.worldscientific.com/doi/abs/10.1142/9789813147355_0002.
- [378] J. H. Hu, Q. Shi, P. Davidovits, D. R. Worsnop, M. S. Zahniser, and C. E. Kolb, “Reactive uptake of $\text{Cl}_2(\text{g})$ and $\text{Br}_2(\text{g})$ by aqueous surfaces as a function of Br^- and I^- ion concentration: The effect of chemical reaction at the interface,” *The Journal of Physical Chemistry*, vol. 99, no. 21, pp. 8768–8776, 1995. DOI: 10.1021/j100021a050. [Online]. Available: <https://doi.org/10.1021/j100021a050>.

- [379] Q. Zou, H. Song, M. Tang, and K. Lu, “Measurements of ho₂ uptake coefficient on aqueous (nh₄)₂so₄ aerosol using aerosol flow tube with lif system,” *Chinese Chemical Letters*, vol. 30, no. 12, pp. 2236–2240, 2019, ISSN: 1001-8417. DOI: <https://doi.org/10.1016/j.cclet.2019.07.041>. [Online]. Available: <https://www.sciencedirect.com/science/article/pii/S1001841719304231>.
- [380] J. Liggió and S.-M. Li, “Reactive uptake of pinonaldehyde on acidic aerosols,” *Journal of Geophysical Research: Atmospheres*, vol. 111, no. D24, 2006. DOI: <https://doi.org/10.1029/2005JD006978>. [Online]. Available: <https://agupubs.onlinelibrary.wiley.com/doi/abs/10.1029/2005JD006978>.
- [381] A. Jammoul, S. Gligorovski, C. George, and B. D’Anna, “Photosensitized heterogeneous chemistry of ozone on organic films,” *The Journal of Physical Chemistry A*, vol. 112, no. 6, pp. 1268–1276, 2008, PMID: 18205335. DOI: [10.1021/jp074348t](https://doi.org/10.1021/jp074348t). [Online]. Available: <https://doi.org/10.1021/jp074348t>.
- [382] S. A. Styler, M. Brigante, B. D’Anna, C. George, and D. J. Donaldson, “Photoenhanced ozone loss on solid pyrene films,” *Phys. Chem. Chem. Phys.*, vol. 11, pp. 7876–7884, 36 2009. DOI: [10.1039/B904180J](https://doi.org/10.1039/B904180J). [Online]. Available: <http://dx.doi.org/10.1039/B904180J>.
- [383] G. Gržinić, T. Bartels-Rausch, T. Berkemeier, A. Türlér, and M. Ammann, “Viscosity controls humidity dependence of n₂o₅ uptake to citric acid aerosol,” *Atmospheric Chemistry and Physics*, vol. 15, no. 23, pp. 13 615–13 625, 2015. DOI: [10.5194/acp-15-13615-2015](https://doi.org/10.5194/acp-15-13615-2015). [Online]. Available: <https://acp.copernicus.org/articles/15/13615/2015/>.
- [384] L. A. Goldberger, L. G. Jahl, J. A. Thornton, and R. C. Sullivan, “N₂o₅ reactive uptake kinetics and chlorine activation on authentic biomass-burning aerosol,” *Environ. Sci.: Processes Impacts*, vol. 21, pp. 1684–1698, 10 2019. DOI: [10.1039/C9EM00330D](https://doi.org/10.1039/C9EM00330D). [Online]. Available: <http://dx.doi.org/10.1039/C9EM00330D>.
- [385] R. P. Staiger and E. B. Miller, “Isatoic anhydride. iv. reactions with various nucleophiles,” *The Journal of Organic Chemistry*, vol. 24, no. 9, pp. 1214–1219, 1959. DOI: [10.1021/jo01091a013](https://doi.org/10.1021/jo01091a013). [Online]. Available: <https://doi.org/10.1021/jo01091a013>.

Chapter 5

Conclusions, Recommendations, and Future Work

Contributions: The conclusion was written by Max Loebel Roson with review and feedback by Dr. Ran Zhao.

5.1 Thesis Summary

The goals for the present thesis were firstly, to develop reproducible methods for the analytical deconvolution of BBE, secondly, to apply the developed methods to obtain molecular data from common and understudied fuels, and finally, to advance our understanding of the heterogeneous processes happening at the interface between biomass burning aerosol and the surrounding gas-phase.

Starting with Chapter 2, I described a tube furnace setup developed to reliably gather particulate matter emitted from the combustion of wood and two distinct types of cow dung biomass. Using this setup, I reported light absorptive, molecular, as well as particle size and distribution data. The use of a tube furnace helped enhance the reproducibility of the combustion process, which has historically been an area of concern among fire scientists. In this chapter, I showed that different biomass fuel emissions can have distinct chemical and light-absorptive properties, even if fuels are often treated uniformly by atmospheric models. This is exemplified using the molecular tracer levoglucosan, which I demonstrate has variable emission factors from wood and cow dung. Despite these findings, it became apparent that the separation methods I employed were not sufficient to reliably separate the complex BBE matrix. As a result, I approached Dr. James J. Harynuk to apply GC×GC-ToF-MS to the analysis of BBE in Chapter 3. The data I obtained from these analyses shows that highest intensity compounds are consistent between burns. Using PCA, I posit that with the exception of key molecular markers, the bulk of the compositional differences between fuels burned are better explained by flow rate and temperature distinctions rather than by biomass type. These findings further reinforce the importance of precisely controlling combustion conditions.

Throughout Chapter 4, I explored the heterogeneous uptake properties of BBE towards acid anhydrides. Despite their volatility, I demonstrated that maleic and phthalic anhydride are chemically uptaken to the surface of flow tubes coated with BBE. Using a multifaceted approach, I showed that maleic and phthalic anhydride react with a variety of nucleophiles present in BBE to form water stable, higher molecular weight products. These findings have implications for our understanding of how highly volatile atmospheric aerosol can end up irreversibly partitioned to the particle-

phase, the formation of novel compounds, as well as the evolution of biomass burning plumes in the atmosphere.

5.2 Future Work and recommendations

5.2.1 On fire research

As a result of climate change, wildfire incidence and severity are expected to worsen in the coming years [30]. In all likelihood, the study of combustion emissions from biomass will remain highly relevant to our environment's and our own well-being. While there are a few issues which impede our accurate understanding of fire emissions, I posit that the most significant might be, that to this day, we still can not fully explain which burning conditions give rise to which aerosol components, or how these components evolve once emitted into the atmosphere. Hence, it is imperative that we: continue to develop techniques that accurately reproduce fires which occur in the natural environment, work on enhancing the robustness of fire-related experiments (including the combustion process itself for laboratory-based studies), and keep constraining the origin and evolution of fire emissions in the atmosphere.

5.2.2 On the application of GC×GC-MS to biomass burning emission analysis

As described throughout Chapters 1-3, the major components of biomass burning emissions are consistent between burns. Yet, the remaining diverse low intensity fraction has been reported to be responsible for many of the climate effects of biomass burning. Simultaneously, that fraction is also believed to be the most affected by variations in fuel type and burning conditions [43, 109, 124]. This means that high-grade analytical instruments, which are typically suited towards analysing low concentrations due to their small detection limits, can struggle to detect the low intensity fraction while avoiding overloading on the consistent high-intensity components. This is particularly apparent by the results presented in Chapter 3, for which PCA was necessary to accurately differentiate components. To combat this issue in GC×GC-MS, I offer a potential solution:

Once the areas of highest - and potentially damaging - intensity in the chromatogram

have been identified, part of the eluent stream could be purged before transferring it into the MS through the installation of a three-way valve. A relatively simple addition, which as far as I am aware, has not been previously reported. Avoiding areas of maximum intensity allows the use of lower split rates, facilitating the detection of lower-intensity components so long as their tR does not overlap the removed areas. In the following sections, I outline some specific areas of research interest.

5.2.3 Proposed research directions

5.2.3.1 Improving bulk identification - inspiration from metabolomic databases

Since metabolomic studies often involve the simultaneous detection of large numbers of disparate molecules, they generally face similar challenges to the biomass burning experiments outlined throughout this thesis. An interesting point of distinction between the two fields is that metabolomics has more widely adopted the use of screening and absolute quantitation methods into the experimental flow. Targeted, untargeted, and semi-targeted techniques are better interlinked to provide a more accurate representation of the nature of each sample [386]. This inter-linkage is facilitated by the large metabolite databases (many of which are open-access) built and maintained by independent researchers. These online libraries allow users to more easily, and often automatically, identify bulk components so long as the tR and characteristic mass fragments of a molecule of interest are known. Metabolomic libraries are specifically designed for application in metabolite studies.

While similar databases also exist for other sample types, such as the BBE analyzed through GC×GC-ToF-MS in Chapter 3, they are often expensive, overly broad, and/or copyrighted by instrument manufacturers. The field of fire science (and atmospheric chemistry in general), would benefit from the development and maintenance of a centralized open access library of known atmospheric pollutant components. This is a significant undertaking ideally achieved through widespread scientific collaboration, as each database entry must be separately identified, codified, and verified. Once created however, such a database would greatly expedite the analysis process, and avoid the duplication of identification efforts.

5.2.3.2 Re-emission of VOCs from biomass burning films

During the anhydride experiments presented in Chapter 4, I noted the peculiar additional FID peaks - some of which surpassed the anhydride peak itself - which occurred due to the re-emission of material from the biomass burning coated flow tubes. This effect is not unknown to scientists who have sampled a filter coated with only a few mg of biomass burning material, opened it after years of storage, and found that the burning scent emanating from the filter was highly pungent.

The potential health effects of breathing in BBE are nowadays well known. However, with the rising interest in indoor air quality in recent years, it is surprising that the potential health effects of re-emission of material from indoor burning of biomass have not been fully considered. Exposure levels could be better constrained with an understanding of the saturated mass concentrations and Henry's law constants of BBOA. However, obtaining these constants is contingent on accurately identifying the components which are being re-emitted. Emitted compounds could be selectively sampled indoors by coupling solid phase micro-extraction - a solvent-free pre-concentration technique - to the separation and identification methods outlined in Chapters 2 and 3. Solid phase micro-extraction may also help bypass issues associated with detecting low intensity compounds described in the previous section, while allowing for the selective detection of compounds of interest by switching the composition of the extraction fibre [387]. Alternatively, in a laboratory setting, the flow tube setup outlined in Chapter 4 could be easily adapted for direct online GC-MS measurements of re-emitted compounds from a pre-coated tube.

The behaviour of the re-emitted species in an indoor setting can be elucidated with the help of simple modeling. For instance, the two-dimensional chemical partitioning plot utilized by a PhD student in my group is a highly suitable tool for this purpose [388, 389]. The model can simulate the air-surface equilibria of volatile and semi-volatile compounds under a variety of conditions, such as temperature.

As climate change continues driving global temperatures upwards, we may find that compounds which previously did not partition into the gas-phase may begin affecting the quality of the air we breathe. A combination of the proposed measurements and modeling steps above can provide timely insights into the impact of solid fuel

combustion in the indoor environment.

5.2.3.3 Towards low-cost accessible detection of levoglucosan

Due to its high emission factor from wood combustion, levoglucosan is the premier biomass burning molecular tracer used for source apportionment. However, the complex instrumental and derivatization methods required to accurately quantify levoglucosan tether its detection to the laboratory and make routine analysis an inconvenient and costly endeavour [271].

Developed for patients suffering from diabetes, glucose sensors have become a widespread swift detection technique for the analysis of blood sugar levels [390]. As an anhydrosugar, levoglucosan hydrolyses to glucose through acid-hydrolysis. So long as the concentration of levoglucosan isomers mannosan and galactosan is accounted for, the concentration of levoglucosan could conceivably be quantified using a glucose sensor. This would provide a swift, field deployable, and affordable alternative to conventional levoglucosan quantification methods. An affordability which grants the average user the ability to predict if the air they breathe is polluted by biomass fuels, whether wildfire-based or anthropogenic. Fast detection particularly benefits remote and at-risk populations, who may not be able to rely on slower government-based initiatives.

References

- [30] P. Jain, D. Castellanos-Acuna, S. C. P. Coogan, J. T. Abatzoglou, and M. D. Flannigan, “Observed increases in extreme fire weather driven by atmospheric humidity and temperature,” *Nature Climate Change*, vol. 12, no. 1, pp. 63–70, Jan. 2022, ISSN: 1758-6798. DOI: 10.1038/s41558-021-01224-1. [Online]. Available: <https://doi.org/10.1038/s41558-021-01224-1>.
- [43] A. Laskin, J. Laskin, and S. A. Nizkorodov, “Chemistry of atmospheric brown carbon,” *Chemical Reviews*, vol. 115, no. 10, pp. 4335–4382, 2015. DOI: 10.1021/cr5006167. [Online]. Available: <https://doi.org/10.1021/cr5006167>.
- [109] P. Lin, L. T. Fleming, S. A. Nizkorodov, J. Laskin, and A. Laskin, “Comprehensive molecular characterization of atmospheric brown carbon by high resolution mass spectrometry with electrospray and atmospheric pressure photoionization,” *Analytical Chemistry*, vol. 90, no. 21, pp. 12 493–12 502, 2018. DOI: 10.1021/acs.analchem.8b02177. [Online]. Available: <https://doi.org/10.1021/acs.analchem.8b02177>.
- [124] L. T. Fleming *et al.*, “Molecular composition and photochemical lifetimes of brown carbon chromophores in biomass burning organic aerosol,” *Atmospheric Chemistry and Physics*, vol. 20, no. 2, pp. 1105–1129, 2020. DOI: 10.5194/acp-20-1105-2020. [Online]. Available: <https://acp.copernicus.org/articles/20/1105/2020/>.
- [271] Z. Zdráhal, J. Oliveira, R. Vermeylen, M. Claeys, and W. Maenhaut, “Improved method for quantifying levoglucosan and related monosaccharide anhydrides in atmospheric aerosols and application to samples from urban and tropical locations,” *Environmental Science & Technology*, vol. 36, no. 4, pp. 747–753, 2002. DOI: 10.1021/es015619v. [Online]. Available: <https://doi.org/10.1021/es015619v>.
- [386] X. Liu and J. W. Locasale, “Metabolomics: A primer,” *Trends in Biochemical Sciences*, vol. 42, no. 4, pp. 274–284, Apr. 2017, ISSN: 0968-0004. DOI: 10.1016/j.tibs.2017.01.004. [Online]. Available: <https://doi.org/10.1016/j.tibs.2017.01.004>.
- [387] L. Lin, M. L. Lee, and D. J. Eatough, “Gas chromatographic analysis of organic marker compounds in fine particulate matter using solid-phase microextraction,” *Journal of the Air & Waste Management Association*, vol. 57, no. 1, pp. 53–58, 2007. DOI: 10.1080/10473289.2007.10465295. [Online]. Available: <https://doi.org/10.1080/10473289.2007.10465295>.
- [388] S. Wu, E. Kim, D. Vethanayagam, and R. Zhao, “Indoor partitioning and potential thirdhand exposure to carbonyl flavoring agents added in e-cigarettes and hookah tobacco,” *Environ. Sci.: Processes Impacts*, vol. 24, pp. 2294–2309, 12 2022. DOI: 10.1039/D2EM00365A. [Online]. Available: <http://dx.doi.org/10.1039/D2EM00365A>.

- [389] S. Wu *et al.*, “Henry’s law constants and indoor partitioning of microbial volatile organic compounds,” *Environmental Science & Technology*, vol. 56, no. 11, pp. 7143–7152, 2022, PMID: 35522906. DOI: 10.1021/acs.est.1c07882. [Online]. Available: <https://doi.org/10.1021/acs.est.1c07882>.
- [390] H.-C. Wang and A.-R. Lee, “Recent developments in blood glucose sensors,” *Journal of Food and Drug Analysis*, vol. 23, no. 2, pp. 191–200, 2015, ISSN: 1021-9498. DOI: <https://doi.org/10.1016/j.jfda.2014.12.001>. [Online]. Available: <https://www.sciencedirect.com/science/article/pii/S1021949815000174>.

Bibliography

- [1] M. Loebel Roson *et al.*, “Chemical characterization of emissions arising from solid fuel combustion—contrasting wood and cow dung burning,” *ACS Earth and Space Chemistry*, vol. 5, no. 10, pp. 2925–2937, 2021. DOI: 10.1021/acsearthspacechem.1c00268.
- [2] M. Loebel Roson *et al.*, “Unexpected electrophiles in the atmosphere – anhydride nucleophile reactions and uptake to biomass burning emissions,” *Phys. Chem. Chem. Phys.*, 2023. DOI: 10.1039/D3CP01751F.
- [3] J. D. Clark and J. W. K. Harris, “Fire and its roles in early hominid lifeways,” *African Archaeological Review*, vol. 3, no. 1, pp. 3–27, Dec. 1985, ISSN: 1572-9842. DOI: 10.1007/BF01117453. [Online]. Available: <https://doi.org/10.1007/BF01117453>.
- [4] N. Alperson-Afil, “Archaeology of fire: Methodological aspects of reconstructing fire history of prehistoric archaeological sites,” *Earth-Science Reviews*, vol. 113, no. 3, pp. 111–119, 2012, ISSN: 0012-8252. DOI: <https://doi.org/10.1016/j.earscirev.2012.03.012>. [Online]. Available: <https://www.sciencedirect.com/science/article/pii/S0012825212000499>.
- [5] K. Balakrishnan *et al.*, “Air pollution from household solid fuel combustion in india: An overview of exposure and health related information to inform health research priorities,” *Global Health Action*, vol. 4, no. 1, p. 5638, 2011, PMID: 21987631. DOI: 10.3402/gha.v4i0.5638. [Online]. Available: <https://doi.org/10.3402/gha.v4i0.5638>.
- [6] W. H. O. (WHO), “Global household energy database,” 2023. [Online]. Available: <https://www.who.int/data/gho/data/themes/air-pollution/household-air-pollution>.
- [7] J. Popp, S. Kovács, J. Oláh, Z. Divéki, and E. Balázs, “Bioeconomy: Biomass and biomass-based energy supply and demand,” *New Biotechnology*, vol. 60, pp. 76–84, 2021, ISSN: 1871-6784. DOI: <https://doi.org/10.1016/j.nbt.2020.10.004>. [Online]. Available: <https://www.sciencedirect.com/science/article/pii/S1871678420301825>.
- [8] P. McKendry, “Energy production from biomass (part 1): Overview of biomass,” *Bioresource Technology*, vol. 83, no. 1, pp. 37–46, 2002, Reviews Issue, ISSN: 0960-8524. DOI: [https://doi.org/10.1016/S0960-8524\(01\)00118-3](https://doi.org/10.1016/S0960-8524(01)00118-3).

[Online]. Available: <https://www.sciencedirect.com/science/article/pii/S0960852401001183>.

- [9] T. C. Bond, D. G. Streets, K. F. Yarber, S. M. Nelson, J.-H. Woo, and Z. Klimont, “A technology-based global inventory of black and organic carbon emissions from combustion,” *Journal of Geophysical Research: Atmospheres*, vol. 109, no. D14, 2004, D14203, 10.1029/2003JD003697. DOI: <https://doi.org/10.1029/2003JD003697>. [Online]. Available: <https://agupubs.onlinelibrary.wiley.com/doi/abs/10.1029/2003JD003697>.
- [10] R. G. Barry and R. J. Chorley, *Atmosphere, weather and climate*, 8th ed. Routledge, 2004, ch. 2,12, pp. 9–32,321–385.
- [11] S. S. Lim *et al.*, “A comparative risk assessment of burden of disease and injury attributable to 67 risk factors and risk factor clusters in 21 regions, 1990–2010: A systematic analysis for the Global Burden of Disease Study 2010,” en, *The Lancet*, vol. 380, no. 9859, pp. 2224–2260, Dec. 2012, ISSN: 01406736. DOI: 10.1016/S0140-6736(12)61766-8. [Online]. Available: <https://linkinghub.elsevier.com/retrieve/pii/S0140673612617668> (visited on 06/25/2021).
- [12] D. W. Dockery *et al.*, “An association between air pollution and mortality in six u.s. cities,” *New England Journal of Medicine*, vol. 329, no. 24, pp. 1753–1759, 1993, PMID: 8179653. DOI: 10.1056/NEJM199312093292401. [Online]. Available: <https://doi.org/10.1056/NEJM199312093292401>.
- [13] J. Liu, D. L. Mauzerall, and L. W. Horowitz, “Evaluating inter-continental transport of fine aerosols:(2) global health impact,” *Atmospheric Environment*, vol. 43, no. 28, pp. 4339–4347, 2009, ISSN: 1352-2310. DOI: <https://doi.org/10.1016/j.atmosenv.2009.05.032>. [Online]. Available: <https://www.sciencedirect.com/science/article/pii/S1352231009004610>.
- [14] C. Samara and D. Voutsas, “Size distribution of airborne particulate matter and associated heavy metals in the roadside environment,” *Chemosphere*, vol. 59, no. 8, pp. 1197–1206, 2005, ISSN: 0045-6535. DOI: <https://doi.org/10.1016/j.chemosphere.2004.11.061>. [Online]. Available: <https://www.sciencedirect.com/science/article/pii/S0045653504011361>.
- [15] Y.-F. Xing, Y.-H. Xu, M.-H. Shi, and Y.-X. Lian, “The impact of PM2.5 on the human respiratory system,” en, *J Thorac Dis*, vol. 8, no. 1, E69–74, Jan. 2016.
- [16] C. J. Murray *et al.*, “Global burden of 87 risk factors in 204 countries and territories, 1990–2019: A systematic analysis for the global burden of disease study 2019,” *The lancet*, vol. 396, no. 10258, pp. 1223–1249, 2020.
- [17] M. O. Andreae and P. Merlet, “Emission of trace gases and aerosols from biomass burning,” *Global Biogeochemical Cycles*, vol. 15, no. 4, pp. 955–966, 2001. DOI: <https://doi.org/10.1029/2000GB001382>. [Online]. Available: <https://agupubs.onlinelibrary.wiley.com/doi/abs/10.1029/2000GB001382>.

- [18] M. Pflieger and A. Kroflič, “Acute toxicity of emerging atmospheric pollutants from wood lignin due to biomass burning,” *Journal of Hazardous Materials*, vol. 338, pp. 132–139, 2017, ISSN: 0304-3894. DOI: <https://doi.org/10.1016/j.jhazmat.2017.05.023>. [Online]. Available: <https://www.sciencedirect.com/science/article/pii/S0304389417303667>.
- [19] W. H. Organization *et al.*, “Who global air quality guidelines: Particulate matter (pm2.5 and pm10), ozone, nitrogen dioxide, sulfur dioxide and carbon monoxide: Executive summary,” pp. 73–89, 2021.
- [20] and European Environment Agency, M Pinterits, B Ullrich, and E Kampel, *European Union emission inventory report 1990-2020 Under the UNECE Air Convention*. Publications Office of the European Union, 2022. DOI: [doi/10.2800/928370](https://doi.org/10.2800/928370).
- [21] M. Lippmann *et al.*, “The u.s. environmental protection agency particulate matter health effects research centers program: A midcourse report of status, progress, and plans,” *Environmental Health Perspectives*, vol. 111, no. 8, pp. 1074–1092, 2003. DOI: [10.1289/ehp.5750](https://doi.org/10.1289/ehp.5750). [Online]. Available: <https://ehp.niehs.nih.gov/doi/abs/10.1289/ehp.5750>.
- [22] A. A. May *et al.*, “Gas-particle partitioning of primary organic aerosol emissions: 3. biomass burning,” *Journal of Geophysical Research: Atmospheres*, vol. 118, no. 19, pp. 11,327–11,338, 2013. DOI: <https://doi.org/10.1002/jgrd.50828>. [Online]. Available: <https://agupubs.onlinelibrary.wiley.com/doi/abs/10.1002/jgrd.50828>.
- [23] M. Hallquist *et al.*, “The formation, properties and impact of secondary organic aerosol: Current and emerging issues,” *Atmospheric Chemistry and Physics*, vol. 9, no. 14, pp. 5155–5236, 2009. DOI: [10.5194/acp-9-5155-2009](https://doi.org/10.5194/acp-9-5155-2009). [Online]. Available: <https://acp.copernicus.org/articles/9/5155/2009/>.
- [24] M. Kanakidou *et al.*, “Organic aerosol and global climate modelling: A review,” *Atmospheric Chemistry and Physics*, vol. 5, no. 4, pp. 1053–1123, 2005. DOI: [10.5194/acp-5-1053-2005](https://doi.org/10.5194/acp-5-1053-2005). [Online]. Available: <https://acp.copernicus.org/articles/5/1053/2005/>.
- [25] M. B. Fernandes, J. O. Skjemstad, B. B. Johnson, J. D. Wells, and P. Brooks, “Characterization of carbonaceous combustion residues. i. morphological, elemental and spectroscopic features,” *Chemosphere*, vol. 51, no. 8, pp. 785–795, 2003, ISSN: 0045-6535. DOI: [https://doi.org/10.1016/S0045-6535\(03\)00098-5](https://doi.org/10.1016/S0045-6535(03)00098-5). [Online]. Available: <https://www.sciencedirect.com/science/article/pii/S0045653503000985>.
- [26] C. E. Kolb *et al.*, “An overview of current issues in the uptake of atmospheric trace gases by aerosols and clouds,” *Atmospheric Chemistry and Physics*, vol. 10, no. 21, pp. 10 561–10 605, 2010. DOI: [10.5194/acp-10-10561-2010](https://doi.org/10.5194/acp-10-10561-2010). [Online]. Available: <https://acp.copernicus.org/articles/10/10561/2010/>.

- [27] V. H. Grassian, “Heterogeneous uptake and reaction of nitrogen oxides and volatile organic compounds on the surface of atmospheric particles including oxides, carbonates, soot and mineral dust: Implications for the chemical balance of the troposphere,” *International Reviews in Physical Chemistry*, vol. 20, no. 3, pp. 467–548, 2001. DOI: 10.1080/01442350110051968. [Online]. Available: <https://doi.org/10.1080/01442350110051968>.
- [28] U. Pöschl, Y. Rudich, and M. Ammann, “Kinetic model framework for aerosol and cloud surface chemistry and gas-particle interactions — part 1: General equations, parameters, and terminology,” *Atmospheric Chemistry and Physics*, vol. 7, no. 23, pp. 5989–6023, 2007. DOI: 10.5194/acp-7-5989-2007. [Online]. Available: <https://acp.copernicus.org/articles/7/5989/2007/>.
- [29] T. Xia, M. Kovoichich, and A. Nel, “The role of reactive oxygen species and oxidative stress in mediating particulate matter injury,” en, *Clin Occup Environ Med*, vol. 5, no. 4, pp. 817–836, 2006.
- [30] P. Jain, D. Castellanos-Acuna, S. C. P. Coogan, J. T. Abatzoglou, and M. D. Flannigan, “Observed increases in extreme fire weather driven by atmospheric humidity and temperature,” *Nature Climate Change*, vol. 12, no. 1, pp. 63–70, Jan. 2022, ISSN: 1758-6798. DOI: 10.1038/s41558-021-01224-1. [Online]. Available: <https://doi.org/10.1038/s41558-021-01224-1>.
- [31] A. L. Westerling, “Increasing western us forest wildfire activity: Sensitivity to changes in the timing of spring,” *Philosophical Transactions of the Royal Society B: Biological Sciences*, vol. 371, no. 1696, p. 20150178, 2016. DOI: 10.1098/rstb.2015.0178. [Online]. Available: <https://royalsocietypublishing.org/doi/abs/10.1098/rstb.2015.0178>.
- [32] S. Szopa *et al.*, “Short-lived climate forcers,” in *Climate Change 2021: The Physical Science Basis. Contribution of Working Group I to the Sixth Assessment Report of the Intergovernmental Panel on Climate Change*, V. Masson-Delmotte *et al.*, Eds. Cambridge, United Kingdom and New York, NY, USA: Cambridge University Press, 2021, 817–922. DOI: 10.1017/9781009157896.008.
- [33] “Nasa worldview,” [Online]. Available: <https://worldview.earthdata.nasa.gov/>.
- [34] I. P. on Climate Change, “Anthropogenic and natural radiative forcing,” in *Climate Change 2013 – The Physical Science Basis: Working Group I Contribution to the Fifth Assessment Report of the Intergovernmental Panel on Climate Change*. Cambridge University Press, 2014, 659–740, 923–1055. DOI: 10.1017/CBO9781107415324.018.
- [35] V. Ramanathan and G. Carmichael, “Global and regional climate changes due to black carbon,” *Nature Geoscience*, vol. 1, no. 4, pp. 221–227, Apr. 2008, ISSN: 1752-0908. DOI: 10.1038/ngeo156. [Online]. Available: <https://doi.org/10.1038/ngeo156>.

- [36] R. J. Park, M. J. Kim, J. I. Jeong, D. Youn, and S. Kim, “A contribution of brown carbon aerosol to the aerosol light absorption and its radiative forcing in east asia,” *Atmospheric Environment*, vol. 44, no. 11, pp. 1414–1421, 2010, ISSN: 1352-2310. DOI: <https://doi.org/10.1016/j.atmosenv.2010.01.042>. [Online]. Available: <https://www.sciencedirect.com/science/article/pii/S1352231010001019>.
- [37] Z. Lu *et al.*, “Light absorption properties and radiative effects of primary organic aerosol emissions,” *Environmental Science & Technology*, vol. 49, no. 8, pp. 4868–4877, 2015. DOI: 10.1021/acs.est.5b00211. [Online]. Available: <https://doi.org/10.1021/acs.est.5b00211>.
- [38] I. P. on Climate Change, J. T. Houghton, and W. M. Organization, *IPCC first assessment report*, eng. Geneva: WMO, 1990.
- [39] J. T. Kiehl and B. P. Briegleb, “The relative roles of sulfate aerosols and greenhouse gases in climate forcing,” *Science*, vol. 260, no. 5106, pp. 311–314, 1993. DOI: 10.1126/science.260.5106.311. [Online]. Available: <https://www.science.org/doi/abs/10.1126/science.260.5106.311>.
- [40] S. H. Schneider, “A comment on “climate: The influence of aerosols”,” *Journal of Applied Meteorology and Climatology*, vol. 10, no. 4, pp. 840–841, 1971. DOI: [https://doi.org/10.1175/1520-0450\(1971\)010<0840:ACOTIO>2.0.CO;2](https://doi.org/10.1175/1520-0450(1971)010<0840:ACOTIO>2.0.CO;2). [Online]. Available: https://journals.ametsoc.org/view/journals/apme/10/4/1520-0450_1971_010_0840_acotio_2_0_co_2.xml.
- [41] H. Brown *et al.*, “Biomass burning aerosols in most climate models are too absorbing,” *Nature communications*, vol. 12, no. 1, pp. 1–15, 2021.
- [42] C. E. Stockwell *et al.*, “Nepal ambient monitoring and source testing experiment (namaste): Emissions of trace gases and light-absorbing carbon from wood and dung cooking fires, garbage and crop residue burning, brick kilns, and other sources,” *Atmospheric Chemistry and Physics*, vol. 16, no. 17, pp. 11 043–11 081, 2016. DOI: 10.5194/acp-16-11043-2016. [Online]. Available: <https://acp.copernicus.org/articles/16/11043/2016/>.
- [43] A. Laskin, J. Laskin, and S. A. Nizkorodov, “Chemistry of atmospheric brown carbon,” *Chemical Reviews*, vol. 115, no. 10, pp. 4335–4382, 2015. DOI: 10.1021/cr5006167. [Online]. Available: <https://doi.org/10.1021/cr5006167>.
- [44] M. O. Andreae and A. Gelencsér, “Black carbon or brown carbon? the nature of light-absorbing carbonaceous aerosols,” *Atmospheric Chemistry and Physics*, vol. 6, no. 10, pp. 3131–3148, 2006. DOI: 10.5194/acp-6-3131-2006. [Online]. Available: <https://acp.copernicus.org/articles/6/3131/2006/>.
- [45] N. A. Janssen *et al.*, *Health effects of black carbon*. World Health Organization. Regional Office for Europe, 2012, viii, 86 p.
- [46] J. Hansen, M. Sato, and R. Ruedy, “Radiative forcing and climate response,” *Journal of Geophysical Research: Atmospheres*, vol. 102, no. D6, pp. 6831–6864, 1997. DOI: <https://doi.org/10.1029/96JD03436>. [Online]. Available: <https://agupubs.onlinelibrary.wiley.com/doi/abs/10.1029/96JD03436>.

- [47] T. Novakov and H. Rosen, “The black carbon story: Early history and new perspectives,” en, *Ambio*, vol. 42, no. 7, pp. 840–851, Apr. 2013.
- [48] R. Saleh, “From measurements to models: Toward accurate representation of brown carbon in climate calculations,” *Current Pollution Reports*, vol. 6, no. 2, pp. 90–104, Jun. 2020, ISSN: 2198-6592. DOI: 10.1007/s40726-020-00139-3. [Online]. Available: <https://doi.org/10.1007/s40726-020-00139-3>.
- [49] M. Xie, G. Shen, A. L. Holder, M. D. Hays, and J. J. Jetter, “Light absorption of organic carbon emitted from burning wood, charcoal, and kerosene in household cookstoves,” *Environmental Pollution*, vol. 240, pp. 60–67, 2018, ISSN: 0269-7491. DOI: <https://doi.org/10.1016/j.envpol.2018.04.085>. [Online]. Available: <https://www.sciencedirect.com/science/article/pii/S0269749118303476>.
- [50] Y. Feng, V. Ramanathan, and V. R. Kotamarthi, “Brown carbon: A significant atmospheric absorber of solar radiation?” *Atmospheric Chemistry and Physics*, vol. 13, no. 17, pp. 8607–8621, 2013. DOI: 10.5194/acp-13-8607-2013. [Online]. Available: <https://acp.copernicus.org/articles/13/8607/2013/>.
- [51] Y. Inuma, O. Böge, R. Gräfe, and H. Herrmann, “Methyl-nitrocatechols: Atmospheric tracer compounds for biomass burning secondary organic aerosols,” *Environmental Science & Technology*, vol. 44, no. 22, pp. 8453–8459, 2010. DOI: 10.1021/es102938a. [Online]. Available: <https://doi.org/10.1021/es102938a>.
- [52] K. M. Updyke, T. B. Nguyen, and S. A. Nizkorodov, “Formation of brown carbon via reactions of ammonia with secondary organic aerosols from biogenic and anthropogenic precursors,” *Atmospheric Environment*, vol. 63, pp. 22–31, 2012, ISSN: 1352-2310. DOI: <https://doi.org/10.1016/j.atmosenv.2012.09.012>. [Online]. Available: <https://www.sciencedirect.com/science/article/pii/S1352231012008710>.
- [53] D. O. De Haan *et al.*, “Brown carbon production in ammonium- or amine-containing aerosol particles by reactive uptake of methylglyoxal and photolytic cloud cycling,” *Environmental Science & Technology*, vol. 51, no. 13, pp. 7458–7466, 2017, PMID: 28562016. DOI: 10.1021/acs.est.7b00159. [Online]. Available: <https://doi.org/10.1021/acs.est.7b00159>.
- [54] C. Li *et al.*, “Formation of secondary brown carbon in biomass burning aerosol proxies through no₃ radical reactions,” *Environmental Science & Technology*, vol. 54, no. 3, pp. 1395–1405, 2020, PMID: 31730747. DOI: 10.1021/acs.est.9b05641. [Online]. Available: <https://doi.org/10.1021/acs.est.9b05641>.
- [55] A. K. Y. Lee *et al.*, “Single-particle characterization of biomass burning organic aerosol (bboa): Evidence for non-uniform mixing of high molecular weight organics and potassium,” *Atmospheric Chemistry and Physics*, vol. 16, no. 9, pp. 5561–5572, 2016. DOI: 10.5194/acp-16-5561-2016. [Online]. Available: <https://acp.copernicus.org/articles/16/5561/2016/>.

- [56] R. Suresh, V. Singh, J. Malik, A. Datta, and R. Pal, “Evaluation of the performance of improved biomass cooking stoves with different solid biomass fuel types,” *Biomass and Bioenergy*, vol. 95, pp. 27–34, 2016, ISSN: 0961-9534. DOI: <https://doi.org/10.1016/j.biombioe.2016.08.002>. [Online]. Available: <https://www.sciencedirect.com/science/article/pii/S0961953416302616>.
- [57] M. A. Johnson *et al.*, “Impacts on household fuel consumption from biomass stove programs in india, nepal, and peru,” *Energy for Sustainable Development*, vol. 17, no. 5, pp. 403–411, 2013, ISSN: 0973-0826. DOI: <https://doi.org/10.1016/j.esd.2013.04.004>. [Online]. Available: <https://www.sciencedirect.com/science/article/pii/S0973082613000343>.
- [58] N. M. Donahue, J. H. Kroll, S. N. Pandis, and A. L. Robinson, “A two-dimensional volatility basis set – part 2: Diagnostics of organic-aerosol evolution,” *Atmospheric Chemistry and Physics*, vol. 12, no. 2, pp. 615–634, 2012. DOI: 10.5194/acp-12-615-2012. [Online]. Available: <https://acp.copernicus.org/articles/12/615/2012/>.
- [59] R. Atkinson, “Atmospheric chemistry of vocs and nox,” *Atmospheric Environment*, vol. 34, no. 12, pp. 2063–2101, 2000, ISSN: 1352-2310. DOI: [https://doi.org/10.1016/S1352-2310\(99\)00460-4](https://doi.org/10.1016/S1352-2310(99)00460-4). [Online]. Available: <https://www.sciencedirect.com/science/article/pii/S1352231099004604>.
- [60] R. Atkinson and J. Arey, “Atmospheric degradation of volatile organic compounds,” *Chemical Reviews*, vol. 103, no. 12, pp. 4605–4638, 2003, PMID: 14664626. DOI: 10.1021/cr0206420. [Online]. Available: <https://doi.org/10.1021/cr0206420>.
- [61] B. R. Simoneit, “Biomass burning — a review of organic tracers for smoke from incomplete combustion,” *Applied Geochemistry*, vol. 17, no. 3, pp. 129–162, 2002, ISSN: 0883-2927. DOI: [https://doi.org/10.1016/S0883-2927\(01\)00061-0](https://doi.org/10.1016/S0883-2927(01)00061-0). [Online]. Available: <https://www.sciencedirect.com/science/article/pii/S0883292701000610>.
- [62] R. K. Chakrabarty *et al.*, “Brown carbon aerosols from burning of boreal peatlands: Microphysical properties, emission factors, and implications for direct radiative forcing,” *Atmospheric Chemistry and Physics*, vol. 16, no. 5, pp. 3033–3040, 2016. DOI: 10.5194/acp-16-3033-2016. [Online]. Available: <https://acp.copernicus.org/articles/16/3033/2016/>.
- [63] W. O. Osburn and T. W. Kensler, “Nrf2 signaling: An adaptive response pathway for protection against environmental toxic insults,” *Mutation Research/Reviews in Mutation Research*, vol. 659, no. 1, pp. 31–39, 2008, Proceedings of the 5th International Conference on Environmental Mutagens in Human Populations (ICEMHP), ISSN: 1383-5742. DOI: <https://doi.org/10.1016/j.mrrev.2007.11.006>. [Online]. Available: <https://www.sciencedirect.com/science/article/pii/S1383574207000695>.

- [64] K. M. Venables, “Low molecular weight chemicals, hypersensitivity, and direct toxicity: The acid anhydrides,” *Occupational and Environmental Medicine*, vol. 46, no. 4, pp. 222–232, 1989, ISSN: 0007-1072. DOI: 10.1136/oem.46.4.222. [Online]. Available: <https://oem.bmj.com/content/46/4/222>.
- [65] V. Feron, H. Til, F. de Vrijer, and P. van Bladeren, “Review : Toxicology of volatile organic compounds in indoor air and strategy for further research,” *Indoor Environment*, vol. 1, no. 2, pp. 69–81, 1992. DOI: 10.1177/1420326X9200100204. [Online]. Available: <https://doi.org/10.1177/1420326X9200100204>.
- [66] X. Shen, Y. Zhao, Z. Chen, and D. Huang, “Heterogeneous reactions of volatile organic compounds in the atmosphere,” *Atmospheric Environment*, vol. 68, pp. 297–314, 2013, ISSN: 1352-2310. DOI: <https://doi.org/10.1016/j.atmosenv.2012.11.027>. [Online]. Available: <https://www.sciencedirect.com/science/article/pii/S1352231012010898>.
- [67] M. Claeys *et al.*, “Formation of secondary organic aerosols through photooxidation of isoprene,” *Science*, vol. 303, no. 5661, pp. 1173–1176, 2004. DOI: 10.1126/science.1092805. [Online]. Available: <https://www.science.org/doi/abs/10.1126/science.1092805>.
- [68] Y. Kanaya *et al.*, “Urban photochemistry in central tokyo: 2. rates and regimes of oxidant (o₃ + no₂) production,” *Journal of Geophysical Research: Atmospheres*, vol. 113, no. D6, 2008. DOI: <https://doi.org/10.1029/2007JD008671>. [Online]. Available: <https://agupubs.onlinelibrary.wiley.com/doi/abs/10.1029/2007JD008671>.
- [69] J. Kirkby *et al.*, “Ion-induced nucleation of pure biogenic particles,” *Nature*, vol. 533, no. 7604, pp. 521–526, May 2016.
- [70] J. S. Reid, R. Koppmann, T. F. Eck, and D. P. Eleuterio, “A review of biomass burning emissions part ii: Intensive physical properties of biomass burning particles,” *Atmospheric Chemistry and Physics*, vol. 5, no. 3, pp. 799–825, 2005. DOI: 10.5194/acp-5-799-2005. [Online]. Available: <https://acp.copernicus.org/articles/5/799/2005/>.
- [71] G. Adler, J. M. Flores, A. Abo Riziq, S. Borrmann, and Y. Rudich, “Chemical, physical, and optical evolution of biomass burning aerosols: A case study,” *Atmospheric Chemistry and Physics*, vol. 11, no. 4, pp. 1491–1503, 2011. DOI: 10.5194/acp-11-1491-2011. [Online]. Available: <https://acp.copernicus.org/articles/11/1491/2011/>.
- [72] K. Tsigaridis and M. Kanakidou, “Global modelling of secondary organic aerosol in the troposphere: A sensitivity analysis,” *Atmospheric Chemistry and Physics*, vol. 3, no. 5, pp. 1849–1869, 2003. DOI: 10.5194/acp-3-1849-2003. [Online]. Available: <https://acp.copernicus.org/articles/3/1849/2003/>.

- [73] S. R. Freitas *et al.*, “Monitoring the transport of biomass burning emissions in south america,” *Environmental Fluid Mechanics*, vol. 5, no. 1, pp. 135–167, Apr. 2005, ISSN: 1573-1510. DOI: 10.1007/s10652-005-0243-7. [Online]. Available: <https://doi.org/10.1007/s10652-005-0243-7>.
- [74] R. F. Pueschel *et al.*, “Vertical transport of anthropogenic soot aerosol into the middle atmosphere,” *Journal of Geophysical Research: Atmospheres*, vol. 105, no. D3, pp. 3727–3736, 2000. DOI: <https://doi.org/10.1029/1999JD900505>. [Online]. Available: <https://agupubs.onlinelibrary.wiley.com/doi/abs/10.1029/1999JD900505>.
- [75] M. G. Lawrence and J. Lelieveld, “Atmospheric pollutant outflow from southern asia: A review,” *Atmospheric Chemistry and Physics*, vol. 10, no. 22, pp. 11 017–11 096, 2010. DOI: 10.5194/acp-10-11017-2010. [Online]. Available: <https://acp.copernicus.org/articles/10/11017/2010/>.
- [76] A. F. Stein, R. R. Draxler, G. D. Rolph, B. J. B. Stunder, M. D. Cohen, and F. Ngan, “Noaa’s hysplit atmospheric transport and dispersion modeling system,” *Bulletin of the American Meteorological Society*, vol. 96, no. 12, pp. 2059–2077, 2015. DOI: <https://doi.org/10.1175/BAMS-D-14-00110.1>. [Online]. Available: <https://journals.ametsoc.org/view/journals/bams/96/12/bams-d-14-00110.1.xml>.
- [77] M. Shiraiwa *et al.*, “Global distribution of particle phase state in atmospheric secondary organic aerosols,” *Nature Communications*, vol. 8, no. 1, p. 15 002, Apr. 2017, ISSN: 2041-1723. DOI: 10.1038/ncomms15002. [Online]. Available: <https://doi.org/10.1038/ncomms15002>.
- [78] K. Li, R. Liu, and C. Sun, “Comparison of anaerobic digestion characteristics and kinetics of four livestock manures with different substrate concentrations,” *Bioresourc. Technology*, vol. 198, pp. 133–140, 2015, ISSN: 0960-8524. DOI: <https://doi.org/10.1016/j.biortech.2015.08.151>. [Online]. Available: <https://www.sciencedirect.com/science/article/pii/S0960852415012675>.
- [79] B. R. Simoneit and V. Elias, “Detecting organic tracers from biomass burning in the atmosphere,” *Marine Pollution Bulletin*, vol. 42, no. 10, pp. 805–810, 2001, ISSN: 0025-326X. DOI: [https://doi.org/10.1016/S0025-326X\(01\)00094-7](https://doi.org/10.1016/S0025-326X(01)00094-7). [Online]. Available: <https://www.sciencedirect.com/science/article/pii/S0025326X01000947>.
- [80] L. Ganzeveld and J. Lelieveld, “Dry deposition parameterization in a chemistry general circulation model and its influence on the distribution of reactive trace gases,” *Journal of Geophysical Research: Atmospheres*, vol. 100, no. D10, pp. 20 999–21 012, 1995. DOI: <https://doi.org/10.1029/95JD02266>. [Online]. Available: <https://agupubs.onlinelibrary.wiley.com/doi/abs/10.1029/95JD02266>.

- [81] N. A. Esmen and M. Corn, “Residence time of particles in urban air,” *Atmospheric Environment (1967)*, vol. 5, no. 8, pp. 571–578, 1971, ISSN: 0004-6981. DOI: [https://doi.org/10.1016/0004-6981\(71\)90113-2](https://doi.org/10.1016/0004-6981(71)90113-2). [Online]. Available: <https://www.sciencedirect.com/science/article/pii/0004698171901132>.
- [82] C. Textor *et al.*, “Analysis and quantification of the diversities of aerosol life cycles within aerocom,” *Atmospheric Chemistry and Physics*, vol. 6, no. 7, pp. 1777–1813, 2006. DOI: 10.5194/acp-6-1777-2006. [Online]. Available: <https://acp.copernicus.org/articles/6/1777/2006/>.
- [83] J. Pandey and U. Pandey, “Accumulation of heavy metals in dietary vegetables and cultivated soil horizon in organic farming system in relation to atmospheric deposition in a seasonally dry tropical region of india,” *Environmental Monitoring and Assessment*, vol. 148, no. 1, pp. 61–74, Jan. 2009, ISSN: 1573-2959. DOI: 10.1007/s10661-007-0139-8. [Online]. Available: <https://doi.org/10.1007/s10661-007-0139-8>.
- [84] A. Łukowski, R. Popek, and P. Karolewski, “Particulate matter on foliage of *betula pendula*, *quercus robur*, and *tilia cordata*: Deposition and ecophysiology,” *Environmental Science and Pollution Research*, vol. 27, no. 10, pp. 10 296–10 307, Apr. 2020, ISSN: 1614-7499. DOI: 10.1007/s11356-020-07672-0. [Online]. Available: <https://doi.org/10.1007/s11356-020-07672-0>.
- [85] K. Nicholson, “A review of particle resuspension,” *Atmospheric Environment (1967)*, vol. 22, no. 12, pp. 2639–2651, 1988, ISSN: 0004-6981. DOI: [https://doi.org/10.1016/0004-6981\(88\)90433-7](https://doi.org/10.1016/0004-6981(88)90433-7). [Online]. Available: <https://www.sciencedirect.com/science/article/pii/0004698188904337>.
- [86] M. Possanzini, P. Buttini, and V. Di Palo, “Characterization of a rural area in terms of dry and wet deposition,” *Science of The Total Environment*, vol. 74, pp. 111–120, 1988, ISSN: 0048-9697. DOI: [https://doi.org/10.1016/0048-9697\(88\)90132-5](https://doi.org/10.1016/0048-9697(88)90132-5). [Online]. Available: <https://www.sciencedirect.com/science/article/pii/0048969788901325>.
- [87] L. A. Barrie, “Scavenging ratios, wet deposition, and in-cloud oxidation: An application to the oxides of sulphur and nitrogen,” *Journal of Geophysical Research: Atmospheres*, vol. 90, no. D3, pp. 5789–5799, 1985. DOI: <https://doi.org/10.1029/JD090iD03p05789>. [Online]. Available: <https://agupubs.onlinelibrary.wiley.com/doi/abs/10.1029/JD090iD03p05789>.
- [88] M. Z. Jacobson, “Development of mixed-phase clouds from multiple aerosol size distributions and the effect of the clouds on aerosol removal,” *Journal of Geophysical Research: Atmospheres*, vol. 108, no. D8, 2003. DOI: <https://doi.org/10.1029/2002JD002691>. [Online]. Available: <https://agupubs.onlinelibrary.wiley.com/doi/abs/10.1029/2002JD002691>.
- [89] R. G. Barry and R. J. Chorley, *Atmosphere, weather and climate*, 8th ed. Routledge, 2004, ch. 3-4, pp. 32–89.

- [90] W. Guelle, Y. J. Balkanski, M. Schulz, F. Dulac, and P. Monfray, “Wet deposition in a global size-dependent aerosol transport model: 1. comparison of a 1 year 210pb simulation with ground measurements,” *Journal of Geophysical Research: Atmospheres*, vol. 103, no. D10, pp. 11 429–11 445, 1998. DOI: <https://doi.org/10.1029/97JD03680>. [Online]. Available: <https://agupubs.onlinelibrary.wiley.com/doi/abs/10.1029/97JD03680>.
- [91] L. Iavorivska, E. W. Boyer, and D. R. DeWalle, “Atmospheric deposition of organic carbon via precipitation,” *Atmospheric Environment*, vol. 146, pp. 153–163, 2016, Acid Rain and its Environmental Effects: Recent Scientific Advances, ISSN: 1352-2310. DOI: <https://doi.org/10.1016/j.atmosenv.2016.06.006>. [Online]. Available: <https://www.sciencedirect.com/science/article/pii/S135223101630437X>.
- [92] Y. Pan *et al.*, “Study on dissolved organic carbon in precipitation in northern china,” *Atmospheric Environment*, vol. 44, no. 19, pp. 2350–2357, 2010, ISSN: 1352-2310. DOI: <https://doi.org/10.1016/j.atmosenv.2010.03.033>. [Online]. Available: <https://www.sciencedirect.com/science/article/pii/S1352231010002591>.
- [93] “Construction of a $1^\circ \times 1^\circ$ fossil fuel emission data set for carbonaceous aerosol and implementation and radiative impact in the echam4 model,” *Journal of Geophysical Research: Atmospheres*, vol. 104, no. D18, pp. 22 137–22 162, 1999. DOI: <https://doi.org/10.1029/1999JD900187>. [Online]. Available: <https://agupubs.onlinelibrary.wiley.com/doi/abs/10.1029/1999JD900187>.
- [94] R. J. Park *et al.*, “Export efficiency of black carbon aerosol in continental outflow: Global implications,” *Journal of Geophysical Research: Atmospheres*, vol. 110, no. D11, 2005. DOI: <https://doi.org/10.1029/2004JD005432>. [Online]. Available: <https://agupubs.onlinelibrary.wiley.com/doi/abs/10.1029/2004JD005432>.
- [95] P. S. Tourinho, V. Kočí, S. Loureiro, and C. A. van Gestel, “Partitioning of chemical contaminants to microplastics: Sorption mechanisms, environmental distribution and effects on toxicity and bioaccumulation,” *Environmental Pollution*, vol. 252, pp. 1246–1256, 2019, ISSN: 0269-7491. DOI: <https://doi.org/10.1016/j.envpol.2019.06.030>. [Online]. Available: <https://www.sciencedirect.com/science/article/pii/S0269749118356744>.
- [96] J. F. Pankow, “An absorption model of gas/particle partitioning of organic compounds in the atmosphere,” *Atmospheric Environment*, vol. 28, no. 2, pp. 185–188, 1994, ISSN: 1352-2310. DOI: [https://doi.org/10.1016/1352-2310\(94\)90093-0](https://doi.org/10.1016/1352-2310(94)90093-0). [Online]. Available: <https://www.sciencedirect.com/science/article/pii/S1352231094900930>.
- [97] G. Rao and E. P. Vejerano, “Partitioning of volatile organic compounds to aerosols: A review,” *Chemosphere*, vol. 212, pp. 282–296, 2018, ISSN: 0045-6535. DOI: <https://doi.org/10.1016/j.chemosphere.2018.08.073>. [Online]. Available: <https://www.sciencedirect.com/science/article/pii/S0045653518315534>.

- [98] N. M. Donahue, S. A. Epstein, S. N. Pandis, and A. L. Robinson, “A two-dimensional volatility basis set: 1. organic-aerosol mixing thermodynamics,” *Atmospheric Chemistry and Physics*, vol. 11, no. 7, pp. 3303–3318, 2011. DOI: 10.5194/acp-11-3303-2011. [Online]. Available: <https://acp.copernicus.org/articles/11/3303/2011/>.
- [99] D. Mackay and P. J. Leinonen, “Rate of evaporation of low-solubility contaminants from water bodies to atmosphere,” *Environmental Science & Technology*, vol. 9, no. 13, pp. 1178–1180, 1975. DOI: 10.1021/es60111a012. [Online]. Available: <https://doi.org/10.1021/es60111a012>.
- [100] A. Neftel, A. Blatter, R. Hesterberg, and T. Staffelbach, “Measurements of concentration gradients of hno₂ and hno₃ over a semi-natural ecosystem,” *Atmospheric Environment*, vol. 30, no. 17, pp. 3017–3025, 1996, ISSN: 1352-2310. DOI: [https://doi.org/10.1016/1352-2310\(96\)00011-8](https://doi.org/10.1016/1352-2310(96)00011-8). [Online]. Available: <https://www.sciencedirect.com/science/article/pii/S1352231096000118>.
- [101] J. W. Telford and S. K. Chai, “A new aspect of condensation theory,” *pure and applied geophysics*, vol. 118, no. 2, pp. 720–742, Sep. 1980, ISSN: 1420-9136. DOI: 10.1007/BF01593025. [Online]. Available: <https://doi.org/10.1007/BF01593025>.
- [102] T. Novakov and J. E. Penner, “Large contribution of organic aerosols to cloud-condensation-nuclei concentrations,” *Nature*, vol. 365, no. 6449, pp. 823–826, Oct. 1993, ISSN: 1476-4687. DOI: 10.1038/365823a0. [Online]. Available: <https://doi.org/10.1038/365823a0>.
- [103] K. Hämeri *et al.*, “Hygroscopic and ccn properties of aerosol particles in boreal forests,” *Tellus B: Chemical and Physical Meteorology*, vol. 53, no. 4, pp. 359–379, 2001. DOI: 10.3402/tellusb.v53i4.16609. [Online]. Available: <https://doi.org/10.3402/tellusb.v53i4.16609>.
- [104] K. A. Koehler *et al.*, “Cloud condensation nuclei and ice nucleation activity of hydrophobic and hydrophilic soot particles,” *Phys. Chem. Chem. Phys.*, vol. 11, pp. 7906–7920, 36 2009. DOI: 10.1039/B905334B. [Online]. Available: <http://dx.doi.org/10.1039/B905334B>.
- [105] L. Brégonzio-Rozier *et al.*, “Secondary organic aerosol formation from isoprene photooxidation during cloud condensation–evaporation cycles,” *Atmospheric Chemistry and Physics*, vol. 16, no. 3, pp. 1747–1760, 2016. DOI: 10.5194/acp-16-1747-2016. [Online]. Available: <https://acp.copernicus.org/articles/16/1747/2016/>.
- [106] J. H. Kroll and J. H. Seinfeld, “Chemistry of secondary organic aerosol: Formation and evolution of low-volatility organics in the atmosphere,” *Atmospheric Environment*, vol. 42, no. 16, pp. 3593–3624, 2008, ISSN: 1352-2310. DOI: <https://doi.org/10.1016/j.atmosenv.2008.01.003>. [Online]. Available: <https://www.sciencedirect.com/science/article/pii/S1352231008000253>.

- [107] A. T. Ahern *et al.*, “Production of secondary organic aerosol during aging of biomass burning smoke from fresh fuels and its relationship to voc precursors,” *Journal of Geophysical Research: Atmospheres*, vol. 124, no. 6, pp. 3583–3606, 2019. DOI: <https://doi.org/10.1029/2018JD029068>. [Online]. Available: <https://agupubs.onlinelibrary.wiley.com/doi/abs/10.1029/2018JD029068>.
- [108] J. M. Delgado-Saborit, M. S. Alam, K. J. Godri Pollitt, C. Stark, and R. M. Harrison, “Analysis of atmospheric concentrations of quinones and polycyclic aromatic hydrocarbons in vapour and particulate phases,” *Atmospheric Environment*, vol. 77, pp. 974–982, 2013, ISSN: 1352-2310. DOI: <https://doi.org/10.1016/j.atmosenv.2013.05.080>. [Online]. Available: <https://www.sciencedirect.com/science/article/pii/S1352231013004536>.
- [109] P. Lin, L. T. Fleming, S. A. Nizkorodov, J. Laskin, and A. Laskin, “Comprehensive molecular characterization of atmospheric brown carbon by high resolution mass spectrometry with electrospray and atmospheric pressure photoionization,” *Analytical Chemistry*, vol. 90, no. 21, pp. 12 493–12 502, 2018. DOI: 10.1021/acs.analchem.8b02177. [Online]. Available: <https://doi.org/10.1021/acs.analchem.8b02177>.
- [110] V. Samburova *et al.*, “Polycyclic aromatic hydrocarbons in biomass-burning emissions and their contribution to light absorption and aerosol toxicity,” *Science of The Total Environment*, vol. 568, pp. 391–401, 2016, ISSN: 0048-9697. DOI: <https://doi.org/10.1016/j.scitotenv.2016.06.026>. [Online]. Available: <https://www.sciencedirect.com/science/article/pii/S0048969716311974>.
- [111] T. Jokinen *et al.*, “Production of extremely low volatile organic compounds from biogenic emissions: Measured yields and atmospheric implications,” *Proceedings of the National Academy of Sciences*, vol. 112, no. 23, pp. 7123–7128, 2015. DOI: 10.1073/pnas.1423977112. [Online]. Available: <https://www.pnas.org/doi/abs/10.1073/pnas.1423977112>.
- [112] S. Yu, “Role of organic acids (formic, acetic, pyruvic and oxalic) in the formation of cloud condensation nuclei (ccn): A review,” *Atmospheric Research*, vol. 53, no. 4, pp. 185–217, 2000, ISSN: 0169-8095. DOI: [https://doi.org/10.1016/S0169-8095\(00\)00037-5](https://doi.org/10.1016/S0169-8095(00)00037-5). [Online]. Available: <https://www.sciencedirect.com/science/article/pii/S0169809500000375>.
- [113] J. P. Reid *et al.*, “The viscosity of atmospherically relevant organic particles,” *Nature Communications*, vol. 9, no. 1, p. 956, Mar. 2018, ISSN: 2041-1723. DOI: 10.1038/s41467-018-03027-z. [Online]. Available: <https://doi.org/10.1038/s41467-018-03027-z>.
- [114] E. Saukko, H. Kuuluvainen, and A. Virtanen, “A method to resolve the phase state of aerosol particles,” *Atmospheric Measurement Techniques*, vol. 5, no. 1, pp. 259–265, 2012. DOI: 10.5194/amt-5-259-2012. [Online]. Available: <https://amt.copernicus.org/articles/5/259/2012/>.

- [115] L. Renbaum-Wolff *et al.*, “Observations and implications of liquid–liquid phase separation at high relative humidities in secondary organic material produced by α -pinene ozonolysis without inorganic salts,” *Atmospheric Chemistry and Physics*, vol. 16, no. 12, pp. 7969–7979, 2016. DOI: 10.5194/acp-16-7969-2016. [Online]. Available: <https://acp.copernicus.org/articles/16/7969/2016/>.
- [116] Y. Zhang *et al.*, “Effect of the aerosol-phase state on secondary organic aerosol formation from the reactive uptake of isoprene-derived epoxydiols (iepoxy),” *Environmental Science & Technology Letters*, vol. 5, no. 3, pp. 167–174, 2018. DOI: 10.1021/acs.estlett.8b00044. [Online]. Available: <https://doi.org/10.1021/acs.estlett.8b00044>.
- [117] J. Li, S. M. Forrester, and D. A. Knopf, “Heterogeneous oxidation of amorphous organic aerosol surrogates by O_3 , NO_3 , and oh, at typical tropospheric temperatures,” *Atmospheric Chemistry and Physics*, vol. 20, no. 10, pp. 6055–6080, 2020. DOI: 10.5194/acp-20-6055-2020. [Online]. Available: <https://acp.copernicus.org/articles/20/6055/2020/>.
- [118] A. M. Arangio, J. H. Slade, T. Berkemeier, U. Pöschl, D. A. Knopf, and M. Shiraiwa, “Multiphase chemical kinetics of oh radical uptake by molecular organic markers of biomass burning aerosols: Humidity and temperature dependence, surface reaction, and bulk diffusion,” *The Journal of Physical Chemistry A*, vol. 119, no. 19, pp. 4533–4544, 2015, PMID: 25686209. DOI: 10.1021/jp510489z. [Online]. Available: <https://doi.org/10.1021/jp510489z>.
- [119] S. Madronich, “Photodissociation in the atmosphere: 1. actinic flux and the effects of ground reflections and clouds,” *Journal of Geophysical Research: Atmospheres*, vol. 92, no. D8, pp. 9740–9752, 1987. DOI: <https://doi.org/10.1029/JD092iD08p09740>. [Online]. Available: <https://agupubs.onlinelibrary.wiley.com/doi/abs/10.1029/JD092iD08p09740>.
- [120] Y. Matsumi and M. Kawasaki, “Photolysis of atmospheric ozone in the ultraviolet region,” *Chemical Reviews*, vol. 103, no. 12, pp. 4767–4782, 2003, PMID: 14664632. DOI: 10.1021/cr0205255. [Online]. Available: <https://doi.org/10.1021/cr0205255>.
- [121] T. Staffelbach, A. Neftel, B. Stauffer, and D. Jacob, “A record of the atmospheric methane sink from formaldehyde in polar ice cores,” *Nature*, vol. 349, no. 6310, pp. 603–605, Feb. 1991, ISSN: 1476-4687. DOI: 10.1038/349603a0. [Online]. Available: <https://doi.org/10.1038/349603a0>.
- [122] B. Rappenglück, P. K. Dasgupta, M. Leuchner, Q. Li, and W. Luke, “Formaldehyde and its relation to co, pan, and so₂ in the houston-galveston airshed,” *Atmospheric Chemistry and Physics*, vol. 10, no. 5, pp. 2413–2424, 2010. DOI: 10.5194/acp-10-2413-2010. [Online]. Available: <https://acp.copernicus.org/articles/10/2413/2010/>.

- [123] P. Lin, N. Bluvshstein, Y. Rudich, S. A. Nizkorodov, J. Laskin, and A. Laskin, "Molecular chemistry of atmospheric brown carbon inferred from a nationwide biomass burning event," *Environmental Science & Technology*, vol. 51, no. 20, pp. 11 561–11 570, 2017. DOI: 10.1021/acs.est.7b02276. [Online]. Available: <https://doi.org/10.1021/acs.est.7b02276>.
- [124] L. T. Fleming *et al.*, "Molecular composition and photochemical lifetimes of brown carbon chromophores in biomass burning organic aerosol," *Atmospheric Chemistry and Physics*, vol. 20, no. 2, pp. 1105–1129, 2020. DOI: 10.5194/acp-20-1105-2020. [Online]. Available: <https://acp.copernicus.org/articles/20/1105/2020/>.
- [125] C. F. Fortenberry, M. J. Walker, Y. Zhang, D. Mitroo, W. H. Brune, and B. J. Williams, "Bulk and molecular-level characterization of laboratory-aged biomass burning organic aerosol from oak leaf and heartwood fuels," *Atmospheric Chemistry and Physics*, vol. 18, no. 3, pp. 2199–2224, 2018. DOI: 10.5194/acp-18-2199-2018. [Online]. Available: <https://acp.copernicus.org/articles/18/2199/2018/>.
- [126] J. Clayden, N. Greeves, and S. Warren, *Organic chemistry*. Oxford university press, 2012, pp. 107–124,427–447.
- [127] H. B. Burgi, J. D. Dunitz, and E. Shefter, "Geometrical reaction coordinates. ii. nucleophilic addition to a carbonyl group," *Journal of the American Chemical Society*, vol. 95, no. 15, pp. 5065–5067, 1973. DOI: 10.1021/ja00796a058. [Online]. Available: <https://doi.org/10.1021/ja00796a058>.
- [128] H. Nemoto, T. Kawamura, and N. Miyoshi, "A highly efficient carbon-carbon bond formation reaction via nucleophilic addition to n-alkylaldimines without acids or metallic species," *Journal of the American Chemical Society*, vol. 127, no. 42, pp. 14 546–14 547, 2005, PMID: 16231887. DOI: 10.1021/ja054010h. [Online]. Available: <https://doi.org/10.1021/ja054010h>.
- [129] V Grignard, "Mixed organomagnesium combinations and their application in acid, alcohol, and hydrocarbon synthesis," *Ann. Chim*, vol. 24, pp. 433–490, 1901.
- [130] J. Y. Chen, H. Jiang, S. J. Chen, C. Cullen, C. M. S. Ahmed, and Y.-H. Lin, "Characterization of electrophilicity and oxidative potential of atmospheric carbonyls," *Environ. Sci.: Processes Impacts*, vol. 21, pp. 856–866, 5 2019. DOI: 10.1039/C9EM00033J. [Online]. Available: <http://dx.doi.org/10.1039/C9EM00033J>.
- [131] J. L. Axson, K. Takahashi, D. O. D. Haan, and V. Vaida, "Gas-phase water-mediated equilibrium between methylglyoxal and its geminal diol," *Proceedings of the National Academy of Sciences*, vol. 107, no. 15, pp. 6687–6692, 2010. DOI: 10.1073/pnas.0912121107. [Online]. Available: <https://www.pnas.org/doi/abs/10.1073/pnas.0912121107>.

- [132] J. D. Rindelaub *et al.*, “The acid-catalyzed hydrolysis of an α -pinene-derived organic nitrate: Kinetics, products, reaction mechanisms, and atmospheric impact,” *Atmospheric Chemistry and Physics*, vol. 16, no. 23, pp. 15 425–15 432, 2016. DOI: 10.5194/acp-16-15425-2016. [Online]. Available: <https://acp.copernicus.org/articles/16/15425/2016/>.
- [133] M. Takeuchi and N. L. Ng, “Chemical composition and hydrolysis of organic nitrate aerosol formed from hydroxyl and nitrate radical oxidation of α -pinene and β -pinene,” *Atmospheric Chemistry and Physics*, vol. 19, no. 19, pp. 12 749–12 766, 2019. DOI: 10.5194/acp-19-12749-2019. [Online]. Available: <https://acp.copernicus.org/articles/19/12749/2019/>.
- [134] M. N. Chan *et al.*, “Influence of aerosol acidity on the chemical composition of secondary organic aerosol from β -caryophyllene,” *Atmospheric Chemistry and Physics*, vol. 11, no. 4, pp. 1735–1751, 2011. DOI: 10.5194/acp-11-1735-2011. [Online]. Available: <https://acp.copernicus.org/articles/11/1735/2011/>.
- [135] D. J. Jacob and S. C. Wofsy, “Photochemical production of carboxylic acids in a remote continental atmosphere,” in *Acid Deposition at High Elevation Sites*, M. H. Unsworth and D. Fowler, Eds. Dordrecht: Springer Netherlands, 1988, pp. 73–92, ISBN: 978-94-009-3079-7. DOI: 10.1007/978-94-009-3079-7_3. [Online]. Available: https://doi.org/10.1007/978-94-009-3079-7_3.
- [136] K. K. Crahan, D. Hegg, D. S. Covert, and H. Jonsson, “An exploration of aqueous oxalic acid production in the coastal marine atmosphere,” *Atmospheric Environment*, vol. 38, no. 23, pp. 3757–3764, 2004, ISSN: 1352-2310. DOI: <https://doi.org/10.1016/j.atmosenv.2004.04.009>. [Online]. Available: <https://www.sciencedirect.com/science/article/pii/S1352231004003693>.
- [137] Z. C. J. Decker *et al.*, “Novel analysis to quantify plume crosswind heterogeneity applied to biomass burning smoke,” *Environmental Science & Technology*, vol. 55, no. 23, pp. 15 646–15 657, 2021, PMID: 34817984. DOI: 10.1021/acs.est.1c03803. [Online]. Available: <https://doi.org/10.1021/acs.est.1c03803>.
- [138] E. A. Bruns *et al.*, “Characterization of gas-phase organics using proton transfer reaction time-of-flight mass spectrometry: Fresh and aged residential wood combustion emissions,” *Atmospheric Chemistry and Physics*, vol. 17, no. 1, pp. 705–720, 2017. DOI: 10.5194/acp-17-705-2017. [Online]. Available: <https://acp.copernicus.org/articles/17/705/2017/>.
- [139] A. W. H. Chan *et al.*, “Secondary organic aerosol formation from photooxidation of naphthalene and alkylnaphthalenes: Implications for oxidation of intermediate volatility organic compounds (ivocs),” *Atmospheric Chemistry and Physics*, vol. 9, no. 9, pp. 3049–3060, 2009. DOI: 10.5194/acp-9-3049-2009. [Online]. Available: <https://acp.copernicus.org/articles/9/3049/2009/>.
- [140] L. Zhang, Z. Wang, W. Zhang, Y. Liang, and Q. Shi, “Determination of anhydride in atmospheric fine particles by optimized solvent extraction,” *Atmospheric Environment*, vol. 285, p. 119 249, 2022, ISSN: 1352-2310. DOI: <https://doi.org/10.1016/j.atmosenv.2022.119249>.

//doi.org/10.1016/j.atmosenv.2022.119249. [Online]. Available: <https://www.sciencedirect.com/science/article/pii/S1352231022003144>.

- [141] Y. Iinuma *et al.*, “Source characterization of biomass burning particles: The combustion of selected european conifers, african hardwood, savanna grass, and german and indonesian peat,” *Journal of Geophysical Research: Atmospheres*, vol. 112, no. D8, 2007. DOI: <https://doi.org/10.1029/2006JD007120>. [Online]. Available: <https://agupubs.onlinelibrary.wiley.com/doi/abs/10.1029/2006JD007120>.
- [142] P. L. Cooper and J. P. D. Abbatt, “Heterogeneous interactions of oh and ho₂ radicals with surfaces characteristic of atmospheric particulate matter,” *The Journal of Physical Chemistry*, vol. 100, no. 6, pp. 2249–2254, 1996. DOI: 10.1021/jp952142z. [Online]. Available: <https://doi.org/10.1021/jp952142z>.
- [143] T. Moise and Y. Rudich, “Reactive uptake of ozone by proxies for organic aerosols: Surface versus bulk processes,” *Journal of Geophysical Research: Atmospheres*, vol. 105, no. D11, pp. 14 667–14 676, 2000. DOI: <https://doi.org/10.1029/2000JD900071>. [Online]. Available: <https://agupubs.onlinelibrary.wiley.com/doi/abs/10.1029/2000JD900071>.
- [144] J. D. Hearn and G. D. Smith, “Kinetics and product studies for ozonolysis reactions of organic particles using aerosol cims,” *The Journal of Physical Chemistry A*, vol. 108, no. 45, pp. 10 019–10 029, 2004. DOI: 10.1021/jp0404145. [Online]. Available: <https://doi.org/10.1021/jp0404145>.
- [145] L. Lee and K. Wilson, “The reactive–diffusive length of oh and ozone in model organic aerosols,” *The Journal of Physical Chemistry A*, vol. 120, no. 34, pp. 6800–6812, 2016, PMID: 27509443. DOI: 10.1021/acs.jpca.6b05285. [Online]. Available: <https://doi.org/10.1021/acs.jpca.6b05285>.
- [146] M. M. Galloway *et al.*, “Analysis of photochemical and dark glyoxal uptake: Implications for soa formation,” *Geophysical Research Letters*, vol. 38, no. 17, 2011. DOI: <https://doi.org/10.1029/2011GL048514>. [Online]. Available: <https://agupubs.onlinelibrary.wiley.com/doi/abs/10.1029/2011GL048514>.
- [147] A. Indarto, “Heterogeneous reactions of hono formation from no₂ and hno₃: A review,” *Research on Chemical Intermediates*, vol. 38, no. 3, pp. 1029–1041, Mar. 2012, ISSN: 1568-5675. DOI: 10.1007/s11164-011-0439-z. [Online]. Available: <https://doi.org/10.1007/s11164-011-0439-z>.
- [148] J. Lobert and J Warnatz, “Emissions from the combustion process in vegetation,” *Fire in the Environment*, vol. 13, pp. 15–37, 1993.
- [149] I. A. of Fire Chiefs, “Basic fire science,” in *Fire investigator: Principles and practice to NFPA 921 and 1033*, 5th ed. Jones and Bartlett Learning, 2018, 21–61.
- [150] A. Thygesen, J. Oddershede, H. Lilholt, A. Bjerre, and K. Ståhl, “On the determination of crystallinity and cellulose content in plant fibres,” *Cellulose*, vol. 12, pp. 563–576, Dec. 2005. DOI: 10.1007/s10570-005-9001-8.

- [151] A. L. Sullivan, “Inside the inferno: Fundamental processes of wildland fire behaviour,” *Current Forestry Reports*, vol. 3, no. 2, pp. 132–149, Jun. 2017, ISSN: 2198-6436. DOI: 10.1007/s40725-017-0057-0. [Online]. Available: <https://doi.org/10.1007/s40725-017-0057-0>.
- [152] J. M. Lobert, D. H. Scharffe, W. M. Hao, and P. J. Crutzen, “Importance of biomass burning in the atmospheric budgets of nitrogen-containing gases,” *Nature*, vol. 346, no. 6284, pp. 552–554, Aug. 1990, ISSN: 1476-4687. DOI: 10.1038/346552a0. [Online]. Available: <https://doi.org/10.1038/346552a0>.
- [153] A. P. Sullivan *et al.*, “Biomass burning markers and residential burning in the winter aircraft campaign,” *Journal of Geophysical Research: Atmospheres*, vol. 124, no. 3, pp. 1846–1861, 2019. DOI: <https://doi.org/10.1029/2017JD028153>. [Online]. Available: <https://agupubs.onlinelibrary.wiley.com/doi/abs/10.1029/2017JD028153>.
- [154] M. O. Andreae, “Biomass burning-its history, use, and distribution and its impact on environmental quality and global climate,” in *Global biomass burning- Atmospheric, climatic, and biospheric implications*, 1991.
- [155] S. K. Akagi *et al.*, “Emission factors for open and domestic biomass burning for use in atmospheric models,” *Atmospheric Chemistry and Physics*, vol. 11, no. 9, pp. 4039–4072, 2011. DOI: 10.5194/acp-11-4039-2011. [Online]. Available: <https://acp.copernicus.org/articles/11/4039/2011/>.
- [156] S. P. Urbanski, “Combustion efficiency and emission factors for wildfire-season fires in mixed conifer forests of the northern rocky mountains, us,” *Atmospheric Chemistry and Physics*, vol. 13, no. 14, pp. 7241–7262, 2013. DOI: 10.5194/acp-13-7241-2013. [Online]. Available: <https://acp.copernicus.org/articles/13/7241/2013/>.
- [157] B. Rooney *et al.*, “Impacts of household sources on air pollution at village and regional scales in india,” *Atmospheric Chemistry and Physics*, vol. 19, no. 11, pp. 7719–7742, 2019. DOI: 10.5194/acp-19-7719-2019. [Online]. Available: <https://acp.copernicus.org/articles/19/7719/2019/>.
- [158] A. L. Hodshire *et al.*, “Aging effects on biomass burning aerosol mass and composition: A critical review of field and laboratory studies,” *Environmental Science & Technology*, vol. 53, no. 17, pp. 10 007–10 022, 2019. DOI: 10.1021/acs.est.9b02588. [Online]. Available: <https://doi.org/10.1021/acs.est.9b02588>.
- [159] Y. H. Kim *et al.*, “Mutagenicity and lung toxicity of smoldering vs. flaming emissions from various biomass fuels: Implications for health effects from wild-land fires,” *Environmental Health Perspectives*, vol. 126, no. 1, p. 017011, 2018. DOI: 10.1289/EHP2200. [Online]. Available: <https://ehp.niehs.nih.gov/doi/abs/10.1289/EHP2200>.

- [160] Y. H. Kim *et al.*, “The role of fuel type and combustion phase on the toxicity of biomass smoke following inhalation exposure in mice,” *Archives of Toxicology*, vol. 93, no. 6, pp. 1501–1513, Jun. 2019, ISSN: 1432-0738. DOI: 10.1007/s00204-019-02450-5. [Online]. Available: <https://doi.org/10.1007/s00204-019-02450-5>.
- [161] Z. C. J. Decker *et al.*, “Nighttime chemical transformation in biomass burning plumes: A box model analysis initialized with aircraft observations,” *Environmental Science & Technology*, vol. 53, no. 5, pp. 2529–2538, 2019, PMID: 30698424. DOI: 10.1021/acs.est.8b05359. [Online]. Available: <https://doi.org/10.1021/acs.est.8b05359>.
- [162] A. Hecobian *et al.*, “Comparison of chemical characteristics of 495 biomass burning plumes intercepted by the nasa dc-8 aircraft during the arctas/carb-2008 field campaign,” *Atmospheric Chemistry and Physics*, vol. 11, no. 24, pp. 13 325–13 337, 2011. DOI: 10.5194/acp-11-13325-2011. [Online]. Available: <https://acp.copernicus.org/articles/11/13325/2011/>.
- [163] D. J. Jacob *et al.*, “The arctic research of the composition of the troposphere from aircraft and satellites (arctas) mission: Design, execution, and first results,” *Atmospheric Chemistry and Physics*, vol. 10, no. 11, pp. 5191–5212, 2010. DOI: 10.5194/acp-10-5191-2010. [Online]. Available: <https://acp.copernicus.org/articles/10/5191/2010/>.
- [164] M. Müller *et al.*, “In situ measurements and modeling of reactive trace gases in a small biomass burning plume,” *Atmospheric Chemistry and Physics*, vol. 16, no. 6, pp. 3813–3824, 2016. DOI: 10.5194/acp-16-3813-2016. [Online]. Available: <https://acp.copernicus.org/articles/16/3813/2016/>.
- [165] J. Tian *et al.*, “A biomass combustion chamber: Design, evaluation, and a case study of wheat straw combustion emission tests,” *Aerosol and Air Quality Research*, vol. 15, no. 5, pp. 2104–2114, 2015. DOI: 10.4209/aaqr.2015.03.0167. [Online]. Available: <https://doi.org/10.4209/aaqr.2015.03.0167>.
- [166] C. D. McClure, C. Y. Lim, D. H. Hagan, J. H. Kroll, and C. D. Cappa, “Biomass-burning-derived particles from a wide variety of fuels – part 1: Properties of primary particles,” *Atmospheric Chemistry and Physics*, vol. 20, no. 3, pp. 1531–1547, 2020. DOI: 10.5194/acp-20-1531-2020. [Online]. Available: <https://acp.copernicus.org/articles/20/1531/2020/>.
- [167] L. E. Hatch, A. Rivas-Ubach, C. N. Jen, M. Lipton, A. H. Goldstein, and K. C. Barsanti, “Measurements of i/svocs in biomass-burning smoke using solid-phase extraction disks and two-dimensional gas chromatography,” *Atmospheric Chemistry and Physics*, vol. 18, no. 24, pp. 17 801–17 817, 2018. DOI: 10.5194/acp-18-17801-2018. [Online]. Available: <https://acp.copernicus.org/articles/18/17801/2018/>.

- [168] R. P. Pokhrel, J. Gordon, M. N. Fiddler, and S. Bililign, “Determination of emission factors of pollutants from biomass burning of african fuels in laboratory measurements,” *Journal of Geophysical Research: Atmospheres*, vol. 126, no. 20, e2021JD034731, 2021, e2021JD034731 2021JD034731. DOI: <https://doi.org/10.1029/2021JD034731>. [Online]. Available: <https://agupubs.onlinelibrary.wiley.com/doi/abs/10.1029/2021JD034731>.
- [169] E. Sarpong, D. Smith, R. Pokhrel, M. N. Fiddler, and S. Bililign, “Refractive indices of biomass burning aerosols obtained from african biomass fuels using rdg approximation,” *Atmosphere*, vol. 11, no. 1, 2020, ISSN: 2073-4433. DOI: 10.3390/atmos11010062. [Online]. Available: <https://www.mdpi.com/2073-4433/11/1/62>.
- [170] R. P. Pokhrel, J. Gordon, M. N. Fiddler, and S. Bililign, “Impact of combustion conditions on physical and morphological properties of biomass burning aerosol,” *Aerosol Science and Technology*, vol. 55, no. 1, pp. 80–91, 2021. DOI: 10.1080/02786826.2020.1822512. [Online]. Available: <https://doi.org/10.1080/02786826.2020.1822512>.
- [171] R. J. Yokelson, T. J. Christian, T. G. Karl, and A. Guenther, “The tropical forest and fire emissions experiment: Laboratory fire measurements and synthesis of campaign data,” *Atmospheric Chemistry and Physics*, vol. 8, no. 13, pp. 3509–3527, 2008. DOI: 10.5194/acp-8-3509-2008. [Online]. Available: <https://acp.copernicus.org/articles/8/3509/2008/>.
- [172] M. F. S. Laboratory, “Experimental fire studied in the fire lab’s combustion chamber,” [Online]. Available: <https://firelab.org/image-gallery>.
- [173] M. Fawaz, A. Avery, T. B. Onasch, L. R. Williams, and T. C. Bond, “Technical note: Pyrolysis principles explain time-resolved organic aerosol release from biomass burning,” *Atmospheric Chemistry and Physics*, vol. 21, no. 20, pp. 15 605–15 618, 2021. DOI: 10.5194/acp-21-15605-2021. [Online]. Available: <https://acp.copernicus.org/articles/21/15605/2021/>.
- [174] S. JIMÉNEZ and J. BALLESTER, “Particulate matter formation and emission in the combustion of different pulverized biomass fuels,” *Combustion Science and Technology*, vol. 178, no. 4, pp. 655–683, 2006. DOI: 10.1080/00102200500241248. [Online]. Available: <https://doi.org/10.1080/00102200500241248>.
- [175] S. Jiménez and J. Ballester, “Formation of alkali sulphate aerosols in biomass combustion,” *Fuel*, vol. 86, no. 4, pp. 486–493, 2007, ISSN: 0016-2361. DOI: <https://doi.org/10.1016/j.fuel.2006.08.005>. [Online]. Available: <https://www.sciencedirect.com/science/article/pii/S0016236106003127>.
- [176] S. Jennings, “The mean free path in air,” *Journal of Aerosol Science*, vol. 19, no. 2, pp. 159–166, 1988, ISSN: 0021-8502. DOI: [https://doi.org/10.1016/0021-8502\(88\)90219-4](https://doi.org/10.1016/0021-8502(88)90219-4). [Online]. Available: <https://www.sciencedirect.com/science/article/pii/0021850288902194>.

- [177] S.-H. Hong and J. Winter, “Size dependence of optical properties and internal structure of plasma grown carbonaceous nanoparticles studied by in situ Rayleigh-Mie scattering ellipsometry,” *Journal of Applied Physics*, vol. 100, no. 6, Sep. 2006, 064303, ISSN: 0021-8979. DOI: 10.1063/1.2338132. [Online]. Available: <https://doi.org/10.1063/1.2338132>.
- [178] R. G. Pinnick, J. M. Rosen, and D. J. Hofmann, “Measured light-scattering properties of individual aerosol particles compared to mie scattering theory,” *Appl. Opt.*, vol. 12, no. 1, pp. 37–41, Jan. 1973. DOI: 10.1364/AO.12.000037. [Online]. Available: <https://opg.optica.org/ao/abstract.cfm?URI=ao-12-1-37>.
- [179] I. Tegen and A. A. Lacis, “Modeling of particle size distribution and its influence on the radiative properties of mineral dust aerosol,” *Journal of Geophysical Research: Atmospheres*, vol. 101, no. D14, pp. 19 237–19 244, 1996. DOI: <https://doi.org/10.1029/95JD03610>. [Online]. Available: <https://agupubs.onlinelibrary.wiley.com/doi/abs/10.1029/95JD03610>.
- [180] S.-S. Park, S. Y. Sim, M.-S. Bae, and J. J. Schauer, “Size distribution of water-soluble components in particulate matter emitted from biomass burning,” *Atmospheric Environment*, vol. 73, pp. 62–72, 2013, ISSN: 1352-2310. DOI: <https://doi.org/10.1016/j.atmosenv.2013.03.025>. [Online]. Available: <https://www.sciencedirect.com/science/article/pii/S135223101300201X>.
- [181] P. J. Silva, D.-Y. Liu, C. A. Noble, and K. A. Prather, “Size and chemical characterization of individual particles resulting from biomass burning of local southern california species,” *Environmental Science & Technology*, vol. 33, no. 18, pp. 3068–3076, 1999. DOI: 10.1021/es980544p. [Online]. Available: <https://doi.org/10.1021/es980544p>.
- [182] J. Rissler *et al.*, “Size distribution and hygroscopic properties of aerosol particles from dry-season biomass burning in amazonia,” *Atmospheric Chemistry and Physics*, vol. 6, no. 2, pp. 471–491, 2006. DOI: 10.5194/acp-6-471-2006. [Online]. Available: <https://acp.copernicus.org/articles/6/471/2006/>.
- [183] P. A. Baron, “Calibration and use of the aerodynamic particle sizer (aps 3300),” *Aerosol Science and Technology*, vol. 5, no. 1, pp. 55–67, 1986. DOI: 10.1080/02786828608959076. [Online]. Available: <https://doi.org/10.1080/02786828608959076>.
- [184] T. M. Peters and D. Leith, “Concentration measurement and counting efficiency of the aerodynamic particle sizer 3321,” *Journal of Aerosol Science*, vol. 34, no. 5, pp. 627–634, 2003, ISSN: 0021-8502. DOI: [https://doi.org/10.1016/S0021-8502\(03\)00030-2](https://doi.org/10.1016/S0021-8502(03)00030-2). [Online]. Available: <https://www.sciencedirect.com/science/article/pii/S0021850203000302>.
- [185] C. Sioutas, “Evaluation of the measurement performance of the scanning mobility particle sizer and aerodynamic particle sizer,” *Aerosol Science and Technology*, vol. 30, no. 1, pp. 84–92, 1999. DOI: 10.1080/027868299304903. [Online]. Available: <https://doi.org/10.1080/027868299304903>.

- [186] B. T. Chen, Y. S. Cheng, and H. C. Yeh, "Performance of a tsi aerodynamic particle sizer," *Aerosol Science and Technology*, vol. 4, no. 1, pp. 89–97, 1985. DOI: 10.1080/02786828508959041. [Online]. Available: <https://doi.org/10.1080/02786828508959041>.
- [187] J. D. Yanosky, P. L. Williams, and D. L. MacIntosh, "A comparison of two direct-reading aerosol monitors with the federal reference method for pm_{2.5} in indoor air," *Atmospheric Environment*, vol. 36, no. 1, pp. 107–113, 2002, ISSN: 1352-2310. DOI: [https://doi.org/10.1016/S1352-2310\(01\)00422-8](https://doi.org/10.1016/S1352-2310(01)00422-8). [Online]. Available: <https://www.sciencedirect.com/science/article/pii/S1352231001004228>.
- [188] S. Shen, P. A. Jaques, Y. Zhu, M. D. Geller, and C. Sioutas, "Evaluation of the smps-aps system as a continuous monitor for measuring pm_{2.5}, pm₁₀ and coarse (pm_{2.5-10}) concentrations," *Atmospheric Environment*, vol. 36, no. 24, pp. 3939–3950, 2002, ISSN: 1352-2310. DOI: [https://doi.org/10.1016/S1352-2310\(02\)00330-8](https://doi.org/10.1016/S1352-2310(02)00330-8). [Online]. Available: <https://www.sciencedirect.com/science/article/pii/S1352231002003308>.
- [189] J. P. Shi, R. M. Harrison, and D. Evans, "Comparison of ambient particle surface area measurement by epiphaniometer and smps/aps," *Atmospheric Environment*, vol. 35, no. 35, pp. 6193–6200, 2001, ISSN: 1352-2310. DOI: [https://doi.org/10.1016/S1352-2310\(01\)00382-X](https://doi.org/10.1016/S1352-2310(01)00382-X). [Online]. Available: <https://www.sciencedirect.com/science/article/pii/S135223100100382X>.
- [190] B. Sarangi, S. G. Aggarwal, D. Sinha, and P. K. Gupta, "Aerosol effective density measurement using scanning mobility particle sizer and quartz crystal microbalance with the estimation of involved uncertainty," *Atmospheric Measurement Techniques*, vol. 9, no. 3, pp. 859–875, 2016. DOI: 10.5194/amt-9-859-2016. [Online]. Available: <https://amt.copernicus.org/articles/9/859/2016/>.
- [191] T. Incorporated, *Scanning mobility particle sizer model 3938 spec sheet us*, 2022.
- [192] P. H. McMurry, X. Wang, K. Park, and K. Ehara, "The relationship between mass and mobility for atmospheric particles: A new technique for measuring particle density," *Aerosol Science and Technology*, vol. 36, no. 2, pp. 227–238, 2002. DOI: 10.1080/027868202753504083. [Online]. Available: <https://doi.org/10.1080/027868202753504083>.
- [193] B. Y. Liu and D. Y. Pui, "A submicron aerosol standard and the primary, absolute calibration of the condensation nuclei counter," *Journal of Colloid and Interface Science*, vol. 47, no. 1, pp. 155–171, 1974, ISSN: 0021-9797. DOI: [https://doi.org/10.1016/0021-9797\(74\)90090-3](https://doi.org/10.1016/0021-9797(74)90090-3). [Online]. Available: <https://www.sciencedirect.com/science/article/pii/0021979774900903>.
- [194] J. L. Hand and S. M. Kreidenweis, "A new method for retrieving particle refractive index and effective density from aerosol size distribution data," *Aerosol Science and Technology*, vol. 36, no. 10, pp. 1012–1026, 2002. DOI:

- 10.1080/02786820290092276. [Online]. Available: <https://doi.org/10.1080/02786820290092276>.
- [195] M. M. Maricq, D. H. Podsiadlik, and R. E. Chase, “Size distributions of motor vehicle exhaust pm: A comparison between elpi and smps measurements,” *Aerosol Science and Technology*, vol. 33, no. 3, pp. 239–260, 2000. DOI: 10.1080/027868200416231. [Online]. Available: <https://doi.org/10.1080/027868200416231>.
- [196] G. Buonanno, M. Dell’Isola, L. Stabile, and A. Viola, “Uncertainty budget of the smps-aps system in the measurement of pm₁, pm_{2.5}, and pm₁₀,” *Aerosol Science and Technology*, vol. 43, no. 11, pp. 1130–1141, 2009. DOI: 10.1080/02786820903204078. [Online]. Available: <https://doi.org/10.1080/02786820903204078>.
- [197] E. Mikhailov, S. Vlasenko, S. T. Martin, T. Koop, and U. Pöschl, “Amorphous and crystalline aerosol particles interacting with water vapor: Conceptual framework and experimental evidence for restructuring, phase transitions and kinetic limitations,” *Atmospheric Chemistry and Physics*, vol. 9, no. 24, pp. 9491–9522, 2009. DOI: 10.5194/acp-9-9491-2009. [Online]. Available: <https://acp.copernicus.org/articles/9/9491/2009/>.
- [198] M. Shiraiwa, M. Ammann, T. Koop, and U. Pöschl, “Gas uptake and chemical aging of semisolid organic aerosol particles,” *Proceedings of the National Academy of Sciences*, vol. 108, no. 27, pp. 11 003–11 008, 2011. DOI: 10.1073/pnas.1103045108. [Online]. Available: <https://www.pnas.org/doi/abs/10.1073/pnas.1103045108>.
- [199] L. Renbaum-Wolff *et al.*, “Viscosity of α -pinene secondary organic material and implications for particle growth and reactivity,” *Proceedings of the National Academy of Sciences*, vol. 110, no. 20, pp. 8014–8019, 2013. DOI: 10.1073/pnas.1219548110. [Online]. Available: <https://www.pnas.org/doi/abs/10.1073/pnas.1219548110>.
- [200] A. M. Maclean *et al.*, “Humidity-dependent viscosity of secondary organic aerosol from ozonolysis of β -caryophyllene: Measurements, predictions, and implications,” *ACS Earth and Space Chemistry*, vol. 5, no. 2, pp. 305–318, 2021. DOI: 10.1021/acsearthspacechem.0c00296. [Online]. Available: <https://doi.org/10.1021/acsearthspacechem.0c00296>.
- [201] M. L. Hinks *et al.*, “Effect of viscosity on photodegradation rates in complex secondary organic aerosol materials,” *Phys. Chem. Chem. Phys.*, vol. 18, pp. 8785–8793, 13 2016. DOI: 10.1039/C5CP05226B. [Online]. Available: <http://dx.doi.org/10.1039/C5CP05226B>.
- [202] A. Laskin, J. S. Smith, and J. Laskin, “Molecular characterization of nitrogen-containing organic compounds in biomass burning aerosols using high-resolution mass spectrometry,” *Environmental Science & Technology*, vol. 43, no. 10, pp. 3764–3771, 2009, PMID: 19544885. DOI: 10.1021/es803456n. [Online]. Available: <https://doi.org/10.1021/es803456n>.

- [203] P. Lin *et al.*, “Molecular characterization of brown carbon in biomass burning aerosol particles,” *Environmental Science & Technology*, vol. 50, no. 21, pp. 11 815–11 824, 2016. DOI: 10.1021/acs.est.6b03024. [Online]. Available: <https://doi.org/10.1021/acs.est.6b03024>.
- [204] R. J. Sheesley, J. J. Schauer, Z. Chowdhury, G. R. Cass, and B. R. Simoneit, “Characterization of organic aerosols emitted from the combustion of biomass indigenous to south asia,” *Journal of Geophysical Research: Atmospheres*, vol. 108, no. D9, 2003, 4285, 10.1029/2002JD002981.
- [205] I. J. George and J. P. D. Abbatt, “Heterogeneous oxidation of atmospheric aerosol particles by gas-phase radicals,” *Nature Chemistry*, vol. 2, no. 9, pp. 713–722, Sep. 2010, ISSN: 1755-4349. DOI: 10.1038/nchem.806. [Online]. Available: <https://doi.org/10.1038/nchem.806>.
- [206] R. Volkamer *et al.*, “Secondary organic aerosol formation from anthropogenic air pollution: Rapid and higher than expected,” *Geophysical Research Letters*, vol. 33, no. 17, 2006. DOI: <https://doi.org/10.1029/2006GL026899>. [Online]. Available: <https://agupubs.onlinelibrary.wiley.com/doi/abs/10.1029/2006GL026899>.
- [207] M. Canagaratna *et al.*, “Chemical and microphysical characterization of ambient aerosols with the aerodyne aerosol mass spectrometer,” *Mass Spectrometry Reviews*, vol. 26, no. 2, pp. 185–222, 2007. DOI: <https://doi.org/10.1002/mas.20115>. [Online]. Available: <https://analyticalsciencejournals.onlinelibrary.wiley.com/doi/abs/10.1002/mas.20115>.
- [208] J. T. Jayne *et al.*, “Development of an aerosol mass spectrometer for size and composition analysis of submicron particles,” *Aerosol Science and Technology*, vol. 33, no. 1-2, pp. 49–70, 2000. DOI: 10.1080/027868200410840. [Online]. Available: <https://doi.org/10.1080/027868200410840>.
- [209] W. Lindinger, A. Hansel, and A. Jordan, “On-line monitoring of volatile organic compounds at pptv levels by means of proton-transfer-reaction mass spectrometry (ptr-ms) medical applications, food control and environmental research,” *International Journal of Mass Spectrometry and Ion Processes*, vol. 173, no. 3, pp. 191–241, 1998, ISSN: 0168-1176. DOI: [https://doi.org/10.1016/S0168-1176\(97\)00281-4](https://doi.org/10.1016/S0168-1176(97)00281-4). [Online]. Available: <https://www.sciencedirect.com/science/article/pii/S0168117697002814>.
- [210] C. N. Hewitt, S. Hayward, and A. Tani, “The application of proton transfer reaction-mass spectrometry (ptr-ms) to the monitoring and analysis of volatile organic compounds in the atmosphere,” *J. Environ. Monit.*, vol. 5, pp. 1–7, 1 2003. DOI: 10.1039/B204712H. [Online]. Available: <http://dx.doi.org/10.1039/B204712H>.
- [211] R. S. Blake, P. S. Monks, and A. M. Ellis, “Proton-transfer reaction mass spectrometry,” *Chemical Reviews*, vol. 109, no. 3, pp. 861–896, 2009, PMID: 19215144. DOI: 10.1021/cr800364q. [Online]. Available: <https://doi.org/10.1021/cr800364q>.

- [212] R. Holzinger, J. Williams, F. Herrmann, J. Lelieveld, N. M. Donahue, and T. Röckmann, “Aerosol analysis using a thermal-desorption proton-transfer-reaction mass spectrometer (td-ptr-ms): A new approach to study processing of organic aerosols,” *Atmospheric Chemistry and Physics*, vol. 10, no. 5, pp. 2257–2267, 2010. DOI: 10.5194/acp-10-2257-2010. [Online]. Available: <https://acp.copernicus.org/articles/10/2257/2010/>.
- [213] J. Dallüge, J. Beens, and U. A. Brinkman, “Comprehensive two-dimensional gas chromatography: A powerful and versatile analytical tool,” *Journal of Chromatography A*, vol. 1000, no. 1, pp. 69–108, 2003, A Century of Chromatography 1903-2003, ISSN: 0021-9673. DOI: [https://doi.org/10.1016/S0021-9673\(03\)00242-5](https://doi.org/10.1016/S0021-9673(03)00242-5). [Online]. Available: <https://www.sciencedirect.com/science/article/pii/S0021967303002425>.
- [214] P. Marriott and R. Shellie, “Principles and applications of comprehensive two-dimensional gas chromatography,” *TrAC Trends in Analytical Chemistry*, vol. 21, no. 9, pp. 573–583, 2002, ISSN: 0165-9936. DOI: [https://doi.org/10.1016/S0165-9936\(02\)00814-2](https://doi.org/10.1016/S0165-9936(02)00814-2). [Online]. Available: <https://www.sciencedirect.com/science/article/pii/S0165993602008142>.
- [215] R. L. Grob and E. F. Barry, *Modern practice of gas chromatography*. John Wiley & Sons, 2004, ch. 7, pp. 339–403.
- [216] W. Wardencki, “Problems with the determination of environmental sulphur compounds by gas chromatography,” *Journal of Chromatography A*, vol. 793, no. 1, pp. 1–19, 1998, ISSN: 0021-9673. DOI: [https://doi.org/10.1016/S0021-9673\(97\)00997-7](https://doi.org/10.1016/S0021-9673(97)00997-7). [Online]. Available: <https://www.sciencedirect.com/science/article/pii/S0021967397009977>.
- [217] Z. Yang, N. T. Tsona, C. George, and L. Du, “Nitrogen-containing compounds enhance light absorption of aromatic-derived brown carbon,” *Environmental Science & Technology*, vol. 56, no. 7, pp. 4005–4016, 2022, PMID: 35192318. DOI: 10.1021/acs.est.1c08794. [Online]. Available: <https://doi.org/10.1021/acs.est.1c08794>.
- [218] K. S. Chow, X. H. H. Huang, and J. Z. Yu, “Quantification of nitroaromatic compounds in atmospheric fine particulate matter in hong kong over 3 years: Field measurement evidence for secondary formation derived from biomass burning emissions,” *Environmental Chemistry*, vol. 13, no. 4, pp. 665–673, 2016. DOI: 10.1071/EN15174. [Online]. Available: <https://doi.org/10.1071/EN15174>.
- [219] A. R. Koss *et al.*, “Non-methane organic gas emissions from biomass burning: Identification, quantification, and emission factors from ptr-tof during the firex 2016 laboratory experiment,” *Atmospheric Chemistry and Physics*, vol. 18, no. 5, pp. 3299–3319, 2018. DOI: 10.5194/acp-18-3299-2018. [Online]. Available: <https://acp.copernicus.org/articles/18/3299/2018/>.

- [220] M. C. Jacobson, H. C. Hansson, K. J. Noone, and R. J. Charlson, “Organic atmospheric aerosols: Review and state of the science,” *Reviews of Geophysics*, vol. 38, no. 2, pp. 267–294, 2000. DOI: <https://doi.org/10.1029/1998RG000045>. [Online]. Available: <https://agupubs.onlinelibrary.wiley.com/doi/abs/10.1029/1998RG000045>.
- [221] H. Bhattarai *et al.*, “Levoglucosan as a tracer of biomass burning: Recent progress and perspectives,” *Atmospheric Research*, vol. 220, pp. 20–33, 2019, ISSN: 0169-8095. DOI: <https://doi.org/10.1016/j.atmosres.2019.01.004>. [Online]. Available: <https://www.sciencedirect.com/science/article/pii/S0169809518311098>.
- [222] A. P. Sullivan *et al.*, “A method for smoke marker measurements and its potential application for determining the contribution of biomass burning from wild-fires and prescribed fires to ambient pm2.5 organic carbon,” *Journal of Geophysical Research: Atmospheres*, vol. 113, no. D22, 2008. DOI: <https://doi.org/10.1029/2008JD010216>. [Online]. Available: <https://agupubs.onlinelibrary.wiley.com/doi/abs/10.1029/2008JD010216>.
- [223] B. Simoneit *et al.*, “Levoglucosan, a tracer for cellulose in biomass burning and atmospheric particles,” *Atmospheric Environment*, vol. 33, no. 2, pp. 173–182, 1999, ISSN: 1352-2310. DOI: [https://doi.org/10.1016/S1352-2310\(98\)00145-9](https://doi.org/10.1016/S1352-2310(98)00145-9). [Online]. Available: <https://www.sciencedirect.com/science/article/pii/S1352231098001459>.
- [224] Y. Huo *et al.*, “Chemical fingerprinting of hulis in particulate matters emitted from residential coal and biomass combustion,” *Environmental Science & Technology*, vol. 55, no. 6, pp. 3593–3603, 2021, PMID: 33656861. DOI: [10.1021/acs.est.0c08518](https://doi.org/10.1021/acs.est.0c08518). [Online]. Available: <https://doi.org/10.1021/acs.est.0c08518>.
- [225] H. Wang *et al.*, “Source profiles of volatile organic compounds from biomass burning in yangtze river delta, china,” *Aerosol and Air Quality Research*, vol. 14, no. 3, pp. 818–828, 2014. DOI: [10.4209/aaqr.2013.05.0174](https://doi.org/10.4209/aaqr.2013.05.0174). [Online]. Available: <https://doi.org/10.4209/aaqr.2013.05.0174>.
- [226] A. Bertrand *et al.*, “Evolution of the chemical fingerprint of biomass burning organic aerosol during aging,” *Atmospheric Chemistry and Physics*, vol. 18, no. 10, pp. 7607–7624, 2018. DOI: [10.5194/acp-18-7607-2018](https://doi.org/10.5194/acp-18-7607-2018). [Online]. Available: <https://acp.copernicus.org/articles/18/7607/2018/>.
- [227] C. Warneke *et al.*, “An important contribution to springtime arctic aerosol from biomass burning in russia,” *Geophysical Research Letters*, vol. 37, no. 1, 2010. DOI: <https://doi.org/10.1029/2009GL041816>. [Online]. Available: <https://agupubs.onlinelibrary.wiley.com/doi/abs/10.1029/2009GL041816>.
- [228] K. Sekimoto *et al.*, “High- and low-temperature pyrolysis profiles describe volatile organic compound emissions from western us wildfire fuels,” *Atmospheric Chemistry and Physics*, vol. 18, no. 13, pp. 9263–9281, 2018. DOI: [10.5194/acp-18-9263-2018](https://doi.org/10.5194/acp-18-9263-2018). [Online]. Available: <https://acp.copernicus.org/articles/18/9263/2018/>.

- [229] C. Y. Lim *et al.*, “Secondary organic aerosol formation from the laboratory oxidation of biomass burning emissions,” *Atmospheric Chemistry and Physics*, vol. 19, no. 19, pp. 12 797–12 809, 2019. DOI: 10.5194/acp-19-12797-2019. [Online]. Available: <https://acp.copernicus.org/articles/19/12797/2019/>.
- [230] W. Li *et al.*, “Tracers from biomass burning emissions and identification of biomass burning,” *Atmosphere*, vol. 12, no. 11, 2021, ISSN: 2073-4433. DOI: 10.3390/atmos12111401. [Online]. Available: <https://www.mdpi.com/2073-4433/12/11/1401>.
- [231] C. E. Stockwell, P. R. Veres, J. Williams, and R. J. Yokelson, “Characterization of biomass burning emissions from cooking fires, peat, crop residue, and other fuels with high-resolution proton-transfer-reaction time-of-flight mass spectrometry,” *Atmospheric Chemistry and Physics*, vol. 15, no. 2, pp. 845–865, 2015. DOI: 10.5194/acp-15-845-2015. [Online]. Available: <https://acp.copernicus.org/articles/15/845/2015/>.
- [232] K. E. Pickering *et al.*, “Convective transport of biomass burning emissions over brazil during trace a,” *Journal of Geophysical Research: Atmospheres*, vol. 101, no. D19, pp. 23 993–24 012, 1996. DOI: <https://doi.org/10.1029/96JD00346>. [Online]. Available: <https://agupubs.onlinelibrary.wiley.com/doi/abs/10.1029/96JD00346>.
- [233] J. S. Fu *et al.*, “Evaluating the influences of biomass burning during 2006 base-asia: A regional chemical transport modeling,” *Atmospheric Chemistry and Physics*, vol. 12, no. 9, pp. 3837–3855, 2012. DOI: 10.5194/acp-12-3837-2012. [Online]. Available: <https://acp.copernicus.org/articles/12/3837/2012/>.
- [234] K. D. Bartle and P. Myers, “History of gas chromatography,” *TrAC Trends in Analytical Chemistry*, vol. 21, no. 9, pp. 547–557, 2002, ISSN: 0165-9936. DOI: [https://doi.org/10.1016/S0165-9936\(02\)00806-3](https://doi.org/10.1016/S0165-9936(02)00806-3). [Online]. Available: <https://www.sciencedirect.com/science/article/pii/S0165993602008063>.
- [235] R. L. Grob and E. F. Barry, *Modern practice of gas chromatography*. John Wiley & Sons, 2004, ch. 2-3,6, pp. 25–193,277–339.
- [236] I. G. McWILLIAM and R. A. DEWAR, “Flame ionization detector for gas chromatography,” *Nature*, vol. 181, no. 4611, pp. 760–760, Mar. 1958, ISSN: 1476-4687. DOI: 10.1038/181760a0. [Online]. Available: <https://doi.org/10.1038/181760a0>.
- [237] W. M. Niessen, *Liquid chromatography-mass spectrometry*. CRC press, 2006, ch. 1-2, pp. 3–53.
- [238] F. Gritti and G. Guiochon, “Mass transfer kinetics, band broadening and column efficiency,” *Journal of Chromatography A*, vol. 1221, pp. 2–40, 2012, Editors’ Choice VI, ISSN: 0021-9673. DOI: <https://doi.org/10.1016/j.chroma.2011.04.058>. [Online]. Available: <https://www.sciencedirect.com/science/article/pii/S0021967311005681>.

- [239] W. Niessen and A. Tinke, "Liquid chromatography-mass spectrometry general principles and instrumentation," *Journal of Chromatography A*, vol. 703, no. 1, pp. 37–57, 1995, ISSN: 0021-9673. DOI: [https://doi.org/10.1016/0021-9673\(94\)01198-N](https://doi.org/10.1016/0021-9673(94)01198-N). [Online]. Available: <https://www.sciencedirect.com/science/article/pii/002196739401198N>.
- [240] S. Banerjee and S. Mazumdar, "Electrospray ionization mass spectrometry: A technique to access the information beyond the molecular weight of the analyte," *International Journal of Analytical Chemistry*, vol. 2012, p. 282574, Mar. 2012, ISSN: 1687-8760. DOI: 10.1155/2012/282574. [Online]. Available: <https://doi.org/10.1155/2012/282574>.
- [241] L. E. Hatch, W. Luo, J. F. Pankow, R. J. Yokelson, C. E. Stockwell, and K. C. Barsanti, "Identification and quantification of gaseous organic compounds emitted from biomass burning using two-dimensional gas chromatography–time-of-flight mass spectrometry," *Atmospheric Chemistry and Physics*, vol. 15, no. 4, pp. 1865–1899, 2015. DOI: 10.5194/acp-15-1865-2015. [Online]. Available: <https://acp.copernicus.org/articles/15/1865/2015/>.
- [242] W. Welthagen, J. Schnelle-Kreis, and R. Zimmermann, "Search criteria and rules for comprehensive two-dimensional gas chromatography–time-of-flight mass spectrometry analysis of airborne particulate matter," *Journal of Chromatography A*, vol. 1019, no. 1, pp. 233–249, 2003, First International Symposium on Comprehensive Multidimensional Gas Chromatography, ISSN: 0021-9673. DOI: <https://doi.org/10.1016/j.chroma.2003.08.053>. [Online]. Available: <https://www.sciencedirect.com/science/article/pii/S0021967303015498>.
- [243] C. N. Jen *et al.*, "Speciated and total emission factors of particulate organics from burning western us wildland fuels and their dependence on combustion efficiency," *Atmospheric Chemistry and Physics*, vol. 19, no. 2, pp. 1013–1026, 2019. DOI: 10.5194/acp-19-1013-2019. [Online]. Available: <https://acp.copernicus.org/articles/19/1013/2019/>.
- [244] M. Abou-Ghanem *et al.*, "Significant variability in the photocatalytic activity of natural titanium-containing minerals: Implications for understanding and predicting atmospheric mineral dust photochemistry," *Environmental Science & Technology*, vol. 54, no. 21, pp. 13509–13516, 2020, PMID: 33058682. DOI: 10.1021/acs.est.0c05861. [Online]. Available: <https://doi.org/10.1021/acs.est.0c05861>.
- [245] J. W. Adams, D. Rodriguez, and R. A. Cox, "The uptake of so₂ on saharan dust: A flow tube study," *Atmospheric Chemistry and Physics*, vol. 5, no. 10, pp. 2679–2689, 2005. DOI: 10.5194/acp-5-2679-2005. [Online]. Available: <https://acp.copernicus.org/articles/5/2679/2005/>.
- [246] Y. Liu, A. V. Ivanov, and M. J. Molina, "Temperature dependence of oh diffusion in air and he," *Geophysical Research Letters*, vol. 36, no. 3, 2009. DOI: <https://doi.org/10.1029/2008GL036170>. [Online]. Available: <https://agupubs.onlinelibrary.wiley.com/doi/abs/10.1029/2008GL036170>.

- [247] J. Fast *et al.*, “Evaluating simulated primary anthropogenic and biomass burning organic aerosols during milagro: Implications for assessing treatments of secondary organic aerosols,” *Atmospheric Chemistry and Physics*, vol. 9, no. 16, pp. 6191–6215, 2009. DOI: 10.5194/acp-9-6191-2009. [Online]. Available: <https://acp.copernicus.org/articles/9/6191/2009/>.
- [248] V. Choudhary, M. Loebel Roson, X. Guo, T. Gautam, T. Gupta, and R. Zhao, “Aqueous-phase photochemical oxidation of water-soluble brown carbon aerosols arising from solid biomass fuel burning,” *Environ. Sci.: Atmos.*, pp. –, 2023. DOI: 10.1039/D2EA00151A. [Online]. Available: <http://dx.doi.org/10.1039/D2EA00151A>.
- [249] L. T. Fleming *et al.*, “Emissions from village cookstoves in haryana, india, and their potential impacts on air quality,” *Atmospheric Chemistry and Physics*, vol. 18, no. 20, pp. 15 169–15 182, 2018. DOI: 10.5194/acp-18-15169-2018. [Online]. Available: <https://acp.copernicus.org/articles/18/15169/2018/>.
- [250] M. Mouton *et al.*, “The hygroscopic properties of biomass burning aerosol from eucalyptus and cow dung under different combustion conditions,” *Aerosol Science and Technology*, vol. 0, no. 0, pp. 1–13, 2023. DOI: 10.1080/02786826.2023.2198587. [Online]. Available: <https://doi.org/10.1080/02786826.2023.2198587>.
- [251] G. G. Pfister, C. Wiedinmyer, and L. K. Emmons, “Impacts of the fall 2007 california wildfires on surface ozone: Integrating local observations with global model simulations,” *Geophysical Research Letters*, vol. 35, no. 19, 2008, L19814, 10.1029/2008GL034747. DOI: <https://doi.org/10.1029/2008GL034747>. [Online]. Available: <https://agupubs.onlinelibrary.wiley.com/doi/abs/10.1029/2008GL034747>.
- [252] B. Langmann, B. Duncan, C. Textor, J. Trentmann, and G. R. van der Werf, “Vegetation fire emissions and their impact on air pollution and climate,” *Atmospheric Environment*, vol. 43, no. 1, pp. 107–116, 2009, ISSN: 1352-2310. DOI: <https://doi.org/10.1016/j.atmosenv.2008.09.047>. [Online]. Available: <https://www.sciencedirect.com/science/article/pii/S135223100800900X>.
- [253] R. J. Yokelson *et al.*, “Coupling field and laboratory measurements to estimate the emission factors of identified and unidentified trace gases for prescribed fires,” *Atmospheric Chemistry and Physics*, vol. 13, no. 1, pp. 89–116, 2013. DOI: 10.5194/acp-13-89-2013. [Online]. Available: <https://acp.copernicus.org/articles/13/89/2013/>.
- [254] R. Cordell *et al.*, “Evaluation of biomass burning across north west europe and its impact on air quality,” *Atmospheric Environment*, vol. 141, pp. 276–286, 2016, ISSN: 1352-2310. DOI: <https://doi.org/10.1016/j.atmosenv.2016.06.065>. [Online]. Available: <https://www.sciencedirect.com/science/article/pii/S1352231016304988>.
- [255] “Health effects institute. state of global air 2020,”

- [256] C. J. L. Murray *et al.*, “Global burden of 87 risk factors in 204 countries and territories, 1990–2019: A systematic analysis for the Global Burden of Disease Study 2019,” en, *The Lancet*, vol. 396, no. 10258, pp. 1223–1249, Oct. 2020, ISSN: 01406736. DOI: 10.1016/S0140-6736(20)30752-2. [Online]. Available: <https://linkinghub.elsevier.com/retrieve/pii/S0140673620307522> (visited on 06/25/2021).
- [257] H. Lukács *et al.*, “Seasonal trends and possible sources of brown carbon based on 2-year aerosol measurements at six sites in europe,” *Journal of Geophysical Research*, vol. 112, Sep. 2007, D23S18, 10.1029/2006JD008151. DOI: 10.1029/2006JD008151.
- [258] T. Kirchstetter, T. Novakov, and P. Hobbs, “Evidence that the spectral dependence of light absorption by aerosols is affected by organic carbon,” *Journal of Geophysical Research Atmospheres*, vol. 109, pp. 21 208–, Nov. 2004, D21208, 10.1029/2004JD004999. DOI: 10.1029/2004JD004999.
- [259] R. A. Washenfelder *et al.*, “Biomass burning dominates brown carbon absorption in the rural southeastern united states,” *Geophysical Research Letters*, vol. 42, no. 2, pp. 653–664, 2015, 10.1002/2014GL062444. DOI: <https://doi.org/10.1002/2014GL062444>. [Online]. Available: <https://agupubs.onlinelibrary.wiley.com/doi/abs/10.1002/2014GL062444>.
- [260] J. P. S. Wong, A. Nenes, and R. J. Weber, “Changes in light absorptivity of molecular weight separated brown carbon due to photolytic aging,” *Environmental Science & Technology*, vol. 51, no. 15, pp. 8414–8421, 2017. DOI: 10.1021/acs.est.7b01739. [Online]. Available: <https://doi.org/10.1021/acs.est.7b01739>.
- [261] I. S. Mudway, S. T. Duggan, C. Venkataraman, G. Habib, F. J. Kelly, and J. Grigg, “Combustion of dried animal dung as biofuel results in the generation of highly redox active fine particulates,” *Particle and Fibre Toxicology*, vol. 2, no. 1, p. 6, 2005, ISSN: 17438977. DOI: 10.1186/1743-8977-2-6. [Online]. Available: <http://particleandfibretoxicology.biomedcentral.com/articles/10.1186/1743-8977-2-6> (visited on 06/25/2021).
- [262] D. Park *et al.*, “Emission Characteristics of Particulate Matter and Volatile Organic Compounds in Cow Dung Combustion,” en, *Environmental Science & Technology*, vol. 47, no. 22, pp. 12 952–12 957, Nov. 2013, ISSN: 0013-936X, 1520-5851. DOI: 10.1021/es402822e. [Online]. Available: <https://pubs.acs.org/doi/10.1021/es402822e> (visited on 06/25/2021).
- [263] M. D. Jolleys *et al.*, “Characterizing the aging of biomass burning organic aerosol by use of mixing ratios: A meta-analysis of four regions,” *Environmental Science & Technology*, vol. 46, no. 24, pp. 13 093–13 102, 2012. DOI: 10.1021/es302386v. [Online]. Available: <https://doi.org/10.1021/es302386v>.
- [264] J. Martinsson *et al.*, “Impacts of combustion conditions and photochemical processing on the light absorption of biomass combustion aerosol,” *Environmental science & technology*, vol. 49, Nov. 2015. DOI: 10.1021/acs.est.5b03205.

- [265] B. R. T. Simoneit, W. F. Rogge, M. A. Mazurek, L. J. Standley, L. M. Hildemann, and G. R. Cass, “Lignin pyrolysis products, lignans, and resin acids as specific tracers of plant classes in emissions from biomass combustion,” *Environmental Science & Technology*, vol. 27, no. 12, pp. 2533–2541, 1993. DOI: 10.1021/es00048a034. [Online]. Available: <https://doi.org/10.1021/es00048a034>.
- [266] C. Venkataraman and G. U. M. Rao, “Emission factors of carbon monoxide and size-resolved aerosols from biofuel combustion,” *Environmental Science & Technology*, vol. 35, no. 10, pp. 2100–2107, 2001. DOI: 10.1021/es001603d. [Online]. Available: <https://doi.org/10.1021/es001603d>.
- [267] A. Pandey, S. Pervez, and R. K. Chakrabarty, “Filter-based measurements of uv–vis mass absorption cross sections of organic carbon aerosol from residential biomass combustion: Preliminary findings and sources of uncertainty,” *Journal of Quantitative Spectroscopy and Radiative Transfer*, vol. 182, pp. 296–304, 2016, ISSN: 0022-4073. DOI: <https://doi.org/10.1016/j.jqsrt.2016.06.023>. [Online]. Available: <https://www.sciencedirect.com/science/article/pii/S0022407316300796>.
- [268] M. O. Andreae, “Emission of trace gases and aerosols from biomass burning – an updated assessment,” *Atmospheric Chemistry and Physics*, vol. 19, no. 13, pp. 8523–8546, 2019. DOI: 10.5194/acp-19-8523-2019. [Online]. Available: <https://acp.copernicus.org/articles/19/8523/2019/>.
- [269] J. J. Schauer, M. J. Kleeman, G. R. Cass, and B. R. T. Simoneit, “Measurement of emissions from air pollution sources. 3. c1-c29 organic compounds from fireplace combustion of wood,” *Environmental Science & Technology*, vol. 35, no. 9, pp. 1716–1728, 2001. DOI: 10.1021/es001331e. [Online]. Available: <https://doi.org/10.1021/es001331e>.
- [270] S. Shabbar and I. Janajreh, “Thermodynamic equilibrium analysis of coal gasification using gibbs energy minimization method,” *Energy Conversion and Management*, vol. 65, pp. 755–763, 2013, ISSN: 0196-8904. DOI: <https://doi.org/10.1016/j.enconman.2012.02.032>. [Online]. Available: <https://www.sciencedirect.com/science/article/pii/S0196890412001501>.
- [271] Z. Zdráhal, J. Oliveira, R. Vermeylen, M. Claeys, and W. Maenhaut, “Improved method for quantifying levoglucosan and related monosaccharide anhydrides in atmospheric aerosols and application to samples from urban and tropical locations,” *Environmental Science & Technology*, vol. 36, no. 4, pp. 747–753, 2002. DOI: 10.1021/es015619v. [Online]. Available: <https://doi.org/10.1021/es015619v>.
- [272] D. Fabbri, G. Chiavari, S. Prati, I. Vassura, and M. Vangelista, “Gas chromatography/mass spectrometric characterisation of pyrolysis/silylation products of glucose and cellulose,” *Rapid Communications in Mass Spectrometry*, vol. 16, no. 24, pp. 2349–2355, 2002. DOI: <https://doi.org/10.1002/rcm.856>. [Online]. Available: <https://analyticalsciencejournals.onlinelibrary.wiley.com/doi/abs/10.1002/rcm.856>.

- [273] K. Yang and B. Xing, “Adsorption of fulvic acid by carbon nanotubes from water,” *Environmental Pollution*, vol. 157, no. 4, pp. 1095–1100, 2009, ISSN: 0269-7491. DOI: <https://doi.org/10.1016/j.envpol.2008.11.007>. [Online]. Available: <https://www.sciencedirect.com/science/article/pii/S0269749108005964>.
- [274] B. Wallace, M. Purcell, and J. Furlong, “Total organic carbon analysis as a precursor to disinfection byproducts in potable water: Oxidation technique considerations,” *J. Environ. Monit.*, vol. 4, pp. 35–42, 1 2002. DOI: 10.1039/B106049J. [Online]. Available: <http://dx.doi.org/10.1039/B106049J>.
- [275] I. Bisutti, I. Hilke, and M. Raessler, “Determination of total organic carbon – an overview of current methods,” *TrAC Trends in Analytical Chemistry*, vol. 23, no. 10, pp. 716–726, 2004, ISSN: 0165-9936. DOI: <https://doi.org/10.1016/j.trac.2004.09.003>. [Online]. Available: <https://www.sciencedirect.com/science/article/pii/S0165993604030535>.
- [276] R. Zhao, A. K. Y. Lee, L. Huang, X. Li, F. Yang, and J. P. D. Abbatt, “Photochemical processing of aqueous atmospheric brown carbon,” *Atmospheric Chemistry and Physics*, vol. 15, no. 11, pp. 6087–6100, 2015. DOI: 10.5194/acp-15-6087-2015. [Online]. Available: <https://acp.copernicus.org/articles/15/6087/2015/>.
- [277] L. M. Russell, “Aerosol organic-mass-to-organic-carbon ratio measurements,” *Environmental Science & Technology*, vol. 37, no. 13, pp. 2982–2987, 2003. DOI: 10.1021/es026123w. [Online]. Available: <https://doi.org/10.1021/es026123w>.
- [278] A. Hoffer *et al.*, “Optical properties of humic-like substances (hulis) in biomass-burning aerosols,” *Atmospheric Chemistry and Physics*, vol. 6, no. 11, pp. 3563–3570, 2006. DOI: 10.5194/acp-6-3563-2006. [Online]. Available: <https://acp.copernicus.org/articles/6/3563/2006/>.
- [279] R. Zhao, C. M. Kenseth, Y. Huang, N. F. Dalleska, and J. H. Seinfeld, “Iodometry-assisted liquid chromatography electrospray ionization mass spectrometry for analysis of organic peroxides: An application to atmospheric secondary organic aerosol,” *Environmental Science & Technology*, vol. 52, no. 4, pp. 2108–2117, 2018, PMID: 29370527. DOI: 10.1021/acs.est.7b04863. [Online]. Available: <https://doi.org/10.1021/acs.est.7b04863>.
- [280] R. C. Pettersen, “The chemical composition of wood,” in *The Chemistry of Solid Wood*, ch. 2, pp. 57–126. DOI: 10.1021/ba-1984-0207.ch002. [Online]. Available: <https://pubs.acs.org/doi/abs/10.1021/ba-1984-0207.ch002>.
- [281] G. N. Inari, M. Pétrissans, A. Pétrissans, and P. Gérardin, “Elemental composition of wood as a potential marker to evaluate heat treatment intensity,” *Polymer Degradation and Stability*, vol. 94, no. 3, pp. 365–368, 2009, ISSN: 0141-3910. DOI: <https://doi.org/10.1016/j.polymdegradstab.2008.12.003>. [Online]. Available: <https://www.sciencedirect.com/science/article/pii/S0141391008004023>.

- [282] A. Mohareb, P. Sirmah, M. Pétrissans, and P. Gérardin, “Effect of heat treatment intensity on wood chemical composition and decay durability of *Pinus patula*,” en, *European Journal of Wood and Wood Products*, vol. 70, no. 4, pp. 519–524, Jul. 2012, ISSN: 0018-3768, 1436-736X. DOI: 10.1007/s00107-011-0582-7. [Online]. Available: <http://link.springer.com/10.1007/s00107-011-0582-7> (visited on 05/26/2021).
- [283] M. Choudhary, L. Bailey, and C. Grant, “Review of the use of swine manure in crop production: Effects on yield and composition and on soil and water quality,” *Waste Management & Research*, vol. 14, no. 6, pp. 581–595, 1996. DOI: 10.1177/0734242X9601400606. [Online]. Available: <https://doi.org/10.1177/0734242X9601400606>.
- [284] P. Sørensen, M. R. Weisbjerg, and P. Lund, “Dietary effects on the composition and plant utilization of nitrogen in dairy cattle manure,” *The Journal of Agricultural Science*, vol. 141, no. 1, 79–91, 2003. DOI: 10.1017/S0021859603003368.
- [285] T. S. Griffin, Z. He, and C. W. Honeycutt, “Manure composition affects net transformation of nitrogen from dairy manures,” en, *Plant and Soil*, vol. 273, no. 1-2, pp. 29–38, Jun. 2005, ISSN: 0032-079X, 1573-5036. DOI: 10.1007/s11104-004-6473-5. [Online]. Available: <http://link.springer.com/10.1007/s11104-004-6473-5> (visited on 06/28/2021).
- [286] S. H. Han, J. Y. An, J. Hwang, S. B. Kim, and B. B. Park, “The effects of organic manure and chemical fertilizer on the growth and nutrient concentrations of yellow poplar (*liriodendron tulipifera* lin.) in a nursery system,” *Forest Science and Technology*, vol. 12, no. 3, pp. 137–143, 2016. DOI: 10.1080/21580103.2015.1135827. [Online]. Available: <https://doi.org/10.1080/21580103.2015.1135827>.
- [287] J. Huang *et al.*, “Chemical structures and characteristics of animal manures and composts during composting and assessment of maturity indices,” en, *PLOS ONE*, vol. 12, no. 6, J. Mao, Ed., e0178110, Jun. 2017, ISSN: 1932-6203. DOI: 10.1371/journal.pone.0178110. [Online]. Available: <https://dx.plos.org/10.1371/journal.pone.0178110> (visited on 05/28/2021).
- [288] F.-X. Collard and J. Blin, “A review on pyrolysis of biomass constituents: Mechanisms and composition of the products obtained from the conversion of cellulose, hemicelluloses and lignin,” *Renewable and Sustainable Energy Reviews*, vol. 38, pp. 594–608, 2014, ISSN: 1364-0321. DOI: <https://doi.org/10.1016/j.rser.2014.06.013>. [Online]. Available: <https://www.sciencedirect.com/science/article/pii/S136403211400450X>.
- [289] J. R. Laing, D. A. Jaffe, and J. R. Hee, “Physical and optical properties of aged biomass burning aerosol from wildfires in siberia and the western usa at the mt. bachelor observatory,” *Atmospheric Chemistry and Physics*, vol. 16, no. 23, pp. 15 185–15 197, 2016. DOI: 10.5194/acp-16-15185-2016. [Online]. Available: <https://acp.copernicus.org/articles/16/15185/2016/>.

- [290] K. M. Sakamoto, J. D. Allan, H. Coe, J. W. Taylor, T. J. Duck, and J. R. Pierce, “Aged boreal biomass-burning aerosol size distributions from bortas 2011,” *Atmospheric Chemistry and Physics*, vol. 15, no. 4, pp. 1633–1646, 2015. DOI: 10.5194/acp-15-1633-2015. [Online]. Available: <https://acp.copernicus.org/articles/15/1633/2015/>.
- [291] S. Janhäll, M. O. Andreae, and U. Pöschl, “Biomass burning aerosol emissions from vegetation fires: Particle number and mass emission factors and size distributions,” *Atmospheric Chemistry and Physics*, vol. 10, no. 3, pp. 1427–1439, 2010. DOI: 10.5194/acp-10-1427-2010. [Online]. Available: <https://acp.copernicus.org/articles/10/1427/2010/>.
- [292] M. D. Hays, P. M. Fine, C. D. Geron, M. J. Kleeman, and B. K. Gullett, “Open burning of agricultural biomass: Physical and chemical properties of particle-phase emissions,” *Atmospheric Environment*, vol. 39, no. 36, pp. 6747–6764, 2005, ISSN: 1352-2310. DOI: <https://doi.org/10.1016/j.atmosenv.2005.07.072>. [Online]. Available: <https://www.sciencedirect.com/science/article/pii/S1352231005007247>.
- [293] A. Y. P. Wardoyo, L. Morawska, Z. D. Ristovski, and J. Marsh, “Quantification of particle number and mass emission factors from combustion of queensland trees,” *Environmental Science & Technology*, vol. 40, no. 18, pp. 5696–5703, 2006, PMID: 17007128. DOI: 10.1021/es0609497. [Online]. Available: <https://doi.org/10.1021/es0609497>.
- [294] A. P. Bruins, “Mechanistic aspects of electrospray ionization,” *Journal of Chromatography A*, vol. 794, no. 1, pp. 345–357, 1998, ISSN: 0021-9673. DOI: [https://doi.org/10.1016/S0021-9673\(97\)01110-2](https://doi.org/10.1016/S0021-9673(97)01110-2). [Online]. Available: <https://www.sciencedirect.com/science/article/pii/S0021967397011102>.
- [295] Y. Chen and T. C. Bond, “Light absorption by organic carbon from wood combustion,” *Atmospheric Chemistry and Physics*, vol. 10, no. 4, pp. 1773–1787, 2010. DOI: 10.5194/acp-10-1773-2010. [Online]. Available: <https://acp.copernicus.org/articles/10/1773/2010/>.
- [296] A. L. Robinson *et al.*, “Rethinking organic aerosols: Semivolatile emissions and photochemical aging,” *Science*, vol. 315, no. 5816, pp. 1259–1262, 2007, ISSN: 0036-8075. DOI: 10.1126/science.1133061. [Online]. Available: <https://science.sciencemag.org/content/315/5816/1259>.
- [297] C.-L. Hsu, C.-Y. Cheng, C.-T. Lee, and W.-H. Ding, “Derivatization procedures and determination of levoglucosan and related monosaccharide anhydrides in atmospheric aerosols by gas chromatography–mass spectrometry,” *Talanta*, vol. 72, no. 1, pp. 199–205, 2007, ISSN: 0039-9140. DOI: <https://doi.org/10.1016/j.talanta.2006.10.018>. [Online]. Available: <https://www.sciencedirect.com/science/article/pii/S0039914006006898>.

- [298] I. Sable *et al.*, “Properties of wood and pulp fibers from lodgepole pine (*pinus contorta*) as compared to scots pine (*pinus sylvestris*),” *BioResources*, vol. 7, no. 2, pp. 1771–1783, 2012, ISSN: 1930-2126. [Online]. Available: https://ojs.cnr.ncsu.edu/index.php/BioRes/article/view/BioRes_07_2_1771_Sable_GJVIVT_Props_Wood_Pulp_Fibers_Pines.
- [299] Z. Wen, W. Liao, and S. Chen, “Hydrolysis of animal manure lignocellulosics for reducing sugar production,” *Bioresource Technology*, vol. 91, no. 1, pp. 31–39, 2004, ISSN: 0960-8524. DOI: [https://doi.org/10.1016/S0960-8524\(03\)00166-4](https://doi.org/10.1016/S0960-8524(03)00166-4). [Online]. Available: <https://www.sciencedirect.com/science/article/pii/S0960852403001664>.
- [300] W. Liao, Y. Liu, C. Liu, Z. Wen, and S. Chen, “Acid hydrolysis of fibers from dairy manure,” *Bioresource Technology*, vol. 97, no. 14, pp. 1687–1695, 2006, ISSN: 0960-8524. DOI: <https://doi.org/10.1016/j.biortech.2005.07.028>. [Online]. Available: <https://www.sciencedirect.com/science/article/pii/S096085240500369X>.
- [301] P. Kumar, D. M. Barrett, M. J. Delwiche, and P. Stroeve, “Methods for pretreatment of lignocellulosic biomass for efficient hydrolysis and biofuel production,” *Industrial & Engineering Chemistry Research*, vol. 48, no. 8, pp. 3713–3729, 2009. DOI: 10.1021/ie801542g. [Online]. Available: <https://doi.org/10.1021/ie801542g>.
- [302] A. Piazzalunga, P. Fermo, V. Bernardoni, R. Vecchi, G. Valli, and M. A. D. Gregorio, “A simplified method for levoglucosan quantification in wintertime atmospheric particulate matter by high performance anion-exchange chromatography coupled with pulsed amperometric detection,” *International Journal of Environmental Analytical Chemistry*, vol. 90, no. 12, pp. 934–947, 2010. DOI: 10.1080/03067310903023619. [Online]. Available: <https://doi.org/10.1080/03067310903023619>.
- [303] C. Schmidl *et al.*, “Chemical characterisation of particle emissions from burning leaves,” *Atmospheric Environment*, vol. 42, no. 40, pp. 9070–9079, 2008, ISSN: 1352-2310. DOI: <https://doi.org/10.1016/j.atmosenv.2008.09.010>. [Online]. Available: <https://www.sciencedirect.com/science/article/pii/S1352231008008406>.
- [304] G. Engling, J. J. Lee, Y.-W. Tsai, S.-C. C. Lung, C. C.-K. Chou, and C.-Y. Chan, “Size-resolved anhydrosugar composition in smoke aerosol from controlled field burning of rice straw,” *Aerosol Science and Technology*, vol. 43, no. 7, pp. 662–672, 2009. DOI: 10.1080/02786820902825113. [Online]. Available: <https://doi.org/10.1080/02786820902825113>.
- [305] X. Sang, Z. Zhang, C. Chan, and G. Engling, “Source categories and contribution of biomass smoke to organic aerosol over the southeastern tibetan plateau,” *Atmospheric Environment*, vol. 78, pp. 113–123, 2013, ISSN: 1352-2310. DOI: <https://doi.org/10.1016/j.atmosenv.2012.12.012>. [Online]. Available: <https://www.sciencedirect.com/science/article/pii/S1352231012011624>.

- [306] R. Urban, C. Alves, A. Allen, A. Cardoso, M. Queiroz, and M. Campos, “Sugar markers in aerosol particles from an agro-industrial region in brazil,” *Atmospheric Environment*, vol. 90, pp. 106–112, 2014, ISSN: 1352-2310. DOI: <https://doi.org/10.1016/j.atmosenv.2014.03.034>. [Online]. Available: <https://www.sciencedirect.com/science/article/pii/S135223101400209X>.
- [307] Y. Cheng *et al.*, “Biomass burning contribution to beijing aerosol,” *Atmospheric Chemistry and Physics*, vol. 13, no. 15, pp. 7765–7781, 2013. DOI: 10.5194/acp-13-7765-2013. [Online]. Available: <https://acp.copernicus.org/articles/13/7765/2013/>.
- [308] P. M. Medeiros and B. R. T. Simoneit, “Source profiles of organic compounds emitted upon combustion of green vegetation from temperate climate forests,” *Environmental Science & Technology*, vol. 42, no. 22, pp. 8310–8316, 2008. DOI: 10.1021/es801533b. [Online]. Available: <https://doi.org/10.1021/es801533b>.
- [309] A. Otto, R. Gondokusumo, and M. J. Simpson, “Characterization and quantification of biomarkers from biomass burning at a recent wildfire site in northern alberta, canada,” *Applied Geochemistry*, vol. 21, no. 1, pp. 166–183, 2006, ISSN: 0883-2927. DOI: <https://doi.org/10.1016/j.apgeochem.2005.09.007>. [Online]. Available: <https://www.sciencedirect.com/science/article/pii/S0883292705002003>.
- [310] C. Schmidl *et al.*, “Chemical characterisation of fine particle emissions from wood stove combustion of common woods growing in mid-european alpine regions,” *Atmospheric Environment*, vol. 42, no. 1, pp. 126–141, 2008, ISSN: 1352-2310. DOI: <https://doi.org/10.1016/j.atmosenv.2007.09.028>. [Online]. Available: <https://www.sciencedirect.com/science/article/pii/S1352231007008047>.
- [311] M. Brege, M. Paglione, S. Gilardoni, S. Decesari, M. C. Facchini, and L. R. Mazzoleni, “Molecular insights on aging and aqueous-phase processing from ambient biomass burning emissions-influenced po valley fog and aerosol,” *Atmospheric Chemistry and Physics*, vol. 18, no. 17, pp. 13197–13214, 2018. DOI: 10.5194/acp-18-13197-2018. [Online]. Available: <https://acp.copernicus.org/articles/18/13197/2018/>.
- [312] A. Krueve, K. Kaupmees, J. Liigand, and I. Leito, “Negative electrospray ionization via deprotonation: Predicting the ionization efficiency,” *Analytical Chemistry*, vol. 86, no. 10, pp. 4822–4830, 2014. DOI: 10.1021/ac404066v. [Online]. Available: <https://doi.org/10.1021/ac404066v>.
- [313] P. Liigand *et al.*, “Think negative: Finding the best electrospray ionization/ms mode for your analyte,” *Analytical Chemistry*, vol. 89, no. 11, pp. 5665–5668, 2017. DOI: 10.1021/acs.analchem.7b00096. [Online]. Available: <https://doi.org/10.1021/acs.analchem.7b00096>.
- [314] M. Xie, X. Chen, M. D. Hays, and A. L. Holder, “Composition and light absorption of n-containing aromatic compounds in organic aerosols from laboratory biomass burning,” *Atmospheric Chemistry and Physics*, vol. 19, no. 5,

- pp. 2899–2915, 2019. DOI: 10.5194/acp-19-2899-2019. [Online]. Available: <https://acp.copernicus.org/articles/19/2899/2019/>.
- [315] E. A. Higgins Keppler, C. L. Jenkins, T. J. Davis, and H. D. Bean, “Advances in the application of comprehensive two-dimensional gas chromatography in metabolomics,” *TrAC Trends in Analytical Chemistry*, vol. 109, pp. 275–286, 2018, ISSN: 0165-9936. DOI: <https://doi.org/10.1016/j.trac.2018.10.015>. [Online]. Available: <https://www.sciencedirect.com/science/article/pii/S0165993618300633>.
- [316] Y. Gloaguen, J. A. Kirwan, and D. Beule, “Deep learning-assisted peak curation for large-scale lc-ms metabolomics,” *Analytical Chemistry*, vol. 94, no. 12, pp. 4930–4937, 2022, PMID: 35290737. DOI: 10.1021/acs.analchem.1c02220. [Online]. Available: <https://doi.org/10.1021/acs.analchem.1c02220>.
- [317] N. Schauer *et al.*, “Gc–ms libraries for the rapid identification of metabolites in complex biological samples,” *FEBS Letters*, vol. 579, no. 6, pp. 1332–1337, 2005, ISSN: 0014-5793. DOI: <https://doi.org/10.1016/j.febslet.2005.01.029>. [Online]. Available: <https://www.sciencedirect.com/science/article/pii/S0014579305001183>.
- [318] S. L. Nam, A. P. de la Mata, and J. J. Harynyuk, “Automated screening and filtering scripts for gc×gc-tofms metabolomics data,” *Separations*, vol. 8, no. 6, 2021, ISSN: 2297-8739. DOI: 10.3390/separations8060084. [Online]. Available: <https://www.mdpi.com/2297-8739/8/6/84>.
- [319] G. S. Groenewold *et al.*, “Pyrolysis two-dimensional gc-ms of miscanthus biomass: Quantitative measurement using an internal standard method,” *Energy & Fuels*, vol. 31, no. 2, pp. 1620–1630, 2017. DOI: 10.1021/acs.energyfuels.6b02645. [Online]. Available: <https://doi.org/10.1021/acs.energyfuels.6b02645>.
- [320] S. P. Urbanski, W. M. Hao, and S. Baker, “Chapter 4 chemical composition of wildland fire emissions,” in *Wildland Fires and Air Pollution*, ser. Developments in Environmental Science, A. Bytnerowicz, M. J. Arbaugh, A. R. Riebau, and C. Andersen, Eds., vol. 8, Elsevier, 2008, pp. 79–107. DOI: [https://doi.org/10.1016/S1474-8177\(08\)00004-1](https://doi.org/10.1016/S1474-8177(08)00004-1). [Online]. Available: <https://www.sciencedirect.com/science/article/pii/S1474817708000041>.
- [321] M. S. Armstrong, A. P. de la Mata, and J. J. Harynyuk, “An efficient and accurate numerical determination of the cluster resolution metric in two dimensions,” *Journal of Chemometrics*, vol. 35, no. 7-8, e3346, 2021. DOI: <https://doi.org/10.1002/cem.3346>. [Online]. Available: <https://analyticalsciencejournals.onlinelibrary.wiley.com/doi/abs/10.1002/cem.3346>.
- [322] N. A. Sinkov and J. J. Harynyuk, “Cluster resolution: A metric for automated, objective and optimized feature selection in chemometric modeling,” *Talanta*, vol. 83, no. 4, pp. 1079–1087, 2011, Enhancing Chemical Separations with Chemometric Data Analysis, ISSN: 0039-9140. DOI: <https://doi.org/10.1016/>

- j.talanta.2010.10.025. [Online]. Available: <https://www.sciencedirect.com/science/article/pii/S0039914010008210>.
- [323] Y. Song, S. Xie, Y. Zhang, L. Zeng, L. G. Salmon, and M. Zheng, "Source apportionment of pm2.5 in beijing using principal component analysis/absolute principal component scores and unmix," *Science of The Total Environment*, vol. 372, no. 1, pp. 278–286, 2006, ISSN: 0048-9697. DOI: <https://doi.org/10.1016/j.scitotenv.2006.08.041>. [Online]. Available: <https://www.sciencedirect.com/science/article/pii/S0048969706006760>.
- [324] Y. Choi *et al.*, "Survey of whole air data from the second airborne biomass burning and lightning experiment using principal component analysis," *Journal of Geophysical Research: Atmospheres*, vol. 108, no. D5, 2003. DOI: <https://doi.org/10.1029/2002JD002841>. [Online]. Available: <https://agupubs.onlinelibrary.wiley.com/doi/abs/10.1029/2002JD002841>.
- [325] K. Ravindra, T. Singh, V. Singh, S. Chintalapati, G. Beig, and S. Mor, "Understanding the influence of summer biomass burning on air quality in north india: Eight cities field campaign study," *Science of The Total Environment*, vol. 861, p. 160 361, 2023, ISSN: 0048-9697. DOI: <https://doi.org/10.1016/j.scitotenv.2022.160361>. [Online]. Available: <https://www.sciencedirect.com/science/article/pii/S0048969722074630>.
- [326] M. Wang *et al.*, "To distinguish the primary characteristics of agro-waste biomass by the principal component analysis: An investigation in east china," *Waste Management*, vol. 90, pp. 100–120, 2019, ISSN: 0956-053X. DOI: <https://doi.org/10.1016/j.wasman.2019.04.046>. [Online]. Available: <https://www.sciencedirect.com/science/article/pii/S0956053X19302594>.
- [327] W. Li *et al.*, "Tracers from biomass burning emissions and identification of biomass burning," *Atmosphere*, vol. 12, no. 11, 2021, ISSN: 2073-4433. DOI: [10.3390/atmos12111401](https://doi.org/10.3390/atmos12111401). [Online]. Available: <https://www.mdpi.com/2073-4433/12/11/1401>.
- [328] N. G. Lewis and L. B. Davin, "1.25 - lignans: Biosynthesis and function," in *Comprehensive Natural Products Chemistry*, S. D. Barton, K. Nakanishi, and O. Meth-Cohn, Eds., Oxford: Pergamon, 1999, pp. 639–712, ISBN: 978-0-08-091283-7. DOI: <https://doi.org/10.1016/B978-0-08-091283-7.00027-8>. [Online]. Available: <https://www.sciencedirect.com/science/article/pii/B9780080912837000278>.
- [329] J. del Río, M. Speranza, A. Gutiérrez, M. Martínez, and A. Martínez, "Lignin attack during eucalypt wood decay by selected basidiomycetes: A py-gc/ms study," *Journal of Analytical and Applied Pyrolysis*, vol. 64, no. 2, pp. 421–431, 2002, ISSN: 0165-2370. DOI: [https://doi.org/10.1016/S0165-2370\(02\)00043-8](https://doi.org/10.1016/S0165-2370(02)00043-8). [Online]. Available: <https://www.sciencedirect.com/science/article/pii/S0165237002000438>.

- [330] E. Bae, J.-G. Na, S. H. Chung, H. S. Kim, and S. Kim, "Identification of about 30000 chemical components in shale oils by electrospray ionization (esi) and atmospheric pressure photoionization (appi) coupled with 15 t fourier transform ion cyclotron resonance mass spectrometry (ft-icr ms) and a comparison to conventional oil," *Energy & Fuels*, vol. 24, no. 4, pp. 2563–2569, 2010. DOI: 10.1021/ef100060b. [Online]. Available: <https://doi.org/10.1021/ef100060b>.
- [331] B. P. Koch and T. Dittmar, "From mass to structure: An aromaticity index for high-resolution mass data of natural organic matter," *Rapid Communications in Mass Spectrometry*, vol. 20, no. 5, pp. 926–932, 2006. DOI: <https://doi.org/10.1002/rcm.2386>. [Online]. Available: <https://analyticalsciencejournals.onlinelibrary.wiley.com/doi/abs/10.1002/rcm.2386>.
- [332] H. Tong *et al.*, "Molecular composition of organic aerosols at urban background and road tunnel sites using ultra-high resolution mass spectrometry," *Faraday Discuss.*, vol. 189, pp. 51–68, 0 2016. DOI: 10.1039/C5FD00206K. [Online]. Available: <http://dx.doi.org/10.1039/C5FD00206K>.
- [333] J.-H. Park, Z. B. Babar, S. J. Baek, H. S. Kim, and H.-J. Lim, "Effects of nox on the molecular composition of secondary organic aerosol formed by the ozonolysis and photooxidation of α -pinene," *Atmospheric Environment*, vol. 166, pp. 263–275, 2017, ISSN: 1352-2310. DOI: <https://doi.org/10.1016/j.atmosenv.2017.07.022>. [Online]. Available: <https://www.sciencedirect.com/science/article/pii/S1352231017304636>.
- [334] Y. Wei, T. Cao, and J. E. Thompson, "The chemical evolution & physical properties of organic aerosol: A molecular structure based approach," *Atmospheric Environment*, vol. 62, pp. 199–207, 2012, ISSN: 1352-2310. DOI: <https://doi.org/10.1016/j.atmosenv.2012.08.029>. [Online]. Available: <https://www.sciencedirect.com/science/article/pii/S1352231012008011>.
- [335] K. O. Johansson *et al.*, "Formation and emission of large furans and oxygenated hydrocarbons from flames," *Proceedings of the National Academy of Sciences*, vol. 113, no. 30, pp. 8374–8379, 2016. DOI: 10.1073/pnas.1604772113. [Online]. Available: <https://www.pnas.org/doi/abs/10.1073/pnas.1604772113>.
- [336] S. Rowat, "Incinerator toxic emissions: A brief summary of human health effects with a note on regulatory control," *Medical Hypotheses*, vol. 52, no. 5, pp. 389–396, 1999, ISSN: 0306-9877. DOI: <https://doi.org/10.1054/mehy.1994.0675>. [Online]. Available: <https://www.sciencedirect.com/science/article/pii/S030698778470675X>.
- [337] X. Liao *et al.*, "Contamination profiles and health impact of benzothiazole and its derivatives in pm2.5 in typical chinese cities," *Science of The Total Environment*, vol. 755, p. 142617, 2021, ISSN: 0048-9697. DOI: <https://doi.org/10.1016/j.scitotenv.2020.142617>. [Online]. Available: <https://www.sciencedirect.com/science/article/pii/S0048969720361465>.

- [338] J. Chen *et al.*, “A review of biomass burning: Emissions and impacts on air quality, health and climate in china,” *Science of The Total Environment*, vol. 579, pp. 1000–1034, 2017, ISSN: 0048-9697. DOI: <https://doi.org/10.1016/j.scitotenv.2016.11.025>. [Online]. Available: <https://www.sciencedirect.com/science/article/pii/S0048969716324561>.
- [339] V. Vakkari *et al.*, “Rapid changes in biomass burning aerosols by atmospheric oxidation,” *Geophysical Research Letters*, vol. 41, no. 7, pp. 2644–2651, 2014. DOI: <https://doi.org/10.1002/2014GL059396>. [Online]. Available: <https://agupubs.onlinelibrary.wiley.com/doi/abs/10.1002/2014GL059396>.
- [340] M. Claeys *et al.*, “Chemical characterisation of humic-like substances from urban, rural and tropical biomass burning environments using liquid chromatography with uv/vis photodiode array detection and electrospray ionisation mass spectrometry,” *Environmental Chemistry*, vol. 9, no. 3, pp. 273–284, 2012. DOI: 10.1071/EN11163. [Online]. Available: <https://doi.org/10.1071/EN11163>.
- [341] S. N. Pandis, R. A. Harley, G. R. Cass, and J. H. Seinfeld, “Secondary organic aerosol formation and transport,” *Atmospheric Environment. Part A. General Topics*, vol. 26, no. 13, pp. 2269–2282, 1992, ISSN: 0960-1686. DOI: [https://doi.org/10.1016/0960-1686\(92\)90358-R](https://doi.org/10.1016/0960-1686(92)90358-R). [Online]. Available: <https://www.sciencedirect.com/science/article/pii/096016869290358R>.
- [342] P. J. Ziemann and R. Atkinson, “Kinetics, products, and mechanisms of secondary organic aerosol formation,” *Chem. Soc. Rev.*, vol. 41, pp. 6582–6605, 19 2012. DOI: 10.1039/C2CS35122F. [Online]. Available: <http://dx.doi.org/10.1039/C2CS35122F>.
- [343] V. Choudhary, T. Gupta, and R. Zhao, “Evolution of brown carbon aerosols during atmospheric long-range transport in the south asian outflow and himalayan cryosphere,” *ACS Earth and Space Chemistry*, vol. 6, no. 10, pp. 2335–2347, 2022. DOI: 10.1021/acsearthspacechem.2c00047. [Online]. Available: <https://doi.org/10.1021/acsearthspacechem.2c00047>.
- [344] B. Yuan, A. R. Koss, C. Warneke, M. Coggon, K. Sekimoto, and J. A. de Gouw, “Proton-transfer-reaction mass spectrometry: Applications in atmospheric sciences,” *Chemical Reviews*, vol. 117, no. 21, pp. 13 187–13 229, 2017, PMID: 28976748. DOI: 10.1021/acs.chemrev.7b00325. [Online]. Available: <https://doi.org/10.1021/acs.chemrev.7b00325>.
- [345] A. Bierbach, I. Barnes, K. H. Becker, and E. Wiesen, “Atmospheric chemistry of unsaturated carbonyls: Butenedial, 4-oxo-2-pentenal, 3-hexene-2, 5-dione, maleic anhydride, 3h-furan-2-one, and 5-methyl-3h-furan-2-one,” *Environmental science & technology*, vol. 28, no. 4, pp. 715–729, 1994.
- [346] L. Wang *et al.*, “Source characterization of volatile organic compounds measured by proton-transfer-reaction time-of-flight mass spectrometers in delhi, india,” *Atmospheric Chemistry and Physics*, vol. 20, no. 16, pp. 9753–9770, 2020. DOI: 10.5194/acp-20-9753-2020. [Online]. Available: <https://acp.copernicus.org/articles/20/9753/2020/>.

- [347] M. M. Coggon *et al.*, “Oh chemistry of non-methane organic gases (nmogs) emitted from laboratory and ambient biomass burning smoke: Evaluating the influence of furans and oxygenated aromatics on ozone and secondary nmog formation,” *Atmospheric Chemistry and Physics*, vol. 19, no. 23, pp. 14 875–14 899, 2019. DOI: 10.5194/acp-19-14875-2019. [Online]. Available: <https://acp.copernicus.org/articles/19/14875/2019/>.
- [348] P. S. Rickly *et al.*, “Influence of wildfire on urban ozone: An observationally constrained box modeling study at a site in the colorado front range,” *Environmental Science & Technology*, vol. 57, no. 3, pp. 1257–1267, 2023, PMID: 36607321. DOI: 10.1021/acs.est.2c06157. [Online]. Available: <https://doi.org/10.1021/acs.est.2c06157>.
- [349] A. C. D. Rivett and N. V. Sidgwick, “Clvii.—the rate of hydration of acid anhydrides: Succinic, methylsuccinic, itaconic, maleic, citraconic, and phthalic,” *J. Chem. Soc., Trans.*, vol. 97, pp. 1677–1686, 0 1910. DOI: 10.1039/CT9109701677. [Online]. Available: <http://dx.doi.org/10.1039/CT9109701677>.
- [350] J. Rosenfeld and C. Murphy, “Hydrolysis study of organic acid anhydrides by differential thermal analysis—ii: Maleic anhydride and trimellitic anhydride,” *Talanta*, vol. 14, no. 1, pp. 91–96, 1967, ISSN: 0039-9140. DOI: [https://doi.org/10.1016/0039-9140\(67\)80050-X](https://doi.org/10.1016/0039-9140(67)80050-X). [Online]. Available: <https://www.sciencedirect.com/science/article/pii/003991406780050X>.
- [351] B. R. T. Simoneit *et al.*, “Composition and major sources of organic compounds of aerosol particulate matter sampled during the ace-asia campaign,” *Journal of Geophysical Research: Atmospheres*, vol. 109, no. D19, 2004. DOI: <https://doi.org/10.1029/2004JD004598>. [Online]. Available: <https://agupubs.onlinelibrary.wiley.com/doi/abs/10.1029/2004JD004598>.
- [352] K. E. Kautzman *et al.*, “Chemical composition of gas- and aerosol-phase products from the photooxidation of naphthalene,” *The Journal of Physical Chemistry A*, vol. 114, no. 2, pp. 913–934, 2010, PMID: 19904975. DOI: 10.1021/jp908530s. [Online]. Available: <https://doi.org/10.1021/jp908530s>.
- [353] T. E. Kleindienst, M. Jaoui, M. Lewandowski, J. H. Offenberg, and K. S. Docherty, “The formation of soa and chemical tracer compounds from the photooxidation of naphthalene and its methyl analogs in the presence and absence of nitrogen oxides,” *Atmospheric Chemistry and Physics*, vol. 12, no. 18, pp. 8711–8726, 2012. DOI: 10.5194/acp-12-8711-2012. [Online]. Available: <https://acp.copernicus.org/articles/12/8711/2012/>.
- [354] Y. Zhao *et al.*, “Insights into secondary organic aerosol formation mechanisms from measured gas/particle partitioning of specific organic tracer compounds,” *Environmental Science & Technology*, vol. 47, no. 8, pp. 3781–3787, 2013, PMID: 23448102. DOI: 10.1021/es304587x. [Online]. Available: <https://doi.org/10.1021/es304587x>.

- [355] A. A. May, R. Saleh, C. J. Hennigan, N. M. Donahue, and A. L. Robinson, “Volatility of organic molecular markers used for source apportionment analysis: Measurements and implications for atmospheric lifetime,” *Environmental Science & Technology*, vol. 46, no. 22, pp. 12 435–12 444, 2012, PMID: 23013599. DOI: 10.1021/es302276t. [Online]. Available: <https://doi.org/10.1021/es302276t>.
- [356] M. Shrivastava *et al.*, “Global long-range transport and lung cancer risk from polycyclic aromatic hydrocarbons shielded by coatings of organic aerosol,” *Proceedings of the National Academy of Sciences*, vol. 114, no. 6, pp. 1246–1251, 2017. DOI: 10.1073/pnas.1618475114. [Online]. Available: <https://www.pnas.org/doi/abs/10.1073/pnas.1618475114>.
- [357] Q. Mu *et al.*, “Temperature effect on phase state and reactivity controls atmospheric multiphase chemistry and transport of pahs,” *Science Advances*, vol. 4, no. 3, eaap7314, 2018. DOI: 10.1126/sciadv.aap7314. [Online]. Available: <https://www.science.org/doi/abs/10.1126/sciadv.aap7314>.
- [358] Y. Chen, P. McDaid, and L. Deng, “Asymmetric alcoholysis of cyclic anhydrides,” *Chemical Reviews*, vol. 103, no. 8, pp. 2965–2984, 2003, PMID: 12914488. DOI: 10.1021/cr020037x. [Online]. Available: <https://doi.org/10.1021/cr020037x>.
- [359] H. O. T. Pye *et al.*, “The acidity of atmospheric particles and clouds,” *Atmospheric Chemistry and Physics*, vol. 20, no. 8, pp. 4809–4888, 2020. DOI: 10.5194/acp-20-4809-2020. [Online]. Available: <https://acp.copernicus.org/articles/20/4809/2020/>.
- [360] J. Park, A. L. Gomez, M. L. Walser, A. Lin, and S. A. Nizkorodov, “Ozonolysis and photolysis of alkene-terminated self-assembled monolayers on quartz nanoparticles: Implications for photochemical aging of organic aerosol particles,” *Phys. Chem. Chem. Phys.*, vol. 8, pp. 2506–2512, 21 2006. DOI: 10.1039/B602704K. [Online]. Available: <http://dx.doi.org/10.1039/B602704K>.
- [361] J. He, B. Zielinska, and R. Balasubramanian, “Composition of semi-volatile organic compounds in the urban atmosphere of singapore: Influence of biomass burning,” *Atmospheric Chemistry and Physics*, vol. 10, no. 23, pp. 11 401–11 413, 2010. DOI: 10.5194/acp-10-11401-2010. [Online]. Available: <https://acp.copernicus.org/articles/10/11401/2010/>.
- [362] J. J. Schauer, M. P. Fraser, G. R. Cass, and B. R. T. Simoneit, “Source reconciliation of atmospheric gas-phase and particle-phase pollutants during a severe photochemical smog episode,” *Environmental Science & Technology*, vol. 36, no. 17, pp. 3806–3814, 2002, PMID: 12322754. DOI: 10.1021/es011458j. [Online]. Available: <https://doi.org/10.1021/es011458j>.
- [363] P. M. Fine, B. Chakrabarti, M. Krudysz, J. J. Schauer, and C. Sioutas, “Diurnal variations of individual organic compound constituents of ultrafine and accumulation mode particulate matter in the los angeles basin,” *Environmental Science & Technology*, vol. 38, no. 5, pp. 1296–1304, 2004, PMID:

15046329. DOI: 10.1021/es0348389. [Online]. Available: <https://doi.org/10.1021/es0348389>.
- [364] Y.-L. Zhang, K. Kawamura, T. Watanabe, S. Hatakeyama, A. Takami, and W. Wang, “New directions: Need for better understanding of source and formation process of phthalic acid in aerosols as inferred from aircraft observations over china,” *Atmospheric Environment*, vol. 140, pp. 147–149, 2016, ISSN: 1352-2310. DOI: <https://doi.org/10.1016/j.atmosenv.2016.05.058>. [Online]. Available: <https://www.sciencedirect.com/science/article/pii/S135223101630406X>.
- [365] D. Hoffmann, Y. Iinuma, and H. Herrmann, “Development of a method for fast analysis of phenolic molecular markers in biomass burning particles using high performance liquid chromatography/atmospheric pressure chemical ionisation mass spectrometry,” *Journal of Chromatography A*, vol. 1143, no. 1, pp. 168–175, 2007, ISSN: 0021-9673. DOI: <https://doi.org/10.1016/j.chroma.2007.01.035>. [Online]. Available: <https://www.sciencedirect.com/science/article/pii/S0021967307000726>.
- [366] A. P. Mouat, C. Paton-Walsh, J. B. Simmons, J. Ramirez-Gamboa, D. W. T. Griffith, and J. Kaiser, “Measurement report: Observations of long-lived volatile organic compounds from the 2019–2020 australian wildfires during the coala campaign,” *Atmospheric Chemistry and Physics*, vol. 22, no. 17, pp. 11 033–11 047, 2022. DOI: 10.5194/acp-22-11033-2022. [Online]. Available: <https://acp.copernicus.org/articles/22/11033/2022/>.
- [367] J. Y. Lee, D. A. Lane, J. B. Heo, S.-M. Yi, and Y. P. Kim, “Quantification and seasonal pattern of atmospheric reaction products of gas phase pahs in pm2.5,” *Atmospheric Environment*, vol. 55, pp. 17–25, 2012, ISSN: 1352-2310. DOI: <https://doi.org/10.1016/j.atmosenv.2012.03.007>. [Online]. Available: <https://www.sciencedirect.com/science/article/pii/S1352231012002397>.
- [368] G. D. Smith, E. Woods, C. L. DeForest, T. Baer, and R. E. Miller, “Reactive uptake of ozone by oleic acid aerosol particles: Application of single-particle mass spectrometry to heterogeneous reaction kinetics,” *The Journal of Physical Chemistry A*, vol. 106, no. 35, pp. 8085–8095, 2002. DOI: 10.1021/jp020527t. [Online]. Available: <https://doi.org/10.1021/jp020527t>.
- [369] S. Gross, R. Iannone, S. Xiao, and A. K. Bertram, “Reactive uptake studies of no3 and n2o5 on alkenoic acid, alkanoate, and polyalcohol substrates to probe nighttime aerosol chemistry,” *Phys. Chem. Chem. Phys.*, vol. 11, pp. 7792–7803, 36 2009. DOI: 10.1039/B904741G. [Online]. Available: <http://dx.doi.org/10.1039/B904741G>.
- [370] T. Nah, S. H. Kessler, K. E. Daumit, J. H. Kroll, S. R. Leone, and K. R. Wilson, “Influence of molecular structure and chemical functionality on the heterogeneous oh-initiated oxidation of unsaturated organic particles,” *The Journal of Physical Chemistry A*, vol. 118, no. 23, pp. 4106–4119, 2014, PMID: 24840787. DOI: 10.1021/jp502666g. [Online]. Available: <https://doi.org/10.1021/jp502666g>.

- [371] T. Berkemeier, A. Mishra, C. Mattei, A. J. Huisman, U. K. Krieger, and U. Pöschl, “Ozonolysis of oleic acid aerosol revisited: Multiphase chemical kinetics and reaction mechanisms,” *ACS Earth and Space Chemistry*, vol. 5, no. 12, pp. 3313–3323, 2021. DOI: 10.1021/acsearthspacechem.1c00232. [Online]. Available: <https://doi.org/10.1021/acsearthspacechem.1c00232>.
- [372] J. N. Crowley *et al.*, “Evaluated kinetic and photochemical data for atmospheric chemistry: Volume v – heterogeneous reactions on solid substrates,” *Atmospheric Chemistry and Physics*, vol. 10, no. 18, pp. 9059–9223, 2010. DOI: 10.5194/acp-10-9059-2010. [Online]. Available: <https://acp.copernicus.org/articles/10/9059/2010/>.
- [373] F. A. Houle, W. D. Hinsberg, and K. R. Wilson, “Oxidation of a model alkane aerosol by oh radical: The emergent nature of reactive uptake,” *Phys. Chem. Chem. Phys.*, vol. 17, pp. 4412–4423, 6 2015. DOI: 10.1039/C4CP05093B. [Online]. Available: <http://dx.doi.org/10.1039/C4CP05093B>.
- [374] D. A. Knopf, U. Pöschl, and M. Shiraiwa, “Radial diffusion and penetration of gas molecules and aerosol particles through laminar flow reactors, denuders, and sampling tubes,” *Analytical Chemistry*, vol. 87, no. 7, pp. 3746–3754, 2015, PMID: 25744622. DOI: 10.1021/ac5042395. [Online]. Available: <https://doi.org/10.1021/ac5042395>.
- [375] M. J. Tang, M. Shiraiwa, U. Pöschl, R. A. Cox, and M. Kalberer, “Compilation and evaluation of gas phase diffusion coefficients of reactive trace gases in the atmosphere: Volume 2. diffusivities of organic compounds, pressure-normalised mean free paths, and average knudsen numbers for gas uptake calculations,” *Atmospheric Chemistry and Physics*, vol. 15, no. 10, pp. 5585–5598, 2015. DOI: 10.5194/acp-15-5585-2015. [Online]. Available: <https://acp.copernicus.org/articles/15/5585/2015/>.
- [376] N. FUCHS and A. SUTUGIN, “High-dispersed aerosols,” in *Topics in Current Aerosol Research*, ser. International Reviews in Aerosol Physics and Chemistry, G. HIDY and J. BROCK, Eds., Pergamon, 1971, p. 1. DOI: <https://doi.org/10.1016/B978-0-08-016674-2.50006-6>. [Online]. Available: <https://www.sciencedirect.com/science/article/pii/B9780080166742500066>.
- [377] R. Zhao *et al.*, “The role of water in organic aerosol multiphase chemistry: Focus on partitioning and reactivity,” in *Advances in Atmospheric Chemistry*. World Scientific Publishing, Feb. 2017, ch. 2, pp. 95–184. DOI: 10.1142/9789813147355_0002. [Online]. Available: https://www.worldscientific.com/doi/abs/10.1142/9789813147355_0002.
- [378] J. H. Hu, Q. Shi, P. Davidovits, D. R. Worsnop, M. S. Zahniser, and C. E. Kolb, “Reactive uptake of $\text{Cl}_2(\text{g})$ and $\text{Br}_2(\text{g})$ by aqueous surfaces as a function of Br^- and I^- ion concentration: The effect of chemical reaction at the interface,” *The Journal of Physical Chemistry*, vol. 99, no. 21, pp. 8768–8776, 1995. DOI: 10.1021/j100021a050. [Online]. Available: <https://doi.org/10.1021/j100021a050>.

- [379] Q. Zou, H. Song, M. Tang, and K. Lu, "Measurements of ho₂ uptake coefficient on aqueous (nh₄)₂so₄ aerosol using aerosol flow tube with lif system," *Chinese Chemical Letters*, vol. 30, no. 12, pp. 2236–2240, 2019, ISSN: 1001-8417. DOI: <https://doi.org/10.1016/j.cclet.2019.07.041>. [Online]. Available: <https://www.sciencedirect.com/science/article/pii/S1001841719304231>.
- [380] J. Liggió and S.-M. Li, "Reactive uptake of pinonaldehyde on acidic aerosols," *Journal of Geophysical Research: Atmospheres*, vol. 111, no. D24, 2006. DOI: <https://doi.org/10.1029/2005JD006978>. [Online]. Available: <https://agupubs.onlinelibrary.wiley.com/doi/abs/10.1029/2005JD006978>.
- [381] A. Jammoul, S. Gligorovski, C. George, and B. D'Anna, "Photosensitized heterogeneous chemistry of ozone on organic films," *The Journal of Physical Chemistry A*, vol. 112, no. 6, pp. 1268–1276, 2008, PMID: 18205335. DOI: [10.1021/jp074348t](https://doi.org/10.1021/jp074348t). [Online]. Available: <https://doi.org/10.1021/jp074348t>.
- [382] S. A. Styler, M. Brigante, B. D'Anna, C. George, and D. J. Donaldson, "Photoenhanced ozone loss on solid pyrene films," *Phys. Chem. Chem. Phys.*, vol. 11, pp. 7876–7884, 36 2009. DOI: [10.1039/B904180J](https://doi.org/10.1039/B904180J). [Online]. Available: <http://dx.doi.org/10.1039/B904180J>.
- [383] G. Gržinić, T. Bartels-Rausch, T. Berkemeier, A. Türler, and M. Ammann, "Viscosity controls humidity dependence of n₂o₅ uptake to citric acid aerosol," *Atmospheric Chemistry and Physics*, vol. 15, no. 23, pp. 13 615–13 625, 2015. DOI: [10.5194/acp-15-13615-2015](https://doi.org/10.5194/acp-15-13615-2015). [Online]. Available: <https://acp.copernicus.org/articles/15/13615/2015/>.
- [384] L. A. Goldberger, L. G. Jahl, J. A. Thornton, and R. C. Sullivan, "N₂o₅ reactive uptake kinetics and chlorine activation on authentic biomass-burning aerosol," *Environ. Sci.: Processes Impacts*, vol. 21, pp. 1684–1698, 10 2019. DOI: [10.1039/C9EM00330D](https://doi.org/10.1039/C9EM00330D). [Online]. Available: <http://dx.doi.org/10.1039/C9EM00330D>.
- [385] R. P. Staiger and E. B. Miller, "Isatoic anhydride. iv. reactions with various nucleophiles," *The Journal of Organic Chemistry*, vol. 24, no. 9, pp. 1214–1219, 1959. DOI: [10.1021/jo01091a013](https://doi.org/10.1021/jo01091a013). [Online]. Available: <https://doi.org/10.1021/jo01091a013>.
- [386] X. Liu and J. W. Locasale, "Metabolomics: A primer," *Trends in Biochemical Sciences*, vol. 42, no. 4, pp. 274–284, Apr. 2017, ISSN: 0968-0004. DOI: [10.1016/j.tibs.2017.01.004](https://doi.org/10.1016/j.tibs.2017.01.004). [Online]. Available: <https://doi.org/10.1016/j.tibs.2017.01.004>.
- [387] L. Lin, M. L. Lee, and D. J. Eatough, "Gas chromatographic analysis of organic marker compounds in fine particulate matter using solid-phase microextraction," *Journal of the Air & Waste Management Association*, vol. 57, no. 1, pp. 53–58, 2007. DOI: [10.1080/10473289.2007.10465295](https://doi.org/10.1080/10473289.2007.10465295). [Online]. Available: <https://doi.org/10.1080/10473289.2007.10465295>.

- [388] S. Wu, E. Kim, D. Vethanayagam, and R. Zhao, "Indoor partitioning and potential thirdhand exposure to carbonyl flavoring agents added in e-cigarettes and hookah tobacco," *Environ. Sci.: Processes Impacts*, vol. 24, pp. 2294–2309, 12 2022. DOI: 10.1039/D2EM00365A. [Online]. Available: <http://dx.doi.org/10.1039/D2EM00365A>.
- [389] S. Wu *et al.*, "Henry's law constants and indoor partitioning of microbial volatile organic compounds," *Environmental Science & Technology*, vol. 56, no. 11, pp. 7143–7152, 2022, PMID: 35522906. DOI: 10.1021/acs.est.1c07882. [Online]. Available: <https://doi.org/10.1021/acs.est.1c07882>.
- [390] H.-C. Wang and A.-R. Lee, "Recent developments in blood glucose sensors," *Journal of Food and Drug Analysis*, vol. 23, no. 2, pp. 191–200, 2015, ISSN: 1021-9498. DOI: <https://doi.org/10.1016/j.jfda.2014.12.001>. [Online]. Available: <https://www.sciencedirect.com/science/article/pii/S1021949815000174>.
- [391] H. E. Gottlieb, V. Kotlyar, and A. Nudelman, "Nmr chemical shifts of common laboratory solvents as trace impurities," *The Journal of Organic Chemistry*, vol. 62, no. 21, pp. 7512–7515, 1997, PMID: 11671879. DOI: 10.1021/jo971176v. [Online]. Available: <https://doi.org/10.1021/jo971176v>.

Appendix A: Chapter 2

A.1 Supplementary information for Chapter 2

A.1.1 Levoglucosan Derivatization

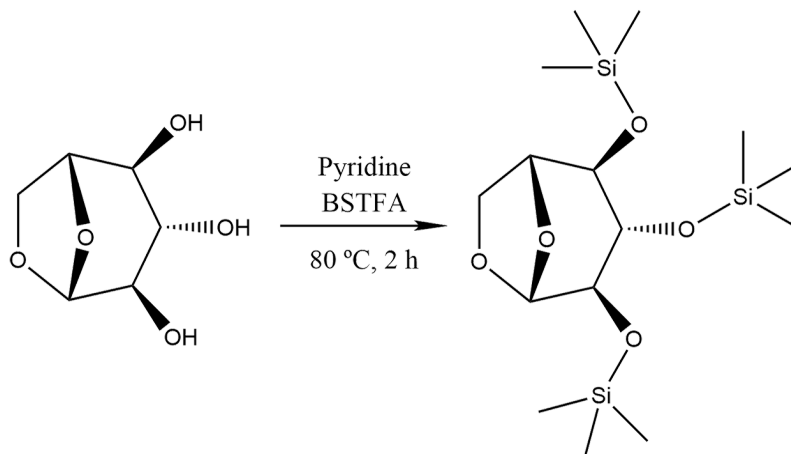


Figure A.1: Levoglucosan Derivatization Mechanism

Levoglucosan was silylated by heating in a water bath at 80 °C for 2 hours with the addition of pyridine and N,O-Bis(trimethylsilyl)trifluoroacetamide (BSTFA). Completion of the derivatization was confirmed from the absence of a GC-MS peak attributed to incompletely-derived levoglucosan.

A.1.2 Particle Emission from Biomass Burning

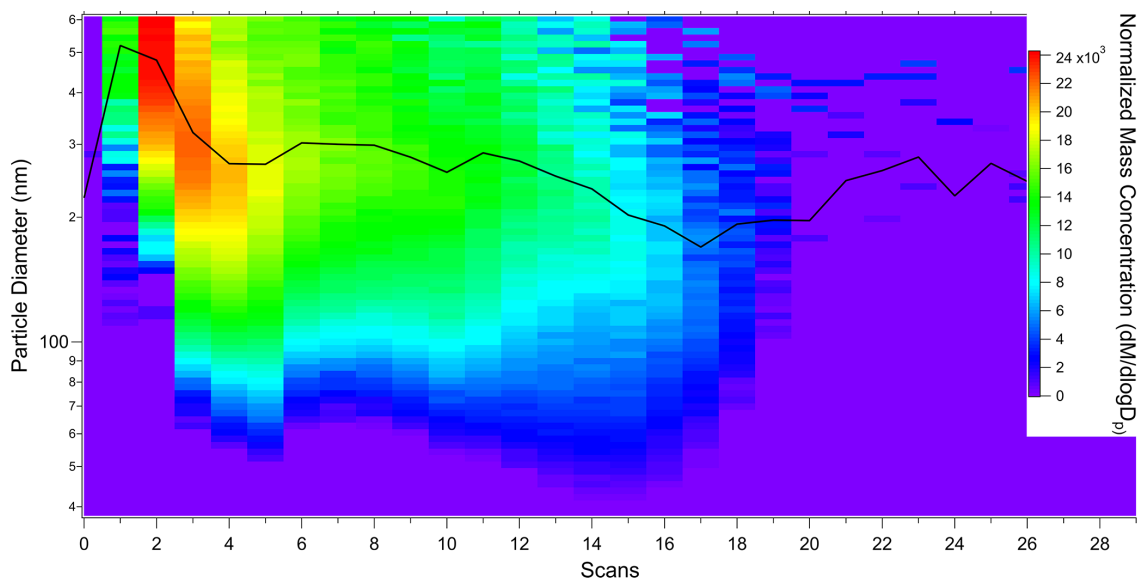


Figure A.2: Normalized mass concentration ($dM/d\log D_p$) and particle diameter (nm) of biomass burning emissions throughout the wood heating process. The heatmap represents the particle mass concentration (dM) in $\mu\text{g}/\text{m}^3$ normalized by the number of channels per decade of particle resolution ($d\log D_p$) of the instrument. The black line represents the median particle diameter.

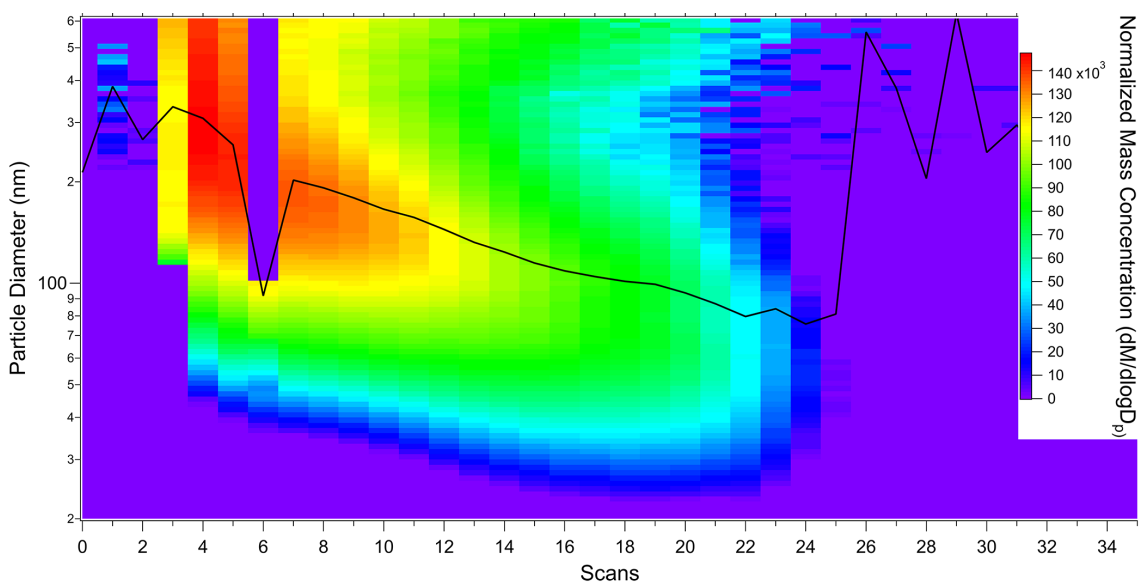


Figure A.3: Normalized mass concentration ($dM/d\log D_p$) and particle diameter (nm) of biomass burning emissions throughout the CAD heating process. The heatmap represents the particle mass concentration (dM) in $\mu\text{g}/\text{m}^3$ normalized by the number of channels per decade of particle resolution ($d\log D_p$) of the instrument. The black line represents the median particle diameter.

Here we present the particle emission data for wood and CAD, in addition to the IND available in the main text in Figure 2 to show the relative agreement between the fuels. Each scan represents a 2 minute interval. Note that as explained in the main text, the total number concentration appears different for each fuel due to the inability of the SMPS to maintain the flow state when pulling a small fraction of the vacuum.

A.1.3 Mass Absorption Coefficients

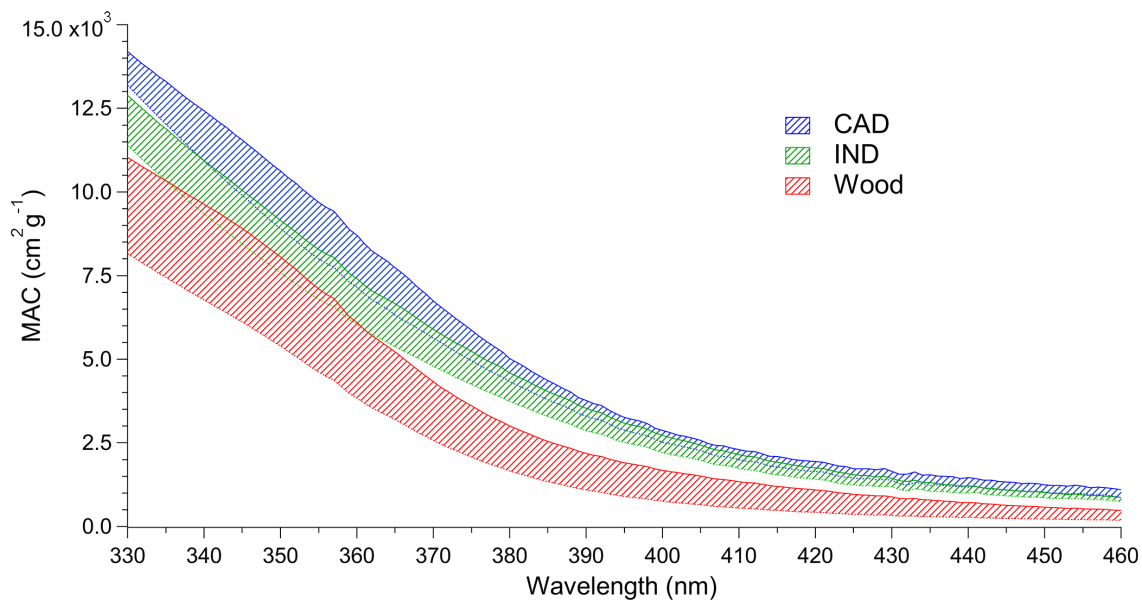


Figure A.4: Mass Absorption Coefficient of water soluble fraction of emissions from the three types of biomass fuels. The shaded area represents the difference between two burns.

The consistency between light absorption measurements is notable considering the isolated burns. Note that the mass absorption values are based on analyses with two separate instruments after extraction of the particulate matter, TOC/TN and UV-Vis.

A.1.4 Individual GC-MS Chromatograms

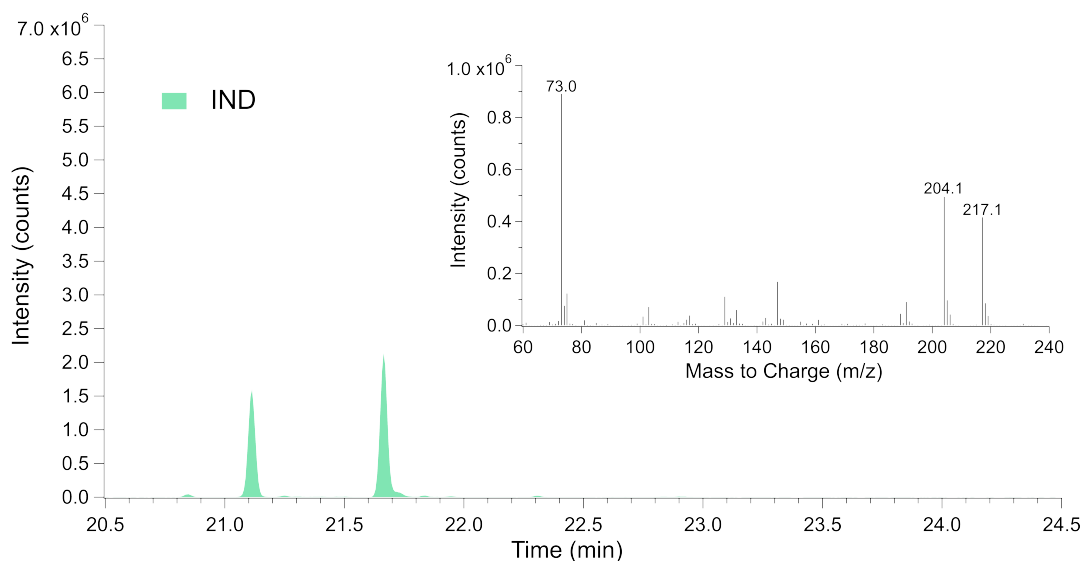


Figure A.5: GC-MS chromatogram of IND biomass burning filter extracts.

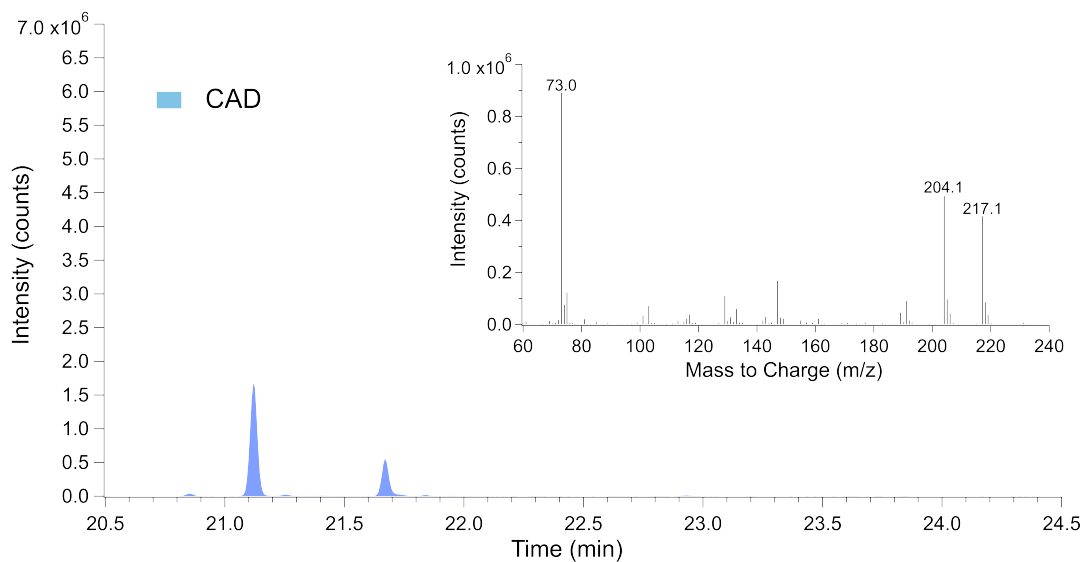


Figure A.6: GC-MS chromatogram of CAD biomass burning filter extracts.

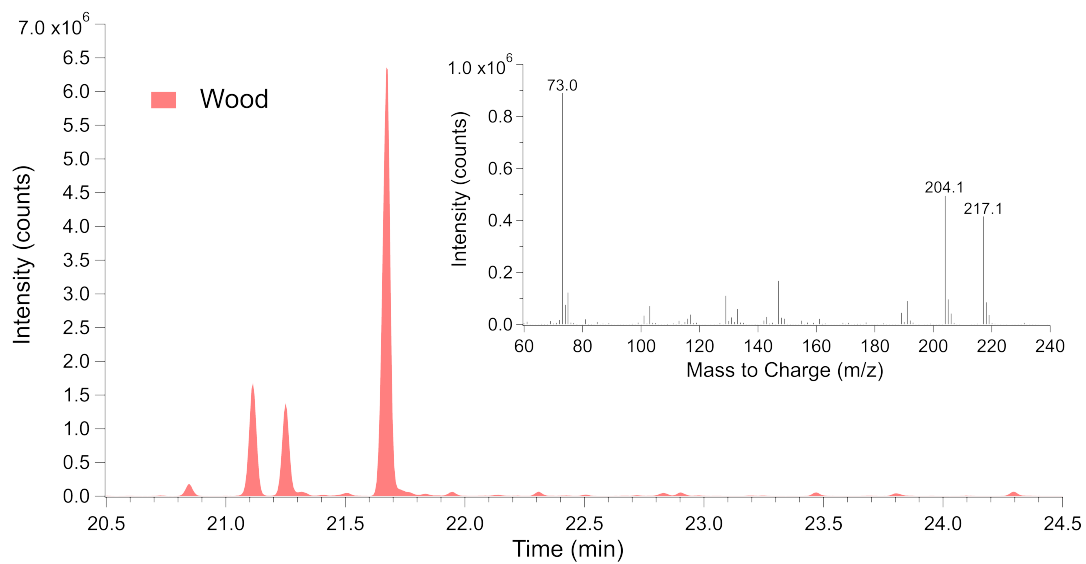


Figure A.7: GC-MS chromatogram of Wood biomass burning filter extracts.

A.1.5 Levoglucosan Fragmentation Pattern

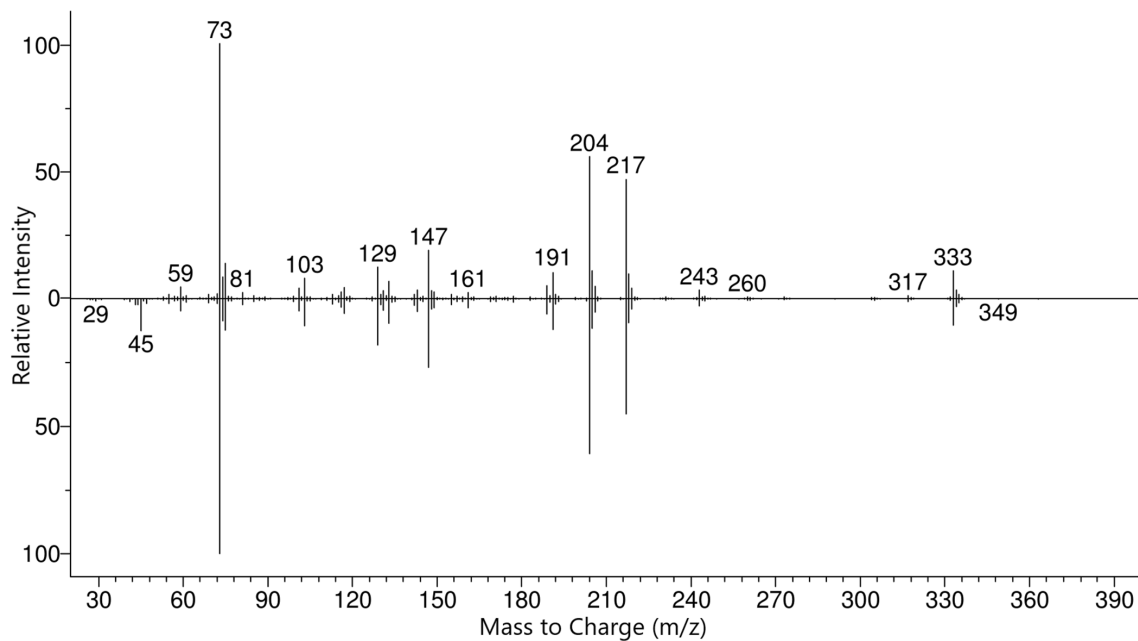


Figure A.8: Fragmentation pattern observed for silylated levoglucosan (top) vs NISTMS library pattern (bottom)

The mass spectrometer was set to detect only $m/z > 50$. Both the observed and library patterns contained the silylated levoglucosan molecular ion (MW of 378), with a relative intensity too low to appear in Figure A.8.

A.1.6 Individual ESI- MS Chromatograms

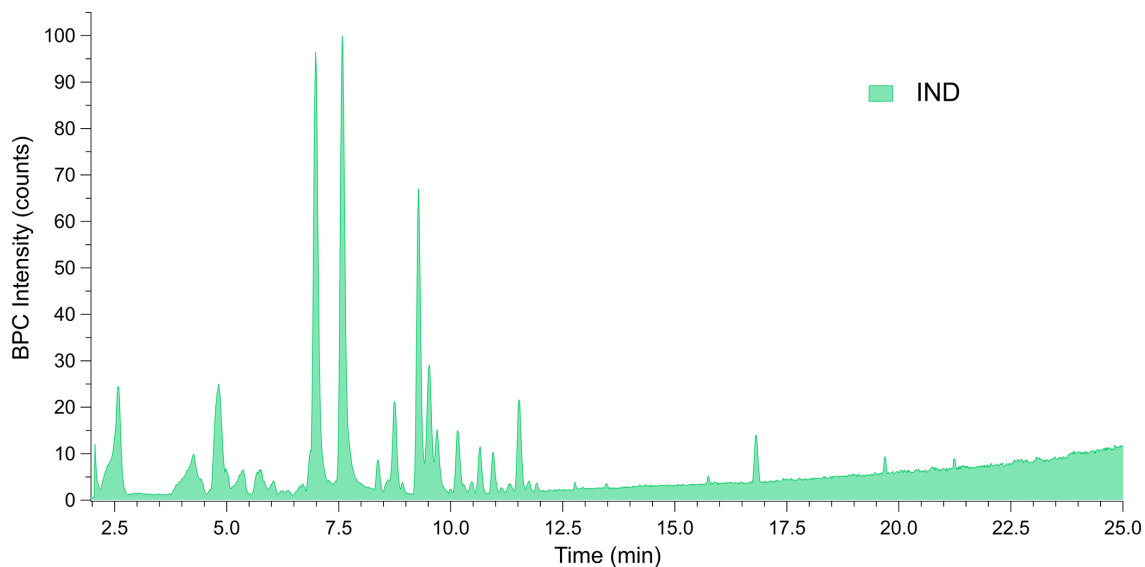


Figure A.9: ESI- LC-MS Base Peak Chromatogram (BPC) of IND biomass burning emissions.

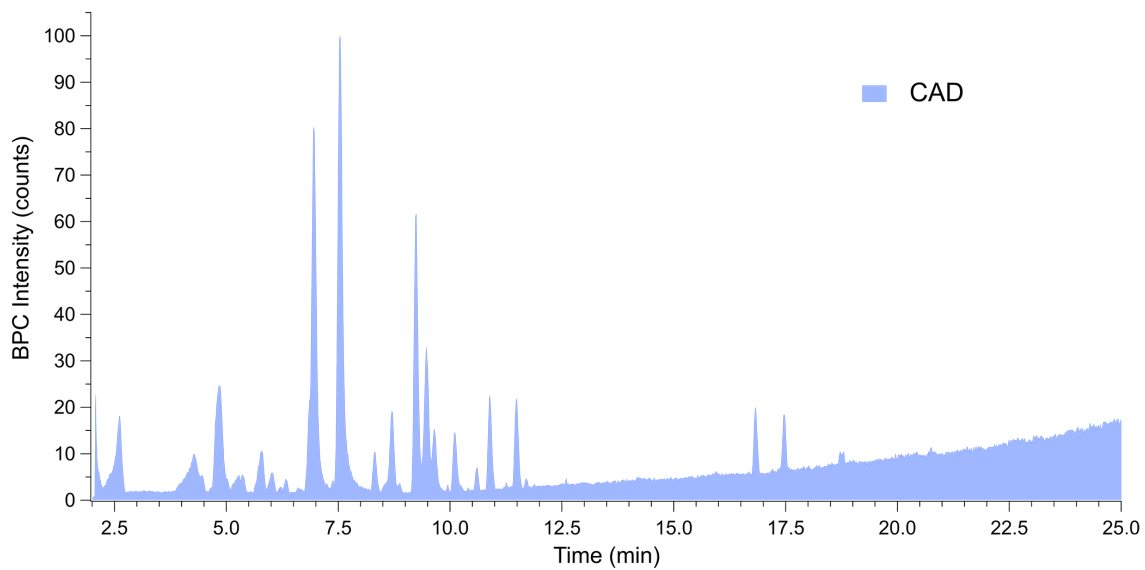


Figure A.10: ESI- LC-MS Base Peak Chromatogram (BPC) of CAD biomass burning emissions.

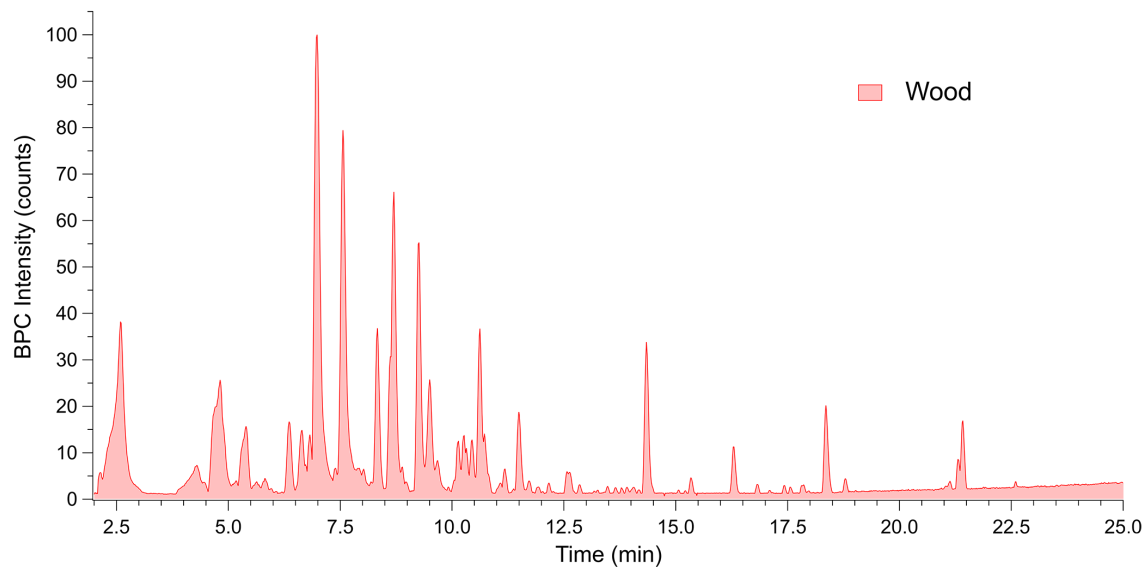


Figure A.11: ESI- LC-MS Base Peak Chromatogram (BPC) of Wood biomass burning emissions.

A.1.7 Individual ESI+ MS Chromatograms

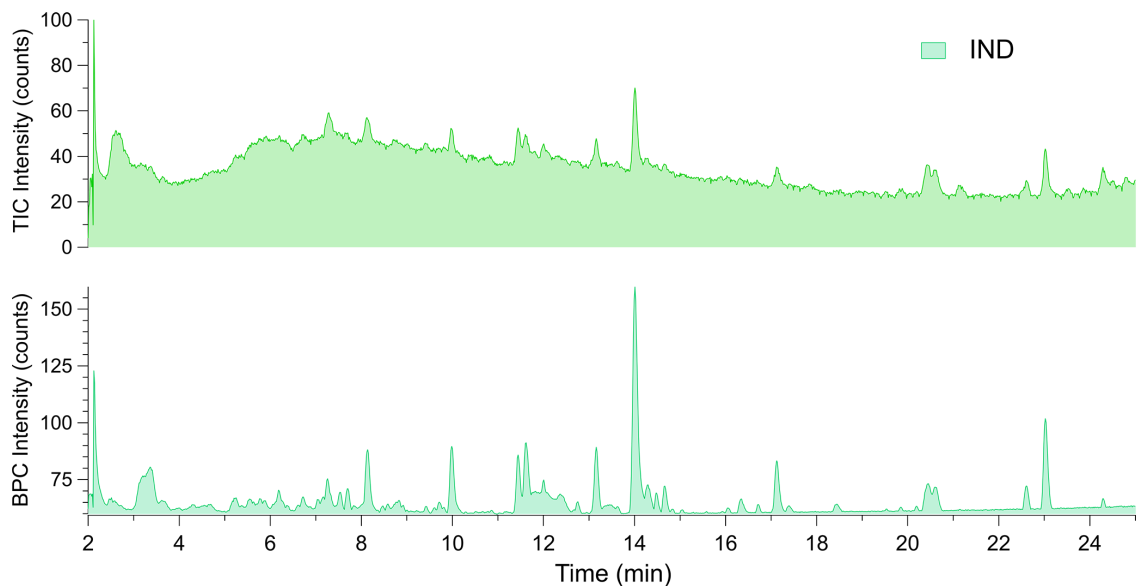


Figure A.12: Total Ion Chromatogram (TIC)(a) and Base Peak Chromatogram (BPC)(b) ESI+ LC-MS chromatograms of IND biomass burning emissions.

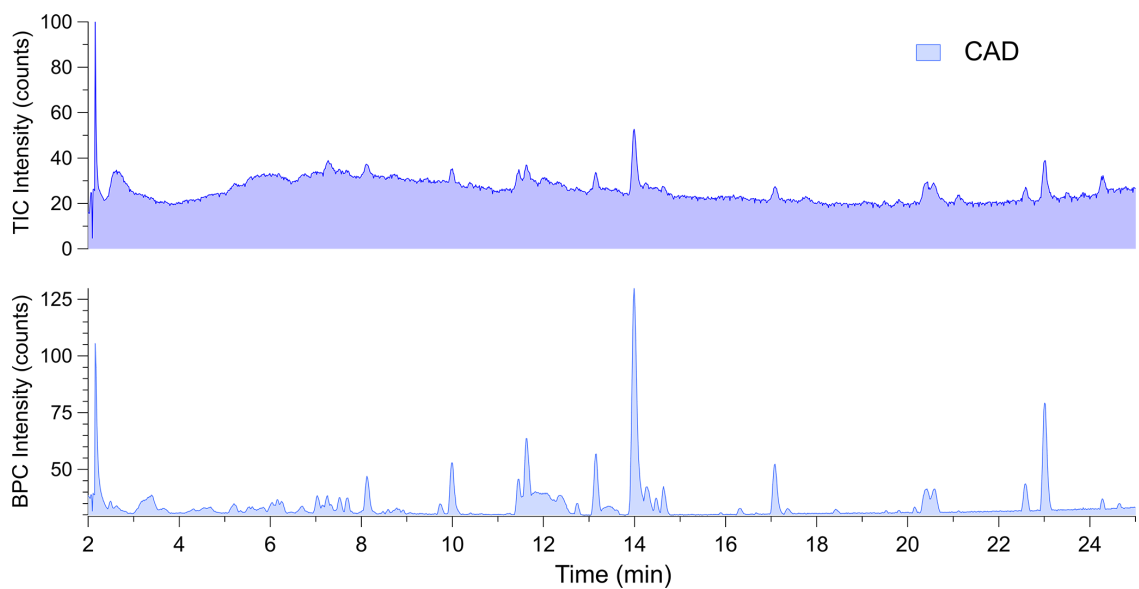


Figure A.13: Total Ion Chromatogram (TIC)(a) and Base Peak Chromatogram (BPC)(b) ESI+ LC-MS chromatograms of CAD biomass burning emissions.

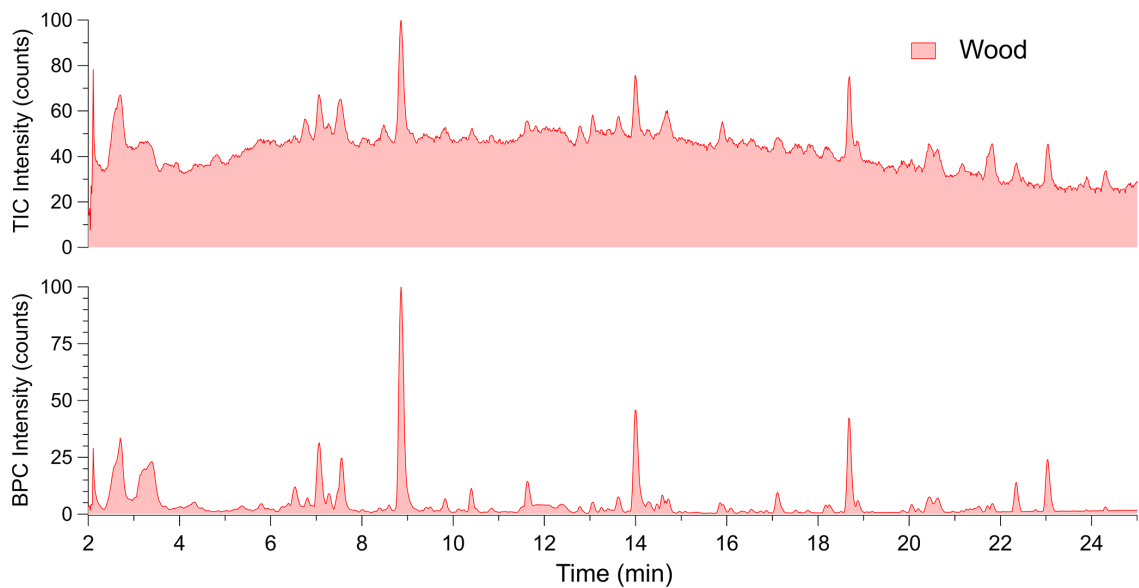


Figure A.14: Total Ion Chromatogram (TIC)(a) and Base Peak Chromatogram (BPC)(b) ESI+ LC-MS chromatograms of Wood biomass burning emissions.

A.1.8 MS Assignments

Table A.1: Top 100 Molecular Assignments Unique to Indian and Canadian Dung using the ESI+ mode. High (left column) to low (right column) in descending order of intensity. Columns 3. and 6. ‘Prev. Rep.’ list whether a compound has been identified in a study by Fleming *et al.*[249] as unique to dung samples (1), common to wood and dung samples (2), or not detected (0).

Calculated Mass to Charge (m/z)	Molecular Formula	Prev. Rep.	Mass to Charge (m/z) contd.	Formula contd.	P. R. contd.
169.0849	C ₉ H ₁₂ O ₃	0	227.1528	C ₁₂ H ₂₀ NO ₃	0
211.0967	C ₁₁ H ₁₄ O ₄	2	318.2777	C ₁₈ H ₃₇ O ₄	0
179.1533	C ₁₁ H ₁₈ N ₂	2	149.0945	C ₈ H ₁₀ N ₃	1
158.0812	C ₇ H ₁₁ NO ₃	0	245.1267	C ₁₄ H ₁₆ N ₂ O ₂	1
144.0654	C ₆ H ₉ NO ₃	0	388.2534	C ₁₉ H ₃₅ N ₂ O ₆	0
209.0789	C ₁₁ H ₁₂ O ₄	2	213.1374	C ₁₁ H ₁₈ NO ₃	0
209.1644	C ₁₂ H ₂₀ N ₂ O	0	279.2307	C ₁₈ H ₃₀ O ₂	0
195.1012	C ₁₁ H ₁₄ O ₃	0	356.3521	C ₂₂ H ₄₅ NO ₂	0
284.2938	C ₁₈ H ₃₇ NO	0	326.3770	C ₂₂ H ₄₇ N	0
181.1322	C ₁₀ H ₁₆ N ₂ O	0	270.2785	C ₁₇ H ₃₅ NO	0
156.0790	C ₁₁ H ₉ N	0	116.1061	C ₆ H ₁₃ NO	0
183.0932	C ₁₂ H ₁₀ N ₂	2	147.0796	C ₁₀ H ₁₀ O	0
265.2624	C ₁₇ H ₃₂ N ₂	0	343.2125	C ₂₁ H ₂₈ NO ₃	0
239.2362	C ₁₆ H ₃₀ O	0	268.2633	C ₁₇ H ₃₃ NO	0
187.0842	C ₈ H ₁₂ NO ₄	0	155.1055	C ₉ H ₁₄ O ₂	0
257.2467	C ₁₆ H ₃₂ O ₂	0	219.1730	C ₁₅ H ₂₂ O	0
228.1496	C ₁₆ H ₁₉ O	0	177.0547	C ₁₀ H ₈ O ₃	2
229.1322	C ₁₄ H ₁₆ N ₂ O	2	290.2678	C ₁₆ H ₃₅ NO ₃	0
299.2575	C ₁₈ H ₃₄ O ₃	0	215.1169	C ₁₃ H ₁₄ N ₂ O	1
228.1496	C ₁₁ H ₁₉ N ₂ O ₃	0	135.0796	C ₉ H ₁₀ O	1
254.2470	C ₁₆ H ₃₁ NO	0	151.0378	C ₈ H ₆ O ₃	0
141.0542	C ₇ H ₈ O ₃	0	195.1040	C ₁₄ H ₁₂ N	0
201.0984	C ₉ H ₁₄ NO ₄	0	355.3196	C ₂₂ H ₄₂ O ₃	0
193.1688	C ₁₂ H ₂₀ N ₂	2	117.0543	C ₅ H ₈ O ₃	0
339.3251	C ₂₂ H ₄₂ O ₂	0	183.1844	C ₁₁ H ₂₂ N ₂	2
150.0893	C ₆ H ₁₃ O ₄	0	230.2471	C ₁₄ H ₃₁ NO	0
293.2939	C ₁₉ H ₃₆ N ₂	0	330.2996	C ₁₉ H ₃₉ NO ₃	0
279.2782	C ₁₈ H ₃₄ N ₂	0	209.1993	C ₁₃ H ₂₄ N ₂	2
259.1197	C ₁₅ H ₁₆ NO ₃	0	324.2891	C ₂₀ H ₃₇ NO ₂	0
328.2848	C ₁₉ H ₃₄ O ₃	0	228.2315	C ₁₄ H ₂₉ NO	0
165.0538	C ₉ H ₈ O ₃	0	125.1068	C ₇ H ₁₂ N ₂	2
148.0747	C ₉ H ₉ NO	0	183.0643	C ₉ H ₁₀ O ₄	0
183.1012	C ₁₀ H ₁₄ O ₃	0	344.3150	C ₂₀ H ₄₁ NO ₃	0
269.1642	C ₁₇ H ₂₀ N ₂ O	0	315.2524	C ₁₈ H ₃₄ O ₄	0
197.0817	C ₁₀ H ₁₂ O ₄	0	170.0945	C ₉ H ₁₃ O ₃	0

Table A.1 continued from previous page

Calculated Mass to Charge (m/z)	Molecular Formula	Prev. Rep.	Mass to Charge (m/z) contd.	Formula contd.	P. R. contd.
169.1686	C ₁₀ H ₂₀ N ₂	1	219.1716	C ₁₀ H ₂₂ N ₂ O ₃	0
167.1531	C ₁₀ H ₁₈ N ₂	2	375.3476	C ₂₂ H ₄₆ O ₄	0
134.0596	C ₈ H ₉ NO ₂	0	181.1222	C ₁₁ H ₁₆ O ₂	0
310.3100	C ₂₀ H ₃₉ NO	0	102.0912	C ₅ H ₁₁ NO	0
149.0600	C ₉ H ₈ O ₂	0	130.1215	C ₇ H ₁₅ NO	0
243.1485	C ₁₅ H ₁₈ N ₂ O	2	113.0228	C ₅ H ₄ O ₃	0
281.2469	C ₁₈ H ₃₂ O ₂	0	181.1314	C ₇ H ₁₈ NO ₄	0
139.1219	C ₈ H ₁₄ N ₂	2	175.0748	C ₁₁ H ₁₀ O ₂	2
156.0789	C ₈ H ₁₁ O ₃	0	112.0749	C ₆ H ₉ NO	0
193.0819	C ₆ H ₁₂ N ₂ O ₅	0	215.1541	C ₁₄ H ₁₈ N ₂	2
191.1155	C ₈ H ₁₆ NO ₄	0	187.0867	C ₁₁ H ₁₀ N ₂ O	1
217.1684	C ₁₄ H ₂₀ N ₂	2	298.3106	C ₁₉ H ₃₉ NO	0
157.0486	C ₇ H ₈ O ₄	0	201.1015	C ₁₂ H ₁₂ N ₂ O	1
273.1131	C ₁₉ H ₁₄ NO	0	301.1086	C ₂₀ H ₁₄ NO ₂	0
244.1330	C ₁₅ H ₁₇ NO ₂	2	169.1220	C ₁₀ H ₁₆ O ₂	0

A.1.9 Standard Compounds

Table A.2: Standard Analysis: ESI- Compound Detection Intensity

Standard Compound	Mix ESI-	Wood ESI-	CAD ESI-	IND ESI-
Vanillin	6.17×10^5	2.26×10^6	2.22×10^5	1.59×10^5
Sinapaldehyde	2.27×10^6	1.21×10^5	2.75×10^4	3.05×10^4
4-Nitroguaiacol	1.22×10^7	1.43×10^4	4.84×10^4	3.19×10^4
4-Nitrocatechol	1.67×10^7	1.24×10^4	6.61×10^4	3.63×10^4
Coniferyl aldehyde	3.50×10^6	9.85×10^6	6.93×10^5	4.71×10^5

Table A.3: Standard Analysis: ESI+ Compound Detection Intensity

Standard Compound	Mix ESI+	Wood ESI+	CAD ESI+	IND ESI+
Vanillin	2.21×10^5	5.06×10^6	5.56×10^5	4.04×10^5
Sinapaldehyde	1.08×10^6	-	8.31×10^4	7.98×10^4
4-Nitroguaiacol	4.55×10^4	-	-	-
4-Nitrocatechol	2.69×10^4	-	-	-
Coniferyl aldehyde	7.31×10^5	1.30×10^7	-	-

Mix refers to an aggregate of the standard compounds - 100 μM each - jointly dissolved in acetonitrile. Detection intensity represents the peak area counts. ESI+ inability to detect sinapaldehyde and coniferyl aldehyde can be explained by the large chemical background of biomass burning emissions.

Appendix B: Chapter 3

B.1 Supplementary information for Chapter 3

B.1.1 GC×GC-ToF-MS Results

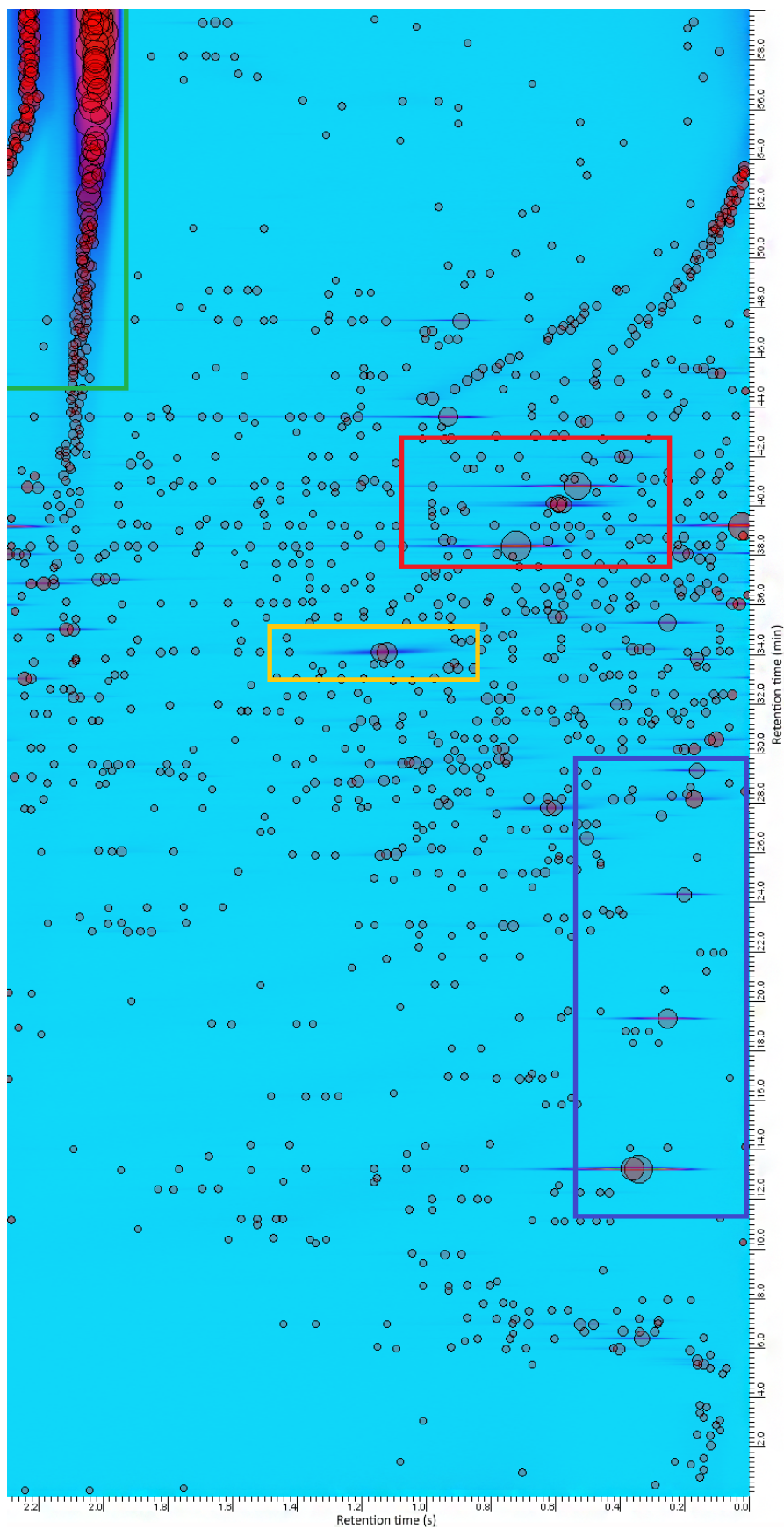


Figure B.1: Two-dimensional gas chromatography time of flight mass spectrometry (GC×GC-ToF-MS) chromatogram of wood biomass burning particulate matter gathered at 500 °C and 0.2 slpm of airflow. Each circle represents a series of syringaldehyde compounds. The red square represents the biomass burning tracer levoglucosan. The blue and green squares represent interferences from the glass wool and column bleed of increasing carbon chain length. The yellow square represents the biomass burning tracer levoglucosan. The blue and green squares represent interferences from the glass wool and column bleed respectively.

Appendix C: Chapter 4

C.1 Supplementary information for Chapter 4

C.1.1 NMR Analysis

As shown in Figure C.2, maleic anhydride will hydrolyse in the protic solvent (D_2O), yielding a peak at ~ 6.4 ppm. Both (Figures C.3 and C.4) also display the same peak, indicating it is due to maleic acid. The acid peak is not present in the aprotic solvent (Figure C.1) which instead displays a peak shift of ~ 7.1 ppm due to the anhydride. As can be seen in Table C.1, the calculated concentration of maleic anhydride in D_2O (obtained from the acid peak shift of ~ 6.4 ppm) is similar to the concentration of the maleic acid standards. This indicates the anhydride fully hydrolyses into its acid form. The peak shifts of ~ 4.7 and ~ 7.4 ppm represent the solvents D_2O and $CDCl_3$ respectively. All samples display a strong internal standard (DMSO) peak shift, at 2.62 ppm using $CDCl_3$ as a solvent, and 2.71 for D_2O , as predicted by established literature [391]. The calculated concentration is obtained from the anhydride or acid peak intensity compared to that of the internal standard.

Table C.1: 1H NMR anhydride and acid analysis in protic (D_2O) and aprotic ($CDCl_3$) solvents. The calculated concentration range represents duplicate analyses.

Chemical	Solvent	DMSO (mM)	Calculated Conc. (mM)
Maleic Anhydride*	D_2O	0.5	0.00342 - 0.00362
Maleic Anhydride	$CDCl_3$	0.5	0.00345 - 0.00367
Maleic Acid	D_2O	0.5	0.00399 - 0.00407
Maleic Acid	$CDCl_3$	0.5	0.00365 - 0.00408

*Lacking maleic anhydride peak, concentration calculated from maleic acid.

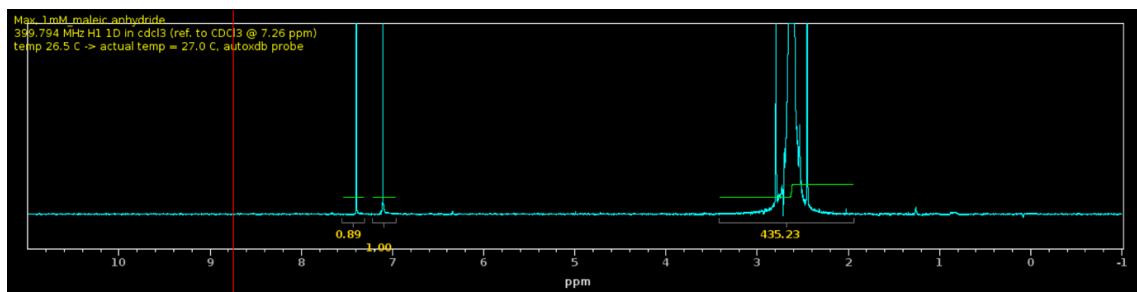


Figure C.1: ^1H NMR plot of Maleic Anhydride dissolved in CDCl_3

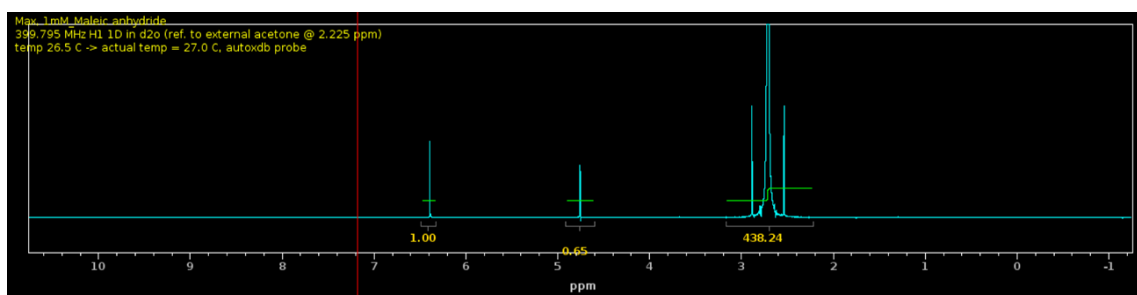


Figure C.2: ^1H NMR plot of Maleic Anhydride dissolved in D_2O

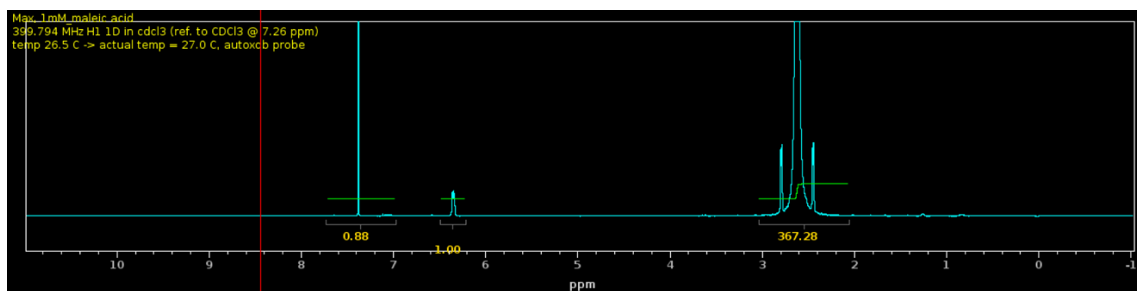


Figure C.3: ^1H NMR plot of Maleic Acid dissolved in CDCl_3

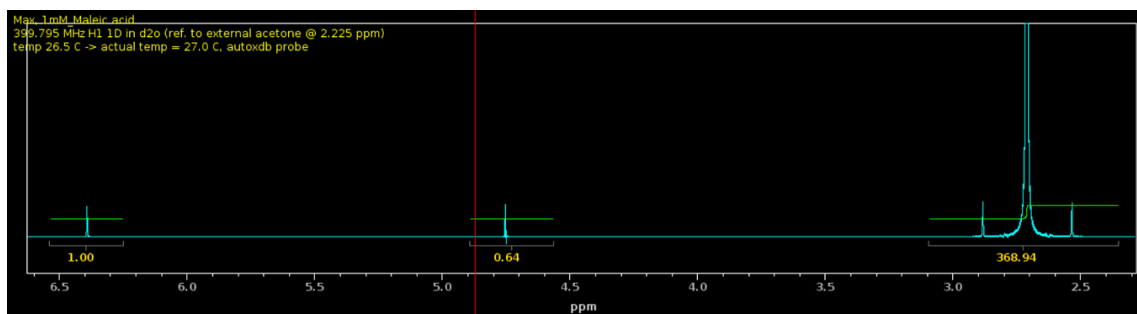


Figure C.4: ^1H NMR plot of Maleic Acid dissolved in D_2O

C.1.2 Anhydride Gas-Phase Concentration Determination

The gas-phase concentration of each anhydride was estimated using LC-MS and GC-FID. By flowing 200 sccm of dry air through the anhydride containing cell followed by the GC-FID and a bubbler, anhydride molecules remain trapped in the liquid water contained in the bubbler, where they rapidly hydrolyze. The water is then sampled and analyzed using the LC-MS method described in the main text. Anhydride detection is achieved through their corresponding acid peak and quantified using acid standards of known concentration. The gas-phase concentration of the anhydride flowing through the system is then back-calculated from the acid concentration in the bubbler water. The trapping efficiency of the bubbler was examined by routing the anhydride through the GC-FID after passing through the bubbler. Anhydride molecules which are not captured by the bubbler are then detected as a peak on the GC-FID. Using a similar quantity of solid anhydride as the coated tube experiments, less than 0.25% of the maleic anhydride broke-through the bubbler and was detected by the GC-FID. The breakthrough peak height did not vary significantly over a 24 h experimental period and matched background signal levels. No breakthrough peak was observed for phthalic anhydride.

C.1.3 Typical LC-MS Chromatograms

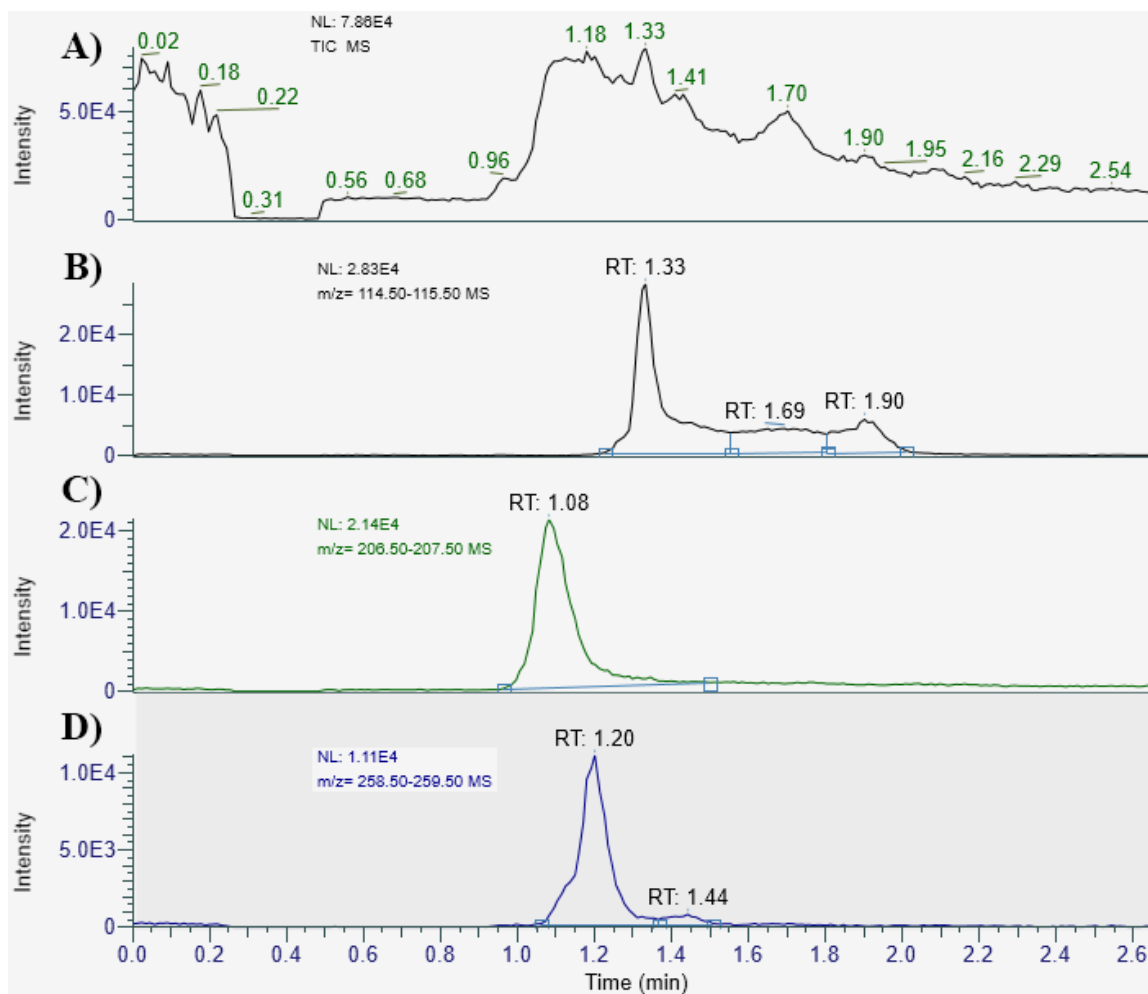


Figure C.5: Liquid Chromatography Negative Electrospray Ionization Mass Spectrometry (LC-MS) Plots of Coated Tube Extract After Maleic Anhydride Uptake in: (A) Total Ion Chromatogram (TIC), (B) Maleic Acid Extracted Ion Chromatogram (EIC) at a mass to charge (m/z) of 115, (C) Levoglucosan EIC at m/z 207, (D) Maleic Anhydride Levoglucosan Product EIC at m/z 259. NL represents the intensity of the largest peak in each chromatogram.

In this section, we provide typical Liquid Chromatography Mass Spectrometry (LC-MS) plots for an extracted tube (C.5), maleic anhydride and acid standards (C.7 and C.6), as well as phthalic acid (C.8) standard. As can be seen from the total ion chromatogram (TIC) in Figure C.5(A), a large “wave” of compounds elute at the beginning of the separation. This is usual of biomass burning emissions analyzed through LC-MS, as they contain numerous compounds with a variety of properties

and functional groups [1]. (B), (C) and (D) are extracted ion chromatograms obtained from (A). As maleic anhydride does not readily ionize in negative electrospray ionization (ESI⁻) mode, it is instead detected in its hydrolysed form as maleic acid. The peak tailing in Figure C.5(B) and Figure C.7 is typical for anhydrides samples dissolved in acetonitrile, and does not occur in the acids (Figures C.6 and C.8). Presumably, water in the LC-MS mobile phase hydrolyses the anhydride during the separation, affecting the corresponding acids retention time and peak intensity.

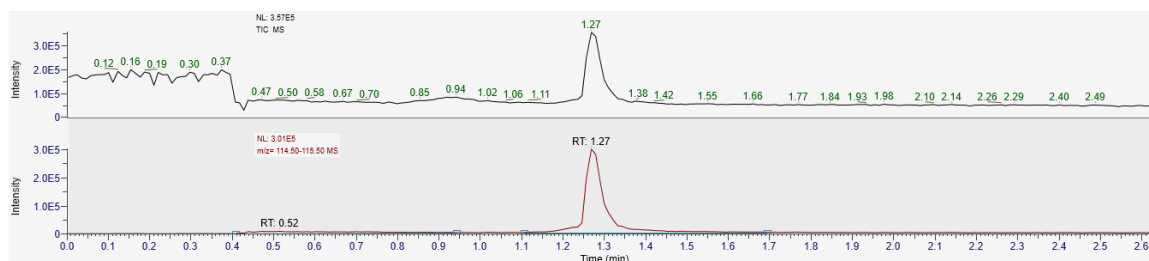


Figure C.6: LC-MS chromatogram of 0.01mM maleic acid dissolved in acetonitrile, TIC (top) and EIC at 115 m/z (bottom).

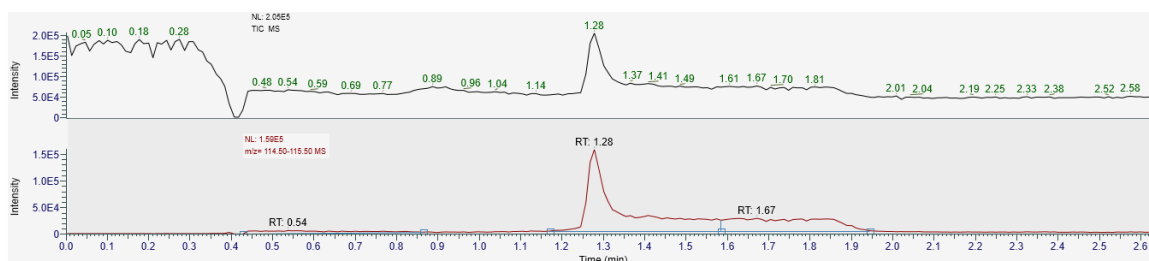


Figure C.7: LC-MS chromatogram of 0.1mM maleic anhydride dissolved in acetonitrile, TIC (top) and EIC at 115 m/z (bottom).

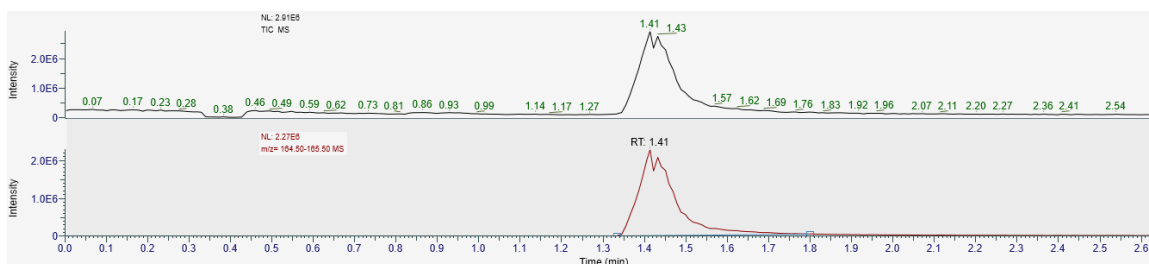


Figure C.8: LC-MS chromatogram of 1mM phthalic acid dissolved in acetonitrile, TIC (top) and EIC at 165 m/z (bottom).

C.1.4 Burn Parameters

Table C.2 displays the burn and airflow parameters for each filter gathered. Emissions were gathered during the temperature ramping process and for 10 minutes after reaching 500 °C, totalling to a 14.9 min collection time. As covered in the main text, each filter was separately extracted in acetonitrile after collection, and mixed together to form a composite sample from which the tubes were coated. Assuming complete extraction, the final concentration of the composite sample was 0.00176 g/ml.

Table C.2: Individual filter burn parameters.

Sample	Temp (°C)	Flow Rate (SLPM)	Ext Vol (mL)	Sample Mass (g)	Filter Load (g)
Wood	500	0.2	10	0.7162	0.0238
Wood	500	0.2	20	1.0905	0.0345
Wood	500	0.2	20	0.8827	0.0199
Wood	500	0.2	20	2.0464	0.0450
Total			70	4.7358	0.1232

C.1.5 Coated Tube Uptake Parameters

Parameter	Experimental	Equation
Temperature (T)	296.15 K	
Air Density (ρ)	1.192 kg m ⁻³	
Air Viscosity (η)	0.0183 mPA s	
Coated Tube Length (L)	20.0 cm	
Coated Tube Internal Diameter (D_{tube})	0.950 cm	
Volumetric Flow (F)	0.204 L min ⁻¹	
Linear Velocity (v)	4.80 cm s ⁻¹	$v = \frac{F}{A}$
Residence Time (t)	4.2 s	$t = \frac{v}{L}$
Reynolds Number (Re) ³	29.7	$Re = \frac{\rho \times D_{tube} \times v}{\eta}$
Length to Laminar Flow (l) ⁴	0.989 cm	$l = 0.035 \times Re \times D_{tube}$
Molecular Velocity (ω_x) ⁵	205.8 m s ⁻¹	$\omega_x = \sqrt{\frac{8 \times k \times T}{\pi \times m}}$
Air Dimensionless Diffusion Volume (V_{Air}) ⁵	19.7	
PA Dimensionless Diff Vol (V_{phthal}) ⁵	136.5	$V = \sum n_i V_i$ $8 \times 15.9 + 4 \times 2.31 + 3 \times 6.11 - 18.3$
RM of the PA(m_A)-Air(m_B) Pair (m(A,B)) ⁵	48.45	$m(A,B) = \frac{2}{\frac{1}{m_A} + \frac{1}{m_B}}$ $m_A = 148.1$ $m_B = 28.96$
PA Diff Coefficient (D(A,B)) ⁵	0.071 cm ² s ⁻²	$D(A,B) = \frac{1.0868 \times T^{1.75}}{\sqrt{m(A,B)} \times (\sqrt[3]{V_{phthal}} + \sqrt[3]{V_{air}})^2 \times 760}$
Mean Free Path (λ) ⁴	102.8 nm	$\lambda = \frac{D}{\omega_x}$
Knudsen Number (Knx) ⁶	2.16 $\times 10^{-5}$	$Knx = \frac{2 \times \lambda}{D_{tube}}$
Dimensionless Axial Distance (z^*) ⁴	0.651	$z^* = L \frac{\pi \times D}{2F}$
Effective Sherwood Number (N_{Shw}^{eff}) ⁴	3.80	$N_{Shw}^{eff} = 3.6568 + \frac{A}{z^* + B}$ A = 0.0978 and B = 0.0154

Table C.3: Parameters used to calculate the uptake coefficient (γ) in Chapter 4
PA = Phthalic Anhydride, RM = Molecular Reduced Mass

C.1.6 Anhydride Nucleophilic Addition

Figure C.9 displays the structures predicted from the LC-MS analysis of anhydride nucleophile mixtures. In each case, the m/z of the product peak was detected as the addition of the anhydride to the nucleophile. For example, vanillin (m/z 152) and maleic anhydride (m/z 98), reacted to form a product with a m/z of 250 (detected as 249 in ESI⁻ mode). Maleic and phthalic anhydride are used interchangeably as -

with the exception of coniferyl aldehyde - both were observed to react with the listed nucleophiles.

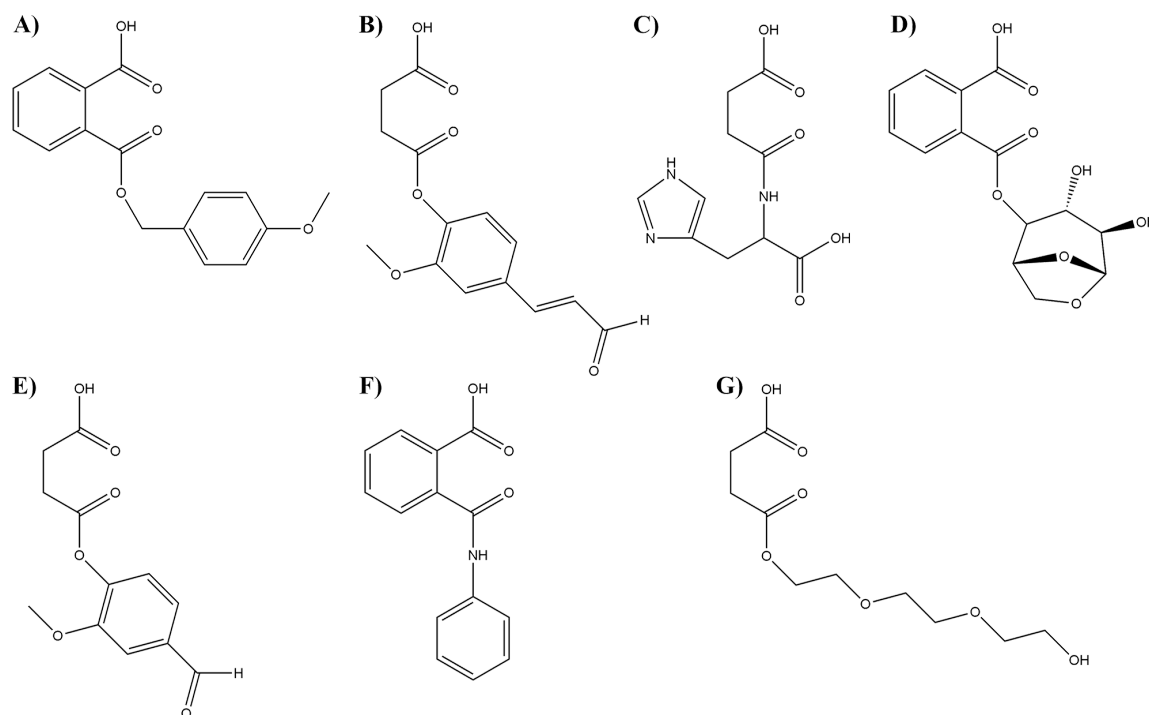


Figure C.9: Predicted product structures of the nucleophilic addition of anhydrides where: A) Anisyl Alcohol + Phthalic Anhydride, B) Coniferyl Aldehyde + Maleic Anhydride, C) Histidine + Maleic Anhydride, D) Levoglucosan + Phthalic Anhydride, E) Vanillin + Maleic Anhydride, F) Aniline + Phthalic Anhydride, and G) Triethylene Glycol + Maleic Anhydride.

C.1.7 Reaction Competition and Product Stability in Water

As can be seen in Figure C.10, the products follow similar trends as those in the main text. For MLP (B), PAP (C), and MAP (D), the presence of water (1-25%) initially enhances the formation of the product. However, the signal swiftly decays as the fraction of available water is increased. As described in the main text, it is likely that water is acting as a proton carrier during the nucleophilic addition reaction, which kick-starts the formation of the product at low water contents. As more water is made available, the hydrolysis reaction takes over and the product is formed in lower quantities.

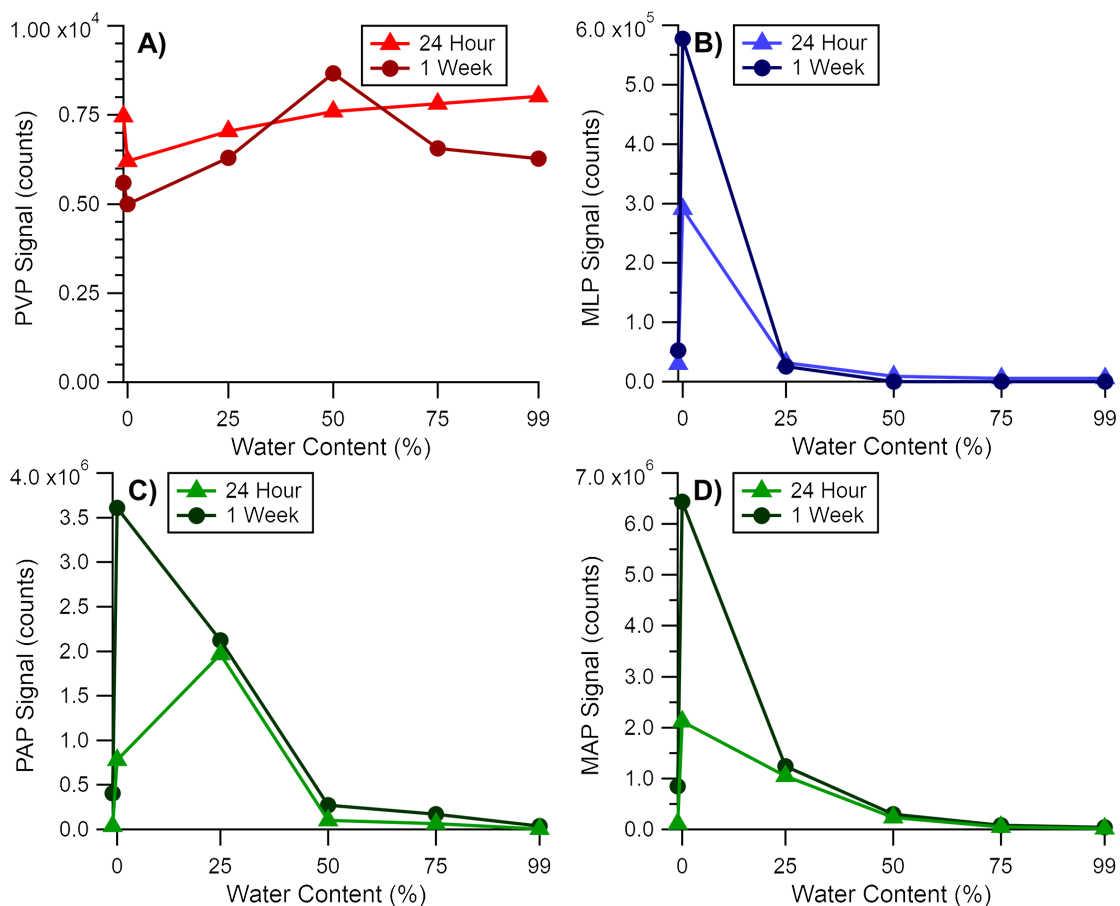


Figure C.10: LC-MS peak area signals obtained from increasing fractions of water in acetonitrile after the 24 hour and 1 week-long analysis period for A) Phthalic Anhydride Vanillin Product (PVP), B) Maleic Anhydride Levoglucosan Product (MLP), C) Phthalic Anhydride Anisyl Alcohol Product (PAP), D) Maleic Anhydride Anisyl Alcohol Product (MAP).